NBSIR 83-2679-2

Technical Aspects of Critical Materials Use by the Steel Industry

Volume II B

Proceedings of a Public Workshop; "Trends in Critical Materials Requirements for Steels of the Future; Conservation and Substitution Technology for Chromium".

4-7 October 1982

Vanderbilt University
Nashville, TN

Public Workshop Sponsored by:
U.S. Department of Commerce, National Bureau of Standards
U.S. Department of the Interior, Bureau of Mines
U.S. Department of Defense, Army Research Office

June 1983

Center for Materials Science
U.S. Department of Commerce
National Bureau of Standards

NBSIR 83-2679-2

Technical Aspects of Critical Materials Use by the Steel Industry

Volume II B:

Proceedings of a Public Workshop; "Trends in Critical Materials Requirement for Steels of the Future; Conservation and Substitution Technology for Chromiun."

Sponsored by:
U.S. Department of Commerce, National Bureau of Standards
U.S. Department of the Interior, Bureau of Mines
U.S. Department of Defense, Army Research Office

4-7 October 1982

Vanderbilt University
Nashville, TN

Chairman
Allen G. Gray
American Society for Metals
Adjunct Professor of Metallurgy
Vanderbilt University

June 1983

U.S. Department of Commerce, Malcolm Baldrige, Secretary
National Bureau of Standards, Ernest Ambler, Director

Contents

VOLUME II A: Proceedings of a Public Workshop; "Trends in Critical Materials Requirements for Steels of the Future; Conservation and Substitution Technology for Chromium".

Impact of Developments in Manufacturing and Process Controls on Conservation and Recovery of Critical Materials

Conservation and Substitution For Chromium in Stainless Steels for Chemical Use and For Corrosion Resistant Applications

VOLUME II B: Proceedings of a Public Workshop; "Trends in Critical Materials Requirements for Steels of the Future; Conservation and Substitution Technology for Chromium".

Potential For Advanced Technologies in Chromium Conservation-Coating Systems And Surface Modification Technology; Ceramics, Composites And Intermetallics

Information Stockpile - Summary of Comments

OUTLOOK FOR CONSERVATION OF CHROMIUM IN SUPERALLOYS

John K. Tien, Juan M. Sanchez and Robert N. Jarrett
Center for Strategic Materials
Henry Krumb School of Mines
Columbia University
New York, New York 10027

I. INTRODUCTION AND BACKGROUND

Chromium is widely recognized as an essential alloying element in superalloys. This point is illustrated in Table I, which shows chromium contents for typical superalloys. Wrought nickel-base and iron/nickel-base alloys constitute the majority of superalloys and contain roughly 15-20% Cr. Cast nickel-base alloys contain typically 10-15% Cr and cobalt-base alloys 20-30% Cr.

Since the total tonnage of superalloy production is a mere fraction of the steel production, the amount of chromium used in superalloys does not constitute a very sizable portion of the total end use chromium in the U.S.[1,2,3] (see Fig. 1). However, the readily available ferrochrome used in stainless steels cannot be used as the source of chromium in the production of superalloys, since steel-grade ferrochrome usually contains too many deleterious tramp elements and impurities. Moreover, iron certainly is a major contaminant in the nickel-base and cobalt-base superalloys. Thus, the more expensive vacuum grade,

TABLE I. Chromium Content of Typical Superalloys

Wrought Ni-Base	Cr Content, %
Waspaloy	19.5
Udimet 720	18.0
Udimet 700	15.0
Nimonic 115	15.0
Cast Ni-Base	
IN 738	16.0
Mar M200	9.0
IN 100	10.0
Alloy 713C	12.5
Iron-Base	
Inconel 718	18.5
Alloy 901	13.5
Incoloy 903	0.0
Cobalt-Base	
X 40	25.5
Mar M509	21.5
Mar M322	21.5

Waspaloy, Udimet, Mar M, and Nimonic, IN, Inconel and Incoloy are trademarks of United Technologies, Inc., Special Metals Corp., Martin-Marietta Inc., and International Nickel Company, Inc., respectively.

spectral grade, or electrolytic* chromium metal is required.[4,5] Figure 2 shows the superalloy use of refined chromium and since over 50% of this chromium metal is refined overseas, this data clearly indicates the critical role played by chromium in superalloy production. Although superalloys use only a small fraction of the total chromium imported, they are the largest user of high quality chromium metal for which the U.S. has a limited production capacity.

In order to establish the feasibility of a Cr conservation program in superalloys, we will next briefly assess the role played by chromium in the structural (or bulk) properties and in the corrosion (or surface) properties of these alloys.

As a bulk alloying element, Cr is found to be the major component of $M_{23}C_6$ and M_7C_3 carbides, a minor component of M_6C, and not present in MC carbides[6,7,8] (Table II). In cobalt-base alloys carbides play a very important role since they are the strengthening phases. Table III shows the basic types of cobalt-base alloys. Note that the total amount of carbide formers in these alloys are about constant, but as the tungsten to chromium ratio increases, M_6C carbides replace the $Cr_{23}C_6$. Furthermore, with the addition of Ti-Ta type

* Difficulties also arise in using electrolytic chromium due to salt impurities resulting from that process(4).

TABLE II. Carbides in Cobalt-Base Superalloys

Alloy	C	Cr	W+Mo	Ti+Cb+Ta+Zr	Total Carbide Formers	Carbide Type
X 40	0.5	25.5	7.5	-	33.0	$Cr_{23}C_6$
Mar M509	0.6	21.5	7.0	4.2	32.5	$Cr_{23}C_6$ $(W,Cr)_6C$ $(Ta,Ti)C$
Mar M322	1.0	21.5	9.0	7.5	38.0	W_6C TaC

TABLE III. Carbide Types in Superalloys and Their Metal Content

Carbide	Metal Atoms
M_7C_3	Cr
$M_{23}C_6$	Cr + (Mo,W)
M_6C	(Mo,W) + Cr
MC	(Hf,Ta,Nb,Ti,V)

refractory elements, the $Cr_{23}C_6$ carbides are replaced with MC's which do not contain Cr. In fact, refractory metals are purposely added to Co-base superalloys in order to replace chromium carbides, which in general play a detrimental role in the alloy's mechanical properties. When $Cr_{23}C_6$ forms, it precipitates heterogeneously at the grain boundaries and at stacking faults. This stacking fault precipitation, in turn, acts as a crack initiation site resulting in low temperature embrittlement. Chromium, however, is always present in Co-based superalloys at a concentration of about 20% Cr, in order to form a protective oxide layer. The latter is necessary since cobalt oxide is volatile, offering no protection of its own.

The same carbide decomposition reaction seen in Co-base superalloys is used in the heat treatment of nickel-base superalloys. However, in the latter system, the reaction is used to produce the typical grain boundary morphology shown in Fig. 3, with both forms of carbide (MC and $M_{23}C_6$) present after heat treatment.

In a study* on the role of cobalt in superalloys, we found that cobalt affected the type of carbide found in nickel-base superalloys[6,7] (see Fig. 4). Removing cobalt from the standard

---

* "The Role of Cobalt on Nickel-Base Superalloys", NASA COSAM (Conservation of Strategic Aerospace Materials) Grant NAG 3-57 conducted at NASA-Lewis Research Center, Special Metals Corporation, Purdue University and Columbia University.

alloy destabilizes the MC carbide and results in more $M_{23}C_6$. Despite this effect the mechanical properties were essentially unaffected (Fig. 5), indicating again that the chromium carbides are replaceable.

As part of the same investigation, it was found that the precipitation of $Cr_{23}C_6$ carbides resulted in a drastic reduction in the hot workability of Nimonic 115. The effect is illustrated in Fig. 6, which shows the failure during the first reduction of the chromium carbide containing alloy, while the alloy with the standard was rolled to the final 3/4" bar. The carbide morphologies are shown in Fig. 7. The spheroidized MC carbides aid workability, while the chromium carbides at the grain boundaries embrittle the alloy. Thus, it was concluded that in Ni-base superalloys the $Cr_{23}C_6$ carbides are not essential for mechanical properties and, indeed, sometimes such carbides are detrimental.

Beside carbide effects, chromium also affects the properties of the matrix since, like cobalt, it partitions to that phase. Similarly, chromium is a relatively weak solid solution strengthener compared to the refractory elements. The chromium effect on gamma prime fraction is also expected to be small, like cobalt's effect, since the Ni-Al-Cr and the Ni-Al-Co ternary phase diagrams are quite similar. Certainly a chromium free alloy would be less prone to sigma formation since chromium is a major component of that phase. The effects of chromium on stacking fault

energy and gamma prime anti-phase boundary energy should certainly be considered, but no intrinsic mechanical problems would be expected if chromium were removed from a superalloy as was the case of 903, a chromium free version of alloy 901.

The main reason for the presence of chromium in superalloys is, of course, the marked improvement in oxidation/hot corrosion resistance it imparts to the alloys. For hot corrosion resistance an alloy should simply have as much chromium as possible[8] (Fig. 8). This amount is limited, however, by the 20-25% chromium solubility in the matrix[6,9], beyond which sigma will form. Since the solubility of chromium in gamma prime is small (about 3-4%), high gamma prime volume fraction alloys are limited in their total chromium content. Thus, such alloys have intrinsically poor hot corrosion resistance.

In applications, the superalloys are usually divided into two groups according to their operating temperatures: the intermediate temperature range (above 800°C) for turbine blades. At the lower temperatures fine grain, wrought alloys with up to about 40% gamma prime are used. At high temperatures, the strength requirement precludes all but the high gamma prime fraction, high strength cast alloys. Because of the large gamma prime fraction, high temperature alloys have less chromium and must be coated for adequate corrosion protection.

The mechanism of corrosion protection in the complex

superalloys is not simple. In the case of iron-nickel and cobalt base alloys Cr_2O_3 forms as the predominant oxide. If the alloy contains sufficient chromium (Fig. 9), this Cr_2O_3 layer is continuous and it has a low enough permeability for oxygen to prevent oxidation of the other metallic species. Such an oxide is protective by itself. However, if an alloy does not contain enough chromium (see Fig. 10), a continuous layer does not form and other oxides occur instead, such as volatile CoO or TiO_2 or porous NiO or Fe_2O_3, which are permeable to oxygen. This oxide situation allows continuous oxidation of the exposed surface.[10]

In the case of nickel-base superalloys, the thermodynamically preferred oxide is Al_2O_3, which has the lowest permeability of any of the oxides. However, the aluminum content in these alloys is too low to form a continuous, protective Al_2O_3 layer. As the oxide starts to form aluminum is drawn to the surface, dissolving gamma prime and forming a denuded zone marked 'Y' in Fig. 11. Due to the depletion of aluminum in the denuded zone, other oxides begin to form as fast as oxygen diffuses through the oxide.[10]

In the nickel-base superalloys, the chromium content is high enough that Cr_2O_3 also forms in the initial oxidation reactions. This oxide essentially behaves like a diffusion barrier for the oxygen and the stable configuration in Fig. 12 is reached. The oxygen activity below the Cr_2O_3 layer is

sufficiently low so that Al_2O_3 alone forms and Al diffusion across the denuded zone is the controlling step. This oxide combination is the source of the excellent oxidation resistance of the superalloys. Even though an aluminum oxide layer would provide the best oxidation protection, superalloys require chromium to form a continuous layer.[10]

The Cr_2O_3 layer is irreplaceable for resistance to hot corrosion in the presence of molten salts. Without this layer (due to a low chromium content), the liquid salts and oxygen preferentially attack grain boundaries (Fig. 13) causing premature intergranular failure (Fig. 14). The rupture life of this specimen was considerably shortened by the presence of $NaSO_4$ (see Fig. 15)[11].

For this reason low chromium alloys are protected by coating with corrosion resistant alloys (NiCrAlY, beta, etc.) or plasma spraying (chromizing or aluminizing). The compositional differences between the coating and substrate (such as a beta phase alloy shown in Fig. 16) form a diffusion couple that can result in a multitude of intermetallic phases at the interface. Differences in mechanical and expansion characteristics between these two alloys are unavoidable. Accordingly thermal fatigue failure at the interface are likely to occur so the substrate always contains a considerable amount of chromium as a safety net.

In summary, chromium can be removed from superalloys without a severe effect on mechanical properties, but it is essential at the surface for oxidation resistance especially in the presence of salt contaminants.

II. Possible Chromium Conservation Options in Superalloys

The current solution for resisting hot corrosion in superalloy design is the addition of as much chromium as the matrix can hold without forming sigma phase and then coating the alloy if that amount is not sufficient (see Fig. 17). Aside from the conservation consideration that over 90% of the chromium is not needed, the presence of this chromium, in fact, can deleteriously affect the alloys. As mentioned, these negative aspects include sigma and mu phase instabilities, excessive $M_{23}C_6$ precipitation, and relatively high thermal expansion coefficients.

The chromium requirement of superalloys can be redefined by three criteria:

1. The near surface of the alloy (a minimum of 10 microns) must contain sufficient chromium for corrosion resistance ($\sim$20%).

2. This layer must be integrally bonded to the substrate with no continuous intermetallic layers or physical interfaces.

3. The configuration must be sufficiently stable over prolonged periods ($\sim$1000 hours). We performed a simulation of the

diffusion process (Fig. 18) and determined that the initial 10 micron profile would be stable at 800°C, but a deeper profile of 50-100 microns would be required for 1000 hours of operation at 1000°C (Fig. 19).

The available techniques for producing surface chemical changes are:

1. Claddings and coatings--Using current diffusion technology, chromium-free base alloys can be coated or clad by conventional techniques. However, this approach has been rejected, to date, since a crack forming in the coating would result in disastrous substrate degradation in hot corrosion environments. Currently all base alloys that are coated contain at least 8% chromium for insurance.

2. Plasma spraying and overlays--Overlays also have a distinct interface and the same failure consequences as claddings or coatings.

3. Dual composition powders[12]--By using two different powder compositions for the interior and surface of the disk components, a sizable amount of the chromium could theoretically be saved. However, to our knowledge, this technique has still not been successfully used to produce a reliable crack-free component.

4. Pack chromizing[13,14]--This technique has been successfully used to reproduce a surface alloy on stainless steels. The steel component, for example, is usually packed in a mixture ferro-chrome or chromium metal and alumina powders with a small amount of ammonium chloride and annealed in an inert or reducing

environment until the required diffusion profile is achieved. The gaseous chromium chloride is the carrier exchange gas of the chromium atoms rather than the metal/metal interface as is the case for the true diffusion couple. Currently this technique has been used experimentally to apply coatings to superalloys, but most of the research is unpublished company proprietary or published in the Soviet Union. This technique might be applied to achieve a smooth concentration profile on the surface of a chromium-free alloy by adjusting chromium and nickel activities in the pack or the exchange gas. However, we do not know of any success, to date, of producing a significant surface concentration of chromium without forming an alpha chromium layer.

5. Laser glazing[15,16] or electron beam surface welding--Laser glazing is a rapid solidification technique that has been used to construct disk shapes from layers of nickel-molybdenum alloys roughly 100 microns thick. Conceivably this technique could be used to apply a layer of a chromium containing alloy to a chromium-free superalloy substrate. However, as yet, no conventional alloy has been laser glazed without forming surface cracks.

6. Chromium ion implantation[17,18,19]--Ion implantation is readily used as a surface alloying technique for low temperature wear or for aqueous corrosion resistance. However, the depth of the alloy layer of chromium is on the order of .1 micron, which is well below the 10 micron minimum required. Additional difficulties include sputtering loss and a low beam current (measured in microamps). Hence, straight ion implantation can be eliminated

at this time as a viable alternative.

7. Ion recoil implantation[19]--As an alternative to using chromium ions as the source, recoil implantation can conceivably use a vapor or electrolytically deposited layer (of chromium) as the target for a high current (milliamps) beam of argon ions. The atom localized impact can in theory drive the chromium into the surface to a depth of approximately 1 micron. Multiple anneals and reapplication (Fig. 20) could result in a substantial profile to a depth of 10 microns or more with no sharp chromium alloy interface.

Isothermal annealing of the implanted layer would most likely produce a smooth concentration profile following Fick's law. Since no diffusion barrier exists at the 10 micron depth, repeat implantation/anneal cycles will distribute previous implant layers over an ever-increasing range before a substantial concentration is developed at the 10 micron depth. However, we propose that the diffusion range can be restricted by the application of a steep thermal gradient. Controlled laser annealing[20,21] is such a technique. Laser energy can be concentrated to within a few microns of the surface and thus constrain chromium diffusion in the near surface layer. With this method a high concentration near-surface layer can be built with a minimum number of implantation cycles.

The same recoil mechanism may be used to bond a thicker chromium layer to the alloy surface. The argon ion beam disrupts

the interface yielding a smooth transition layer for the diffusion couple without the problem of decohesion. In this alternative scenario, laser anneal can again serve as the spatially contained heat source for driving the chromium rapidly through the interface resulting in a chromium bearing surface alloy.

In summary, we assert that the chromium metal in superalloys is a critical strategic material which is quite vulnerable to supply side fluctuations. We have shown that chromium is essential for the elevated temperature oxidation and hot corrosion resistance of these alloys. However, the high chromium content required for the surface protection is not needed for the mechanical properties of the superalloys and, indeed, is often considered more detrimental than beneficial for these properties. Accordingly, we have reviewed the various methods of achieving the srface requirement of chromium while eliminating the bulk of the chromium from the alloys. While current methods of protecting low chromium alloys have drawbacks when applied to chromium-free alloys, several alternate methods of surface alloying, including ion implantation and laser annealing, have recently shown possible applications in the area of conservation of chromium in superalloys.

III. References

1. J.L. Morning, N.A. Matthews and E.C. Petersen, in Mineral Facts and Problems 1980, U.S. Bureau of Mines Bulletin 671, 1980, pp. 167-182.

2. U.S. Bureau of Mines Commodity Data Summary, "Chromium," 1980-1981.

3. L.R. Curwick, W. A. Petersen and H.V. Makar, U.S. Bureau of Mines IC #8821, 1980.

4. Private communication, W.J. Boesch, Special Metals Corporation, New Hartford, New York.

5. Private communication, A. FitzGibbon, Elkem Metals, Pittsburgh.

6. R.N. Jarrett and J.K. Tien, Met. Trans. A, Vol. 13A, June 1982, pp. 1021-1032.

7. J.K. Tien and R.N. Jarrett, in High Temperature alloys for Gas Turbines 1982, eds. R. Brunetaud et al., D. Reidel Publishing Co., Dordrecht, The Netherlands, pp. 423-446.

8. The Superalloys, eds. C.T. Sims and W.C. Hagel, John Wiley and Sons, Inc., New York, 1972.

9. O.H. Kriege and J.M. Baris, Trans. ASM, Vol. 62, 1969, pp.195-200.

10. F.S. Pettit and J.K. Tien, in Corrosion Fatigue, 1972, pp. 576-589.

11. J.K. Tien and J.M. Davidson, Advances in Corrosion Science and Technology, Vol. 7, 1980, p. 1-51.

12. Private communication, J. Stulga, Crucible Inc. Research Center, Pittsburgh.

13. R. Sivakumar, Trans. Indian Inst. of Metals, Vol. 33, No. 5, 1980, pp. 398-403.

14. R. Sivakumar and L.L. Seigle, Met. Trans. A, Vol. 7A, 1976, p. 1073.

15. E.M. Breinan, B.H. Kear, C.M. Banas and L.E. Greenwald, in Superalloys: Metallurgy and Manufacture, Claitor's Publishing Div., Baton Rouge, 1976, pp. 435-450.

16. D.B. Snow, E.M. Breinan and B.H. Kear, in Superalloys 1980, ASM, Metals Park, 1980, pp. 189-203.

17. A.B. Campbell III, B.D. Sartwell and P.B. Needham, Jr., U.S. bureau of Mines Report RI #8387, 1979.

18. C.W. Draper, Journal of Metals, June 1982, pp. 24-32.

19. Private Communication, D. Moon and W. Nahemow, Westinghouse Research and Development, Pittsburgh.

20. G. Dearnaley, Journal of Metals, Sept. 1982, pp. 18-28.

21. Private communication, S. Copley, University of Southern California, Los Angeles.

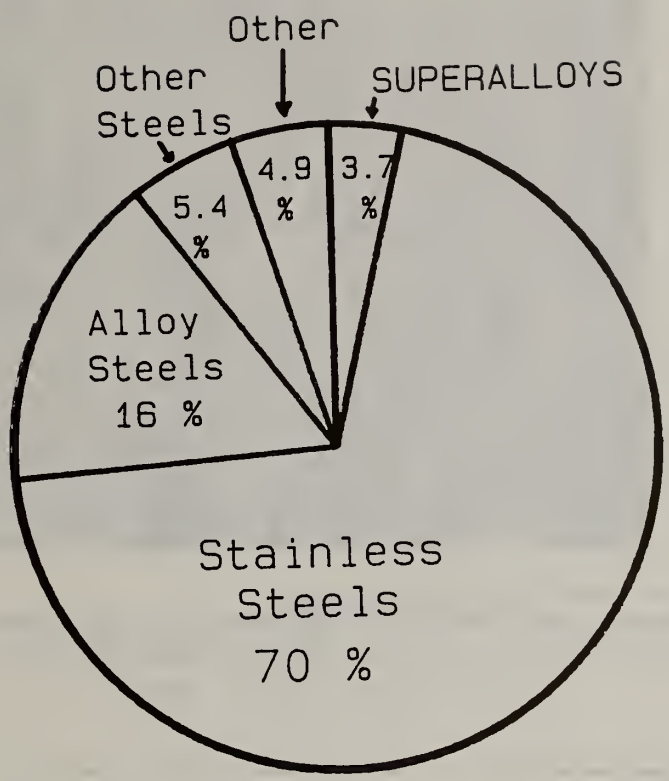

Fig. 1 1980 Total U.S. chromium consumption (849 million pounds)

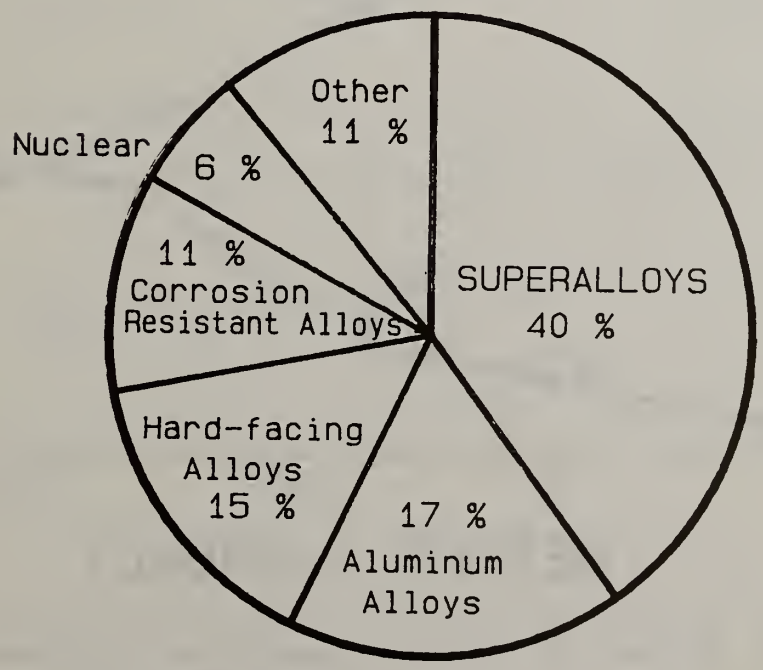

Fig. 2 Superalloy use of refined chromium metal

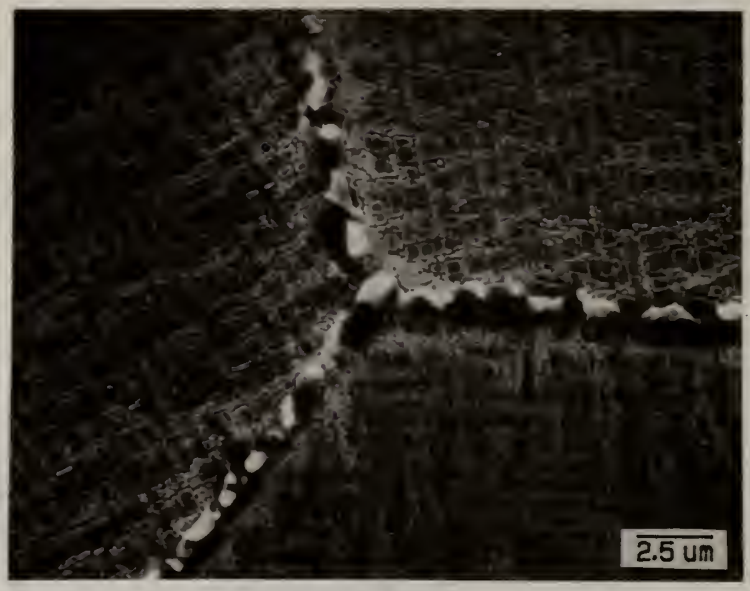

Fig. 3 Microstructure of a typical nickel-base superalloy with carbides at the grain boundaries

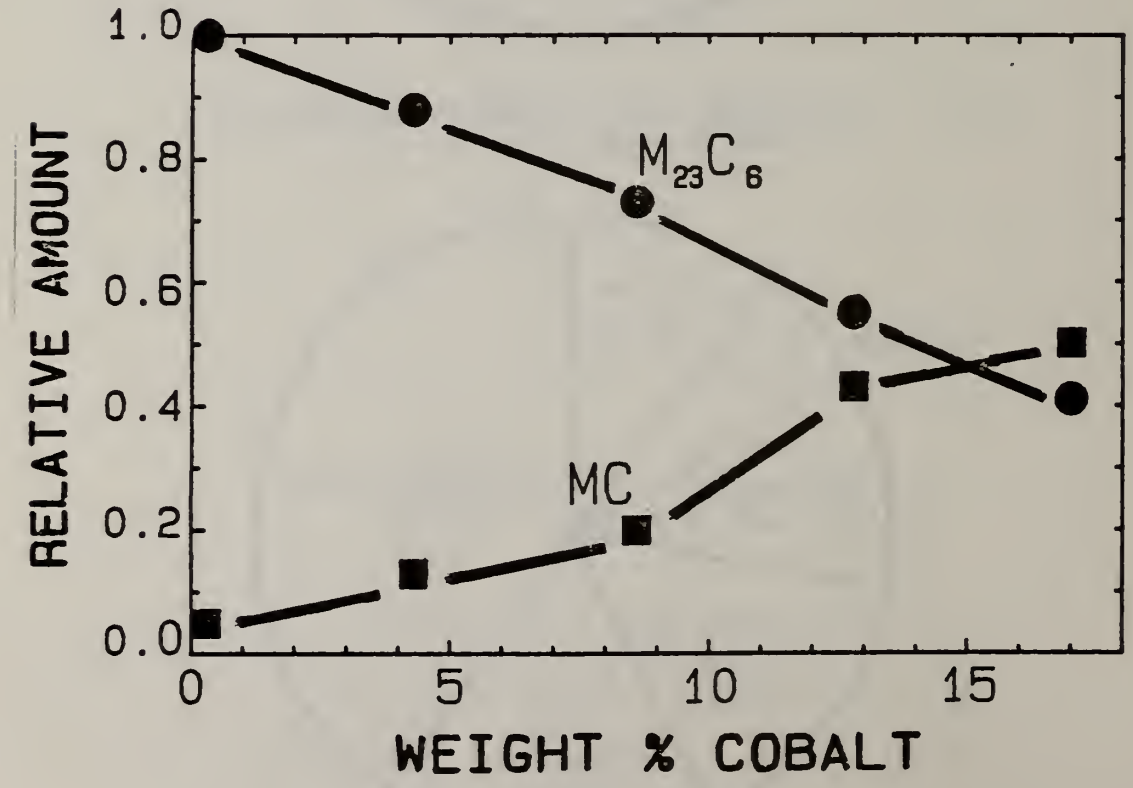

Fig. 4 Effect of cobalt on carbides in Udimet 700

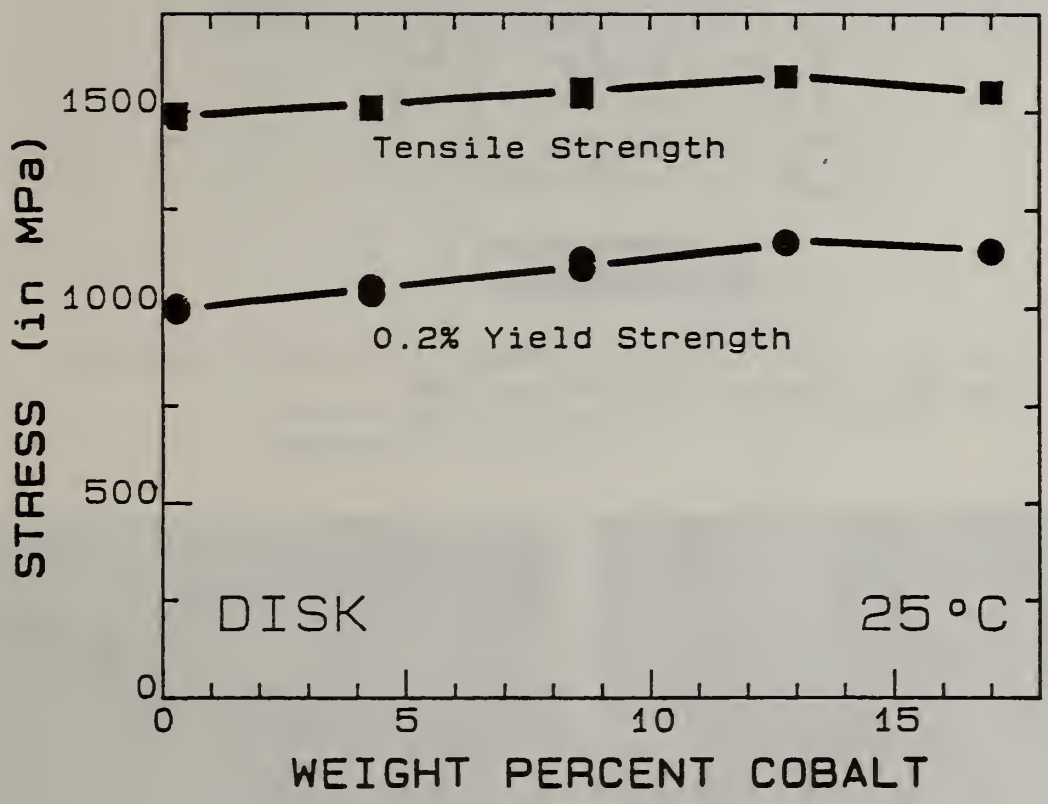

Fig. 5 Room temperature tensile properties of cobalt modified Udimet 700

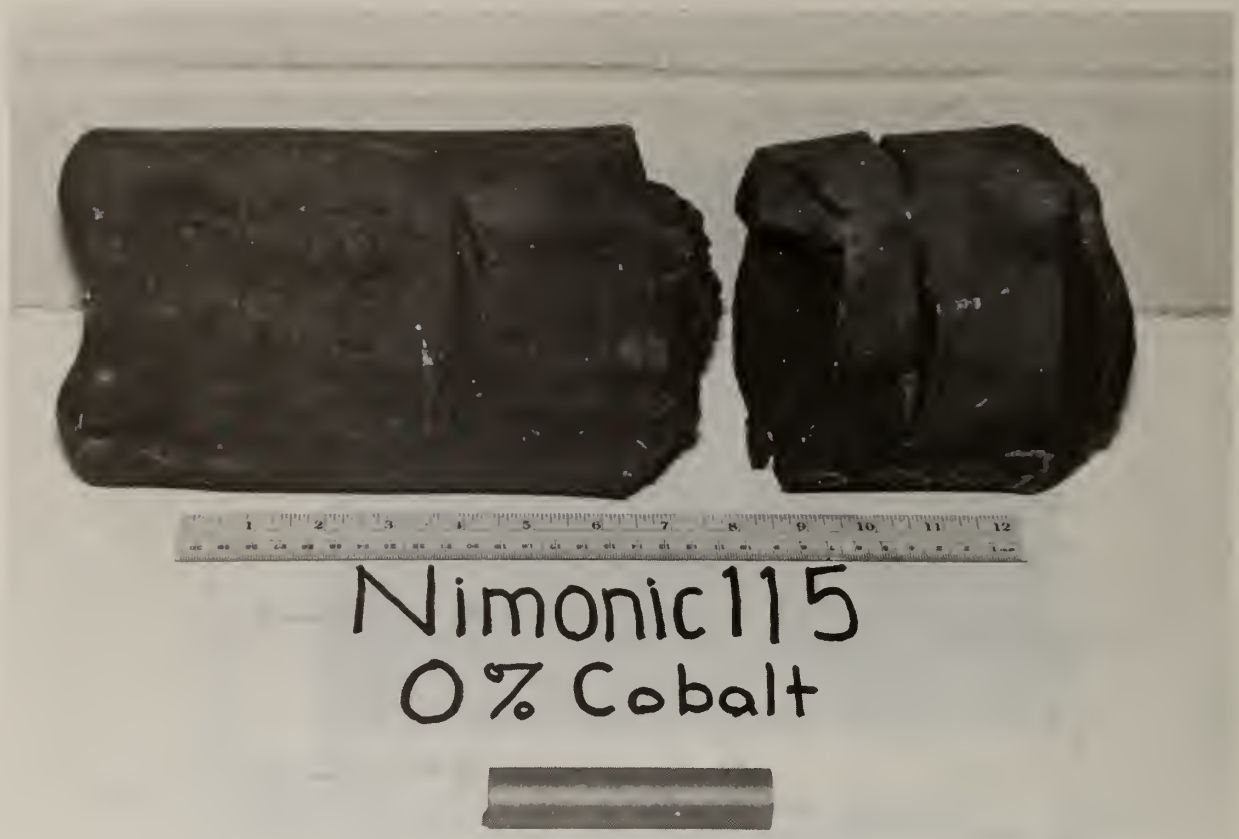

Fig. 6 Failure of low cobalt Nimonic 115 during rolling due to chromium carbide content

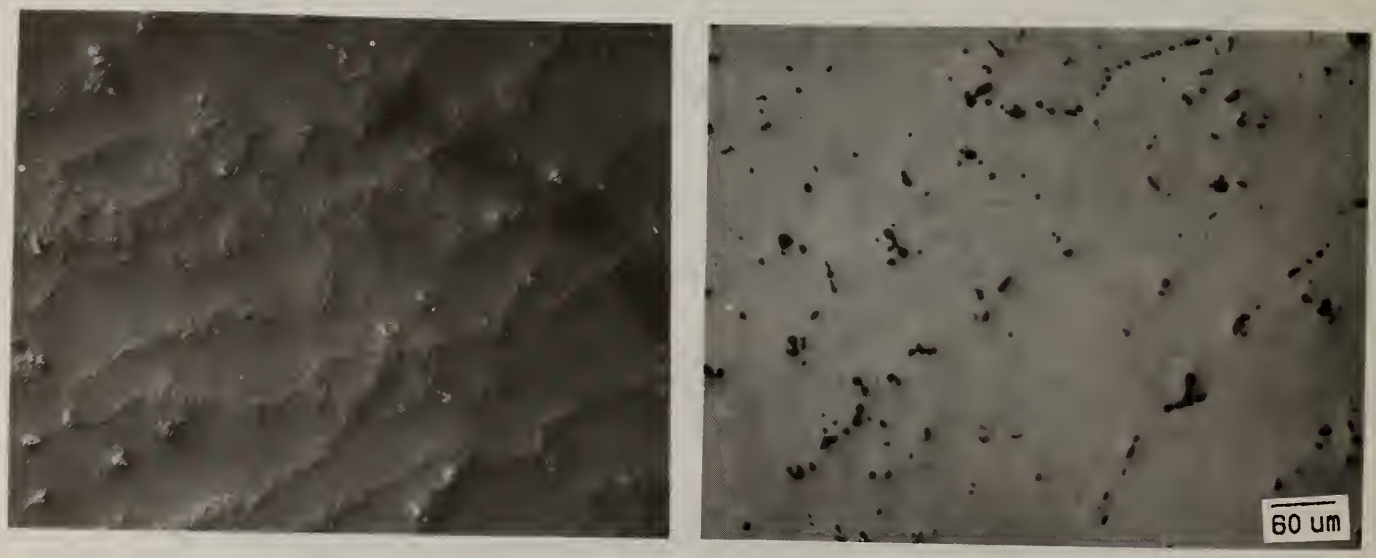

Fig. 7 Carbide microstructure of standard N115 (right) and low cobalt N115 (left). Note the nearly continuous chromium carbides in the cobalt-free alloy.

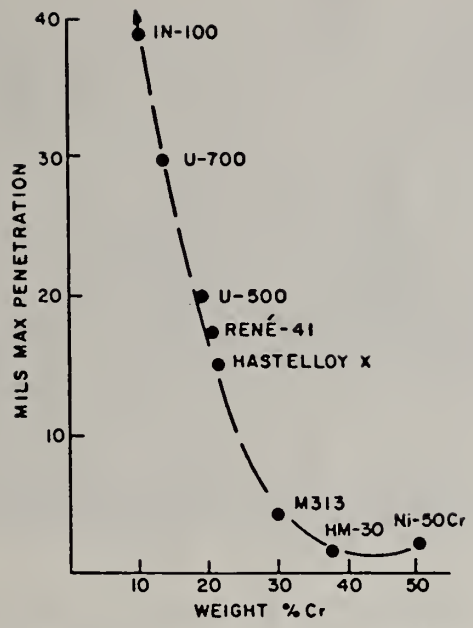

Idcalization of the effect of chromium on the hot-corrosion resistance of nickel-base alloys in burner-rig tests.

ALLOY	CR CONTENT	γ′ FRACTION	CR(IN γ)	CR(IN γ′)
WROUGHT				
WASPALOY	19.5	20.	23.	2.
UDIMET 700	15.0	45.	22.	3.
NIMONIC 115	15.0	50.	24.	4.
CAST				
INCONEL 713C	12.5	50.	23.	3.
IN 100	10.0	65.	22.	3.
MARM 200	9.0	55.	17.	3.

Fig. 8 Phase compositions(9,6) and the effect of chromium on hot corrosion resistance(8). Note the chromium solubility in the the gamma and gamma prime phases of all the alloys as nearly constant. This limit is determined by the sigma phase boundary in the multicomponent phase diagram.

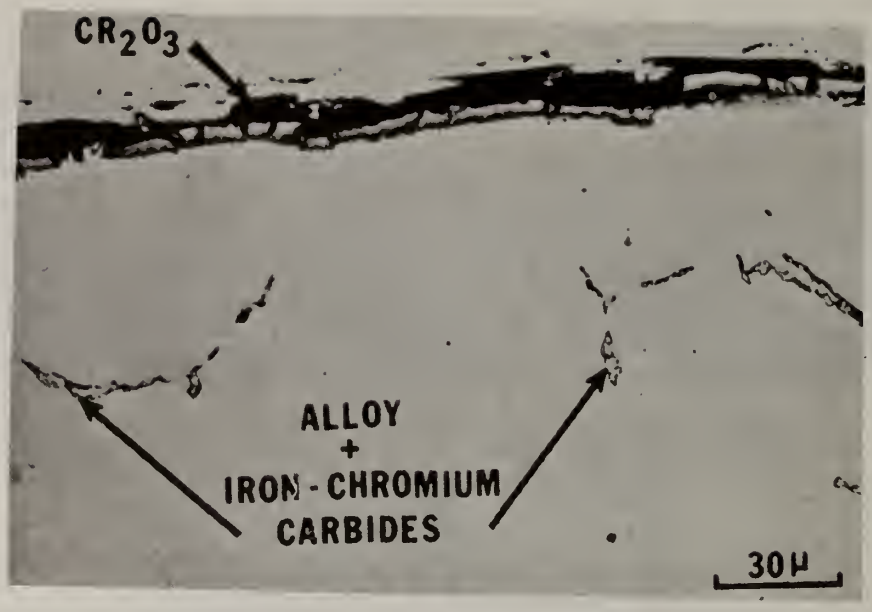

Fig. 9 Iron-chromium alloy with protective chromium oxide layer

Fig. 10 Oxidation of a low chromium alloy

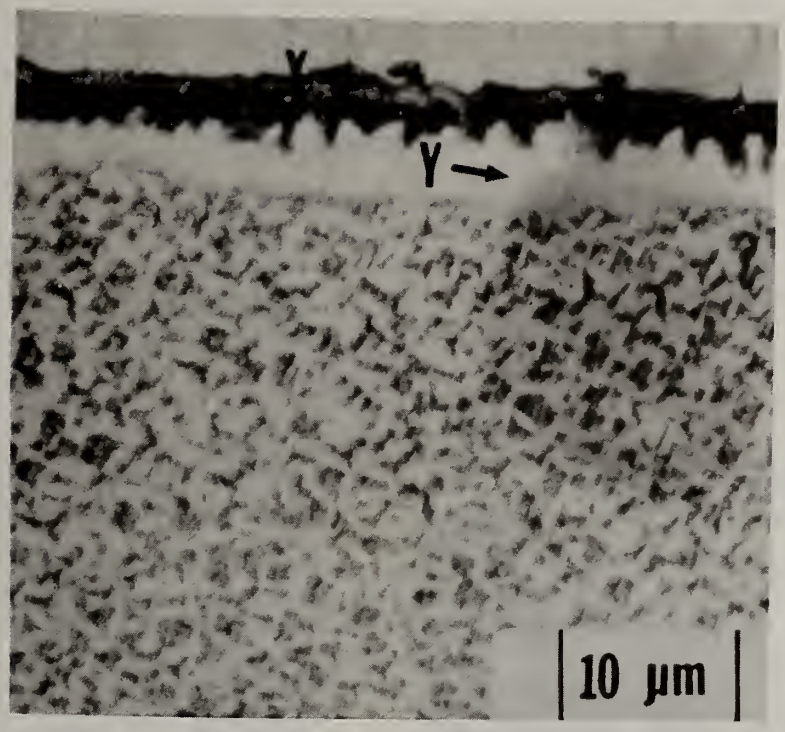

Fig. 11 Formation of a gamma prime denuded zone below the alumium oxide in a nickel-base superalloy

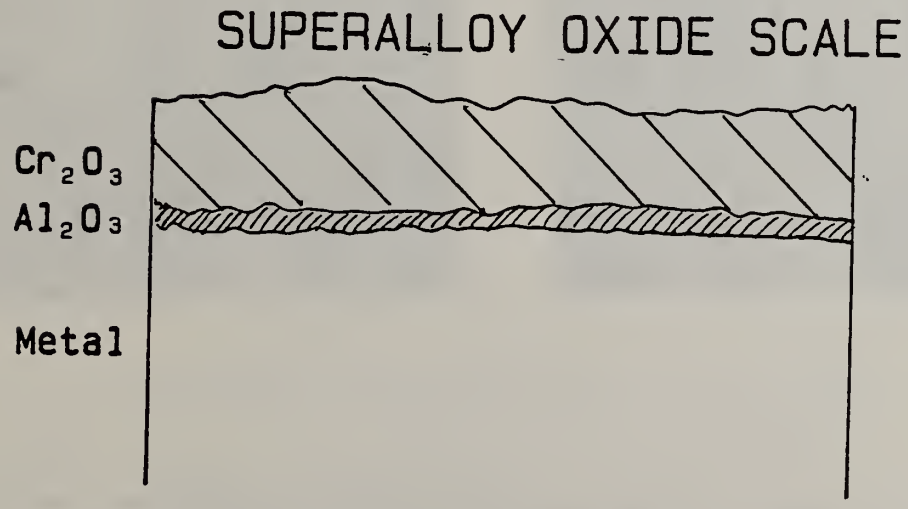

Fig. 12 Superalloy oxide protective scales

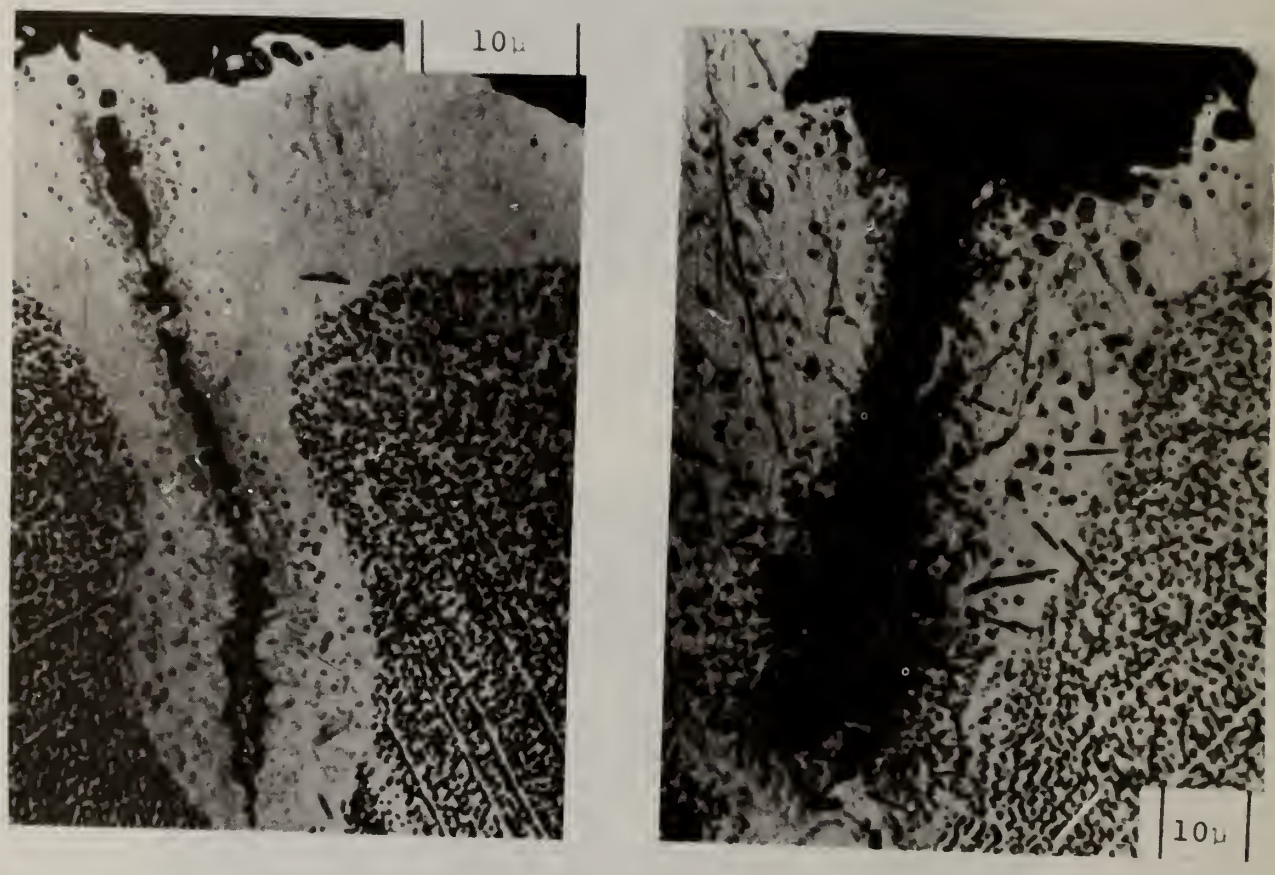

Fig. 13 Preferential grain boundary attack in the hot corrosion of a nickel-base superalloy

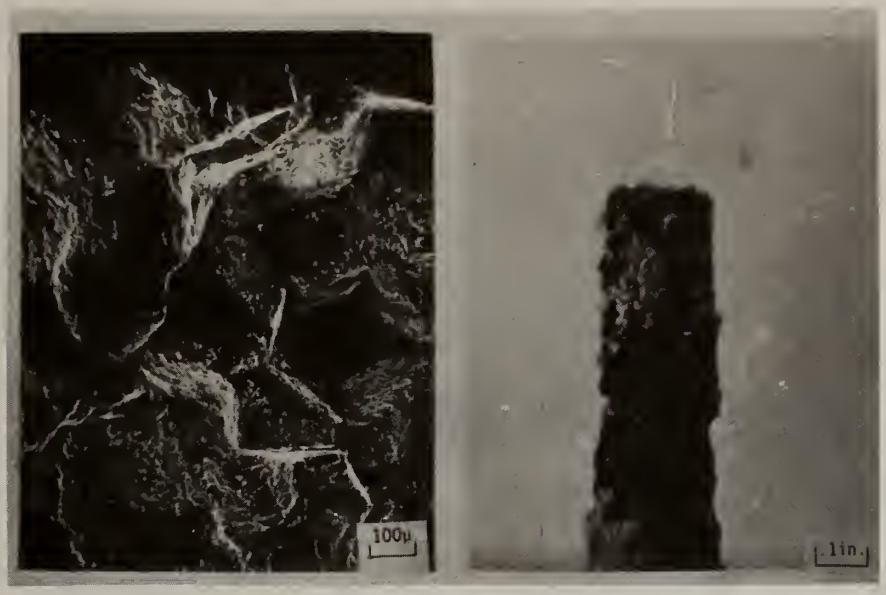

Fig. 14 Intergranular failure of a hot corrosion/ stress rupture specimen

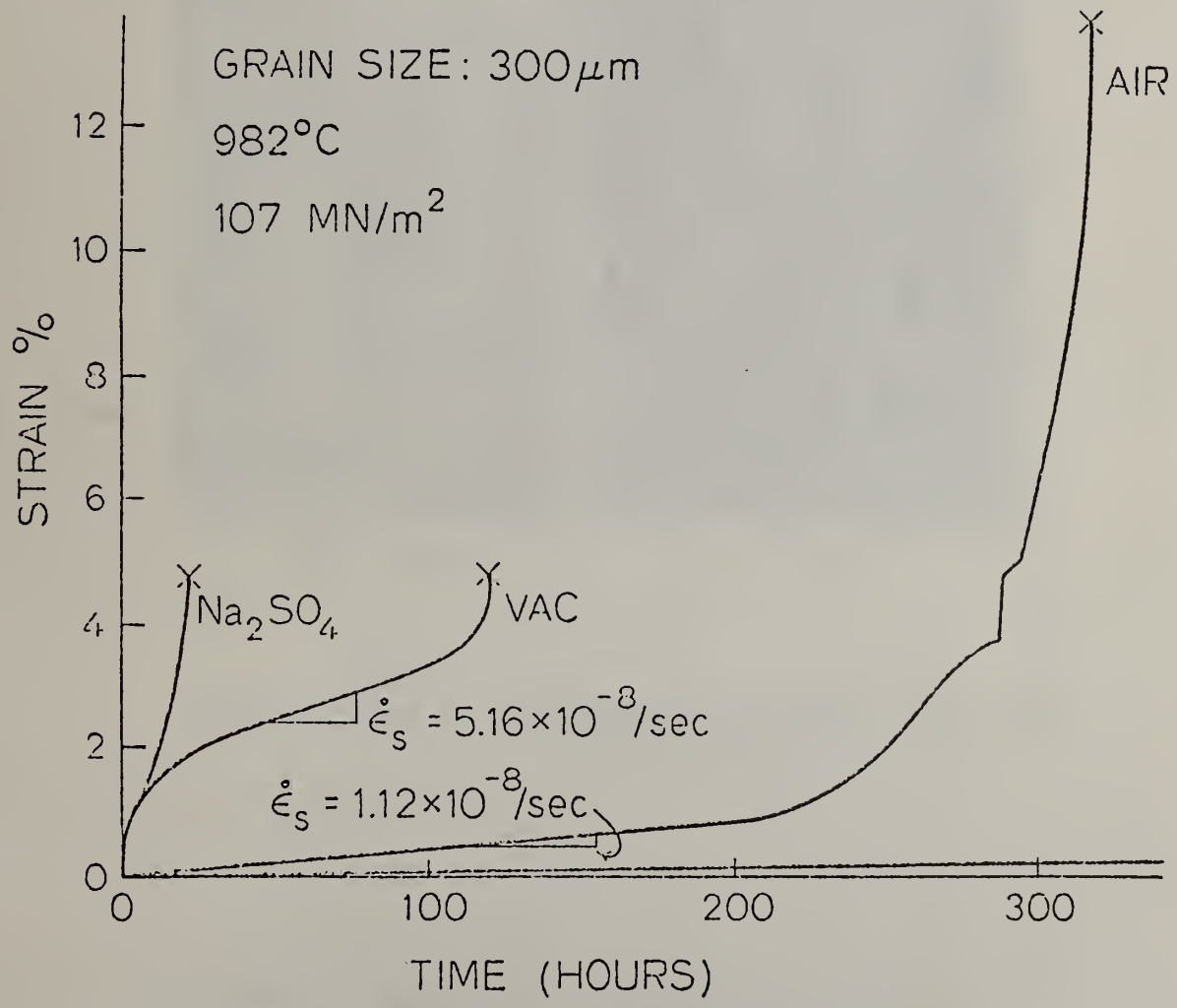

Fig. 15 Corrosion induced premature failure of the above specimen

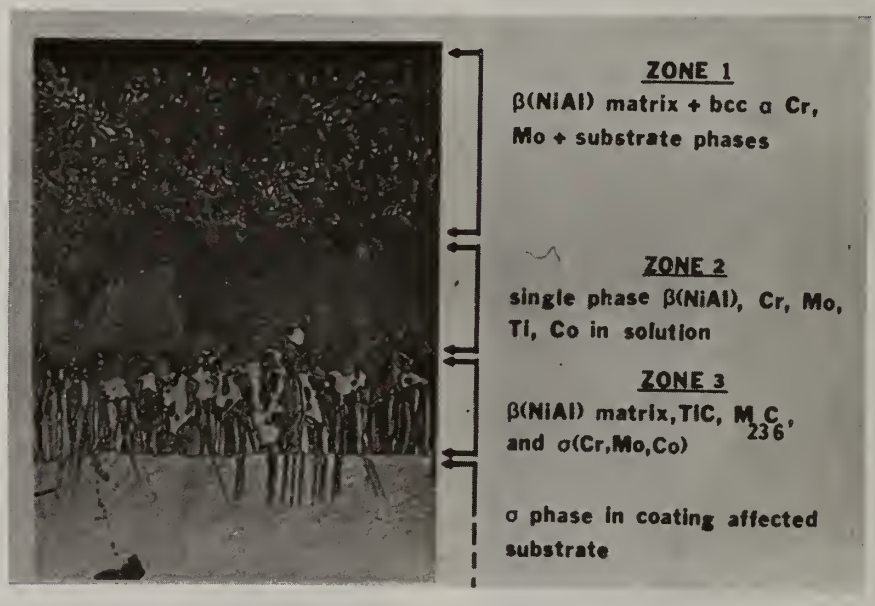

Fig. 16 Diffusion boundaries of a beta phase coated superalloy

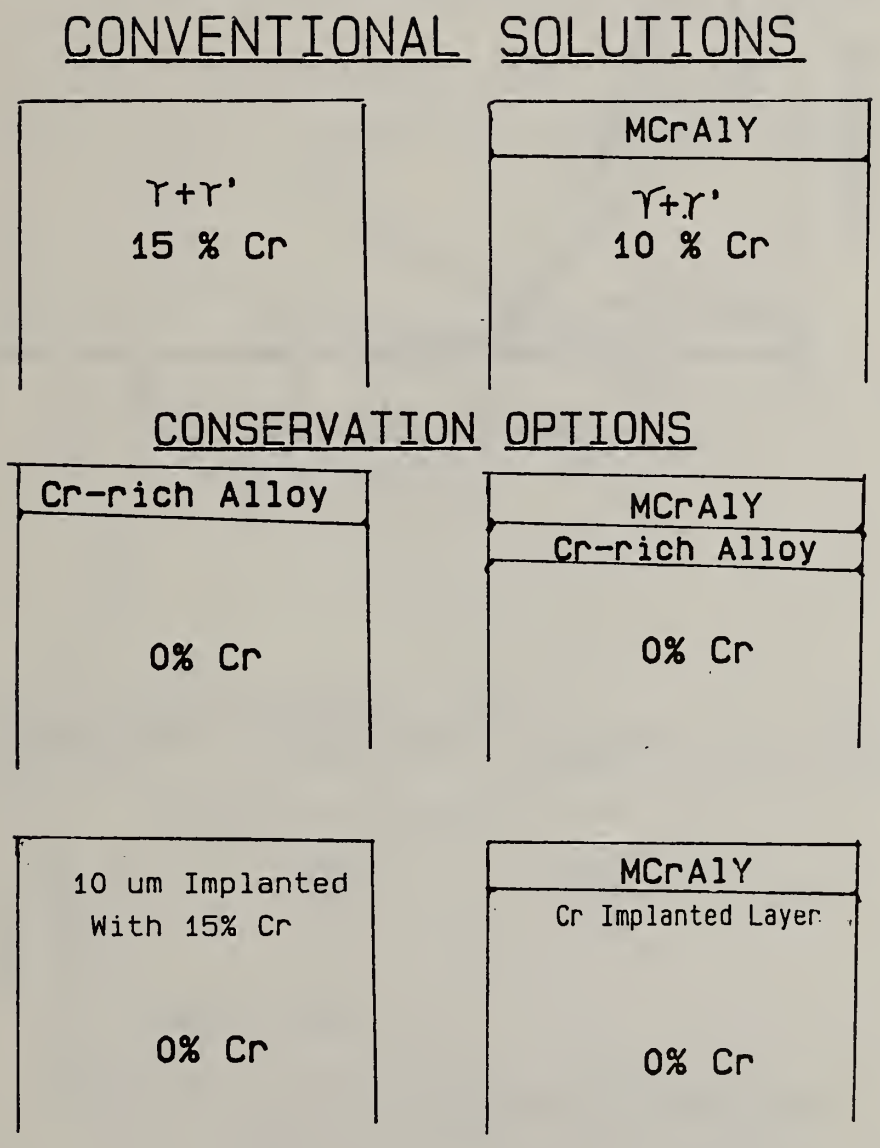

Fig. 17 Methods of providing superalloys with adequate corrosion resistance

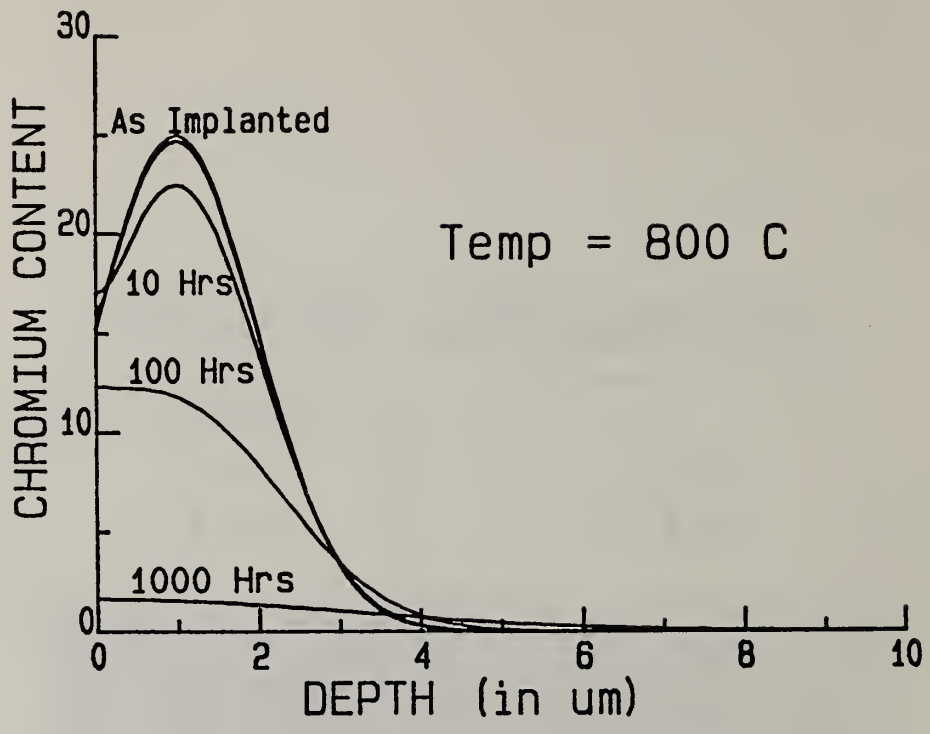

$$c(x,t) = \frac{\Phi_o}{2(2\pi)^{\frac{1}{2}}\delta(1+\tau)^{3/2}} \; EXP[\frac{-\eta}{2(1+\tau)}]ERF\; C[\frac{-\eta-a(1+\tau)}{\sqrt{2}(\tau(1+\tau)^{\frac{1}{2}}}] + EXP[\frac{-(\eta+2a)^2}{2(1+\tau)}]ERF\; C[\frac{\eta+a(1+\tau)}{\sqrt{2}(\tau(1+\tau)}\,^{\frac{1}{2}}]$$

WHERE: $\tau = \frac{2Dt}{\delta 2}$ $\eta = \frac{x-x_o}{\delta}$ $a = \frac{x_o}{\delta}$

Φ_o = total ion dose

AND THE INITIAL PROFILE IS:

$$c(x,o) = \frac{\Phi_o}{2\pi\delta} \exp[-\frac{(x-x_o)^2}{2\delta^2}]$$

Fig. 18 Diffusion profile of a surface alloy in a nickel-base alloy

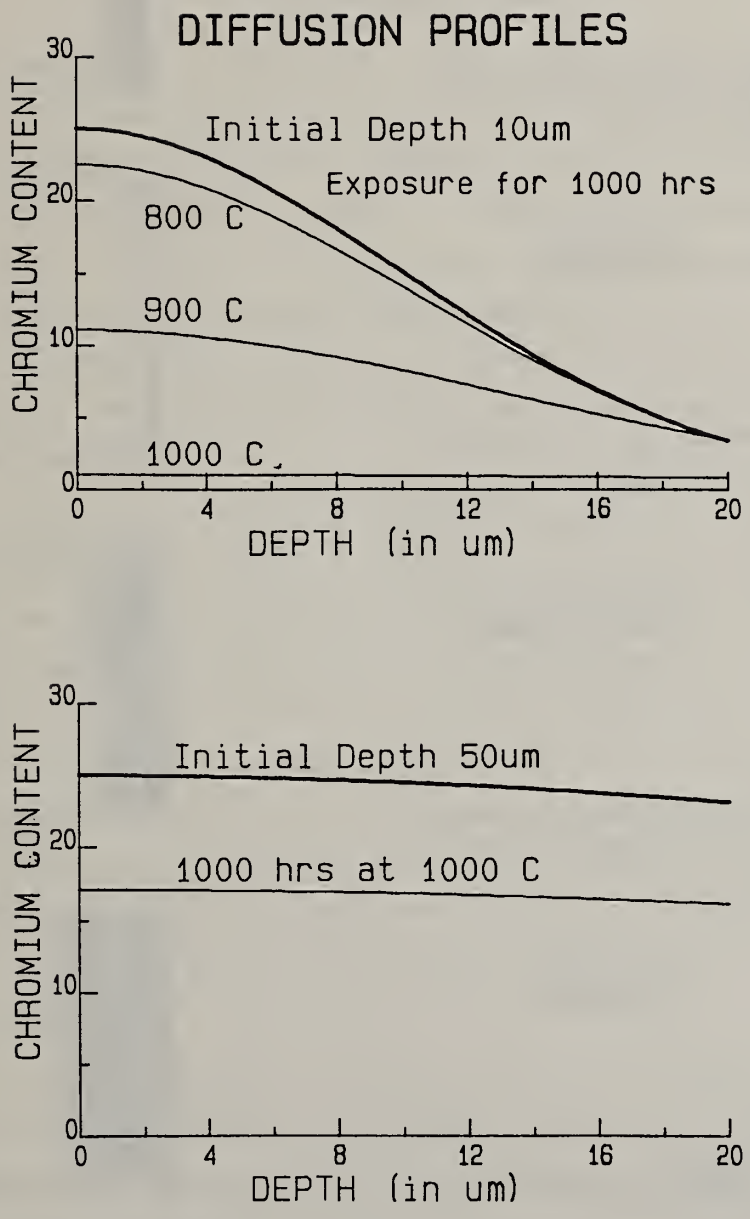

Fig. 19 Required profiles for 800°C and 1000°C exposure

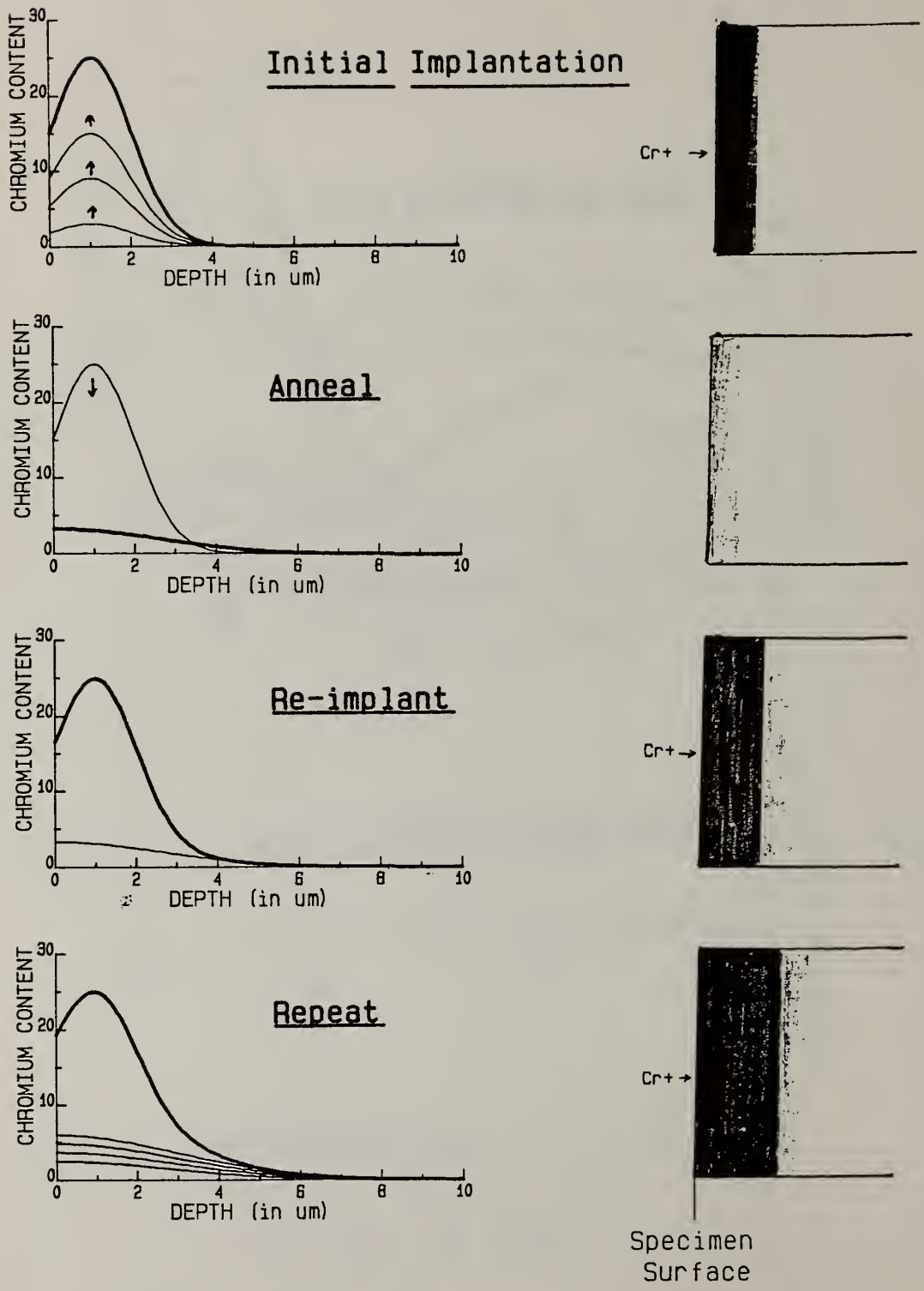

Fig. 20 Multiple implantation approach

DEVELOPMENT OF MODIFIED 9 Cr-1 Mo STEEL[1]

Vinod K. Sikka

Metals and Ceramics Division
Oak Ridge National Laboratory
Oak Ridge, TN 37830

The status of development and commercialization of a modified 9 Cr-1 Mo alloy is presented. The alloy is modified by the addition of 0.06 to 0.10% Nb and 0.18 to 0.25% V. The alloy is recommended for use in the normalized and tempered condition (1038°C for 1 h, air cooled to room temperature; 760°C for 1 h, air cooled to room temperature). Heat treatment, Charpy impact, tensile, and creep properties of the alloy are described in detail along with brief description of other properties.

The modified alloy has creep strength that exceeds that of standard 9 Cr-1 Mo and 2 1/4 Cr-1 Mo steels for the temperature range from 427 to 704°C. The total elongation and reduction of area values for all test temperatures and rupture times up to 22,500 h exceed 15 and 70%, respectively. The estimated design allowable stresses for this alloy are higher than those for standard 9 Cr-1 Mo and 2 1/4 Cr-1 Mo steel. At 550°C and above, these values are twice those of the other alloys. Operating experience on this alloy is being obtained by installing tubes in various steam power plants.

1. Introduction

A 9 Cr-1 Mo steel with properties improved over the 2 1/4 Cr-1 Mo steel and that of other ferritics in the ranges from 9 to 12% Cr and 1 to 2% Mo has been developed recently [1, 2]. The development of this alloy was funded jointly by the U.S. Department of Energy fossil energy

[1]Research sponsored by the Office of Fossil Energy and the Office of Breeder Reactor Technology Project, U.S. Department of Energy, under contract W-7405-eng-26 with Union Carbide Corporation.

and breeder reactor development programs. The purpose of this paper is to describe the status of this development, with special emphasis on the status of approval of this material in the ASTM Specifications and the *ASME Boiler and Pressure Vessel Code*.

2. Chemical Specifications

The composition specifications of modified 9 Cr-1 Mo steel are listed in Table 1 and compared with those of standard 9 Cr-1 Mo steel. The main difference with the modified alloy compared with the standard alloy include

1. addition of niobium and vanadium,
2. a specified range for each element, and
3. a specification for nitrogen, which is not listed for the standard 9 Cr-1 Mo.

Table 1. Chemical analysis of modified 9 Cr-1 Mo steel and its comparison with standard 9 Cr-1 Mo steel

Element	Content range, wt %	
	Modified 9 Cr-1 Mo (Grade 91)	Standard 9 Cr-1 Mo (Grade 9)
Carbon	0.08–0.12	0.15 max
Manganese	0.30–0.60	0.30–0.60
Phosphorus	0.020 max	0.030 max
Sulfur	0.010 max	0.030 max
Silicon	0.20–0.50	1.00 max
Chromium	8.00–9.50	8.00–10.00
Molybdenum	0.85–1.05	0.90–1.10
Nickel	0.40 max	
Vanadium	0.18–0.25	
Niobium	0.06–0.10	
Nitrogen	0.030–0.070	
Aluminum	0.04 max	

Both niobium and vanadium are added to the alloy to improve its elevated-temperature strength properties. Microstructural work has indicated that the improved strength of the modified alloy comes from two factors. First, fine $M_{23}C_6$ precipitate particles nucleate on Nb(C,N), which comes out first during the heat treatment. Second, the vanadium enters $M_{23}C_6$ and retards its growth at the service temperature. The finer distribution of $M_{23}C_6$ adds to strength, and its retarded growth holds the strength for long periods of time at the service temperature.

3. Heat Treatment

The alloy is recommended for use in the normalized and tempered condition. The normalizing treatment consists of heating the alloy to 1040°C, holding for 1 h for material up to 25 mm thick, and then air cooling to room temperature. This treatment produces a fully martensitic structure. The typical hardness in this condition is Rockwell C40. The tempering treatment consists of heating the normalized steel to 760°C, holding for 1 h up to 25-mm thickness, and then air cooling to room temperature. The typical hardness in this condition is Rockwell B95. Optical and transmission electron micrographs of tempered martensite are shown in Figs. 1 and 2. Figure 1 shows that the alloy is single phase

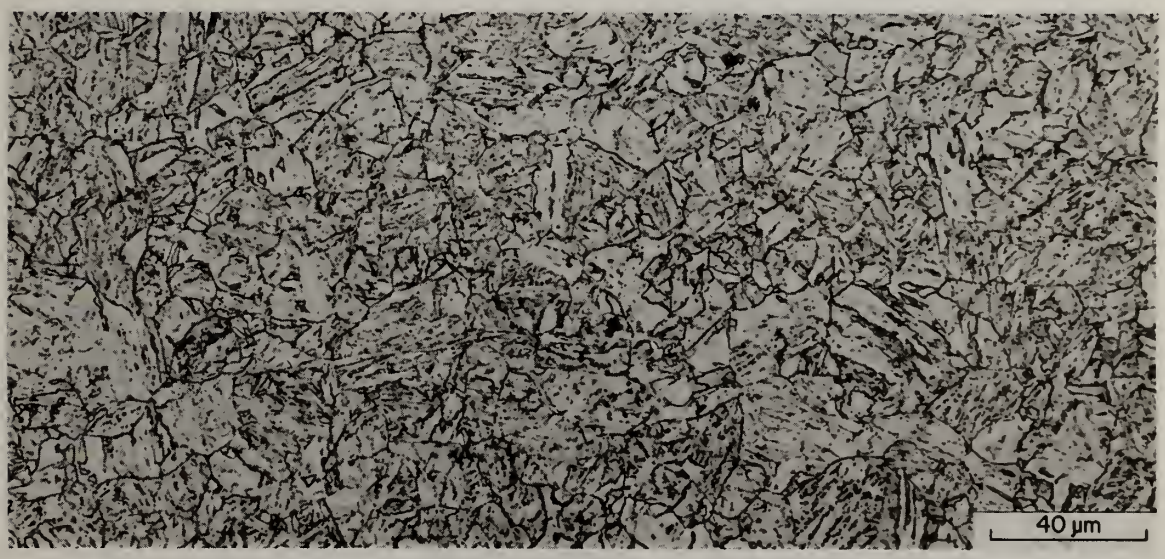

Figure 1. Typical microstructure of modified 9 Cr-1 Mo steel after the nominal normalizing and tempering treatment (1040°C for 1 h, 760°C for 1 h). Note that the grain size is very fine.

Figure 2. Transmission electron micrograph of a specimen normalized at 1040°C for 1 h and tempered at 760°C for 1 h. The micrograph shows that tempered martensite consists of dislocation substructure and carbides ($M_{23}C_6$ and MC) on both the grain and subgrain boundaries.

(free from δ-ferrite) and has a fine grain size (ASTM 8–9). The transmission electron micrograph shows that the tempered microstructure has high-dislocation-density subboundaries in the matrix. The subboundaries are stabilized by the precipitation of carbides on them. Carbides also precipitate at the prior austenite grain boundaries.

The tempering response of the alloy can be described by the Hollomon-Jaffe (HJ) tempering parameter. This parameter is given by

$$HJ = T(C + \log t) , \qquad (1)$$

where

T = temperature in kelvins,

t = time in hours,

C = HJ constant.

The optimized value of C for two commercial heats (30176 and 30394) characterized to date was determined to be 22.3.

The correlation of tempering parameter with hardness, Charpy V-notch energy, 0.2% yield strength, and total elongation at room temperature is shown in Fig. 3. The 0.2% yield and ultimate tensile strengths are well correlated with room-temperature hardness (Fig. 4). Such correlations are useful when the material has to meet both the tensile property and hardness criteria.

The grain coarsening response of the alloy was examined as a function of the normalizing temperature and time (Fig. 5). Grain coarsening of the modified alloy occurred only when the normalizing temperature was increased about 100°C or more above the specified normalizing temperature of 1040°C. Even in the coarsened condition, the grain size for the modified alloy remained near ASTM No. 5.

4. Commercial Melting and Fabrication

Eight heats of this alloy have been melted by commercial vendors (Table 2). Many vendors have fabricated this alloy (Table 3). The overall consensus is that melting and fabrication of this alloy presents no technical problems, although costs will obviously vary depending upon the melting and fabrication process selected.

5. Mechanical Properties

The main emphasis on the mechanical properties of modified alloy was limited to Charpy-impact, tensile, and creep testing. Each of these properties is described here briefly.

5.1 Charpy-Impact Properties

The curves of Charpy V-notch impact energy versus test temperature for two commercial heats of modified 9 Cr-1 Mo steel are compared with a heat of standard 9 Cr-1 Mo steel in Fig. 6. All tests were conducted on

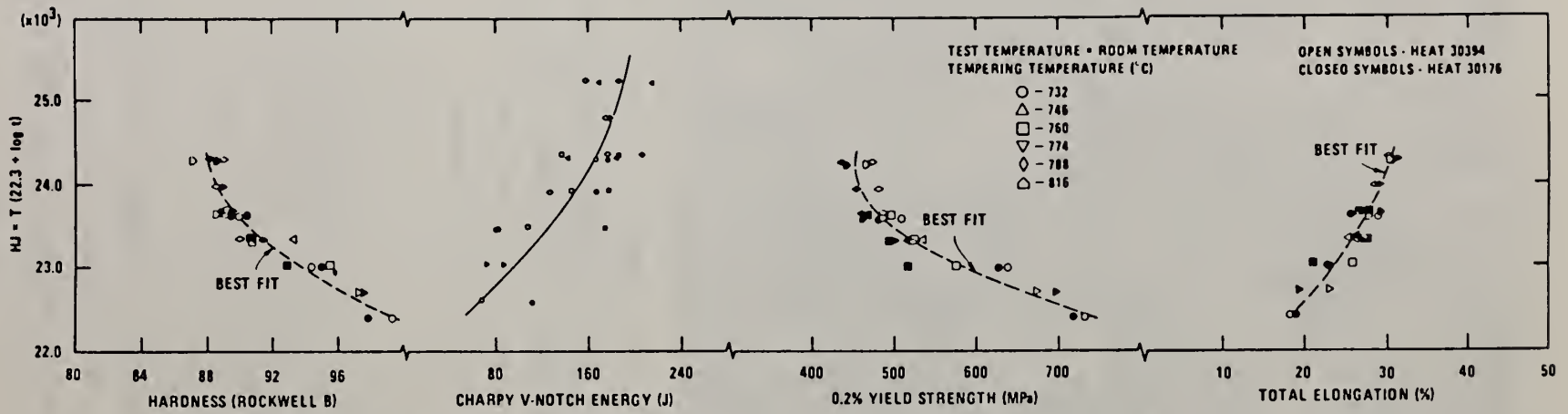

Figure 3. Tempering parameter as a function of hardness, Charpy energy, 0.2% yield strength, and total elongation at room temperature.

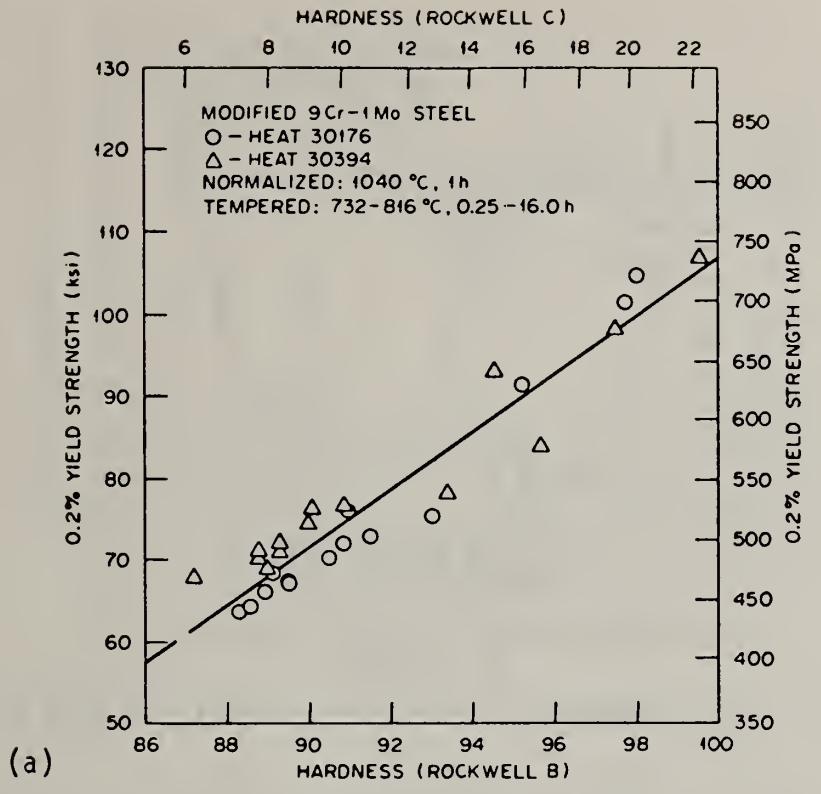

(a)

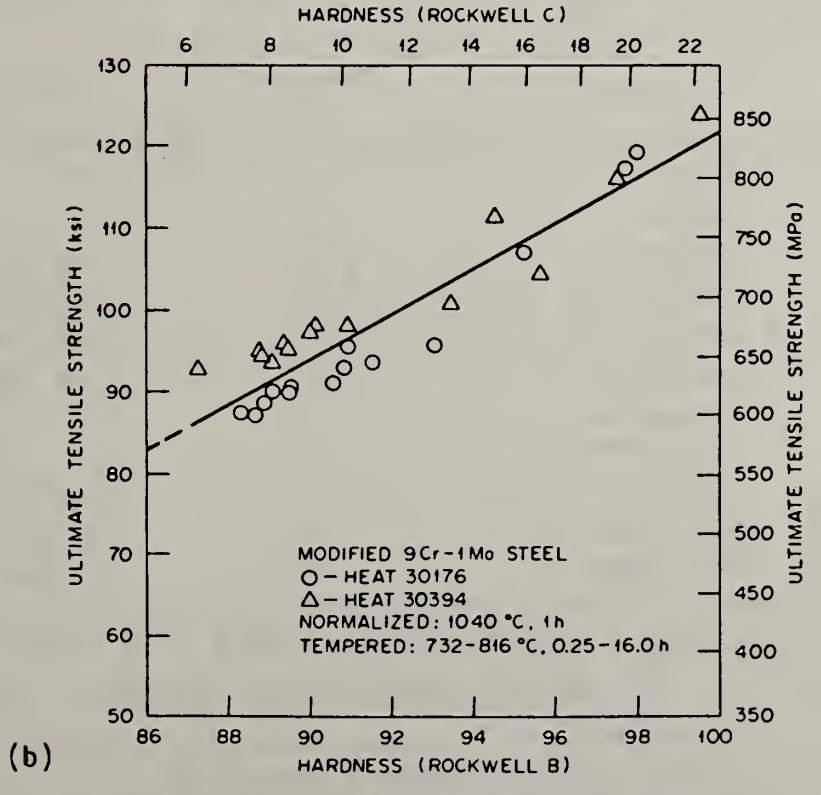

(b)

Figure 4. Room-temperature strength versus hardness for two commercial heats of modified 9 Cr-1 Mo steel. (a) Yield. (b) Ultimate.

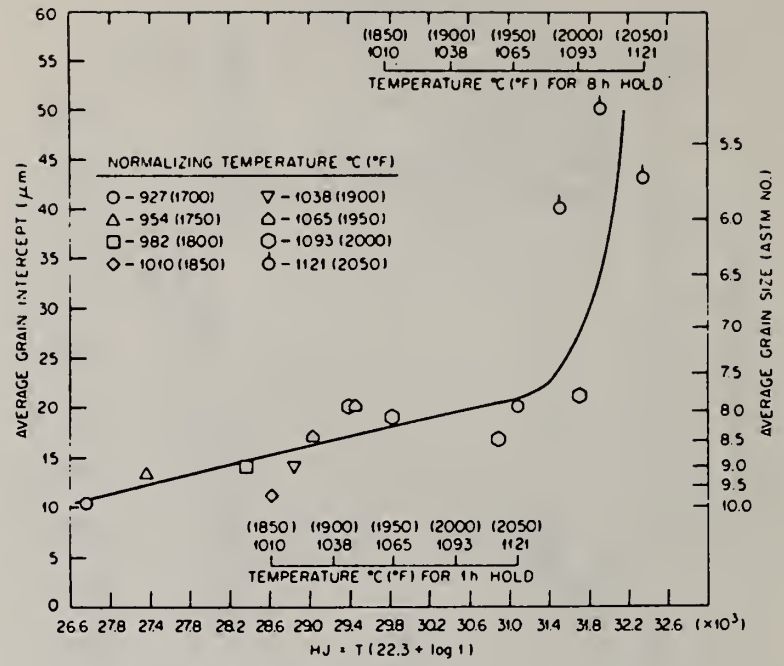

Figure 5. Grain coarsening behavior of modified 9 Cr-1 Mo steel.

Table 2. List of commercial heats melted on modified 9 Cr-1 Mo steel

Heat	Melter	Heat size (tons)	Melting practice[a]
F5349	Quaker	4	AOD
30383	CarTech	15	AOD
30394[b]	CarTech	15	AOD/ESR
30176[c]	CarTech	15	AOD/ESR
30182[c]	CarTech	15	AOD/ESR
10148[d]	Electralloy	15	AOD and AOD/ESR
XA3602	Combustion Engineering	0.5	Air induction
91887	CarTech	2.5	Electric/ESR
YYC982C	Sumitomo, Japan	2.0	Vacuum induction
59020	NKK, Japan	5.0	Vacuum induction

[a]AOD = argon-oxygen decarburization. ESR = electroslag remelting.

[b]Heat 30394 is half of heat 30383 and was electroslag remelted.

[c]Heats 30176 and 30182 are the same heat. Their numbers are different because CarTech identifies ingots separately.

[d]Heat 10148 was melted by AOD process. Half this heat was subsequently electroslag remelted.

Table 3. Summary of information on fabrication of commercial heats of modified 9 Cr-1 Mo alloy

Heat	Melter	Melting practice[a]	Product	Product size, mm		Fabrication method	Fabricator
				OD	Thickness		
F5349	Quaker	AOD	Plate		16	Hot forged, hot rolled	ORNL, Y-12
30383	CarTech	AOD	Plate		51	Hot forged, hot rolled	Jessop
30383	CarTech	AOD	Bar	95		Hot forged, hot rolled	CarTech
30383	CarTech	AOD	Tube	102	15	Hot extruded	Amax
30394	CarTech	AOD-ESR	Plate		25	Hot forged, hot rolled	Jessop
30394	CarTech	AOD-ESR	Bar	232		Hot forged	CarTech
30394	CarTech	AOD-ESR	Tube	102	15	Hot extruded	Amax
30394	CarTech	AOD-ESR	Tube	76	13	Hot rotary pierced	Timken
30182	CarTech	AOD-ESR	Plate		16	Hot forged, hot rolled	CE
30182	CarTech	AOD-ESR	Bar	232		Hot forged	CarTech
30182	CarTech	AOD-ESR	Tube	102	15	Hot extruded	Amax
30182	CarTech	AOD-ESR	Tube	76	13	Hot rotary pierced	Timken
30176	CarTech	AOD-ESR	Plate		25	Hot forged, hot rolled	Jessop
10148	Electralloy	AOD	Plate		16	Hot forged, tempered, cold rolled	ORNL
10148	Electralloy	AOD	Bar	44		Hot extruded	ORNL
10148	Electralloy	AOD	Bar	107		Hot rolled	Bethlehem
10148	Electralloy	AOD	Pipe	245	25	Hot pilgered	Phoenix

Table 3. (Continued)

Heat	Melter	Melting practice[a]	Product	Product size, mm		Fabrication method	Fabricator
				OD	Thickness		
10148	Electralloy/ Universal Cyclops	AOD-ESR	Plate	203		Hot rolled	Universal Cyclops
10148	Electralloy/ Universal Cyclops	AOD-ESR	Plate	51		Hot rolled	Universal Cyclops
10148	Electralloy/ Universal Cyclops	AOD-ESR	Octagon box	200		Hot forged	Universal Cyclops
10148	Electralloy/ Universal Cyclops	AOD-ESR	Round	232		Hot forged	Universal Cyclops
10148	Electralloy/ Universal Cyclops	AOD-ESR	Tube	54	9.45	Hot extruded, cold reduced	TI Stainless (UK)
XA3602	Combustion Engineering	Air induction	Tube	51	8.03	Centrifugally cast and cold pilgered	CE
YYC982C	Sumitomo	VIM	Tube	76	13	Hot extruded, cold drawn	Sumitomo
YYC982C	Sumitomo	VIM	Tube	51	6.4	Hot extruded, cold drawn	Sumitomo
59020	NKK	VIM	Plate		25	Hot forged, hot rolled	NKK
59020	NKK	VIM	Tube	76	13	Hot extruded, cold drawn	NKK
59020	NKK	VIM	Tube	51	6.4	Hot extruded, cold drawn	NKK

[a]AOD = argon-oxygen decarburization, ESR = electroslag remelting, VIM = vacuum induction melting.

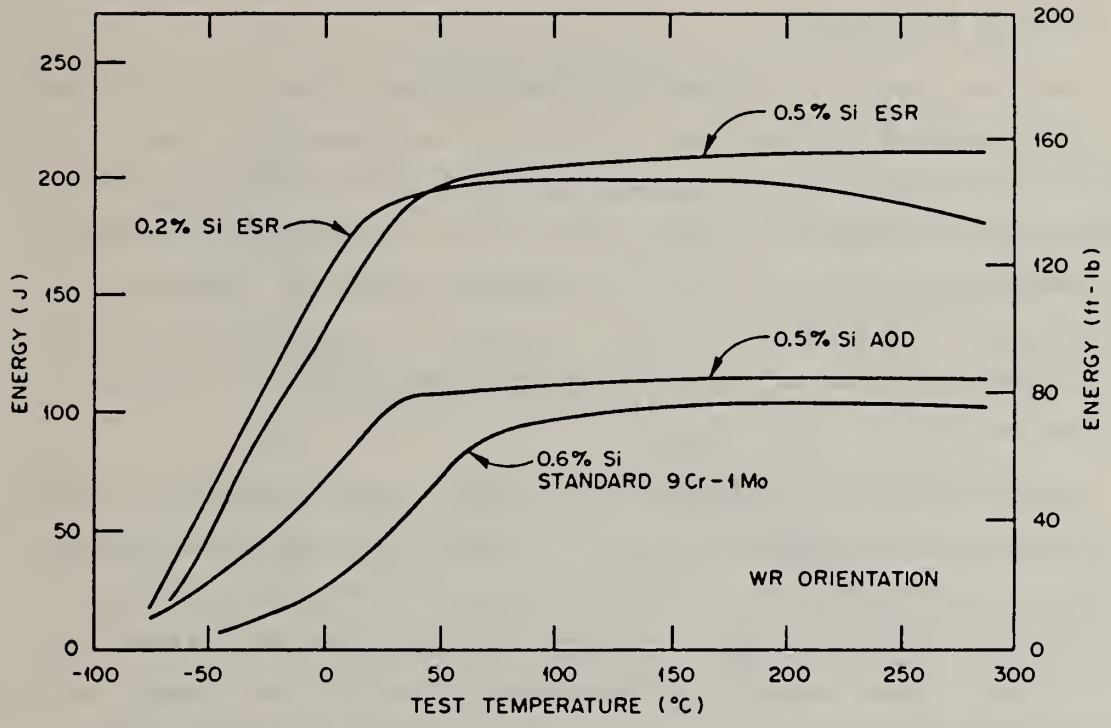

Figure 6. Effect of melting process on the Charpy V-notch toughness from two 14-Mg (15-ton) commercial ESR heats of modified 9 Cr-1 Mo steel and one standard 9 Cr-1 Mo steel plate.

specimens with the V-notch parallel to the rolling direction. The standard 9 Cr-1 Mo heat was electric furnace melted. One modified 9 Cr-1 Mo steel heat was melted by both the AOD (argon-oxygen decarburization) and AOD-ESR combination. All the second heat of modified 9 Cr-1 Mo was melted by the AOD-ESR process. Data in this figure show that the 68 J (50 ft-lb) ductile-to-brittle transition temperatures for both heats of modified 9 Cr-1 Mo are lower than that for the standard 9 Cr-1 Mo heat. The upper-shelf energies for the AOD-ESR-melted modified 9 Cr-1 Mo heats are much higher than those for either AOD-melted modified 9 Cr-1 Mo steel or electric-furnace-melted standard 9 Cr-1 Mo steel. This figure also shows that Charpy properties are affected by both the silicon content and the melting practice [3]. The lower silicon content or electroslag remelting of the material produces lower transition temperatures and higher upper-shelf energies. However, between the two factors, melting practice appears to have a much more potent effect than silicon content.

5.2 Tensile Properties

Tensile properties of commercial heats of modified 9 Cr-1 Mo steel have been measured for test temperatures in the range from room temperature to 760°C. Data include the effects of melting practice, compositional differences, strain rate (8.0 to 0.00008/min), postweld heat treatment (1—112 h at 732°C), isothermal annealing treatment (1038°C for 1 h, fast cool to 704°C, and hold for 14 h, followed by air cooling), and thermal aging treatment (5000 and 11,600 h at 538, 593, and 649°C).

Typical plots of 0.2% yield and ultimate tensile strengths against test temperature are shown in Fig. 7. Similar plots for total elongation and reduction of area are shown in Fig. 8. These plots combine data on plate, tube, and bar. All tests were at a nominal strain rate of 0.004/min. Room-temperature data on individual product forms were used to determine the average values, the standard deviation in the room-temperature data, and the recommended minimum properties for use in ASTM specifications. These values are listed in Table 4, and the recommended minimum values are the same for all three products. The best fit average and minimum curves based on the room-temperature specified minimum properties (see Table 4) are also included in Figs. 7 and 8. These plots show that the minimum specified properties at room temperature are conservative enough to include data on all commercial heats through test temperatures of 760°C.

Tensile data anlysis also showed the following features.

1. Melting practice, AOD versus AOD-ESR, had no effect on tensile properties for test temperatures up to 760°C. This is different from impact properties, which were far superior for AOD-ESR-melted material to those for AOD-melted material.

2. The tensile properties of modified 9 Cr-1 Mo steel are sensitive to strain rate at room temperature and three higher test temperatures: 427, 538, and 649°C. The yield and ultimate tensile strengths decrease some with decreasing strain rate at room temperature. This

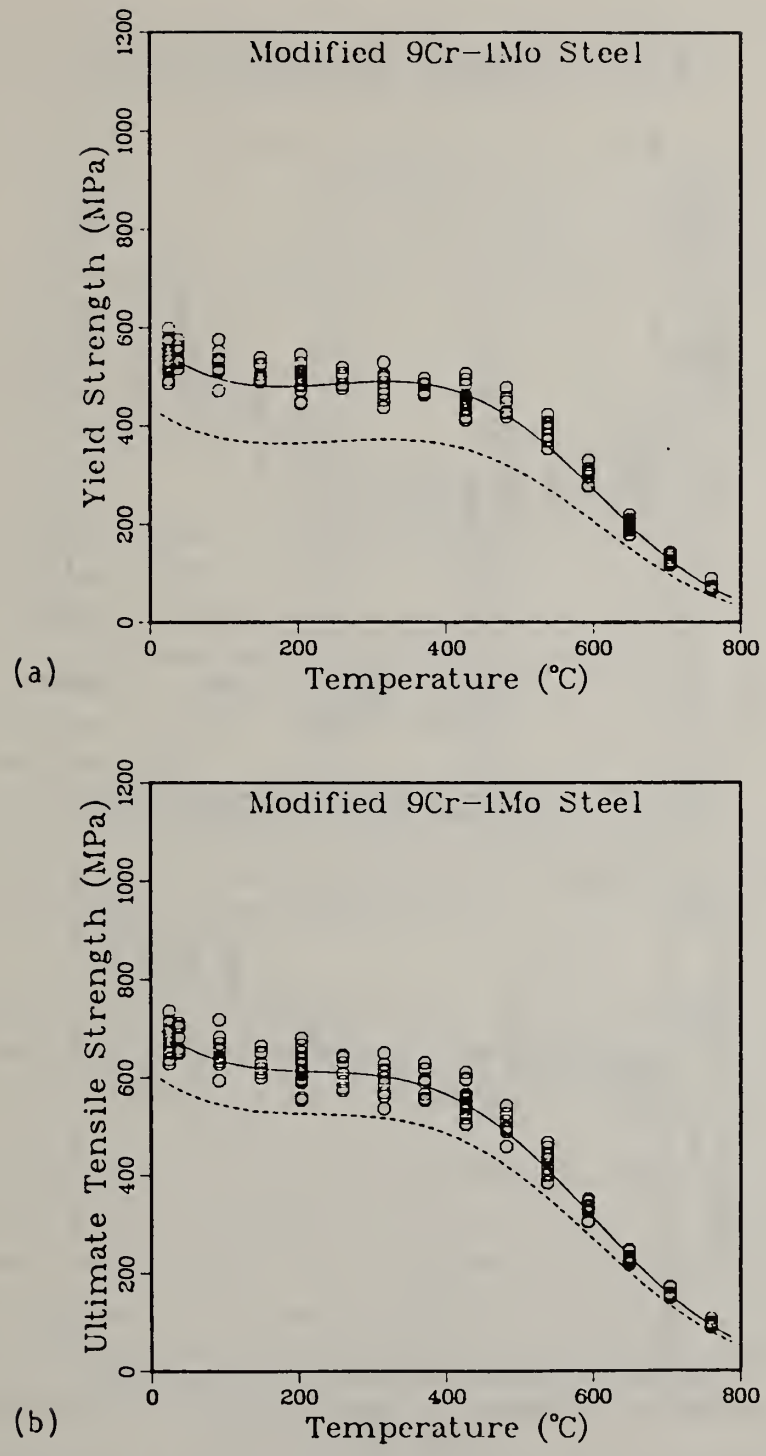

Figure 7. Plots of (a) 0.2% offset yield strength and (b) ultimate tensile strength as functions of test temperature for plate, bar, and tube of commercial heats of modified 9 Cr-1 Mo steel. The best fit average and minimum curves based on room-temperature specified minimum yield and ultimate tensile strength of 414 and 586 MPa are included also in these figures.

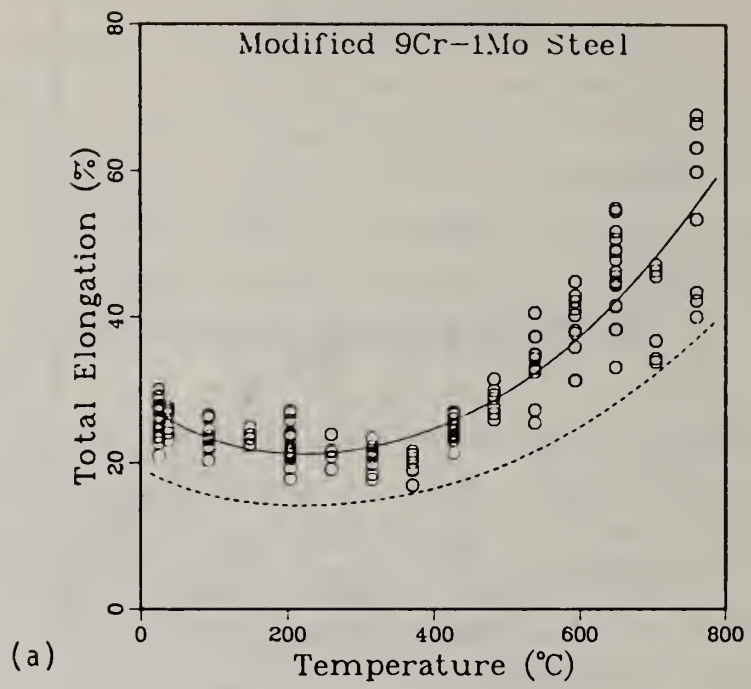

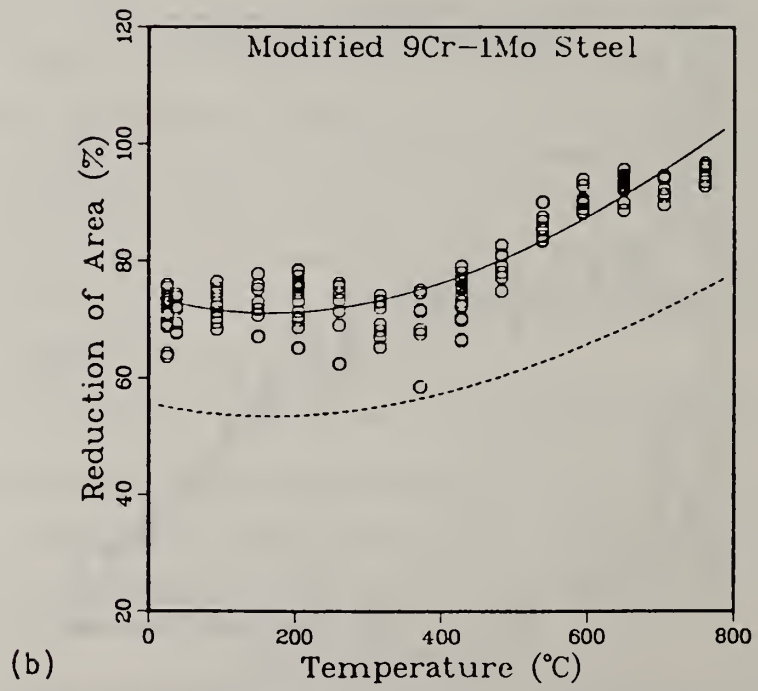

Figure 8. Plots of (a) total elongation and (b) reduction of area as functions of test temperature for plate, bar, and tube of commercial heats of modified 9 Cr-1 Mo steel. The best fit average and minimum curves based on the room-temperature specified minimum total elongation and reduction of area of 18 and 55% are included also in these figures.

Table 4. Minimum tensile properties at room temperature specified for various products of modified 9 Cr-1 Mo steel tested in the normalized and tempered condition[a]

Product	Calculation	Strength, MPa		Total elongation (%)	Reduction of area (%)
		0.2%	Ultimate		
Plate	Average	545	683	24.7	69.8
	Average — 2SD	496	634	20.6	61.6
	Average — 3SD	476	607	18.5	57.5
	Recommended min	414	586	18	55
Tube	Average	524	669	27	74
	Average — 2SD	483	627	23	71
	Average — 3SD	462	607	21	70
	Recommended min	414	586	18	55
Bar	Average	531	676	28	73
	Average — 2SD	469	614	26	70
	Average — 3SD	434	586	25.5	68
	Recommended min	414	586	18	55

[a]At 1038°C for 1 h, air cooled to room temperature, and at 760°C for 1 h, air cooled to room temperature.

occurs without any change in ductility. At 427 and 538°C strength decreases and ductility increases with decreasing strain rate. At 649°C, strength decreases with some decrease in ductility.

3. A decrease of 14 to 28°C in tempering temperature from 760°C substantially increased yield and ultimate tensile strengths for test temperatures through 427°C. At a test temperature of 649°C the increase in strength was relatively small. Ductility was only slightly affected by this drop in tempering temperature. Changes in hardness and Charpy-impact energy as a result of change in tempering temperature are shown in Fig. 3.

4. Tensile tests were conducted at room temperature and at the aging temperature on a single heat (F5349) aged for 5000 and 11,600 h at 538, 593, and 649°C. Only small changes were observed in properties as a result of this treatment.

5.3 Creep Data

A substantial number of creep tests on the commercial heats of modified 9 Cr-1 Mo steel are either ruptured or in progress. These tests are being run at 427, 454, 482, 538, 593, 649, 677, and 704°C. Creep rupture data at 593°C on commercial heats of modified 9 Cr-1 Mo steel are plotted in Fig. 9. Data in this figure are compared with the average curves for the modified 9 Cr-1 Mo, standard British 9 Cr-1 Mo, standard American 9 Cr-1 Mo and 2 1/4 Cr-1 Mo. The modified and standard British 9 Cr-1 Mo steels are both tested in the normalized and tempered condition. The standard American 9 Cr-1 Mo and 2 1/4 Cr-1 Mo steels were tested in the annealed condition. The following observations are derived from Fig. 9.

1. The modified 9 Cr-1 Mo steel is significantly stronger than standard 9 Cr-1 Mo and 2 1/4 Cr-1 Mo. The strength difference becomes even more important for rupture times exceeding 1000 h.

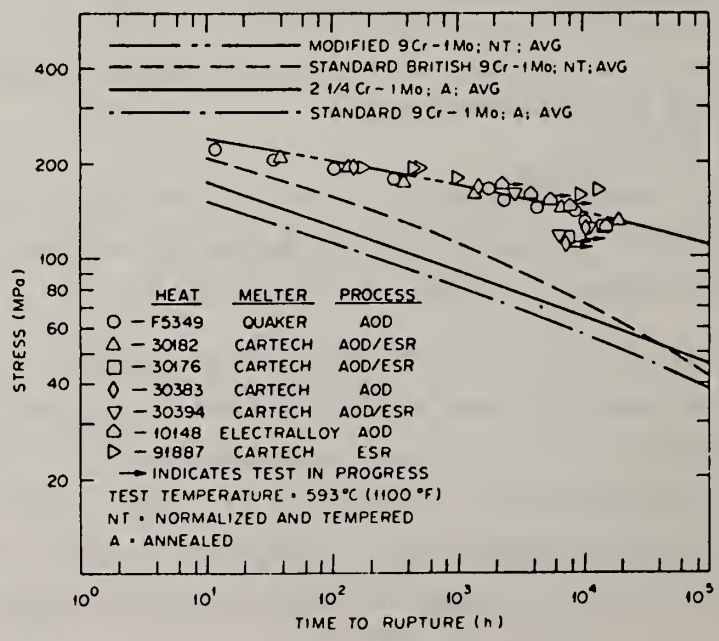

Figure 9. Stress-rupture plot at 593°C comparing data on commercial heats of modified 9 Cr-1 Mo steel (tested in normalized and tempered condition) with the average curves for the standard British 9 Cr-1 Mo steel tested in the normalized and tempered condition and standard American 9 Cr-1 Mo steel and 2 1/4 Cr-1 Mo steel tested in the annealed condition.

2. Changing the heat treatment condition from annealed to normalized and tempered improves the creep-rupture strength only a small amount. However, for the same heat treatment (normalizing and tempering) the composition modification made in our alloy produced a very large improvement in creep-rupture strength.

Figure 9 compares rupture strength only at 593°C. The 10^5-h creep-rupture strength at a range of temperatures (427—732°C) is compared for various alloys in Fig. 10. This figure also includes the curve for 2 1/4 Cr-1 Mo steel tested in the normalized and tempered condition. This figure shows again that the modified 9 Cr-1 Mo alloy is stronger than standard 9 Cr-1 Mo and 2 1/4 Cr-1 Mo steel for the entire temperature range. The strength differences become more significant for temperatures exceeding 500°C.

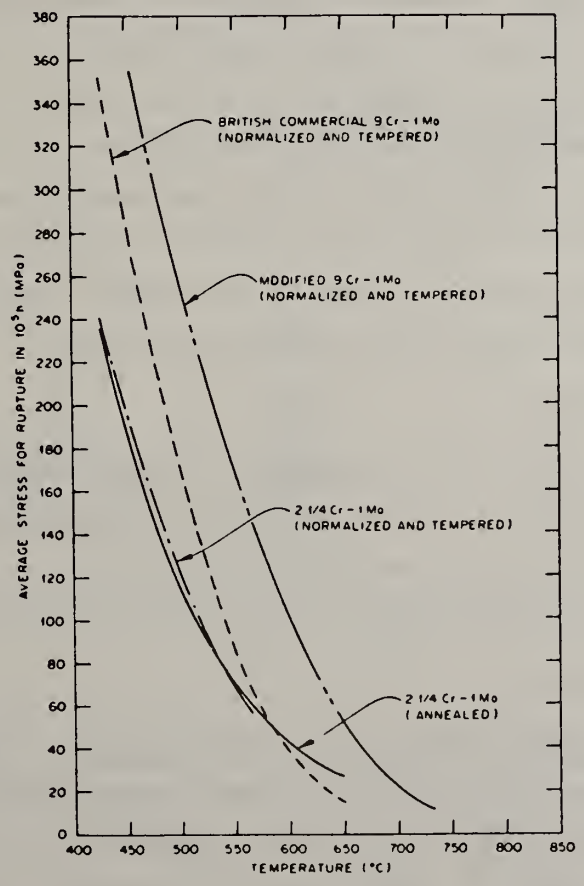

Figure 10. Variation of 10^5-h creep rupture strength with temperature for several materials.

When the creep strength of an alloy is increased, one is concerned with the associated loss in ductility. The total elongation and reduction of area for creep tests ruptured thus far on the commercial heats of modified 9 Cr-1 Mo steel are plotted in Fig. 11. The total elongation for most heats exceed 15%, and the reduction of area exceeds 70%. Furthermore, these data show no indication of drop in ductility with increasing rupture time. This is true for all tests temperatures.

The data presented above show that the alloy we have developed has high creep strength and excellent creep ductility.

5.4 Estimated Design Allowable Stresses

Tensile and creep data were employed to estimate the design allowable stresses for the modified 9 Cr-1 Mo steel. The procedure employed for these estimates was the one used for the ASME Code, Sect. VIII. The maximum design allowable stresses estimated for the modified 9 Cr-1 Mo steel (normalized and tempered) are compared with those for 2 1/4 Cr-1 Mo (annealed and normalized and tempered) and standard 9 Cr-1 Mo steel (normalized and tempered) in Fig. 12. This figure shows that the design allowable stresses for the modified alloy are higher than those of standard 9 Cr-1 Mo and 2 1/4 Cr-1 Mo steels for the entire temperature range. Furthermore, at 550°C and above the design allowable stresses become approximately twice those of the other alloys.

6. Related Properties

Data on both physical and mechanical properties other than these presented in this paper are either available or being collected in an effort to completely characterize the modified 9 Cr-1 Mo alloy. Each of these properties is listed with its status described briefly.

6.1 Physical Properties

In this area effort is under way to determine the thermal expansion coefficient, thermal conductivity, and heat capacity of one heat each of standard and modified 9 Cr-1 Mo alloy. The objective of the study is to determine if there are significant differences in the physical properties of the two alloys.

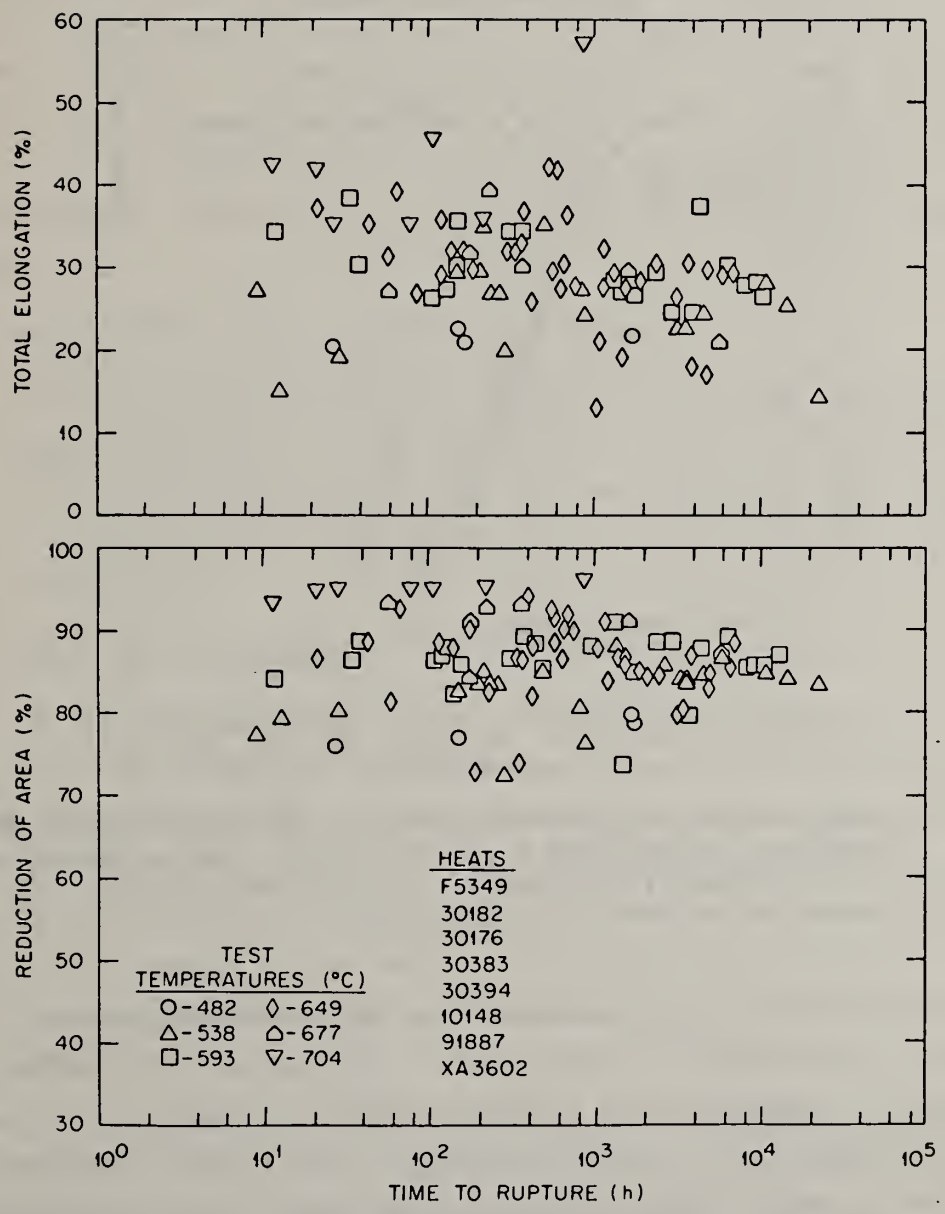

Figure 11. Plots of (top) total elongation and (bottom) reduction of area as functions of rupture time for commercial heats of modified 9 Cr-1 Mo steel tested in the normalized and tempered condition. Data are for test temperatures in the range 482 to 704°C and for eight commercial heats.

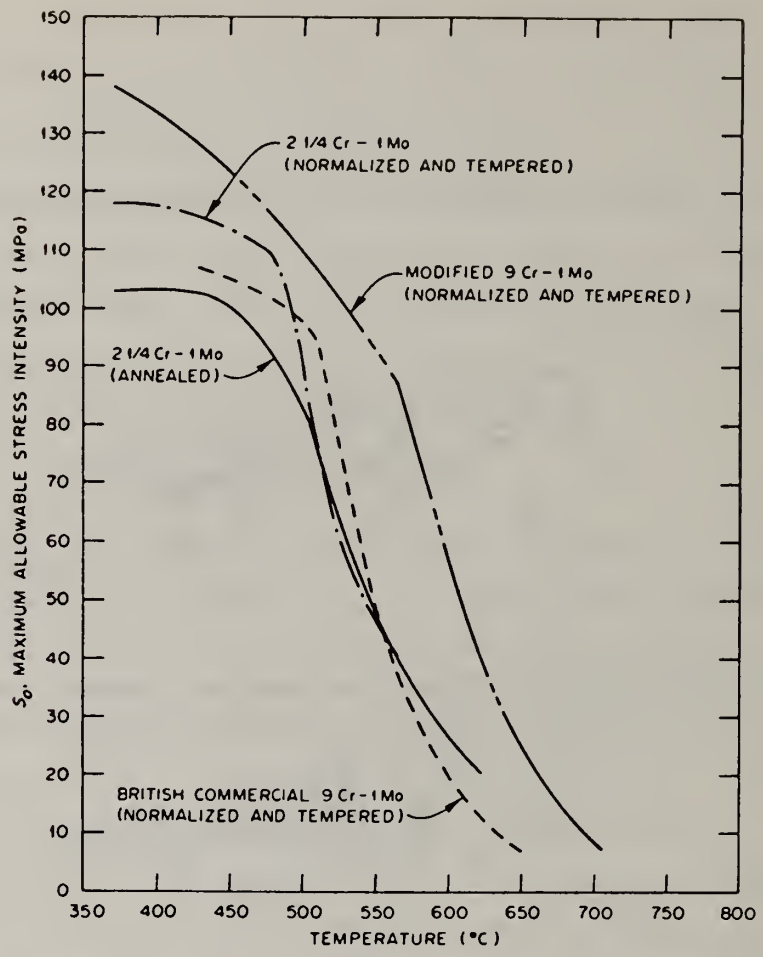

Figure 12. Estimated design allowable stresses as a function of temperature for modified 9 Cr-1 Mo steel. Design allowable stress values for standard 9 Cr-1 Mo and 2 1/4 Cr-1 Mo steel are also included for comparison.

Results of this study have shown that the thermal expansion coefficient of modified 9 Cr-1 Mo steel is the same as that observed in this study and reported in the literature for the standard 9 Cr-1 Mo steel [4]. However, the thermal conductivity was found to be related to the silicon content. Higher silicon content tended to be associated with lower thermal conductivity. We have tested modified 9 Cr-1 Mo heats containing 0.2 and 0.5% Si and recommend that the average values for these two heats be used as typical values.

6.2 Fatigue and Creep-Fatigue Tests

These tests are in progress at Oak Ridge National Laboratory, Sandia National Laboratory, Northwestern University, and the University of Connecticut. Data available have shown that the modified alloy has about the same fatigue strength (total strain range versus number of cycles to failure) as type 316 stainless steel in the range from 525 to 593°C. The alloy also has superior fatigue life beyond 10^5 cycles to 2 1/4 Cr-1 Mo, standard 9 Cr-1 Mo, and type 304 stainless steel. Microstructural observations on fatigue-tested specimens are reported by Jones [5].

6.3 Fatigue Crack Growth and Fracture Toughness

These tests are currently in progress at the Hanford Engineering Development Laboratory. Results available showed that the crack growth rate of the modified 9 Cr-1 Mo steel is about the same as that observed for 2 1/4 Cr-1 Mo and 12 Cr-1 Mo steel in the range from room temperature to 538°C [6].

6.4 Steam and Air Oxidation

The behavior of modified 9 Cr-1 Mo steel and other alloys (2 1/4 Cr-1 Mo, 9 Cr-2 Mo, 12 Cr-1 Mo, and type 304 stainless steel) in superheated steam at 482 and 538°C are available for a period of 28,339 h. Results of this study have shown that silicon is very potent in reducing the oxidation rate in steam at 538°C of chromium-molybdenum steels [7]. Because of its lower silicon content, the modified alloy showed slightly higher weight gain in steam at 538°C than that observed for standard 9 Cr-1 Mo alloy.

Air oxidation data at 593°C were obtained on both the modified 9 Cr-1 Mo and 2 1/4 Cr-1 Mo steel for a period of 20,000 h. These data showed that the weight gain for 2 1/4 Cr-1 Mo steel was about eight times that observed for the modified 9 Cr-1 Mo alloy. Tests are now continuing to measure the weight gain for longer periods.

6.5 Welding

The weldability of modified 9 Cr-1 Mo steel is being investigated with the Varestraint hot cracking test, Battelle under-bead cracking test, Tekken Y-groove test, hydrogen sensitivity test, and stress-relief cracking test. Results available thus far have shown that the material is free from hot cracking susceptibility, a preheat temperature of 200°C can prevent hydrogen sensitivity, and there are no stress-relief cracking problems for a postweld heat-treatment temperature of 732°C. The filler wire composition for gas tungsten arc welding, electrod composition for shielded metal arc welding, and the combination of filler wire and flux for submerged arc welding are currently being optimized to satisfy the strength and ductility criteria set for the alloy.

7. Operating Experience on Modified 9 Cr-1 Mo Steel Tubes

Industrial operating experience, which aids earlier approval of the data package for the ASME Code, is being obtained by installing tubes of this alloy in various conventional power plants. The status of installation of modified 9 Cr-1 Mo tubes in various utility power plants is summarized in Table 5. The range of utilities involved is international: United States, United Kingdom, and Canada. In most cases the tubes being replaced are stainless steel. The longest operating time has been reached for tubes installed at the Kingston Steam Plant. The tubes installed in Kingston plant are shown in Fig. 13. The modified 9 Cr-1 Mo steel tubes were supplied with type 347 stainless steel safe ends. The safe ends were welded on with Inconel 82 (ERNiCr3) filler wire. The final welds between type 347 and type 321 (existing tubes) were made on location.

Tubes in the Agecroft power station went into operation in April 1982 and those in Lambton and Nanticoke are expected to go into operation in October 1982. This operating experience will be very useful for obtaining the approval of this alloy in the ASME Code.

8. Status of Commercialization

The use of a modified or new alloy in actual application requires that it be included in ASTM specifications and various sections of the

Table 5. Current status of testing of modified 9 Cr-1 Mo steel tubes in U.S. and foreign steam power plants

Utility	Plant	Tube location	Operating temperature (°C)	Tubes being replaced	Number of tubes	Date installed	Status
Tennessee Valley Authority	Kingston Steam Plant, Unit 5	Superheater	593	Type 321	8	May 1980	Operating
American Electric Power	Tanners Creek Unit 3	Secondary superheater	593	Type 304	10	April 1981	Operating
Detroit Edison	St. Clair Unit 2	Reheater	538	Type 347	2	February 1981	Operating
Central Electric Generating Board (U.K.)	Agecroft Power Station	Superheater	590–620	2 1/4 Cr-1 Mo	6	April 1982	Operating
Ontario Hydro (Canada)	Lambton TGS	Reheater Reheater	538 538	Type 304H Std 9 Cr-1 Mo	9 9	September 1982	Planned
Ontario Hydro (Canada)	Nanticoke TGS	Secondary superheater	538	2 1/4 Cr-1 Mo	11	September 1982	Planned

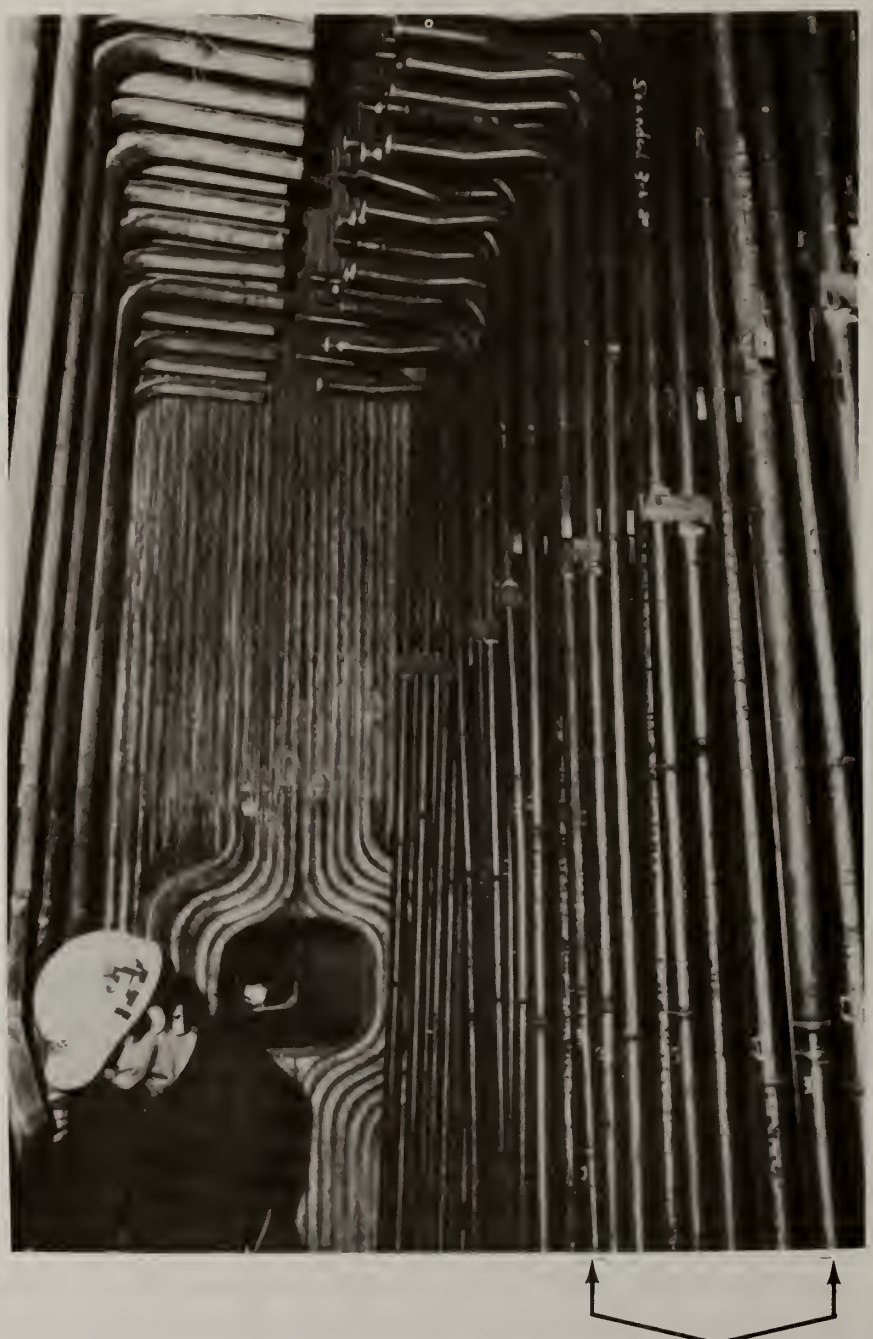

Figure 13. The modified 9 Cr-1 Mo steel tubes before going into operation in the TVA Kingston Steam power plant.

ASME Boiler and Pressure Vessel Code. The ASTM specifications are in fact prerequisites for the consideration of this alloy by the ASME Code Committees. The schedule for the ASTM and ASME Code approval is as follows:

An application for an ASTM specification for the plate and tube product was submitted for approval in May 1981. The specification application for the forgings, piping, and fittings was submitted in May 1982. The tube subcommittee has approved the specifications, which now must be approved by the main committee. The plate specifications are near approval, but the other specifications are still under consideration by the appropriate subcommittees.

The data package for the inclusion of modified 9 Cr-1 Mo steel in Sect. I and VIII of the *ASME Boiler and Pressure Vessel Code* was submitted in June 1982. At the request of various users and producers, the appropriate subcommittees of ASME are expected to start reviewing the data package during September 1982.

8. Summary

The status of development and commercialization of a modified 9 Cr-1 Mo alloy is presented. The alloy is modified by the additions of niobium (0.06—0.10%) and vanadium (0.18—0.25%). The alloy is recommended for use in the noramlized and tempered condition (1038°C for 1 h, air cooled to room temperature; 760°C for 1 h, air cooled to room temperature). Heat-treatment, Charpy impact, tensile, and creep properties of the alloy are discussed in detail and other properties are described briefly. Some of the key facts about modified 9 Cr-1 Mo alloy include the following.

1. The ductile-to-brittle transition temperature (68-J) of modified 9 Cr-1 Mo is lower and the upper-shelf energy higher than those of standard 9 Cr-1 Mo alloy. These properties were much better in the electroslag-remelted material.

2. The creep rupture strength of the modified alloy is higher than that of the standard 9 Cr-1 Mo and 2 1/4 Cr-1 Mo steels for the entire creep temperature range. The improvement in 10^5-h creep-rupture strength

is very significant at temperatures above 500°C. Higher strength is also accompanied by total elongation and reduction of area values higher than 15 and 70%, respectively.

3. Higher creep strength of the modified 9 Cr-1 Mo steel provides design allowable stresses that exceed those of 2 1/4 Cr-1 Mo and standard 9 Cr-1 Mo steel for the entire temperature range. At temperatures of at least 500°C, the design allowable stresses for the modified alloy are twice those observed for 2 1/4 Cr-1 Mo and standard 9 Cr-1 Mo steel.

4. The specifications for various products of this alloy have been submitted to ASTM for approval. A data package has also been submitted to the *ASME Boiler and Pressure Vessel Code* for approval of this material in Sects. I and VIII.

5. Operating experience on this alloy is being obtained by installing its tubes in various steam power plants.

The author thanks the following for their contributions: R. E. McDonald (ORNL) and G. C. Bodine (CE, Chattanooga) for contributions to melting, fabrication, and heat treatment and helping to prepare tubes for installation in various power plants; W. J. Stelzman (ORNL) for Charpy V-notch studies; R. H. Baldwin (ORNL) for tensile and creep testing; M. C. Cowgill (Westinghouse-Advanced Reactors Division) for creep testing; J. F. King (ORNL) and C. D. Lundin (University of Tennessee) for welding studies; R. K. Williams (ORNL) for physical properties; and M. K. Booker (ORNL) for the data analysis. Our special thanks are also due to the research staff of Climax Molybdenum Company of Michigan for its contributions to the success of this program. Continued encouragement and support of E. E. Hoffman (DOE, Oak Ridge Operations) and P. Patriarca (ORNL) to the success of this program also are greatly appreciated.

9. References

[1] Sikka, V. K., Ward, C. T., and Thomas, K. C. "Modified 9 Cr-1 Mo Steel — An Improved Alloy for Steam Generator Application," presented at the ASM International Conference on Production, Fabrication, Properties and Application of Ferritic Steels for High-Temperature Applications, Warren, Pa., Oct. 6—8, 1981, to be published.

[2] Bodine, G. C., and McDonald, R. E. "Laboratory and Pilot Commercial Process/Product Development of Modified 9 Cr-1 Mo Ferritic Alloy," presented at the ASM International Conference on Production, Fabrication, Properties, and Application of Ferritic Steels for High-Temperature Applications, Warren, Pa., Oct. 6—8, 1981, to be published.

[3] Orr, J., et al. "The Physical Metallurgy of Chromium-Molybdenum Steels for Fast Reactor Boilers," pp. 91—109 in *Int. Conf. Ferritic Steels for Fast Reactor Steam Generators, 30 May—2 June 1977*, British Nuclear Energy Society, London.

[4] Williams, R. K., et al. "The Physical Properties of 9 Cr-1 Mo Steel from 300 to 1000 K," paper presented at the 17th Int. Thermal Conductivity Conference, Gaithersburg, Md., June 15—19, 1981, to be published in the proceedings.

[5] Jones, W. B. "Effects of Mechanical Cycling on the Substructure of Modified 9 Cr-1 Mo Ferritic Steel," presented at the ASM International Conference on Production, Fabrication, Properties and Application of Ferritic Steels for High Temperature Applications, Warren, Pa., Oct. 6—8, 1981, to be published.

[6] James, L. A. *Fatigue-Crack Growth Behavior in Ferritic Alloys for Potential GCFR Structural Applications*, HEDL-TME 80-71, Hanford Engineering Development Laboratory, Richland, Wash., December 1980.

[7] Griess, J. C., and Maxwell, W. A. *The Long-Term Oxidation of Selected Alloys in Superheated Steam at 482 and 538°C*, ORNL-5771, Oak Ridge National Laboratory, Oak Ridge, Tenn., July 1981.

SiMo Ductile Iron for Elevated Temperature Service to Conserve Chromium

Jay Janowak*

INTRODUCTION

High silicon molybdenum ductile cast iron is a relatively low cost ferritic heat resistant material. In the trade it is called high silicon moly iron or just plain SiMo. It is already in direct competition with high chromium steels in some applications on a purely economic basis. It is a popular material for turbo charger housings and exhaust manifolds. It has been found to be the superior material for rabble teeth in a moly-sulfide ore roaster. And finally, SiMo is a candidate for furnace grates. All of these either are, or could become, high chrome steel applications. Should there be a "critical" need to reduce our use of chromium or to decrease our dependency on chromium, we believe the high silicon moly ductile cast irons could be considered as an option to high chromium steel. It is probable, but somewhat speculative, that relatively minor design changes could allow SiMo ductile iron to function in place of high chromium steels in numerous situations. In the next few minutes four applications will be reviewed to provide a feeling for the characteristic properties of this material. SiMo ductile is basically a standard ferritic nodular (ASTM 60-40-18) to which 1.5% silicon and 1% molybdenum are added to create the 4 silicon - 1 moly heat resistant ductile cast iron.

* Jay Janowak is Manager of Foundry Development, Climax Molybdenum Company P. O. Box 397, Arlington Heights, Illinois 60006. This is the oral text of a workshop presentation "Trends in Critical Materials Requirements for Steels of the Future Conservation and Substitution Technology for Chromium" at Vanderbilt University, October 5, 1982

TURBOCHARGERS

The Si-Mo nodular iron concept was developed at the Climax research laboratory in the sixties. Among early anticipated applications were relatively low cost tubing for use in hydrogen gas generators and forming dies for titanium. These did not materialize, but Climax engineers brought the concept to the attention of a prominent turbocharger manufacturer, and, after an extensive development program, 4% Si - 0.6% Mo ductile iron emerged as an improved housing material. Figure 1 shows an automotive turbocharger. To give an idea of size, a small car unit would fit inside a 1 gallon milk container. A cut away view is shown in Figure 2.

Turbochargers are like miniature air compressors. Hot exhaust gases spin the turbine which through a common shaft drives the blower. On demand, fresh compressed air can be forced into the combustion chamber of the engine to provide added power in trucks and off-road vehicles. Using a different approach, this concept is applied to improve auto fuel economy through utilization of smaller, lighter weight engines.

Exhaust gases are typically in the 1300 to 1500^{o}F range. Housings can become red hot as shown in Figure 3. Dimensional stability , oxidation resistance, and high temperature strength and toughness are important properties provided by SiMo ductile iron in this application. Let me emphasize the critical criteria.

Containment - Housings must be able to contain a "wheel burst" for obvious safety considerations. On vehicles, heavy walls are prohibitive because of weight and space restrictions. Therefore, the relatively

weaker gray irons are not practical. Consequently, the alternatives are narrowed to ferritic or austenitic ductile irons or stainless steel. However component complexity favors the castability of a ductile iron over stainless steel options. While austenitic irons are stronger at temperature, the ferritic irons have better ductility. Since containment is related to a combination of strength and ductility, either iron will serve the purpose.

Figure 4 shows strength and toughness at 1300°F of a 4% silicon ductile iron with increasing molybdenum contents. Notice that molybdenum substantially increases strength at 1300°F and also note the elongation of over 50% at a level of 1% molybdenum. Ductile behavior is evidenced in Figure 5 which shows a housing that contained a wheel burst at temperature during a scheduled "run-away" test on a dynamometer.

Dimensional Stability - Dimensional stability is essential in general, but, specifically, the turbine blade/housing "air-gap" must be maintained at a minimum level. Divider wall stability is also very important. Thermal expansion, phase changes, oxidation growth and distortion can influence the "air-gap" and other contours visible in the cutaway view (Figure 2). Silicon and molybdenum both work in the direction of improving the dimensional stability of nodular irons. Ferritic ductile iron has a very low coefficient of thermal expansion which is dimensionally beneficial compared to an austenitic material. The addition of silicon further improves dimensional stability by raising the temperature of the phase change to austenite as shown in Figure 6. Note that, at 4% silicon, ferrite is stable up to over 1500°F.

Molybdenum provides dimensional stability by increasing the strength at temperature and by improving creep resistance. In addition, molybdenum adds resistance to stress relaxation, thereby reducing warping and distortion. Figure 7 shows constrained thermal fatigue specimens. Both are high silicon ferritic iron. One sample accumulated a bulge - it had no molybdenum. The other sample contained .6% molybdenum. It showed less bulge and survived 3 times the number of cycles to failure. This benefit of molybdenum applies to both ferritic and austenitic irons.

Oxidation - Ductile iron is inherently more oxidation resistant than gray iron because the graphite is in discreet spheres as will be seen later. This is a mechanical influence related to the transmission of oxygen. Chemically, silicon and aluminum can add greatly to oxidation resistance in cast irons. The silicon effect is shown in Figure 8. Here, weight gain is plotted versus time at 1200°F for various silicon levels. Notice the initial weight gain in all cases. This is explained by the mechanism of oxidation resistance apparent in Figure 9. Silicon preferentially oxidizes at the surface to provide a silicon oxide layer which prevents further penetration of oxygen. Notice also the discreet spheres of graphite characteristic of ductile iron. This is a different graphite shape than that of gray cast iron which has interconnected graphite flakes that create a virtual "pipe line" for oxygen. This silicon scale is particularly tenacious. Without adequate silicon, this scale would exfoliate and rapidly abrade the turbine blades. Silicon provides this benefit to both ferritic and austenitic irons. By limiting oxidation and thereby growth, high silicon irons have additional dimensional stability.

To bring this section to an end let me point out that turbocharger housing materials can be classified according to service temperature. Gray irons can serve up to 1000°F. Unalloyed ferritic nodular irons can serve up to 1300°F, and with additions of silicon and molybdenum up to 1500°F. Austenitic irons with silicon and molybdenum may serve up to 1700°F while temperatures beyond that point may require high chromium steels or superalloys. High chromium stainless steels are alternatives to the irons at all these nominal temperature levels, particularly when special thermal or environmental situations challenge the cast irons. In such cases, silicon and molybdenum additions to ductile iron make it a suitable alternative to high chromium steels.

EXHAUST MANIFOLDS

Exhaust manifolds are another hot engine item (Figure 10). Traditionally, automotive exhaust manifolds were gray iron. However, higher operating temperatures, demand for weight reduction, and the desirable aspect of low thermal conductivity (for faster catalytic converter light off) has resulted in a change to predominantly unalloyed ferritic nodular iron. Most recently, a substantial interest has been shown in fabricated stainless steel exhaust manifolds and there are indications that some of the new cars may have these as standard. The principle advantage of fabricated stainless steel is weight reduction - since the remaining properties should be adequately provided by the SiMo ductile irons. In fact, it is believed that SiMo ferritic ductile irons are superior to the fabricated stainless steel in design flexibility, noise damping and distortion resistance. Thermal distortion can make it impossible to replace an exhaust manifold once removed from the car.

In extreme cases, during operation, thermal distortion can lead to exhaust gas leaks which can be a noise problem and a potential fire hazard. Building a further case for the iron, it is important to recognize that it is now possible, with new casting technology to cast ductile iron exhaust manifolds having sections as thin as one-sixteenth of an inch. The jury is still out on this application but SiMo ductile irons are clearly in competition with stainless steel having more than 12% chromium.

In a specific case involving very large diesel engines with pistons over 15" in diameter, SiMo ductile iron replaced tubular wrought 2¼Cr-1Mo steel exhaust manifolds. A design change was desired by the manufacturer to reduce cost and improve performance. The new design provided a common tuned exhaust system instead of multiple individual exhaust tubes. Initially, unalloyed ferritic nodular iron was considered and had the necessary or improved corrosion resistance to condensate. However, concern over oxidation and creep led to the selection of SiMo ductile iron which provided the necessary confidence level for the new design. In this case, SiMo ductile iron replaced 2¼Cr-1Mo steel for a cost and performance benefit.

GRATES

Furnace grates (Figure 11) are another application where SiMo ductile iron is being considered. An industrial incinerator operator was looking for a lower cost alternative to HC steel. HC steel is 26-30%Cr, 4%Ni (max), .5%C(max), 2%Si(max), and 1%Mn(max). An enterprising foundry looking for new business decided to pursue the SiMo iron with our guidance. A review of the application revealed certain

needs. Metal to metal wear resistance was needed to protect against a sliding action inherent in the design. Resistance to spike heating up to 1500°F was desired, but normal grate operating temperatures were said to be on the order of 400°F because the grates were effectively insulated by the burning rubbish. In addition, the grates were cooled by cold air forced up through the grates from below to provide oxygen for burning. Toughness was important because motor blocks sometimes were dropped from a height of 20 feet onto the grates. There was no feeling for the corrosion resistance needed. A comparison of available properties was made and shown in Figure 12.

Based on this information a decision was made "to go" and trial castings were put into a controlled pilot experiment side by side with HC steel. After 6 months the incinerator was shut down and inspected. SiMo ductile grates showed less wear than HC steel. Then, sometime after the 6 month check, the grates were found to have significantly deteriorated (Figures 13 and 14). A preliminary investigation revealed that molten aluminum had apparently fluxed the iron causing a reduction in the melting point. The iron thus appeared melted in an environment where temperatures only rarely reached 1500°F. The investigation has begun only recently, and as of this moment, the relative resistance of SiMo iron and HC steel to aluminum fluxing is not known. In refuse systems where metal separation occurs after burning, relative resistance to such fluxing action may end up being a critical material selection criteria.

Specific tests are planned to determine the relative resistance of SiMo ductile and HC steel to aluminum fluxing. It is however clear from the results to date that, except for this fluxing by aluminum, the SiMo grates performed equally well or better than those of HC steel.

ROASTER TEETH - The last example is a case where SiMo ductile iron has been found the superior material in an ore roasting furnace. Five years ago, engineers at our moly sulfide roasting plants began a program to improve the life of the roaster rabble teeth.

A number of rabble teeth standing upside down and waiting to be put into service are shown in Figure 15. They hang from a beam that rotates inside a roaster as shown in Figure 16. This view shows the roaster in the empty and cold condition. The main shaft is also visible. The tooth closest to the shaft is in location number one. In Figure 17 is a view showing the red hot rabble teeth doing their job which is to roll over the molybdenum sulfide in an oxidizing atmosphere at up to 1500°F. The rabble teeth are basically plows which must stand up to an abrasive and especially hostile environment of hot molybdenum oxide, oxygen, and high sulfur gases.

At times, during operation, it is necessary to maintain a free flow condition. In Figure 18 is an operator poking to free teeth from the substance being plowed when it becomes gummy creating excessive drag on the shaft. You might say some impact resistance is needed.

The standard material was ferritic nodular iron with a silicon carbide insert at the plow location for abrasion resistance. A number

of materials were involved in the controlled experiment including SiMo ductile iron, high chromium white irons and stainless steels. The basis for selection of these materials for test was fairly straightforward. The SiMo ductile iron was included on the premise that it might last sufficiently longer than standard ferritic ductile iron to meet the objective time and still be low cost. High chromium white iron is well known for abrasion resistance but high temperature endurance in this environment was unknown. Stainless steel was assumed to be the best material to withstand the corrosive environment. It was felt that significantly extended life could justify the added cost of this high chromium-nickel option.

Results after one year of continuous service are apparent from pictures of the teeth in Figures 19-22. Standard teeth in Figure 19 are ferritic ductile iron with about 2% silicon and no alloying elements. The smallest tooth suffered the greatest deterioration and was closest to the shaft where the environment is most hostile. The other teeth were relatively further away from the shaft and in environments of declining hostility. This same pattern follows with all of the materials tested. CF8 (cast 304) stainless steel (19%Cr-9%Ni) is shown in Figure 20, 28% chromium white iron in Figure 21, and 4 silicon - 1 molybdenum ductile iron in Figure 22. Wear data are numerically summarized in Figure 23 in terms of "percent of original weight remaining" on the vertical axis and roaster arm location along the horizontal axis. Position 1 is hotter and more hostile. Position 14 is cooler and less hostile.

The roaster teeth can be classified by performance into two groups; the high silicon alloyed nodular iron (Alloys 1 and 8) - and all the rest, as clearly evident. There is a distinct difference in the way the nodular irons eroded and the way the stainless steels and high Cr white irons eroded. The nodular irons developed a thick oxide scale which appeared to protect the metal surface and reduce the rate of oxidation. The stainless steels, Alloys 3 and 9, did not develop a thick protective scale, and thus, eroded very rapidly. Part of the rapid deterioration of the stainless steel may have been related to the nickel content. However a specific study would be necessary to verify that possibility. The high Cr irons, Alloys 6 and 7, did develop an oxide scale but it apparently had inadequate stability in the roaster environment.

It is clear that the high chromium alloyed materials did not perform any better than the standard alloy in the roaster environment. The oxidation protection normally accompanying high chromium contents in ferrous alloys is apparently just not effective in this environment. On the other hand, it was certainly a pleasant surprise to find the SiMo ductile iron as the most servicing material in this aggressive environment.

In conclusion I would simply like to summarize these case histories and restate our premise.

1. Four silicon - one moly ductile cast iron is currently in competition with high chromium steels for elevated temperature service in exhaust system components such as turbocharger housings and exhaust manifolds. SiMo is a common turbocharger housing material. It has replaced 2¼ Cr - 1 Mo in an exhaust manifold. And, it is being challenged by fabricated stainless steel for automotive exhaust systems.

2. SiMo ductile iron is being considered as a replacement for 27% chromium HC steel in industrial incinerator grates.

3. SiMo ductile iron has been found to be the superior rabble tooth material in the highly corrosive - erosive environment of a moly sulfide roaster over standard ferritic ductile iron, 27% chromium white iron, and 19% chromium - 9% nickel stainless steels.

4. It is probable, but speculative, with relatively minor changes in design or performance requirements, that SiMo ductile cast iron could replace high chromium steels in numerous high temperature applications, should a critical need to do so develop.

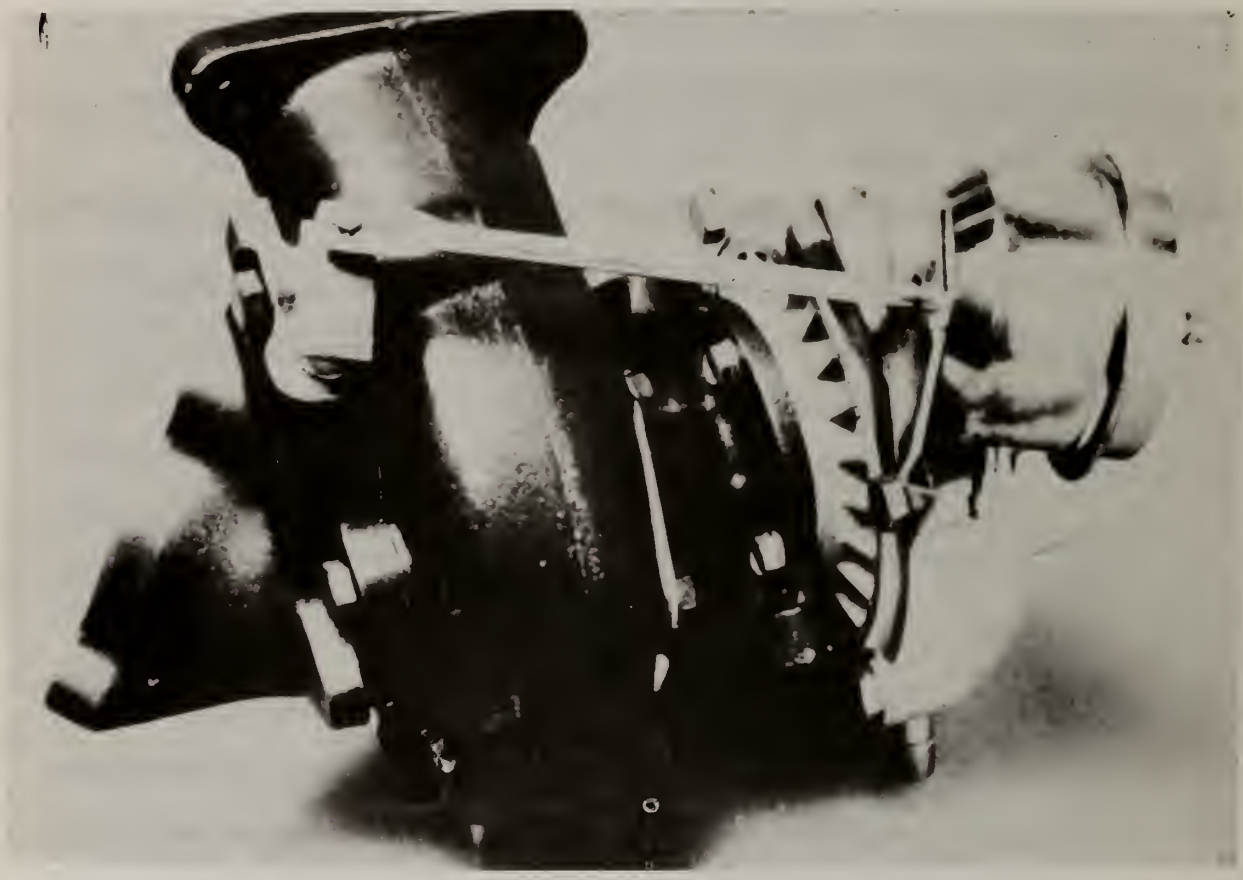

Figure 1 Automotive Turbocharger

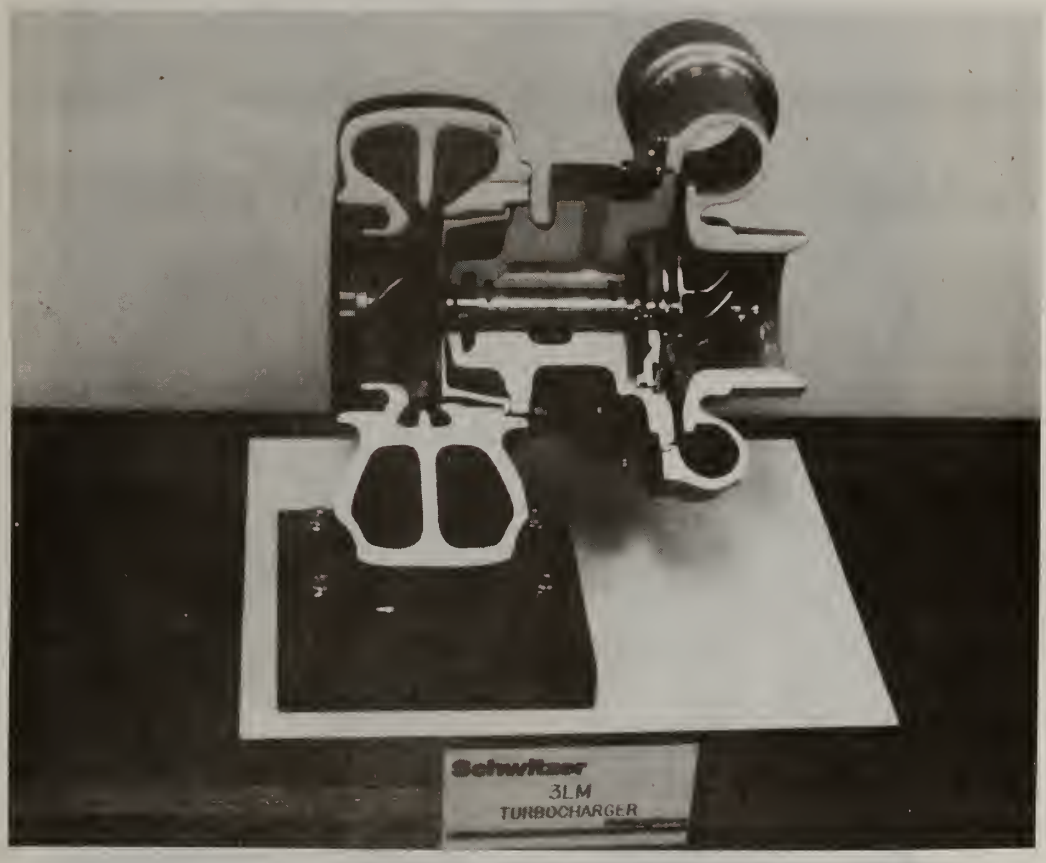

Figure 2 Automotive Turbocharger -- Cutaway View

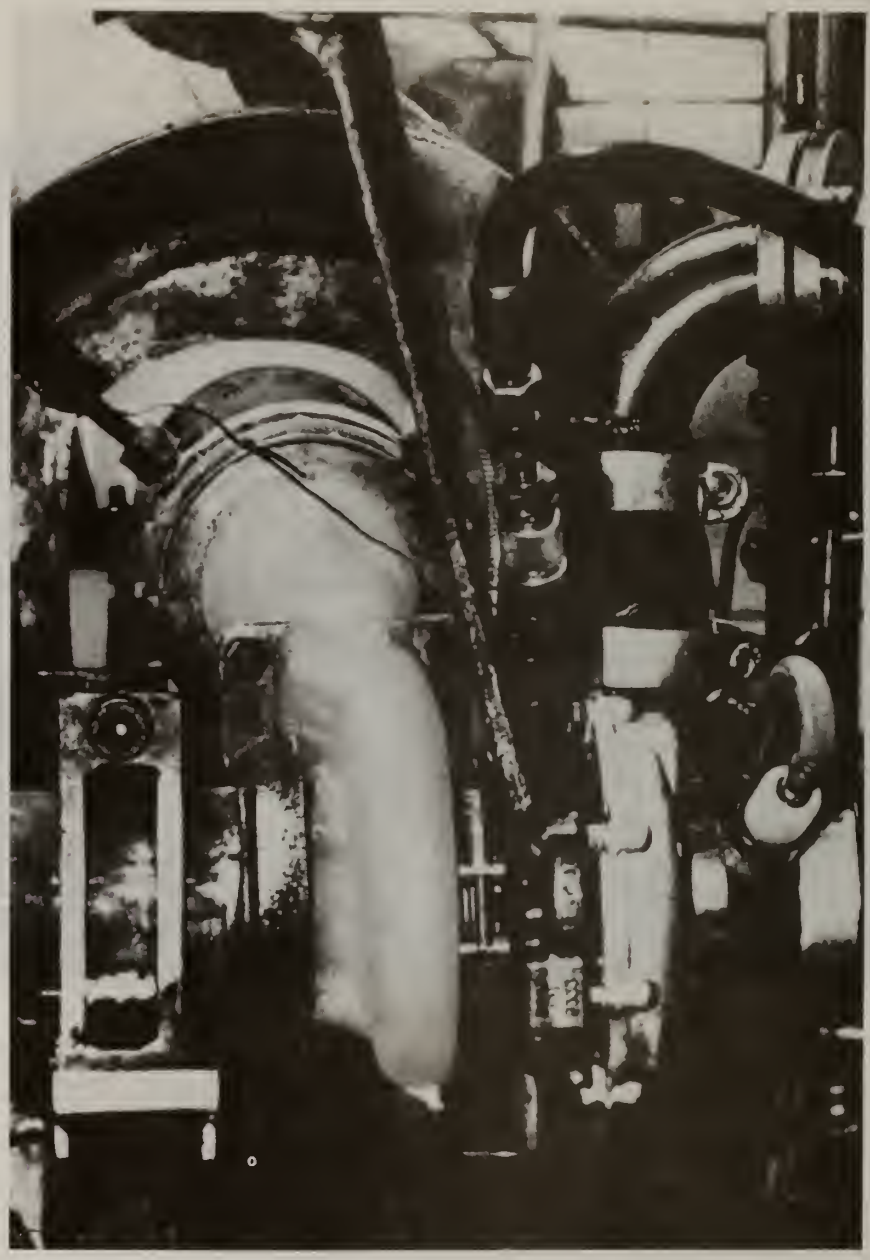

Figure 3 Turbocharger in Service on Test Stand

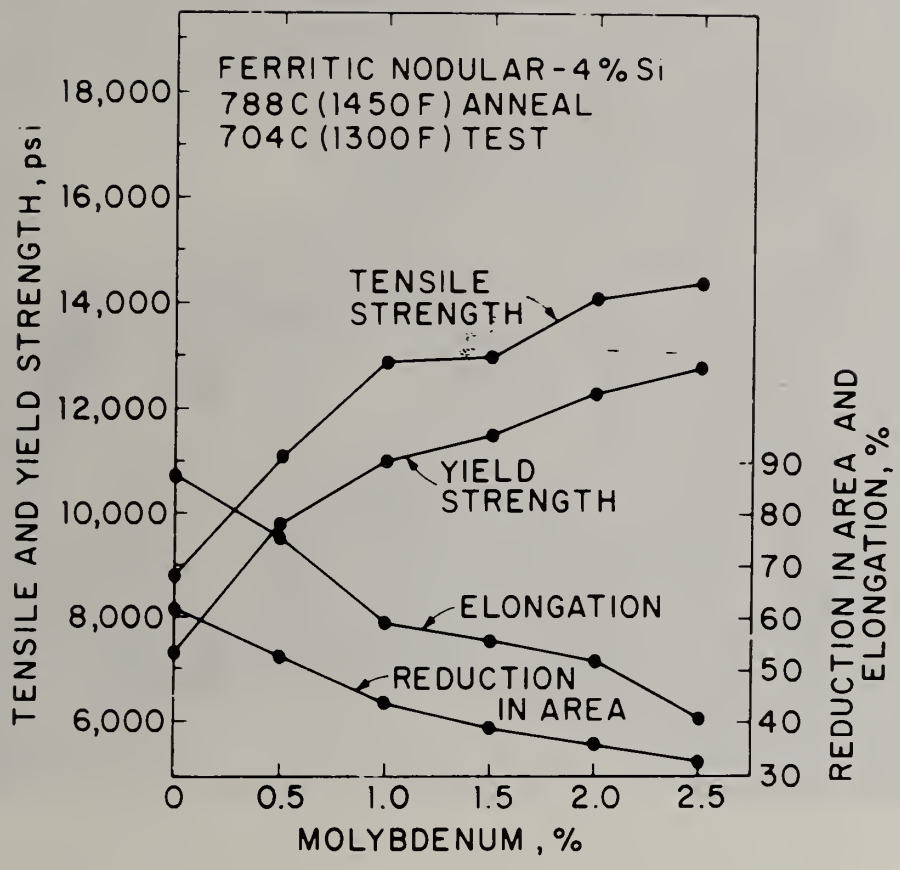

Figure 4 Tensile Properties of 4% Si Nodular Cast Iron at 704 C (1300 F)

Figure 5 Turbocharger Housing Damage After Containment of Wheel Burst

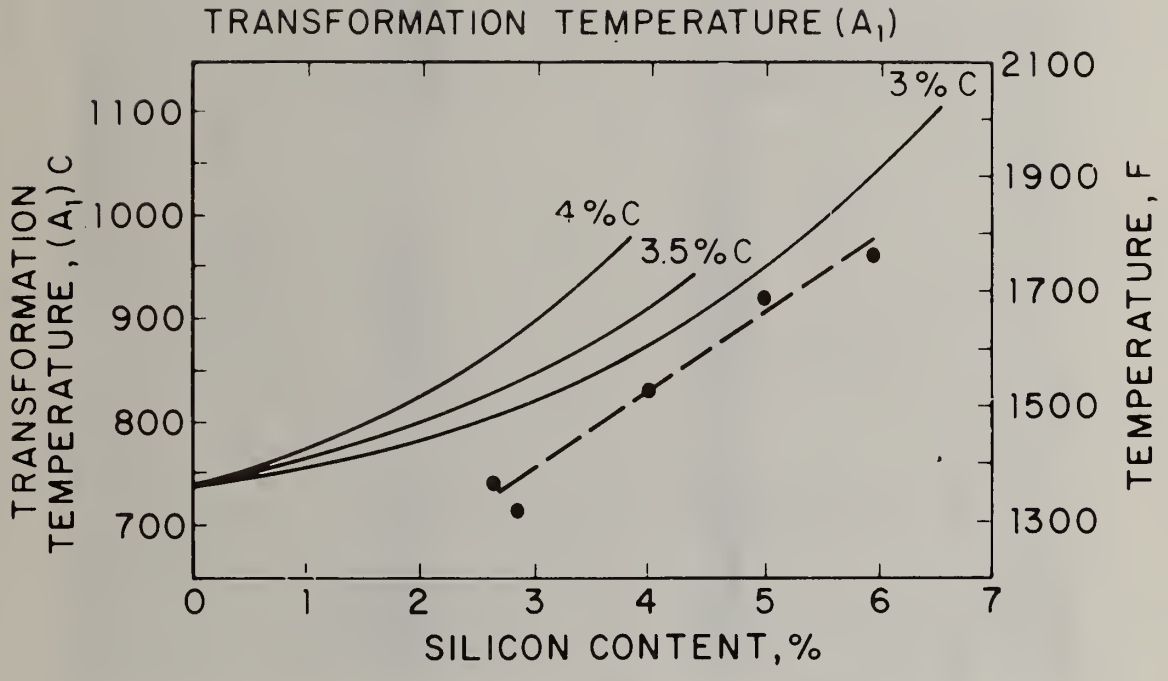

Figure 6 Effect of Silicon Content on Ac_1 of Nodular Irons at Various Carbon Contents. Curves Are From the Literature, Data Points Represent Climax Data (Dilatometry) for $3.1\% < C < 3.8\%$.

Figure 7 Constrained Thermal Fatigue Test Specimens of High-Silicon Nodular Irons. Sample on Left Alloyed with 0.6% Mo.

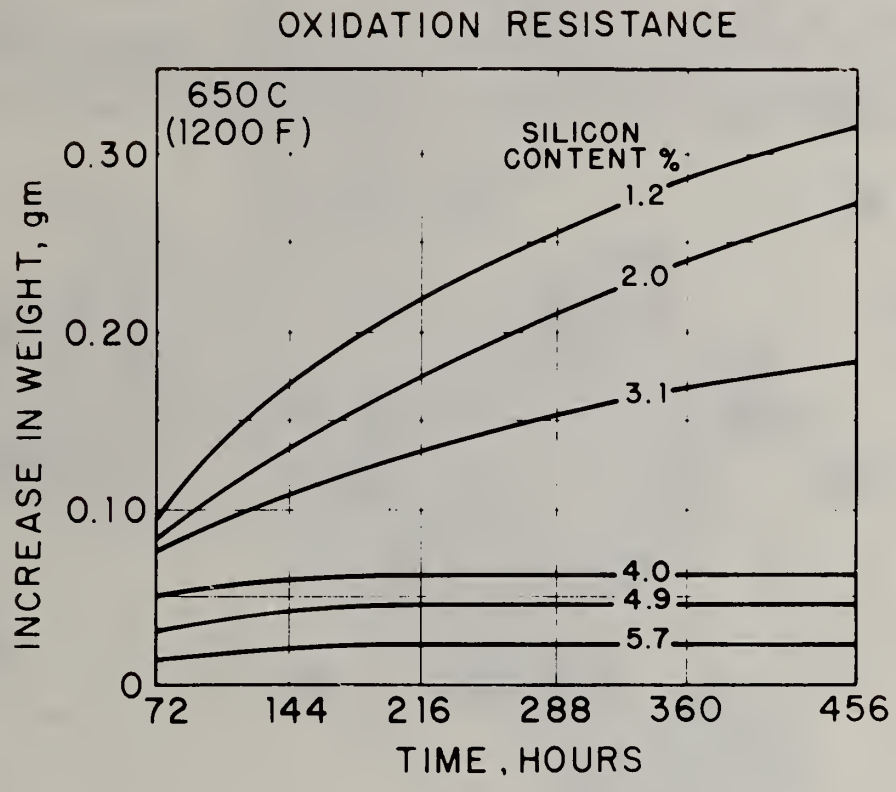

Figure 8 Effect of Silicon Content on Oxidation Resistance of Nodular Iron at 650 C (1200 F)

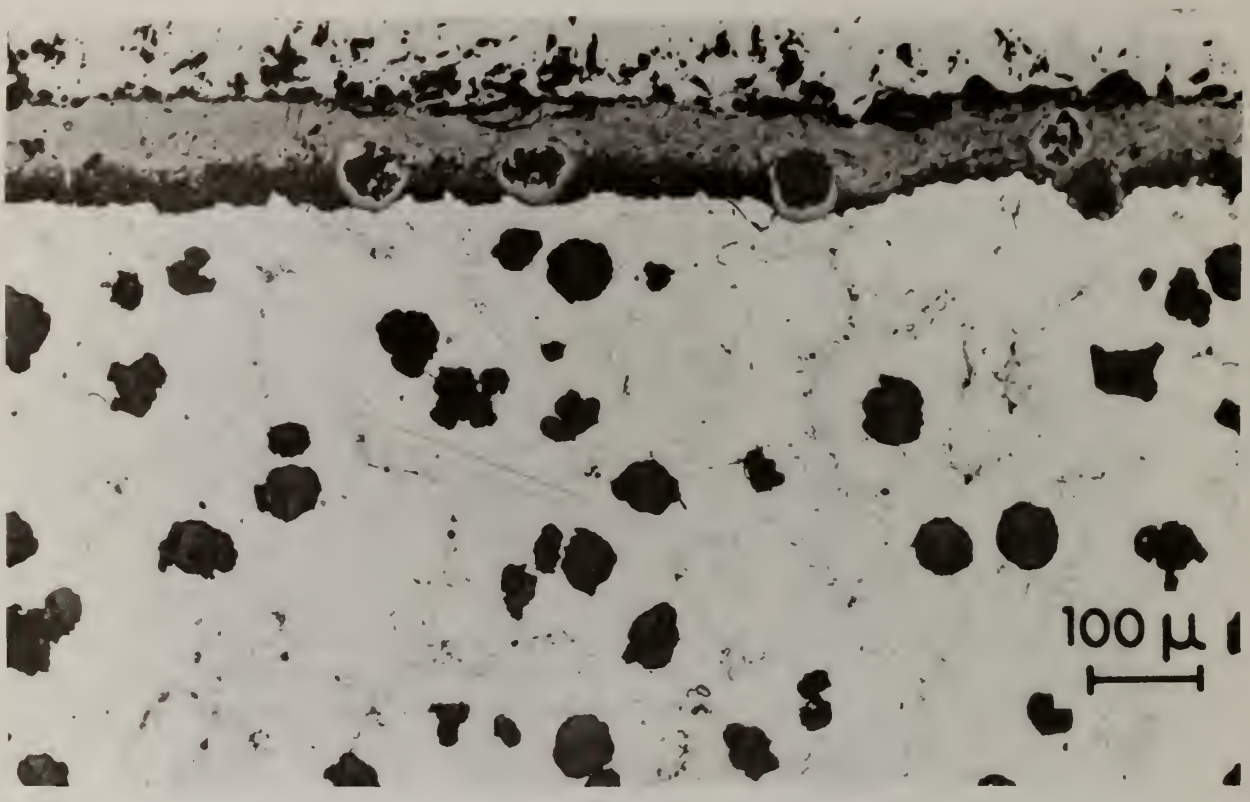

Figure 9 Photomicrograph of Oxidized High-Silicon Nodular Iron Showing Adherent Silicon Oxide Scale

Figure 10 Exhaust Manifold

Figure 11 Commercial Incinerator Furnace Grate Before Service

	HC STEEL	4 Si-1 Mo
Tensile Strength at Room Temperature	55,000 min.	80,000 min.
%Elongation at Room Temperature	2-19	8-19
Brinell Hardness No.	190-223	190-240
Load Bearing Service	up to 1200°F	up to 1500°F
Rupture Stress		
at 1300°F	—	3300 psi
at 1400°F	2300 psi	—

Figure 12 Comparison of Properties of High-Chromium (HC) Steel and 4Si-1Mo Nodular Iron

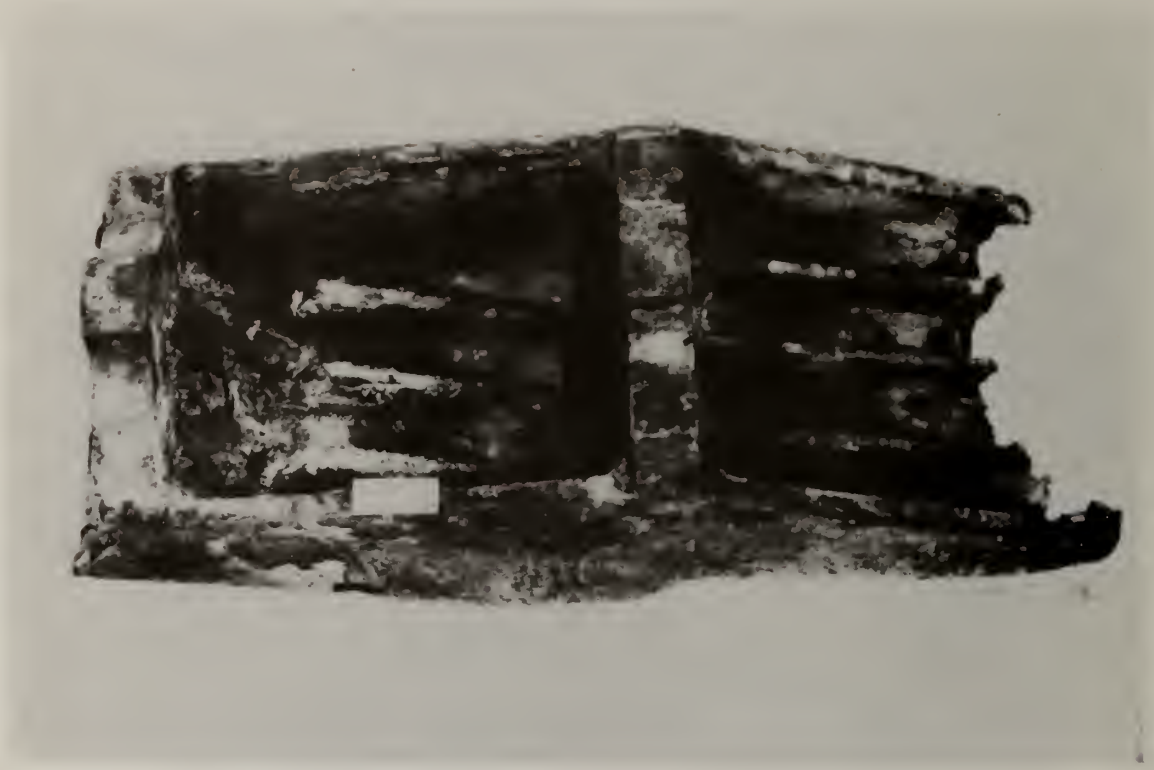

Figure 13 Si-Mo Nodular Iron Furnace Grate Showing Damage Resulting (Apparently) from Exposure to Molten Aluminum

Figure 14 Si-Mo Nodular Iron Furnace Grate Showing Damage Resulting (Apparently) from Exposure to Molten Aluminum

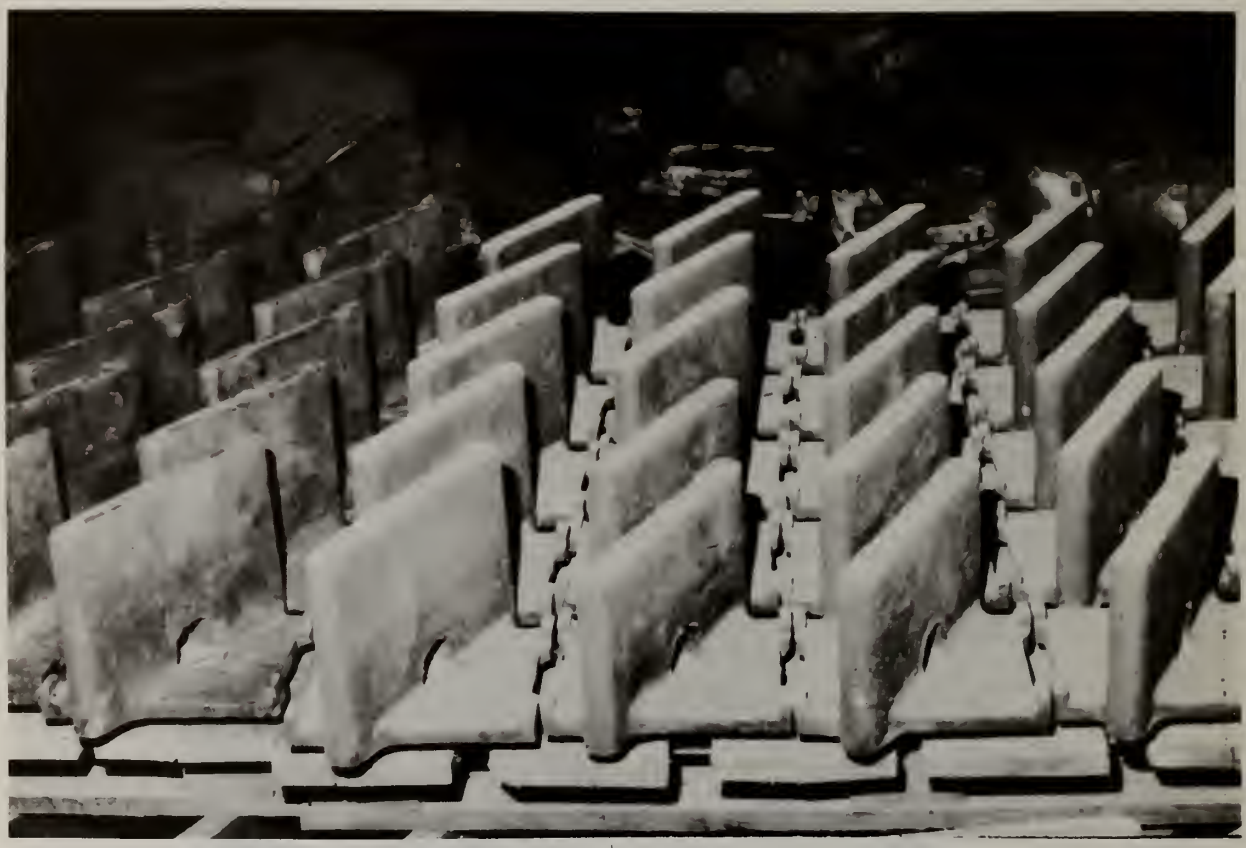

Figure 15 Roaster Teeth Prior to Service

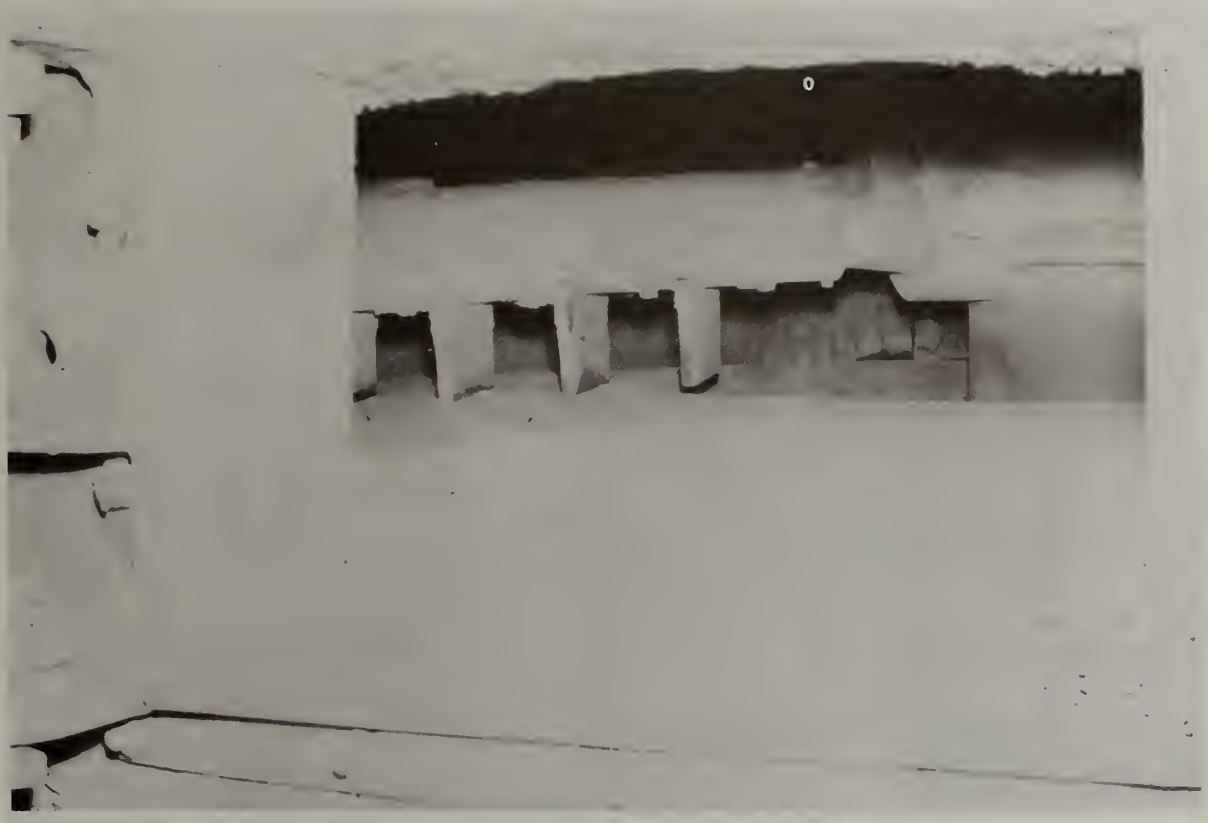

Figure 16 Roaster Teeth in Position on Rabble Arm

Figure 17 Roaster Teeth in Service

Figure 18 Operator Using Steel Rod to Clean Roaster Teeth

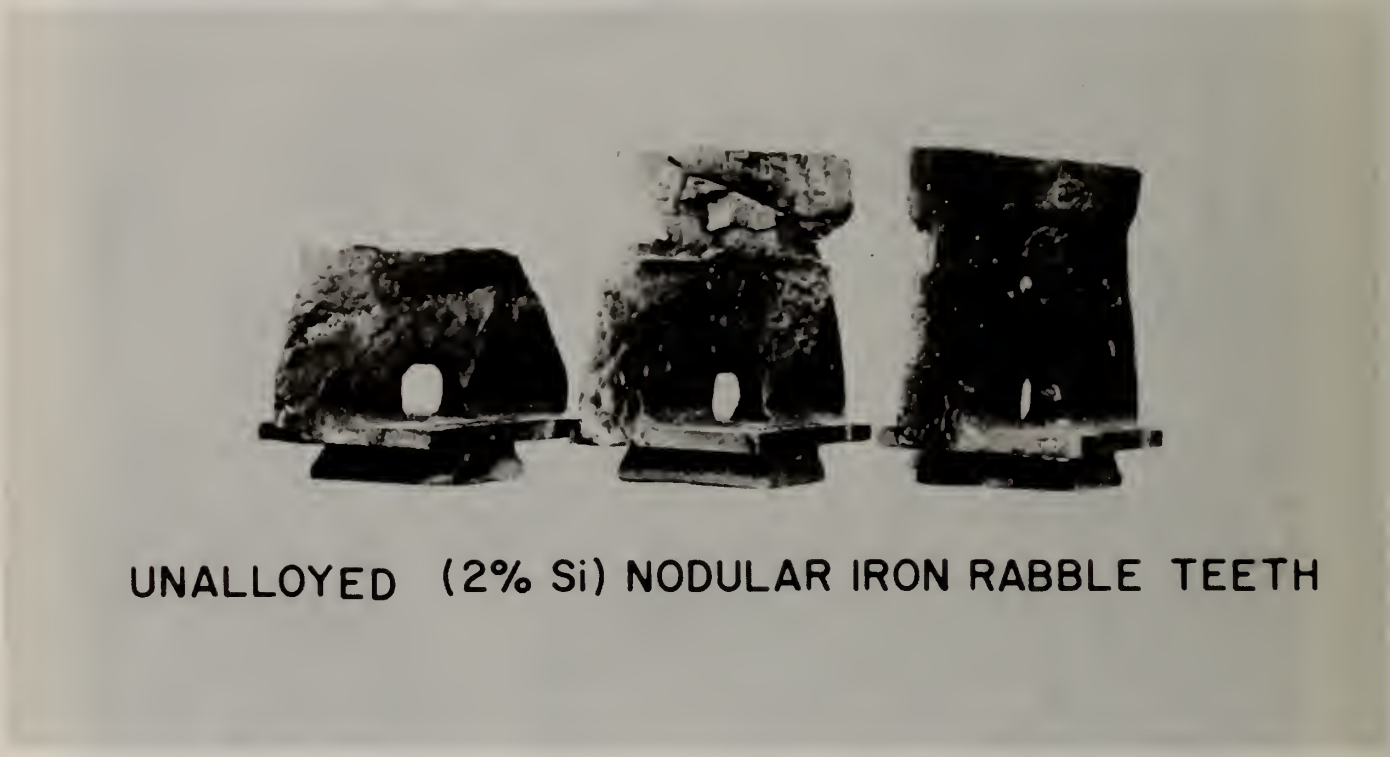

Figure 19 Unalloyed Nodular Iron Roaster Teeth
after One Year of Service

Figure 20 Cast 304 Stainless Roaster Teeth
after One Year of Service

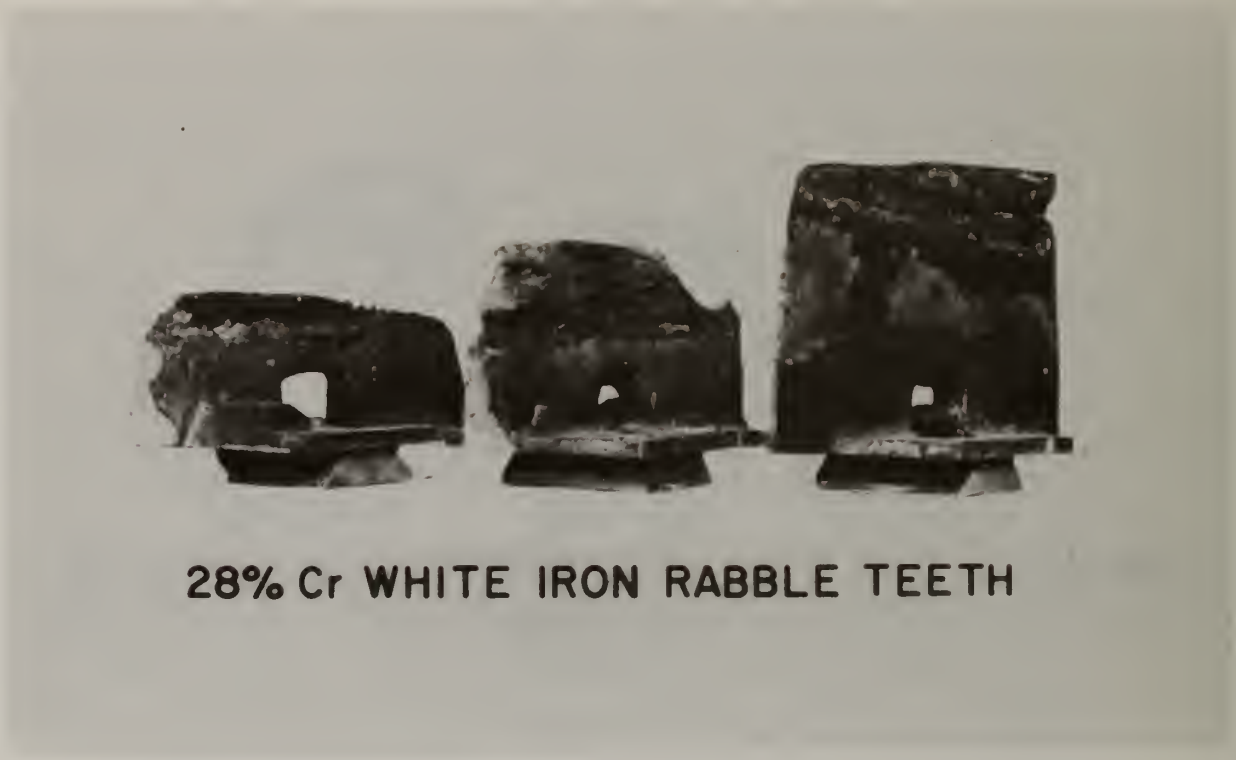

Figure 21 High-Chromium White Cast Iron Roaster Teeth after One Year of Service

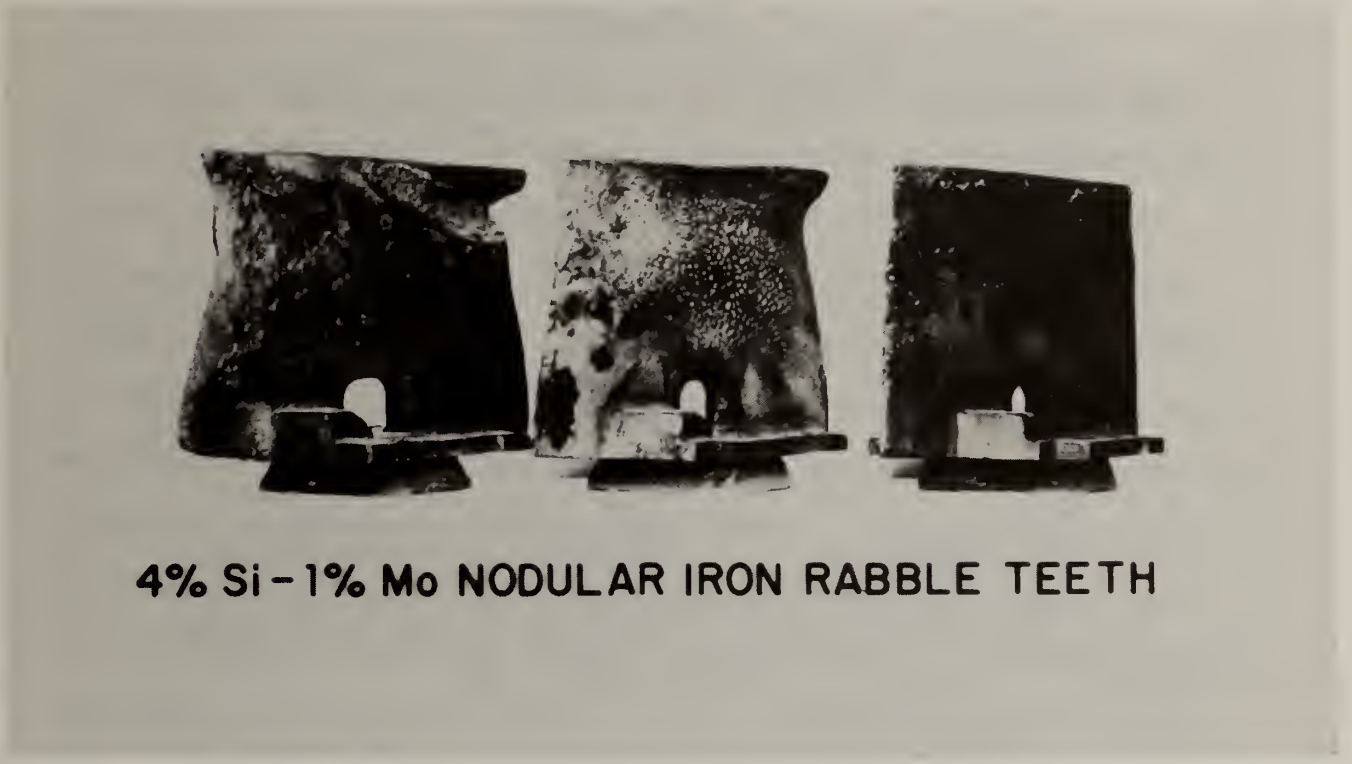

Figure 22 4Si-1Mo Nodular Iron Roaster Teeth
after One Year of Service

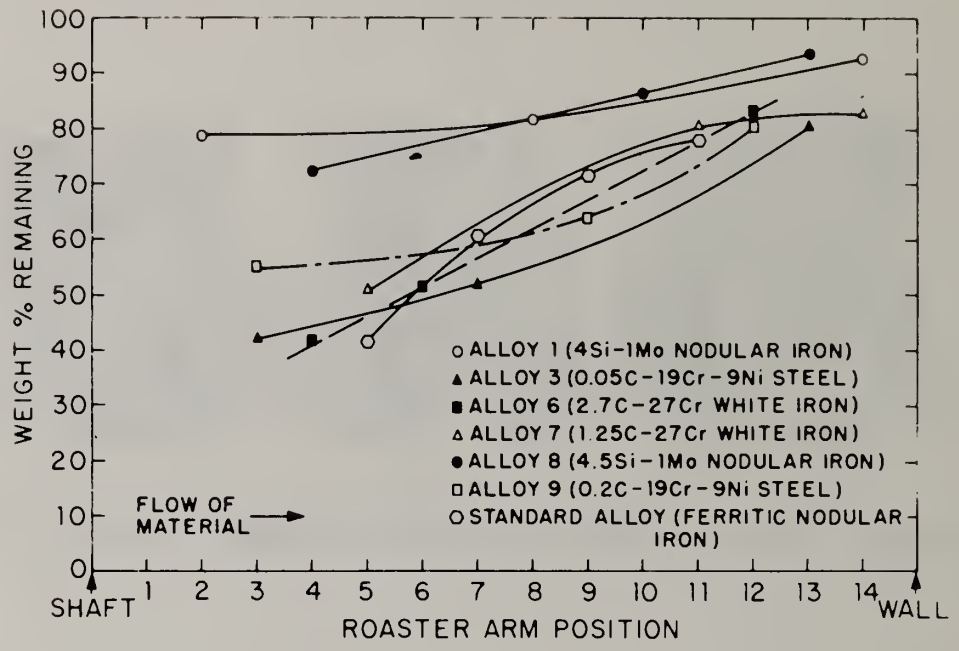

Figure 23 Performance of Various Materials as Roaster Teeth in Climax Test

THE 1982 STATUS REPORT ON FE-MN-AL STEELS*

Samir K. Banerji
Foote Mineral Company
Exton, PA 19341

INTRODUCTION

The development of the Fe-Mn-Al alloy system as a possible substitute for the traditional Ni-Cr austenitic stainless steels in some applications appears to be gaining some momentum. In the June 1981 Workshop on the "Conservation and Substitution Technology for Critical Materials" held at Vanderbilt University, Nashville, Tennessee, the author presented an update of activities on this subject.[1] The available literature until that time was reviewed in that report and a brief summary of some preliminary work spurred by the two earlier papers of the author[2,3] was presented. Some of those efforts have been completed, some have been forgotten, some are still continuing and some new efforts have been started. It is particularly gratifying to see that the results of some of these efforts are beginning to appear in the literature.

A paper on the oxidation resistance of Fe-Mn-Al-C alloys[4] appeared recently and another one on Mn-Al-Si austenitic steels for propellers of sea-going vessels[5] will be forthcoming shortly in the Metal Progress. A third paper on the marine corrosion behavior of several Fe-Mn-Al austenitic steels[6] will be submitted for publication in the near future. Another paper outlining the various properties and characteristics of the Al-Mn-C austenitic steels has been submitted for publication in the Journal of Metals.[7] Six papers were presented on this subject at the XXXVI Brazilian Society for Metals (ABM) Annual Congress in July 1981.[8-13] These

*To be presented at the Public Workshop on "Trends in Critical Materials Requirements for Steels of the Future - Conservation and Substitution Technology for Chromium," Vanderbilt University, Nashville, Tennessee, October 4-7, 1982.

papers provided some preliminary results of a large-scale study undertaken at various universities in cooperation with the Technological Center Foundation of Minas Gerais-CETEC in Brazil. Two papers[14,15] appeared recently at the 35th Annual Conference of the Australasian Institute of Metals dealing with the oxidation and sulfidation resistance of Fe-Mn-Al type alloys. Brief summaries of these and the other ongoing work are presented in this report.

SUMMARY OF THE NEW LITERATURE SINCE THE JUNE 1981 WORKSHOP

1. "Development of Oxidation Resistant Fe-Mn-Al Alloys" by J. C. Garcia et. al. (ref. 4).

The microstructure and oxidation behavior at 500° and 700°C (930° and 1290°F) of several Fe-Mn-Al-Si-C-X alloys, shown in Table 1, were studied. Alloys A and B showed a dual-phase structure, predominantly austenitic with different amounts of an ordered b.c.c. phase, when homogenized at 1100° and 1000°C, respectively. Alloys C and D were single phase austenitic when quenched from 1100° and 1000°C, respectively. Alloys E and F with Cu additions were primarily ordered b.c.c. with the precipitation of a disordered f.c.c. phase. The oxidation behavior of these alloys were measured by weight gain experiments in flowing oxygen (1 atm.) at 700° and 500°C for times up to 24 hours.

Table 1. Composition of six alloys studied by Garcia et. al. (ref. 4).

Alloy	Composition, wt %							
	Al	Mn	Si	C	Cu	P	S	Fe
A	10.84	31.92	3.01	0.74	--	0.05	0.02	bal
B	9.05	33.30	1.41	0.88	--	0.02	0.02	bal
C	8.63	28.60	2.68	0.69	--	0.05	0.02	bal
D	7.25	24.04	2.06	1.01	--	0.02	0.02	bal
E	12.40	4.13	2.12	0.03	0.91	0.02	0.01	bal
F	12.05	4.20	1.93	0.03	8.90	0.02	0.01	bal

Figure 1 shows that alloy E behaves similarly to type 304 stainless steel at 700°C while the behavior of the rest of the alloys in 24 h runs is far superior for the Fe-Al-Mn alloys than for a plain carbon steel. Results reported in Fig. 2 indicate that Fe-Al-Mn alloys behave comparatively and superior to type 304 in 24 h experiments at 500°C. These results are in agreement with other reports.[1,7,8] The formation of aluminum-rich surface oxide scales was a common observation in these alloys during the oxidation tests. Addition of Cu appeared beneficial for oxidation resistance. Finally, alloys A, B, C, and D were hot and cold rolled at room temperature into 1 mm (0.04 in.) thick sheet without intermediate anneals. Alloys E and F became brittle at room temperature probably because of brittleness associated with the ordered parent phase.

2. "An Austenitic Mn-Al-Si Steel for Propellers of Sea-Going Vessels" by R. Wang and F. H. Beck (ref. 5).

This soon to be published paper describes the selection of an Fe-Mn-Al steel for the propeller of a sea-going fishing vessel in People's Republic of China, launched on August 10, 1980, and still sailing safely. The mechanical properties and marine corrosion resistance of as-cast alloys of Table 2 were studied and compared with Mn-Fe brass which is the traditional propeller material and austenitic stainless steel. The strength and hardness of the Fe-Mn-Al alloys were higher than those of the brass. These alloys were approximately 20% lighter than the brass and also lighter than the stainless steel.

The marine corrosion tests were first carried out by immersing samples in boiling seawater for 118 hours. Alloy no. 1 and the Ni-Cr stainless steel showed no evidence of rusting. Alloy no. 3 had a small rust spot but alloys 2 and 4 were obviously rusty. Similar immersion

tests lasting 768 hours (32 days) were also carried out at room temperature. Alloys 2 and 4 were covered by a brown rust film, alloy 3 showed a thin yellowish film, the Ni-Cr stainless had a little track of rust, but alloy no. 1 was free from any obvious rust. Based on this the alloy no. 1 was chosen for the propeller of the fishing vessel mentioned earlier.

Subsequently, the polarization curves in artificial seawater were determined for the alloy no. 1 and the Ni-Cr stainless steel. Interestingly enough, the corrosion current density (I_{corr}) and the corrosion rate (R_{corr}) were nearly identical, being 2.905×10^3 NA/Cm and 1.2 mpy, respectively.

Table 2. Compositions of Alloys Tested by Wang and Beck (ref. 5).

No.	Code Name	%C	%Si	%Mn	%Al	%P	%S	%RE
1	$Mn_{30}Al_{10}Si$	1.01	1.31	30.5	10.4	0.007	0.006	0.056
2	$Mn_{20}Al_7$	0.50	0.30	22.3	7.2	0.005	0.003	0.038
3	$Mn_{30}Al_7$ Si	0.23	1.25	29.2	7.4	0.008	0.003	0.061
4	$Mn_{20}Al_5$	0.13	0.28	20.7	5.6	0.007	0.005	0.063

The Main Composition of the Compared Materials

		%C	%Cr	%Ni	%Ti	%Cu	%Zn	%Mn	%Fe
5	$Cr_{18}Ni_9Ti$	0.08	18.59	9.63	1.07				
6	Mn-Fe Brass 55-3-1					55	41	3	1

3. "Marine Corrosion Behavior of Several Fe-Mn-Al Austenitic Steels" by Wang and Rapp (ref. 6).

This very recent work at the Ohio State University has concentrated on the electrochemical corrosion behavior of several Fe-Mn-Al alloys. The potentiodynamic polarization tests in artificial seawater or in $1NH_2SO_4$ were performed on seven different alloys of varying compositions and the results were compared with two standard austenitic stainless steels

of types 316 and 321. The composition of the various alloys tested and the results of the corrosion tests are shown in Table 3. Alloy no. 3 (30Mn-10Al-1C) showed the best corrosion resistance of all the seven alloys tested with a linear corrosion rate somewhere in between types 316 and 321 stainless. Additionally, this alloy in $1NH_2SO_4$ also showed a passive region within the potential of +0.5V to +1.5V.

The shape of the polarization curves for all these alloys in artificial seawater including the 316 and 321 stainless steels were nearly the same, all lacking an obvious passive region. However, with increasing Al and/or Si and decreasing C contents, there is a more stable region at anodic potential near E_{corr}. The shapes of the polarization curves for alloy no. 3 and 316 stainless were nearly identical. Based on this and the results in Table 3, it was concluded that Al and Si are beneficial in the marine corrosion resistance of these alloys. The carbon content should be kept to a minimum necessary to maintain an austenitic structure.*

4. "An Evaluation of Al-Mn-C Austenitic Steel" by Rao et. al. (ref. 7).

The mechanical properties and preliminary oxidation and corrosion behavior of a 32Mn-9.6Al-1.0C-Fe alloy were studied. The alloy was found to be age-hardenable with the peak hardening occuring around 600°C aging temperature. The mechanical properties of the steel in this peak-aged condition were: yield strength = 90 kg/mm^2 (128 ksi), ultimate tensile strength = 100 kg/mm^2 (142 ksi), and 40% elongation. The impact properties in the solution annealed condition were good, but deteriorated drastically on peak aging. The alloy exhibited excellent formability characteristics, comparable to 304 stainless steel in 1.45 and 0.63 mm gage thicknesses. The oxidation resistance in 100 hour tests in air showed the alloy to be only marginally inferior to 304 SS at 700°C. This is in agreement with the

*Further work is continuing at the Ohio State University by these authors.

Table 3. Chemical Composition and Corrosion Data of the Samples Tested by Wang and Rapp - (ref. 6).

No.	Code Name	Main Composition, wt % C	Mn	Al	Si	Cr	Ni	Mo	Cu	Ti	N	Corr. Potential E_{corr} (V)	Corr. Current I_{corr} $\mu A/cm^2$	Equiv. Weight g/Equ.	Density g/cm^2	Linear Corr. Rate (mpy)	Linear Corr. Rate mm/year
1	316	0.025	1.62		0.46	17.37	10.84	2.15	0.40			-0.414	0.785	25.88	7.83	0.339	0.0085
2	321	0.08				18.59	9.63			1.07		-0.444	2.905	26.02	7.84	1.253	0.032
3	11-1-1A (Cast)	1.01	30.15	9.75	0.12							-0.512	1.740	23.27	7.17	0.735	0.019
4	11-10-3C	1.05	30.60	8.39	0.23							-0.622	17.520	23.84	7.27	7.465	0.188
5	8-24-1	1.24	30.10	8.33	0.12							-0.667	81.740	23.84	7.26	34.840	0.877
6	10-28-1	0.52	29.81	8.28	0.02							-0.679	7.73	23.84	7.28	3.241	0.083
7	11-10-4	1.05	30.5	8.37	1.45							-0.659	6.98	23.37	7.22	2.934	0.074
8	8-24-2	1.07	30.10	8.32	1.54							-0.626	4.76	23.37	7.22	2.002	0.050
9	2-2-1	0.06	30.32	6.68	0.08						0.2	-0.740	10.11	25.42	7.40	4.514	0.113

previous work.[1,4,8] At 900°C the oxidation resistance was considerably inferior, again confirming the results of other workers.[8,9] The corrosion rate of half immersed samples in 7% NaCl at 60°C was nearly twice that of 304 SS. In 50% HCl at room temperature the results were considerably poorer. This work was summarized in my earlier report.[1]

Additional work on the phase stability and transformation characteristics, microstructural correlation, and kinetics of aging are being completed. In view of the higher stability of the austenite on deformation or cooling to liquid nitrogen, these alloys do seem to have a good potential in cryogenic applications.

5. "The Resistance to Oxidation and the Electrical Resistivity of an Fe-Mn-Al System Alloy" by Casteletti and Spinelli (ref. 8).

An alloy with 31.22% Mn, 7.54% Al, 1.34% Si, and 0.93% C (pouring 13) and a non-silicon version of this alloy were tested. Oxidation tests were carried out in air at 700° and 800°C for times up to 70 hours and compared with Type 304 stainless steel. The resistivity of the alloy (pouring 13) was measured over the temperature range of 80°-812°C using 80 mm long wires with 2 mm^2 cross-sectional area. Figure 3 shows that the oxidation resistance of the alloy at 700°C is comparable to 304 SS. This is in agreement with previous work.[1,4,7] At 800°C the oxidation resistance is inferior to that of 304 SS, Fig. 4. Nevertheless, the oxide layer did stabilize after about 40 hours at 800°C. The alloy without Si had a substantially inferior oxidation resistance at both temperatures. The electrical resistivity values shown in Fig. 5 are higher than those of commercial Ni-Cr alloys and Kanthal.

Based on these results it was concluded that these alloys represented a promising option in replacing the heat resistant alloys of Ni-Cr, Fe-Ni-Cr, and Fe-Cr-Al at temperatures up to 800°C.

6. "Study of Oxidation of an Fe-Al-Mn-C Alloy at High Temperatures" by Assuncao et. al. (ref. 9).

A low carbon alloy (36.5 Mn, 7.4 Al, 0.13 C, bal. Fe) was studied in this work. The oxidation behavior at 1000° and 1100°C was investigated in air, pure oxygen and nitrogen for times up to 8 hours (50 hours in one case). The results of the oxidation tests in air do not indicate good performance at 1000°C and 1100°C. This is in agreement with previous results.[7,8] The outer oxide layer which spalled-off was identified to be $MnO.Fe_2O_3$ which is consistent with the work of Rao et. al.[7] The inner adhering oxide layer was rich in Fe_2O_3 followed by a region of an aluminum-rich precipitate, the existence of which was correlated with the presence of nitrogen in the oxidizing gas atmosphere, suggesting the precipitate to be nitride or carbonitride complexes of Al and Fe. The oxidation resistance of the alloy in pure oxygen was excellent at 1000°C.

7. "Study of the Microstructural Transformations in TIG Welding of an Fe-Al-Mn Alloy " by Bushinelli et. al. (ref. 10).

Again, a low carbon alloy was used with a chemistry nearly identical to the previous study.[9] 3 mm thick cold-rolled plates in homogenized (1000°C/2h, water quenched) and cold-worked condition were used for the welding test. Due to the low carbon content (.12%), the alloy in both these conditions showed a duplex microstructure consisting of austenite and δ-ferrite, but the fraction of the ferrite phase was smaller and spheroidized in the homogenized condition. The TIG welding was selected because this is virtually an inconsumable electrode process. The welding parameters were: 105-110A, 14-16V, weld rate of 20 cm/min., and a pass length of 75 cm.

The transformation of δ-ferrite in the weld heat-affected-zone (HAZ) of the cold-rolled plates caused embrittlement and the fracture to occur

in the HAZ at stress values about half the strength of the base metal. The tensile tests of the welded plates in the homogenized condition were invalid due to lack of weld penetration. The composition of the δ-ferrite in these alloys was richer in Al and poorer in Mn. Homogenization reduced the Al content of the ferrite. The transformed δ-ferrite regions in the HAZ of the cold-worked plates were also rich in Al and low in Mn compared to the austenitic matrix. Therefore, it was believed that the embrittlement in this case occurred due to the precipitation of an intermetallic (Fe_3Al type) or carbidic phase in the transformed ferrite regions rather than β-manganese formation.

The homogenized plates did not show any transformation of the ferrite in the HAZ. The HAZ microstructure remained unchanged from the base metal microstructure of the homogenized plates, i.e., spheroidized ferrite with smaller volume fraction and reduced Al content. Although the results of the tensile test in this case were invalid, it is believed that the weld embrittlement could be eliminated by the prior homogenization treatment. However, the ideal solution would be to minimize or eliminate the ferrite phase altogether by increasing the austenite stabilizing element. In this case a higher carbon version of the alloy could be useful.

8. "Mechanical Properties of an Austenitic Steel of the System Fe-Mn-Al" by Casteletti and Spinelli (ref. 11).

The same alloy (pouring 13) used in the other study of these authors,[8] 31Mn-7.5Al-1.3Si-0.93C-Fe, was used for this work as well. Tensile properties were measured in the temperature range of 24°-815°C and also after various levels of cold-reductions ranging from 0 to 80%. Low-temperature impact strength was measured over a temperature range of +20°C to -196°C. The microstructure of the as-cast alloy showed

large austenitic grains with some dendritic structure in the grain interiors. After forging (at 900°C) and solution annealing at 1050°C followed by oil quenching, a typical annealed austenitic microstructure was obtained.

In Table 4 are presented the results of the tensile tests in the as-cast and forged states of the alloy. There is an increase of approximately 35% in the tensile strength and 40% in the yield strength of the worked alloy with practically no loss of ductility compared to the as-cast alloy. The mechanical properties of the as-cast alloy are still better than most standard austenitic stainless steels.

Table 4. Results of the Tensile Strength Tests for the As-Cast and Forged Material (ref. 11)

Material	Tensile Strength $MN.m^{-2}$	0.2% Yield Strength $MN.m^{2}$	Elongation %	Reduction in Area %
As-Cast	738	401	50	--
Forged	997	567	48	59

Figure 6 shows the temperature dependence of the tensile strength of the forged alloy in the temperature range of 24-815°C. Note that over the temperature range 24°-600°C, the tensile strength values for the alloy under study are 30% higher than those of 202 SS; 50% higher than those of 316 SS; and 68% higher than those of 304 SS.

Figure 7 shows the yield strength as a function of temperature for the alloy studied compared to the standard stainless steels. It can be seen that the yield strength values for the Mn-Al steel are on average 87% higher than those for the other alloys, in the entire range of temperatures studied.

One can also see a slight decline in the yield strength values in the temperature range of 150-300°C, where there occurs the phenomenon of dynamic aging of the alloy. Between the temperatures of 400° and 550°C, the yield strength values exhibit a peak, possibly indicating the occurrence of hardening phenomena due to precipitation in this range of temperatures.

Figures 8 and 9 show the dependence of tensile and yield strengths on the percentage of cold reduction. Note that the rate of increase in tensile strength with percent reduction is about the same for the Mn-Al steel (pouring 13) as the standard stainless steels. However, the absolute values are considerably higher due to the initially high tensile strength of the alloy. On the other hand, the yield strength initially increases more rapidly than the other alloys (Figure 9). As expected, the ductility decreases as strength increases with cold reduction, see Figure 10. The rate of drop in ductility is approximately the same as the standard stainless steels, although the absolute values are lower due to higher strength of the Mn-Al alloy.

Figure 11 shows that the strain-hardening response of this alloy is lower than those of two other stainless steels -- Types 201 and 301. Figure 12 compares the impact strength of the Fe-Mn-Al alloy with several other steels from room temperature down to liquid nitrogen temperature. The ductile-brittle transition temperature of this alloy in the as-forged condition is about -80°C and comparable to the 310 SS.

The specific gravity of the alloy was 6.85 g/cm^3. This coupled with the high strength levels provides a very attractive strength-to-weight ratio in this alloy.

9. "Precipitation Reactions in Low-Carbon Fe-Mn-Al Alloys" by Tschiptschin and Goldenstein (ref. 12).

Two low-carbon alloys with .13C, 36.5Mn, 7Al were studied; one without Si (#T-04) and one with 1% Si (#T-05). After homogenizing at 1000°C for times up to 24 hours, the microstructure still consisted of islands of delta ferrite in an austenite matrix. The alloys were aged at 600°-800°C for times ranging from 15 secs. to 200 hours. The transformation of δ-ferrite into lamellar carbide + ferrite was observed as a result of aging. The transformed ferrite was an ordered phase of the Fe_3Al type and caused embrittlement of the alloy. The transformation nucleated at the austenite/δ-ferrite boundaries and the interlamellar spacing increased with temperature.

No significant changes in hardness were observed as a result of aging, as shown in Table 5. This lack of age-hardening is contrary to other observations,[1,7] probably because of the low carbon content of these two alloys. At 1000°C both the alloys developed thick oxide layers when heated in air as observed by other workers.[9]

Table 5. Vickers Hardness of Alloys T-04 and T-05 (ref. 12)

Heat Treatments Carried Out	VH Hardness Alloy T-04	Alloy T-05
1000°C - 2 h	179	163
1000°C - 2 h & 800°C - 1 h	158	158
1000°C - 2 h & 800°C - 3 h	165	157
1000°C - 2 h & 700°C - 1 h	160	165
1000°C - 2 h & 700°C - 3 h	161	171
1000°C - 2 h & 600°C - 15 s	152	159
1000°C - 2 h & 600°C - 30 s	170	155
1000°C - 2 h & 600°C - 2 m	148	154
1000°C - 2 h & 600°C - 10 m	157	164
1000°C - 2 h & 600°C - 30 m	148	162
1000°C - 2 h & 600°C - 1 h	160	145
1000°C - 2 h & 600°C - 3 h	143	153
1000°C - 2 h & 635°C - 200 h	179	175

10. "Domain of the Austenitic Phase in the Fe-Mn-Al System at 1000°C" by Branco and Boratto (ref. 13).

The 1000°C isothermal section of the carbon-free Fe-Mn-Al ternary system was determined to establish the austenitic phase field. The samples were held at 1000°C for 168 hours under 1 atm. argon pressure before quenching in water. X-ray diffractometry, optical microscopy and micro-hardness measurements were used to identify the various phases. The results showed a slightly more limited austenitic phase field than that proposed earlier.[16] The maximum aluminum solubility in the austenite at 1000°C was 15 atomic percent in the carbon-free ternary system.

11. "Elements Essential to High Temperature Sulphidation Resistant Iron-Based Alloys" by Tomas (ref. 14).

Preliminary results of this work on Femnal 30 alloy (30.4Mn, 7.6Al, 0.8C, bal. Fe) was summarized in my report last year.[1] This and some additional work is now completed. The purpose was to develop iron-based alloys free of chromium to resist sulphidation attack at high temperatures encountered in materials used for fossil fuel and coal conversion plants due to the presence of sulfur.

A large number of alloys were tested for sulphidation resistance in a reducing atmosphere of H_2+1 vol.% H_2S for 9 hours at 700° and 800°C. The weight gain data[17] shown in Figure 13 exhibited the best performance by pure Mo and two iron-based alloys containing 5% Al and 7% (Fenbal 7) or 17% (Fenbal 17) niobium. The Femnal 30 and a similar Si-bearing alloy #11-10-4B (30.5Mn, 8.4Al, 1.5Si, 1.05C, bal. Fe), supplied by me to Dr. Tomas, also showed very good performance better than all the standard Ni-Cr stainless and high Mo or Nb alloys.

In both these alloys a relatively thin adherent sulfide scale formed, see for example Figure 14 showing the scale formed in Femnal 30 after 9 hours at 700°C. The scale was duplex in nature, the outer layer being predominantly MnS with very low iron content, Figure 15(a). Underneath this outer layer of MnS there forms a thin layer of niddle-like aluminum sulfides, either Al_2S_3 or $FeAl_2S_4$, protruding into the inner matrix (Figure 14). This provides excellent scale/matrix adhesion and spallation resistance to the scale. The slightly inferior result on the 11-10-4B alloy (Figure 13) was believed[17] to be due to the presence of iron-rich sulfide phase in the outer layer of the scale, the lighter phase in Figure 15(b). This could be due to the presence of Si in this alloy. Apart from this, the scale on both this and the Femnal 30 alloys were similar in nature.

British Gas Corporation has tested both Femnal 30 and the 11-10-4B alloy in an oil gassifier test rig. The conditions were thought to be reducing, containing about 0.5-1.0 vol. % H_2S. However, both alloys failed catastrophically after 300 hours at 750°C. Analysis of the reaction products revealed oxides and a liquid slag. This indicated that more oxygen was present than previously assumed. It has been shown earlier that such alloys do not resist oxidation/sulphidation attack in multicomponent gas mixtures.[18] However, in reducing/sulphidizing atmospheres these alloys offer excellent potential at least up to 700°-800°C. At 700°C in this atmosphere these alloys are at least ten times more resistant than the 300 series stainless steels.

12. "The Development of Fe-Al Alloys for High Temperature Oxidation Resistance" by Jackson and Wallwork (ref. 15).

This work deals with the carbon-free, low-Mn, ferritic alloys of the Fe-Mn-Al system in an attempt to improve oxidation resistance at the higher temperature range of 800°-1000°C. The high-manganese austenitic alloys do not appear to have suitable oxidation resistance at these higher temperatures as discussed earlier.[1,7,9] Approximately fifty Fe-Mn-Al and several Fe-Mn-Cr-Al alloys were prepared by a levitation melting technique. Specimens in the as-cast condition were oxidized at 800°C for 24 hours under an oxygen pressure of 200 torr. Some selected alloys were also tested for 100 hours at 600°, 800°, and 1000°C.

Table 6 shows the weight gain data in 800°C/24 hour tests on the various Fe-Mn-Al alloys. Based on these results the most optimum composition for 800°C service was: 5-10 Mn, 6-10 Al, bal. Fe.

Table 6. Weight Gains for 24 Hours Oxidation ($\Delta W/24$) at 800°C (mg. $cm.^{-2}$). Marked Area Showing Optimum Composition Range for Fe-Mn-Al System (ref. 15).

Al \ Mn	1	2.5	5	7.5	10	15	20	25	30
5				1.043	.167				
6	.828	.157	.123	.046	.054	.223	1.16*		
7	.356	.114	.033		.046	.127	.253	.436	
8	.041	.067	.038			.116	.102	.174	.367
9	.057	.072	.021		.085	.123	.166		.169
10	.062	.061					.155	.138	
11									.166
12									.136
13		.053				.155			
14		.091							
15			.074						
16					.151	.191			

*Specimen only oxidized for 18 hours.

The weight gains and compositions of some of the Fe-Mn-Cr-Al alloys oxidized for 24 and 100 hours at 800°C under 200 torr oxygen pressure are shown in Table 7. The most protective scales with minimum weight gain were found in alloys containing 5% Al, <15% Mn, and >5% Cr.

Table 7. Weight Gain and Composition of Some Fe-Mn-Cr-Al Alloys (ref. 15).

Alloy Composition			Weight gain at 800°C (mg cm^{-2})	
Fe-%Mn-%Al-%Cr			24 Hours	100 hours
5	4	5	.292 (18 hrs)	--
5	5	5	.068	.327
7.5	4	5	.196	.420
7.5	5	3	.122	.493
7.5	5	5	.063	.215
10	4	5	.115	--
10	4	12	.061	--
15	5	5	2.663	--

The results on two alloys tested for 100 hours at 600°, 800°, and 1000°C under 200 torr oxygen pressure are shown in Table 8. Convoluted scales with almost identical morphologies and composed of an outer layer rich in Mn and Al, and an inner layer of Al_2O_3, formed on both alloys oxidized at 1000°C.

Table 8. 100 Hour Oxidation Tests (ref. 15)

Alloy Composition		Weight Gain (mg cm^{-2})		
Fe-%Mn-%Al		600°C	800°C	1000°C
10	6	.171	.117	.450
20	8	.101	.242*	.253*

*Weight gains unreliable due to oxide spallation.

Based on this work the authors concluded that suitable alloys from the Fe-Mn-Al system can be produced with oxidation resistance at 800°-1000°C equivalent to that of heat resisting stainless steels. The final formulation of these alloys by possible addition of Cr, C, and rare earths is now being undertaken in order to develop better room temperature properties and high temperature strength.

OTHER UNPUBLISHED AND ONGOING WORK

1. University of Leeds, U.K. - G. E. Hale (ref. 19)

This work performed by G. E. Hale constitutes a part of his soon to be submitted Ph.D. thesis at the University of Leeds. It concentrated mainly on the austenitic alloy with about 30Mn, 8Al, 0.8-1.0C, bal. Fe. Some work was also done on a duplex austenitic/ferritic alloy and a fully ferritic material. The composition of various alloys studied are shown in Table 9.

Table 9. Alloy Compositions (ref. 19)

ALLOY NO.	ROOM TEMPERATURE MICROSTRUCTURE	COMPOSITION				
		Mn	Al	C	Fe	Others
2	Austenitic	30.4	7.6	0.81	BAL	0.014N, 0.36Si 0.009S, 0.017P
3	Austenitic/ Ferritic	17.1	5.0	0.07	BAL	0.06Si
4	Ferritic	8.9	6.9	0.07	BAL	0.007P
5	Austenitic	30.9	8.0	0.97	BAL	0.008N, 0.17Si 0.011S, 0.007P

The Ferritic Alloy:

The ferritic alloy No. 4 shows a distinct "script" phase together with intergranular grain boundary precipitation in the as-cast state (Figure 16), but this can be removed by hot rolling and/or solution treatment at temperatures of 1100°C and above, followed by water quenching. The exact nature of this "script" phase has not yet been determined. Unfortunately, this alloy has proved extremely difficult to machine and very brittle at room temperature with a Charpy impact energy of only about 4 Joules. Aging after a high temperature solution treatment followed by quenching results in a fine precipitation in both the grain boundaries and grain interiors. No distinct increase in hardness was detected with increasing aging time, however.

The Duplex Alloy:

The duplex alloy No. 3 shows some interesting effects and may well be worth more detailed study. After hot rolling, the alloy contained 73% austenite and 27% ferrite (the relative proportions of the two phases were measured with an X-ray diffractometer), but on solution treating at 1200°C and higher followed by rapid quenching (preferably into iced brine), the alloy becomes single phase ferrite in fairly thin sections (1-2 mm). Larger sections and/or slower cooling rates lead to austenite precipitation both at ferrite grain boundaries and also within the grains.

Reheating the quenched material allows austenite reversion to occur and the amount of austenite formed can be controlled by varying the temperature and time of the reversion treatment as shown in Table 10. This experiment was performed in samples measuring less than 3 mm in thickness. In larger sections the proportion of austenite formed is generally higher due to slower cooling rate.

Table 10. Influence of Reheating on the Percent Austenite Formed in the Duplex Alloy No. 3 (ref. 19)

Reheat Temperature (°C)	% Austenite
1250°C/30 mins/IBQ*	16.5**
150°	10.5
200°	14
400°	18
600°	15.5
700°	51
800°	62
1000°	68.5

All specimens were solution treated at 1250°C for 30 minutes in silica tube (under a partial atmosphere of argon), quenched into iced brine and then reheated at the temperatures shown for one hour followed by water quenching.

* IBQ: Ice Brine Quench
** Quenching out of silica tube gives a slower cooling rate than a direct quench from air and this has caused some austenite precipitation during cooling.

Tensile and impact data have been measured for this alloy in the hot rolled duplex state and are given in Tables 11 and 12, respectively.

Table 11. Tensile Data at Room Temperature for Alloy No. 3 in the Hot Rolled Condition (ref. 19)

UTS(MPa)	0.2% PROOF STRESS (MPa)	% REDUCTION IN AREA	% ELONGATION (15 mm gauge length)
625	485	80	32

Table 12. Energy Absorbed in Charpy V-Notch Test for Alloy No. 3 in the Hot Rolled Condition (ref. 19)

TEMPERATURE (°C)	IMPACT ENERGY (JOULES)
20	193
0	193
-40	148
-70	102
-85	98
-196	32

These figures show acceptable strength levels coupled with fairly good toughness down to at least -85°C (98 Joules). At -85°C, the predominant failure mode was transgranular ductile by microvoid coalescence. Some small areas of cleavage were observed and presumably these are associated with the ductile-to-brittle transition within the ferrite. It is clear, however, that the predominantly austenitic matrix restricts the propagation of any cracks which originate in the ferritic regions.

The absence of a rapid ductile-to-brittle transition in this alloy unlike that observed in certain ferritic steels suggests that alloys of this type could be useful in certain cryogenic applications.

Some limited impact energy data have been measured in samples containing about 25% austenite obtained by a reversion treatment mentioned above. The impact energy of this specimen at -40°C was only about 27 Joules compared to 148 Joules for the hot rolled sample (Table 12) with 73% austenite. This is consistent with previous observations of decreasing ductility with decreasing austenite content of these alloys.(1) The fracture mode of the sample with 25% austenite was predominantly brittle

transgranular cleavage with small areas of ductile fracture around reformed austenite forming a continuous network along the prior ferrite grain boundaries. This amount of austenite is apparently not sufficient to arrest brittle cracks originating from the ferritic matrix. This result again emphasizes the inherently brittle nature of the ferritic Fe-Mn-Al alloys.

The Austenitic Alloys:

A large proportion of this work has been centered on austenitic alloys with compositions close to Fe-30Mn-8Al-1C. Transmission electron microscopy was used to help characterize the aging behavior of these alloys.

Hardness versus Aging Time curves were produced for Alloys 2 and 5 at temperatures between 450° and 650°C. In the case of Alloy No. 2, Figure 17, the classic type of age-hardening response was observed with lower temperatures eventually achieving higher hardness values but at greatly increased times.

For Alloy No. 5, Figure 18, aging between 450°C and 550°C showed the standard type of hardness-time curves, while above 600°C, the maximum hardness was lower and occurred after a longer time due to overaging.

In Alloy No. 5, the hardness values were always somewhat lower than those measured for Alloy No. 2 at the same temperature. The solution treatment temperature in both cases was 1050°C for one hour followed by water quenching. It is not yet clear why there is a difference in the aging behavior of the two alloys; the only compositional difference being the carbon content.

The transmission electron micrographs in Figures 19-23 show the fine structure which develops in this material on aging. Selected area diffraction analysis has indicated that these precipitates form along <100> directions in the austenite matrix and exhibit a cube-cube orientation with

the austenite, Figure 20. Selected area diffraction analysis also shows the presence of super-lattice spots and that the precipitate has a simple cubic structure and is likely to be ordered. This has been confirmed by x-ray analysis of the extracted precipitate particles, from which a lattice parameter of 379.6 pm was measured and this is in good agreement with the published data for Iron Aluminum Carbide Fe_3AlC, although the interplanar spacings for Manganese Aluminum Carbide Mn_3AlC are also similar. It would appear that the precipitate is a Fe_3AlC type in which there has been some partial substitution of manganese for iron. This has been further confirmed by energy dispersive x-ray analysis (EDX) of the precipitate powder in the scanning electron microscope where iron, manganese and aluminum peaks were detected. (EDX analysis does not detect elements below sodium and therefore carbon cannot be observed by this method.)

The tensile and impact properties of the two alloys both in the solution treated (ST) and quenched condition and after aging at close to the peak hardness values have been measured, Table 13, and are similar to those determined by other workers.

The effect of aging time at 550°C (Alloy No. 5 after solution treatment: 1050°C/1h/WQ) on the tensile properties is shown in Figure 24. With short aging times, it is possible to further improve the strength without too great a loss in ductility. However, the low temperature impact strength drops off rather drastically on aging.

For example, the room temperature impact energy after 1 hour aging at 550°C is still a respectable 119 Joules (Table 13) at -196°C it drops to 5 Joules. The impact energy of the solution treated material shows a small drop from 206 Joules at room temperature to 192 Joules at -90°C and then falls to 106 Joules at -196°C -- still a very high value and a low

Table 13. Tensile and Impact Data for Alloy No. 5 and No. 2 (ref. 19)

ALLOY NO. 5

Heat Treatment Condition °C/hr/WQ	UTS (MPa)	0.2%PS (MPa)	% Reduction in Area	% Elongation (over a 15mm gauge length)	Charpy V-Notch Impact Energy (Joules) at 20°C
ST 1050/1/WQ (ST)	860	440	71	71	206
ST + 550/1/WQ	885	660	59	48	119
ST + 550/6/WQ	1030	850	49	46	8.1
ST + 550/16/WQ	1040	890	49	28	N/M
ST + 550/48/WQ	1000	850	28	20	N/M
ST + 500/16/WQ	955	825	52	32	23
ST + 600/16/WQ	1015	890	37	32	5.4
ALLOY NO. 2					
ST 1050/1/WQ	900	460	65	69	--
ST + 600/12/WQ	1100	920	25	34	--

N/M: Not measured for this treatment.

ductile-brittle transition temperature. Therefore, the increases in strength which occur with aging are offset by a substantial decrease in toughness together with a measurable loss of ductility as well. The aged material failed in a predominantly intergranular brittle mode and was caused by the grain boundary precipitates which are present in the peak-hardened state.

2. University of Calgary, Canada - W. J. D. Shaw et. al. (ref. 20)

The work has just started this summer focusing on the creep behavior of an Fe-Mn-Al steel. The high temperature environmental (in steam) creep and electrochemical corrosion behavior will also be studied. Preliminary results of the short time creep tests are shown in Table 14 for an alloy (#SB-8-24-2) containing 30.1Mn-8.3Al-1.5Si-1.07C-Fe bal. in the hot rolled condition. These early results indicate the creep characteristics of this alloy to be equivalent to 9Cr-1Mo steels but infoerior to 304 SS. The microstructural characterization and the corrosion tests will be starting shortly.

3. Virginia Polytechnic Institute and State University, Blacksburg, VA - J. H. Wilson, T. Sudarshan et. al. (ref. 21)

This work is also just getting underway. The major emphasis here will be to study the effects of humidity and hydrogen on the tensile strength and torsional fatigue life of Al-Mn stainless steels. In addition, the effects of oxygen and hydrogen on the crack growth rates will also be determined. The initial alloys being tested have the following compositions (Table 15).

Table 15. Composition of Fe-Mn-Al Alloys Being Studied at VPI&SU

Alloy	%Mn	%Al	%Si	%C	%Fe
SB-8-24-1	30.1	8.3	0.12	1.07	bal.
SB-8-24-2	30.1	8.3	1.54	1.07	bal.

Sept. 15/82
Dr. W.J.D. Shaw
Dept. of Mech. Engg.
Univ. of Calgary

Table 14

Mn-Al Steel
SB-8-24-2
Preliminary Creep Results

Spec. Number	Stress, Psi	Temperature, °F	Time to failure, hrs.	Avg.creep rate in/in/hr $x10^{-3}$	Total extention in$x10^{-3}$
5	40,000	1150	42.4	0.94	60
10	40,000	1000	198.8	0.35	105.1
4	20,000	1300	19.9	2.3	74.2
1	20,000	1300	17.5	2.5	77.2
3	20,000	1150	151	0.62	140.7
9	20,000	1200	84	2.22	280
2+	20,000	1000	1001.4	0.10	146
11*	20,000	1000	136.5	0.05	9.8
7	10,000	1150	763.1	0.14	160
8*	5,000	1150	930	0.02	30

* Test still in progress

\+ Stopped prior to failure occurring

The first samples cathodically charged with hydrogen and also charged during tensile straining showed approximately the same degree of susceptibility to hydrogen embrittlement as most common austenitic stainless steels. Intergranular fracture, typical of hydrogen-induced cracking was observed, Figure 25. Utility of these steels in food processing and fertilizer industries is envisioned depending on the results of this work.

4. EG&G Idaho, Inc., Idaho Falls, ID - G. Korth (ref. 22)

A major program on Mn-Al steels has also started recently at EG&G Idaho. This will be a rather comprehensive study involving tensile, impact, creep, fatigue, corrosion, stress-corrosion and weldability properties of these steels. Two alloys with about 30Mn/8Al/1C/Fe, one without Si and one with 1.5% Si have been produced for the initial tests. Early indication of weldability is encouraging. Some corrosion test coupons in geothermal wells are being tested. Other experimental work is just beginning.

SUMMARY

In summary, it is gratifying to note that considerable progress has been made over the past year and a half on the evaluation and characterization of Fe-Mn-Al alloys. However, most of the work done and the information presented in this report are somewhat preliminary in nature. Much work still remains to be done for complete evaluation and understanding of various properties of this alloy system. It appears that in certain applications such as heat resistant materials at moderate temperatures, corrosion resistance in some environments, higher strength-to-weight ratio materials, and cryogenic applications, etc., these alloys offer good substitution potentials for chromium-bearing steels.

It is hoped that the interested agencies will offer assistance and encouragement for continued and more thorough investigations of this new family of steels, offering one option in the search for conservation and substitution technology for chromium.

ACKNOWLEDGEMENTS

The continued interest of Dr. Allen Gray in the Fe-Mn-Al alloys as potential substitutes for Cr-bearing steels is greatly appreciated. The author is grateful to the ASM and the AIME for providing the preprints of the manuscripts of the two papers by R. Wang et. al. and the paper by K. Narasimha Rao et. al., respectively. The efforts of the individual contributors who have privately communicated with the author and provided the information and results of their work presented in this report are gratefully recognized. I also wish to express my special thanks to F. Boratto and P. Tomas for providing the reprints of the papers published in Brazil and Australia. Finally, I wish to acknowledge the continued support of Foote Mineral Company and its permission to present this report.

REFERENCES

1. S. K. Banerji; "An Update on Fe-Mn-Al Steels," Proc. of the Workshop on "Conservation and Substitution Technology for Critical Materials," Vanderbilt University, Nashville, TN, USA, held June 15-17 (1981).

2. S. K. Banerji; "An Austenitic Stainless Steel Without Nickel and Chromium," Metal Progress, p. 59, April (1978).

3. S. K. Banerji; "An Austenitic Stainless Steel Without Nickel and Chromium," Trans. Indian Inst. of Metals, Vol. 30, No. 3, p. 186, June (1977).

4. J. C. Garcia, N. Rosas and R. J. Rioja; "Development of Oxidation Resistant Fe-Mn-Al Alloys," Metal Progress, p. 47, August (1982).

5. R. Wang and F. H. Beck; "An Austenitic Mn-Al-Si Steel for Propellers of Sea-Going Vessels," to be published in Metal Progress.

6. R. Wang and R. A. Rapp; "Marine Corrosion Behavior of Several Fe-Mn-Al Austenitic Steels," to be submitted for publication.

7. K. Narasimha Rao, R. Sivakumar and M. L. Bhatia; "An Evaluation of Al-Mn-C Austenitic Steel," submitted to Journal of Metals.

8. L. C. Casteletti and D. Spinelli; "The Resistance to Oxidation and the Electrical Resistivity of an Fe-Mn-Al System Alloy," Dept. of Matls. Sci., EESC, Univ. of Sao Paulo, Sao Carlos, Brazil; Proc. XXXVI, Brazilian Soc. for Metals (ABM) Annual Congress, p. 249, held in Recife, Pernambuco, Brazil, July 5-10 (1981).

9. F. C. R. Assuncao and M. F. da S. Lopes; "Study of Oxidation of Fe-Al-Mn-C Alloy at High Temperatures," Dept. Matls. Sci. & Met., Catholic Univ., Rio de Janeiro, Brazil, ibid, p. 329.

10. A. J. A. Bushinelli, J. C. Dutra and W. May; "Study of the Microstructural Transformations in TIG Welding of an Fe-Al-Mn Alloy," Fed. Univ. of Santa Catarina, Florianapolis, Brazil, ibid, p. 521.

11. L. C. Casteletti and D. Spinelli; "Mechanical Properties of an Austenitic Steel of the System Fe-Mn-Al," Dept. Matls. Sci., EESC, Univ. Sao Paulo, Sao Carlos, Brazil, ibid, p. 299.

12. A. P. Tschiptschin and H. Goldenstein; "Precipitation Reactions in Low-Carbon Fe-Mn-Al Alloys," Dept. Met. Eng., Univ. of Sao Paulo, Brazil, ibid, p. 117.

13. J. R. T. Branco and F. J. M. Boratto; "Domain of the Austenitic Phase in the Fe-Mn-Al System at 1000°C," Met. Tech. Section, Tech. Center Found. of Minas Gerais-CETEC, Belo Horizonte, Brazil, ibid, p. 175.

14. P. Tomas; "Elements Essential to High Temperature Sulphidation Resistant Iron-Based Alloys," Univ. of New South Wales, Kensington, NSW, Australia, Proc. 35th Annual Conf. of the Australasian Inst. of Metals, p. 90, held in Sydney, Australia, May (1982).

15. P. R. S. Jackson and G. R. Wallwork: "The Development of Fe-Al Alloys for High Temperature Oxidation Resistance," Univ. of New South Wales, Kensington, NSW, Australia, ibid, p. 78.

16. D. J. Chakrabarti; "Phase Stability in Ternary Systems of Transition Elements with Aluminum," Met. Trans. B, Vol. 8B, p. 121, March (1977).

17. P. Tomas and S. K. Banerji, private communication (1982).

18. R. A. Perkins; "Sulphidation-Resistant Alloy for Coal Gasification Service," Qtrly. Report #FE-2200-6, Lockheed, Palo Alto, CA (1976).

19. G. E. Hale, Dept. of Metallurgy, University of Leeds, Leeds, U.K.; Ph.D. thesis to be submitted, private communication (1982).

20. W. J. D. Shaw, Dept. of Mech. Eng., University of Calgary, Calgary, Alberta, Canada; private communication (1982).

21. T. Sudarshan and J. H. Wilson, Depts. of Materials and Agricultural Eng., VPI&SU, Blacksburg, VA, private communication (1982).

22. G. E. Korth, EG&G Idaho, Inc., Idaho Falls, ID, private communication (1982).

SKBanerji:erd
10/82

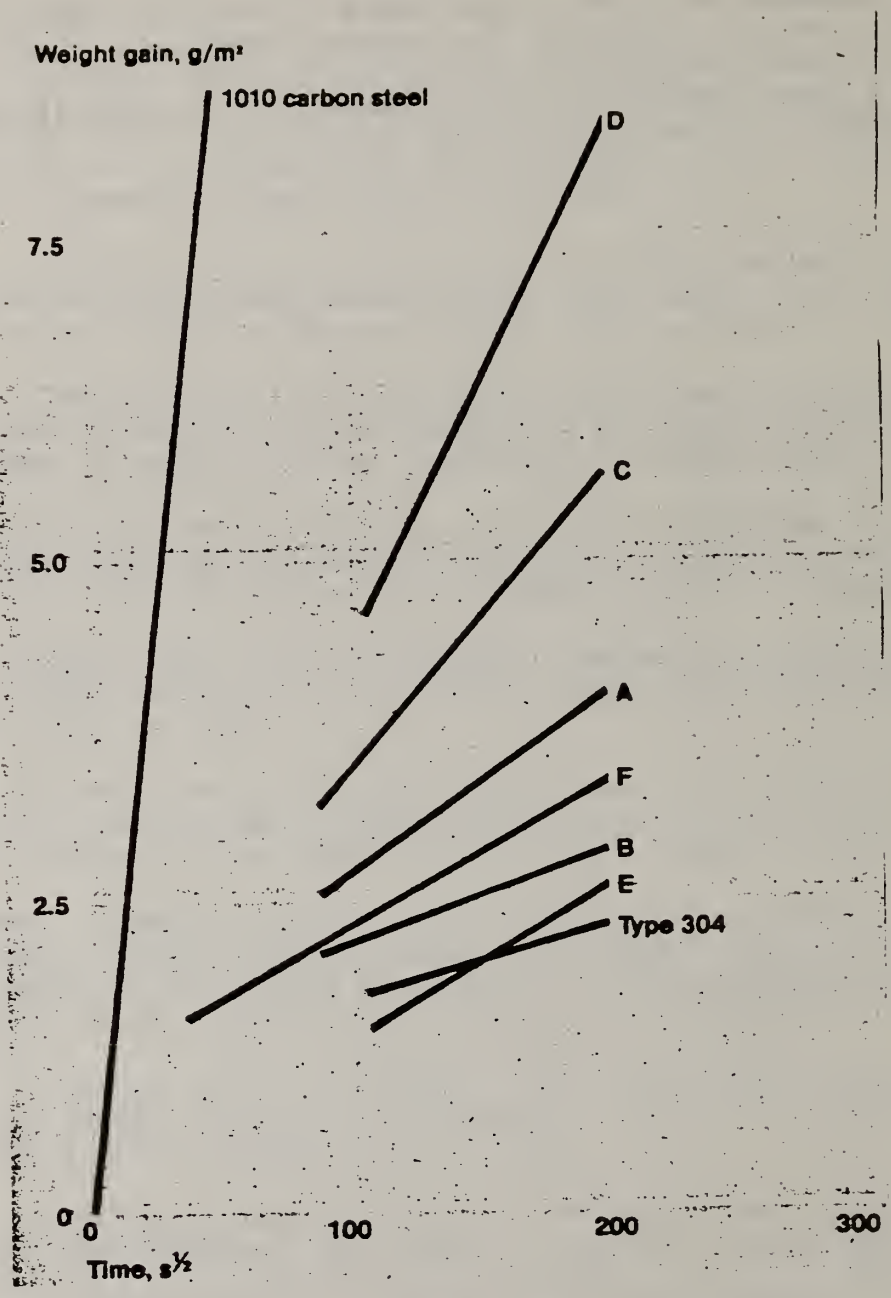

Fig. 1. Plots of weight gained versus time at 700°C (1290°F) for the six experimental alloys of Table 1, type 304 stainless steel, and a 1010 carbon steel. Parabolic regions of the data curves are presented here. Note that the slope for alloy B is similar to that for type 304. Pressure: 1 atm (100 kPa) of flowing oxygen. (ref. 4)

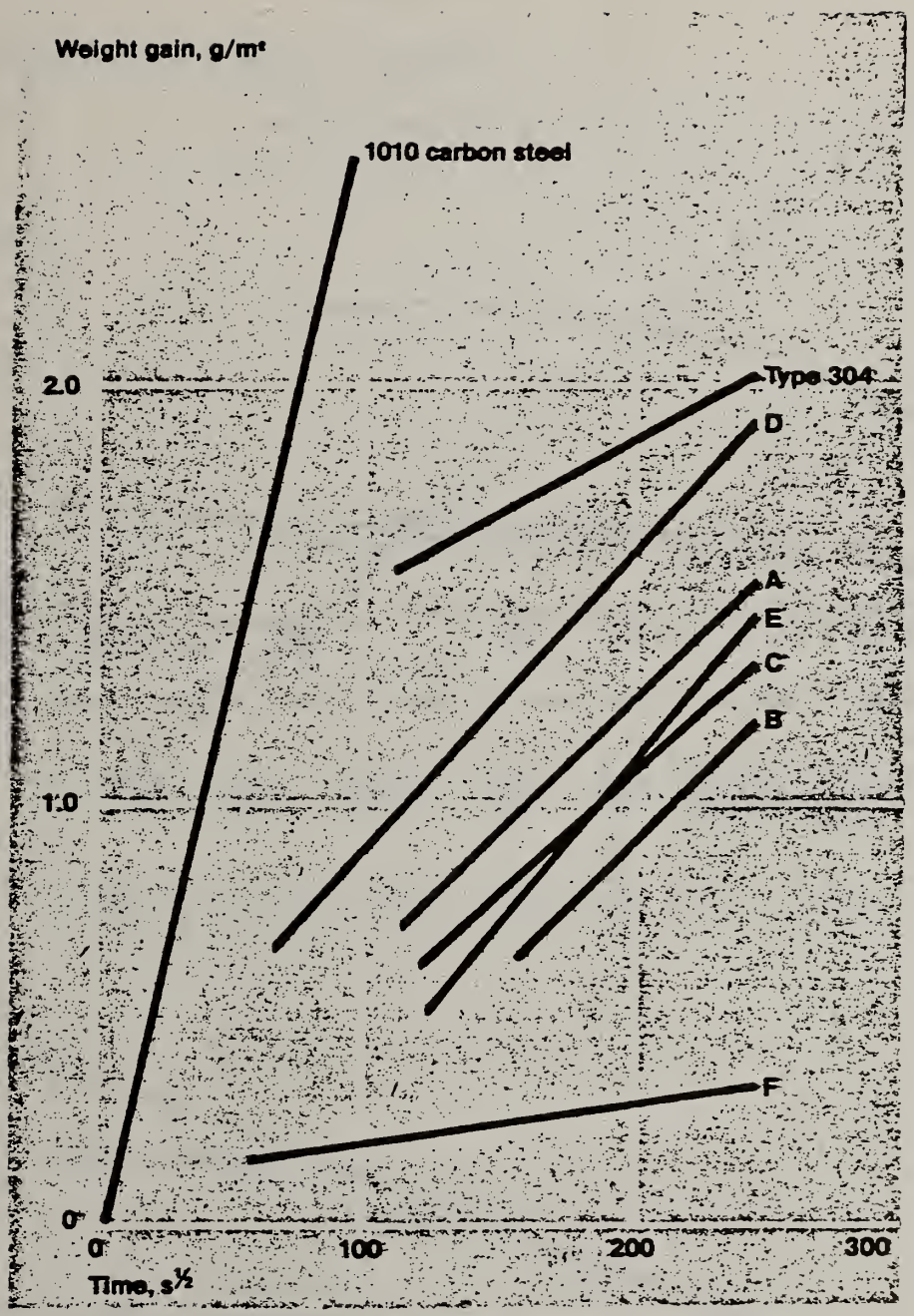

Fig. 2. Plot of weight gained versus time at 500°C (930°F) for the six experimental alloys of Table 1, type 304 stainless steel, and a 1010 carbon steel. Parabolic regions of the data curves are presented here. Note excellent behavior of alloy F. Pressure: 1 atm (100 kPa) of flowing oxygen. (ref. 4)

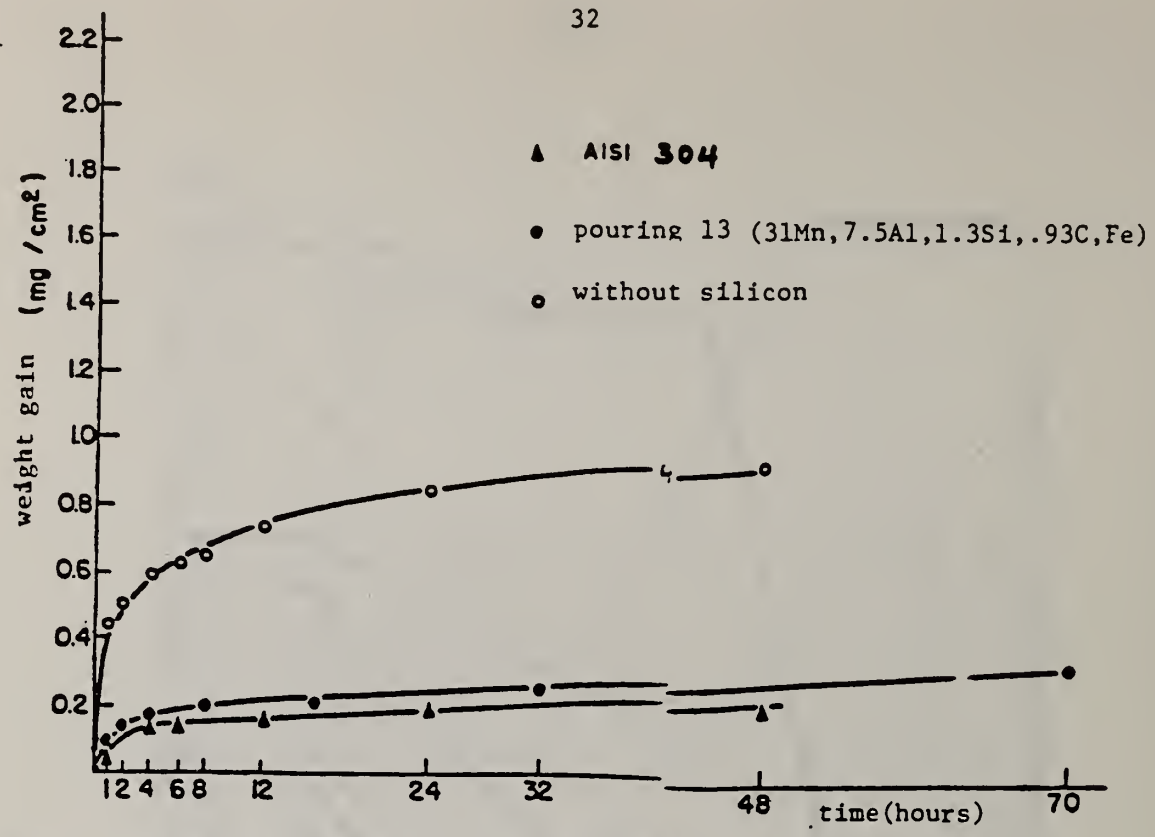

Fig. 3. Weight gain as a function of time at 700°C in air. (ref. 8)

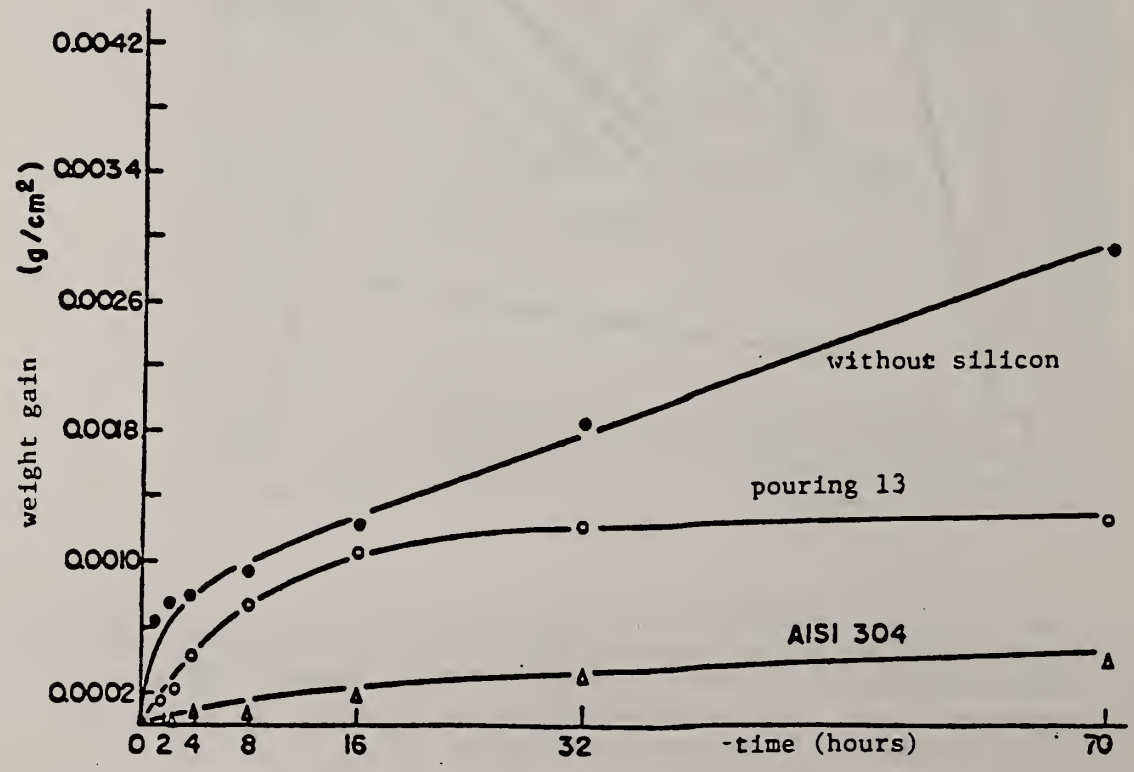

Fig. 4. Weight gain as a function of time at 800°C in air. (ref. 8)

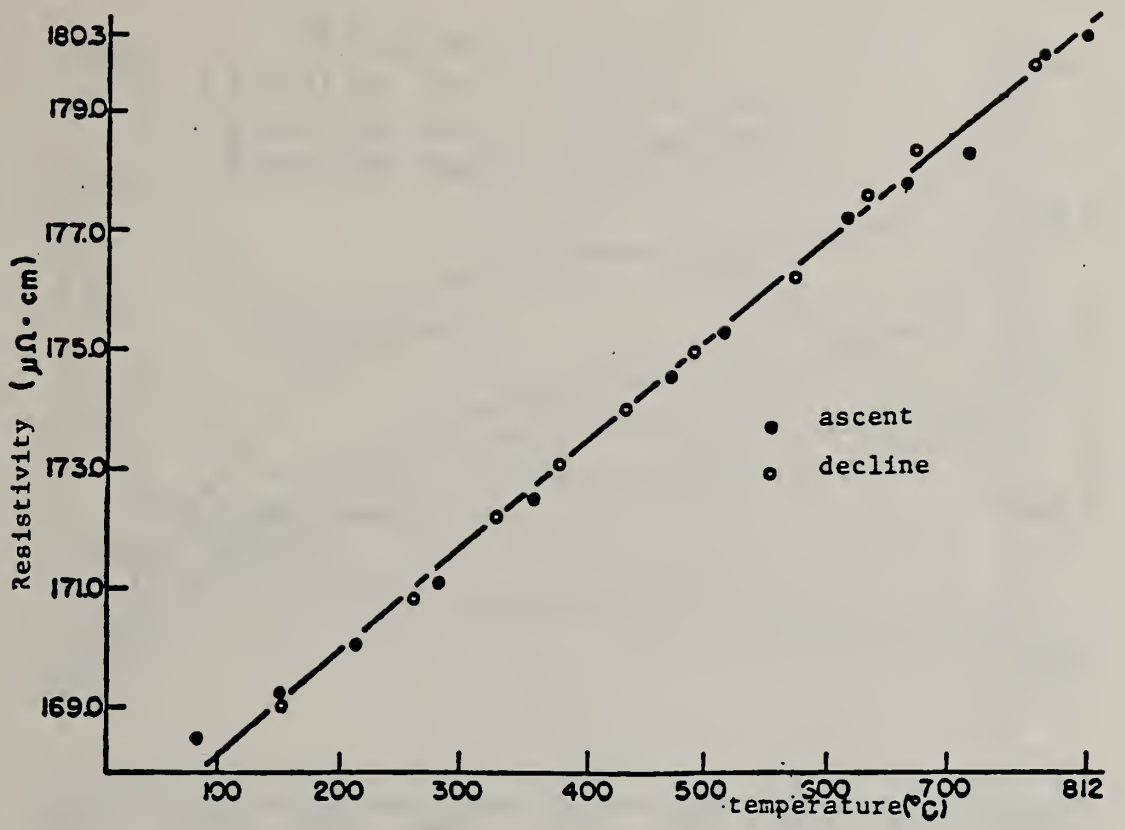

Fig. 5. Temperature dependence of resistivity for an Fe-31Mn, 7.5Al, 1.3Si, 0.93C alloy. (ref. 8)

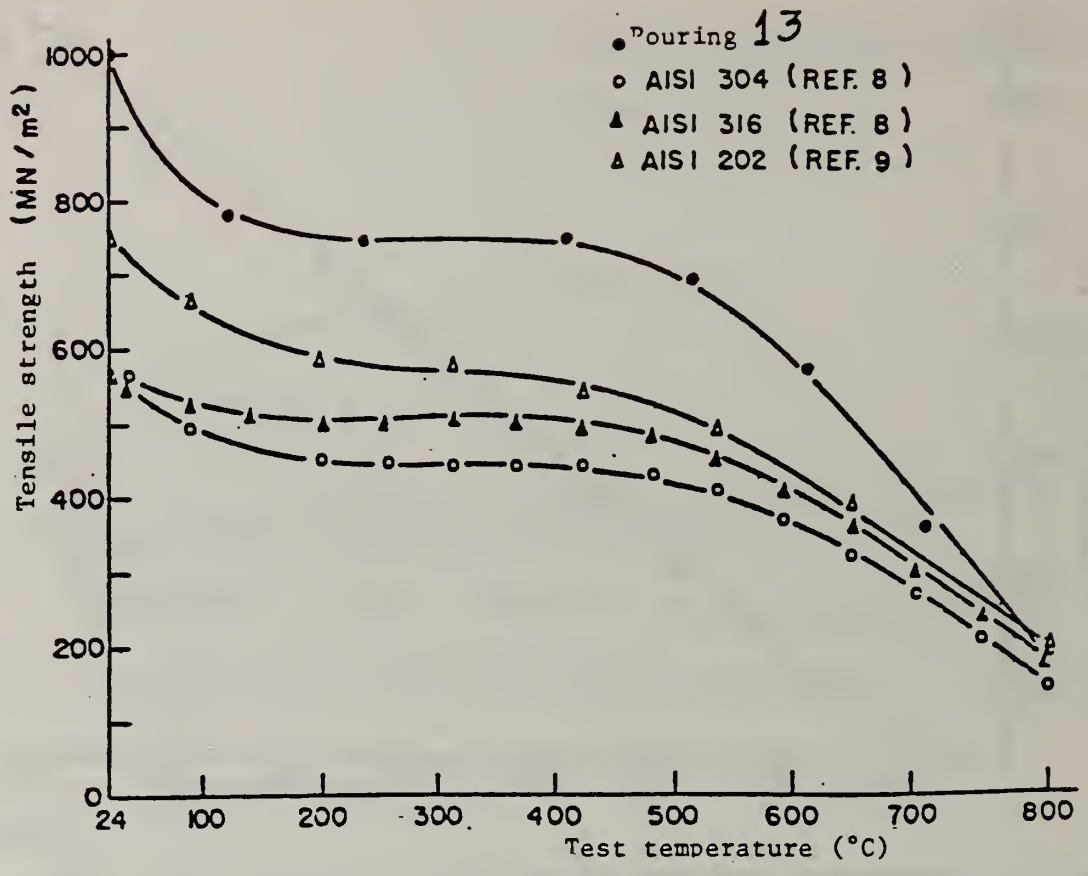

Fig. 6. Variation in tensile strength with temperature. (ref. 11)

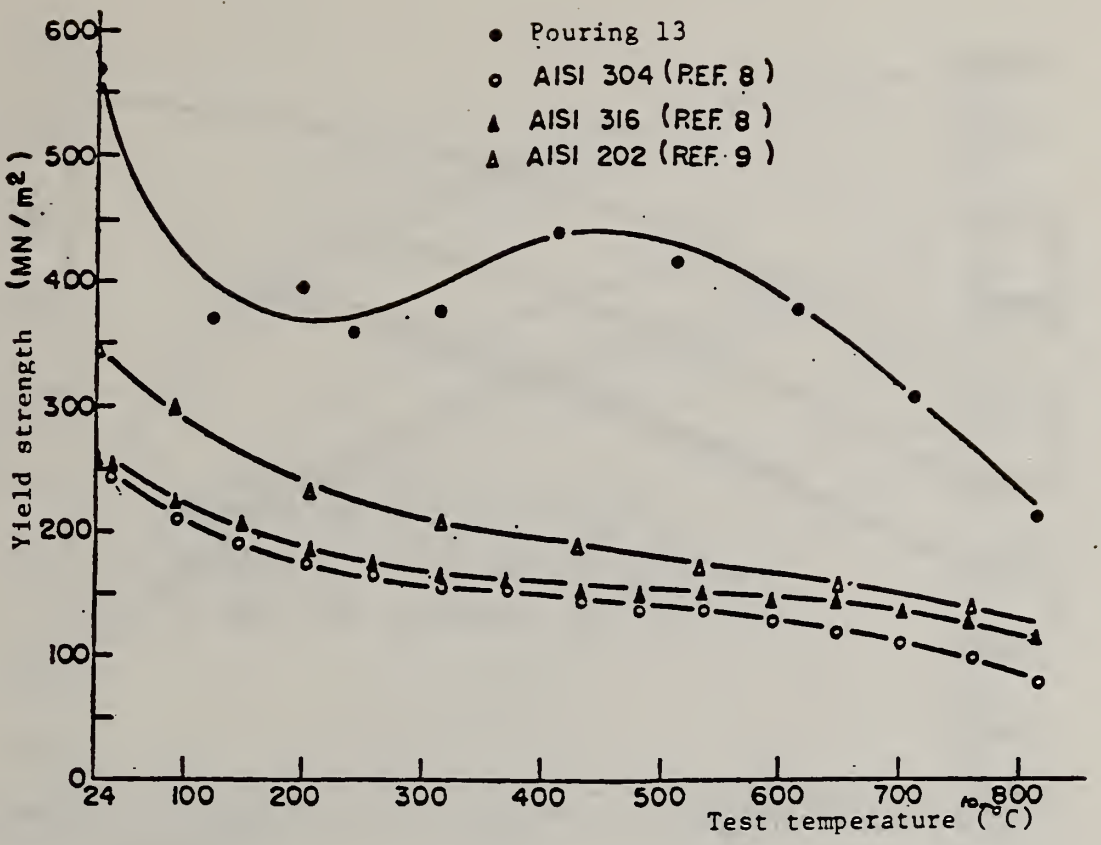

Fig. 7. Variation in yield strength with temperature. (ref. 11)

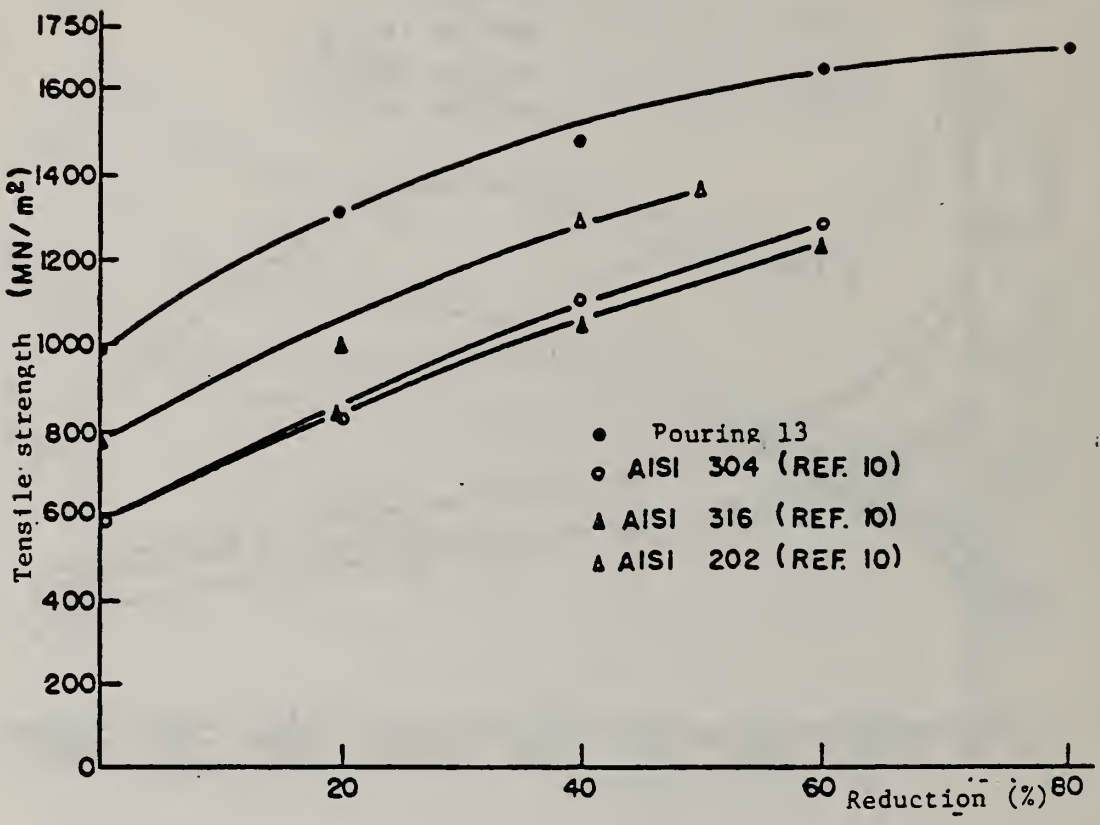

Fig. 8. Variation in tensile strength with the degree of reduction. (ref. 11)

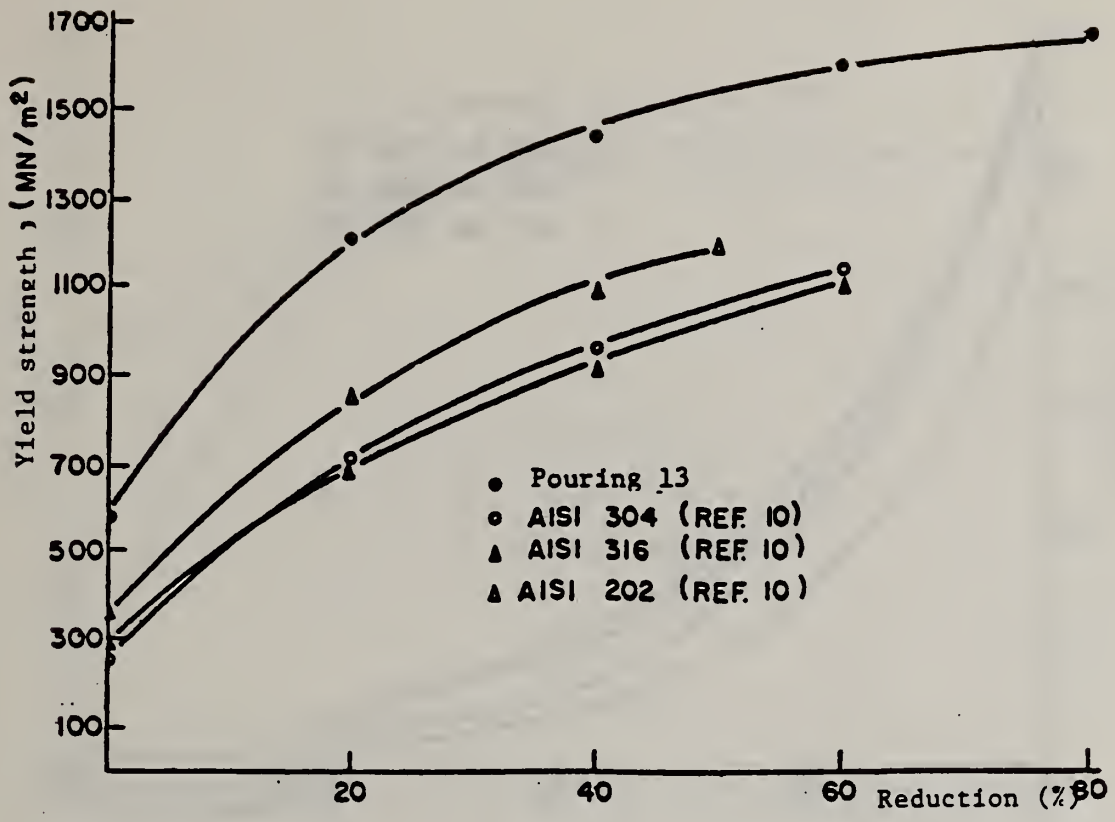

Fig. 9. Variation in yield strength with the degree of reduction. (ref. 11)

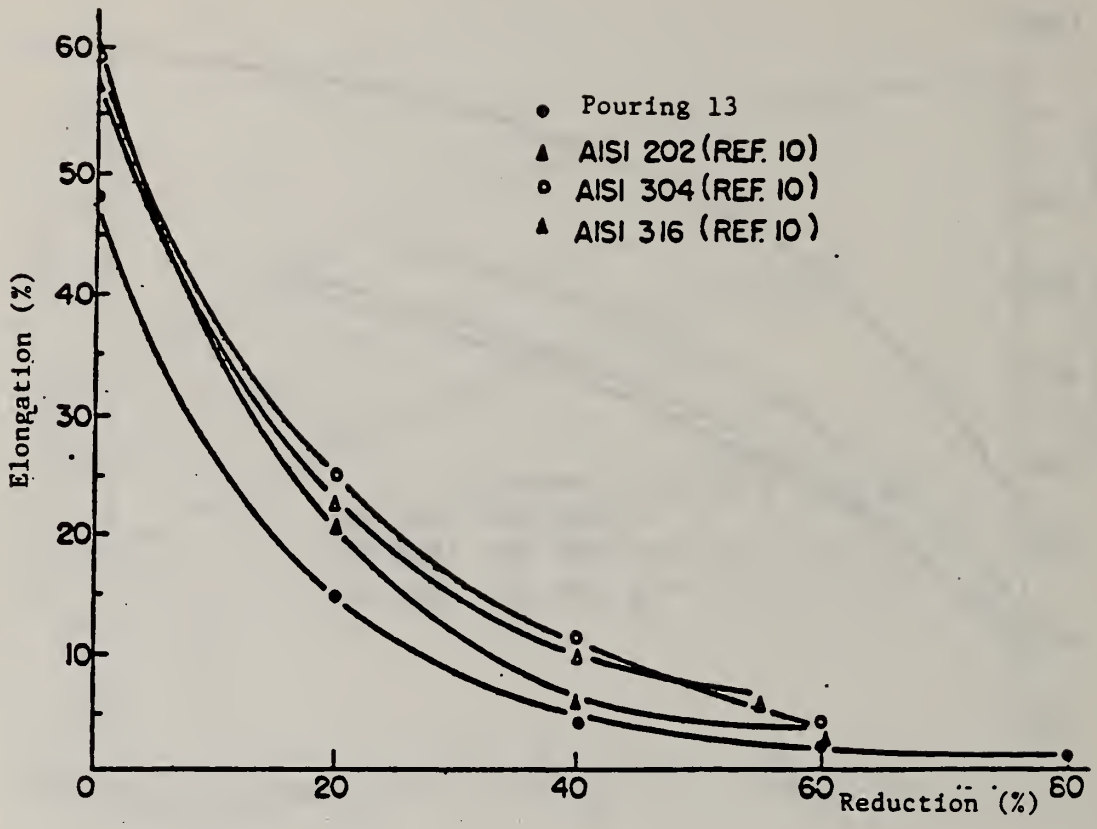

Fig. 10. Variation in elongation with the degree of reduction. (ref. 11)

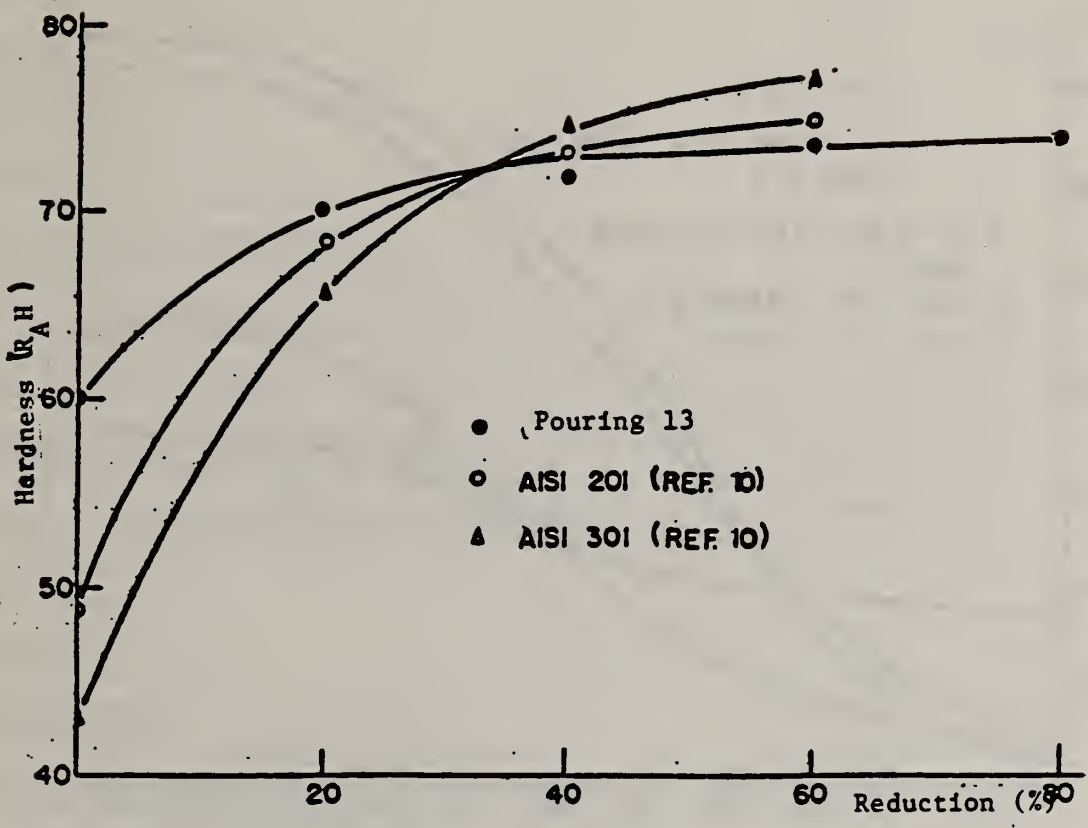

Fig. 11. Variation in hardness with the degree of reduction. (ref. 11)

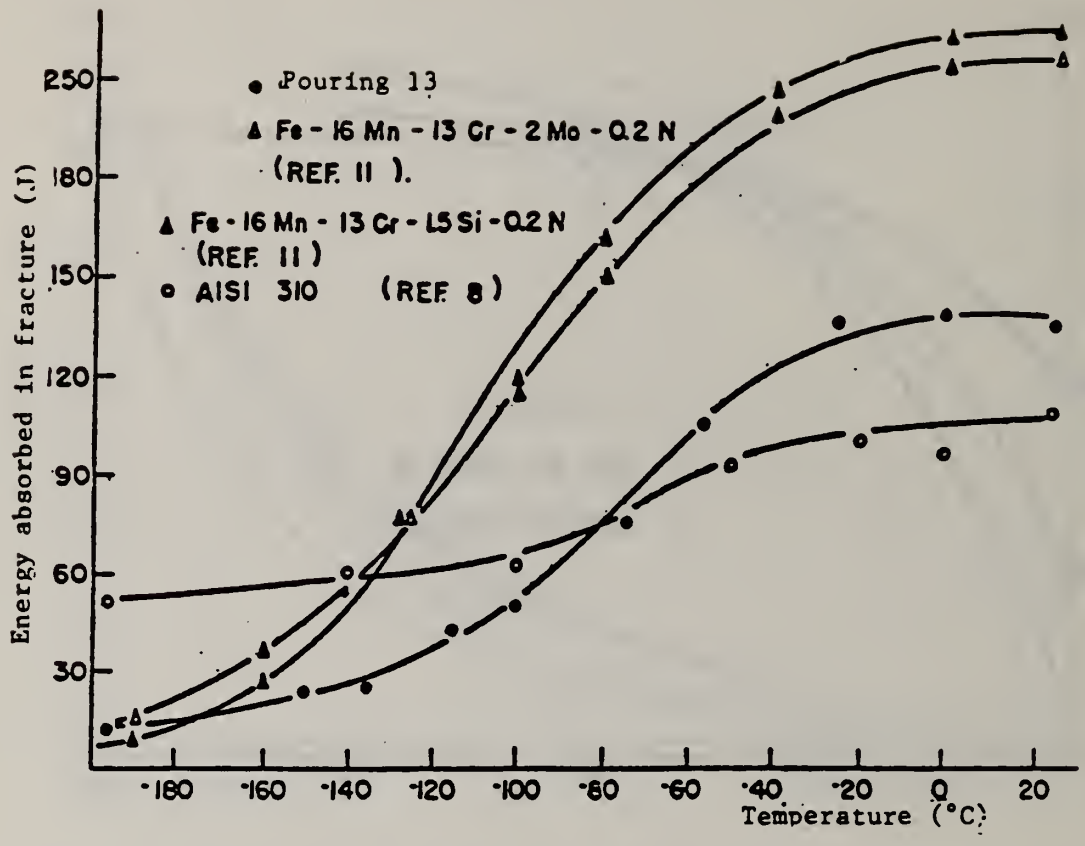

Fig. 12. Variation in the energy absorbed in impact with temperature. (ref. 11)

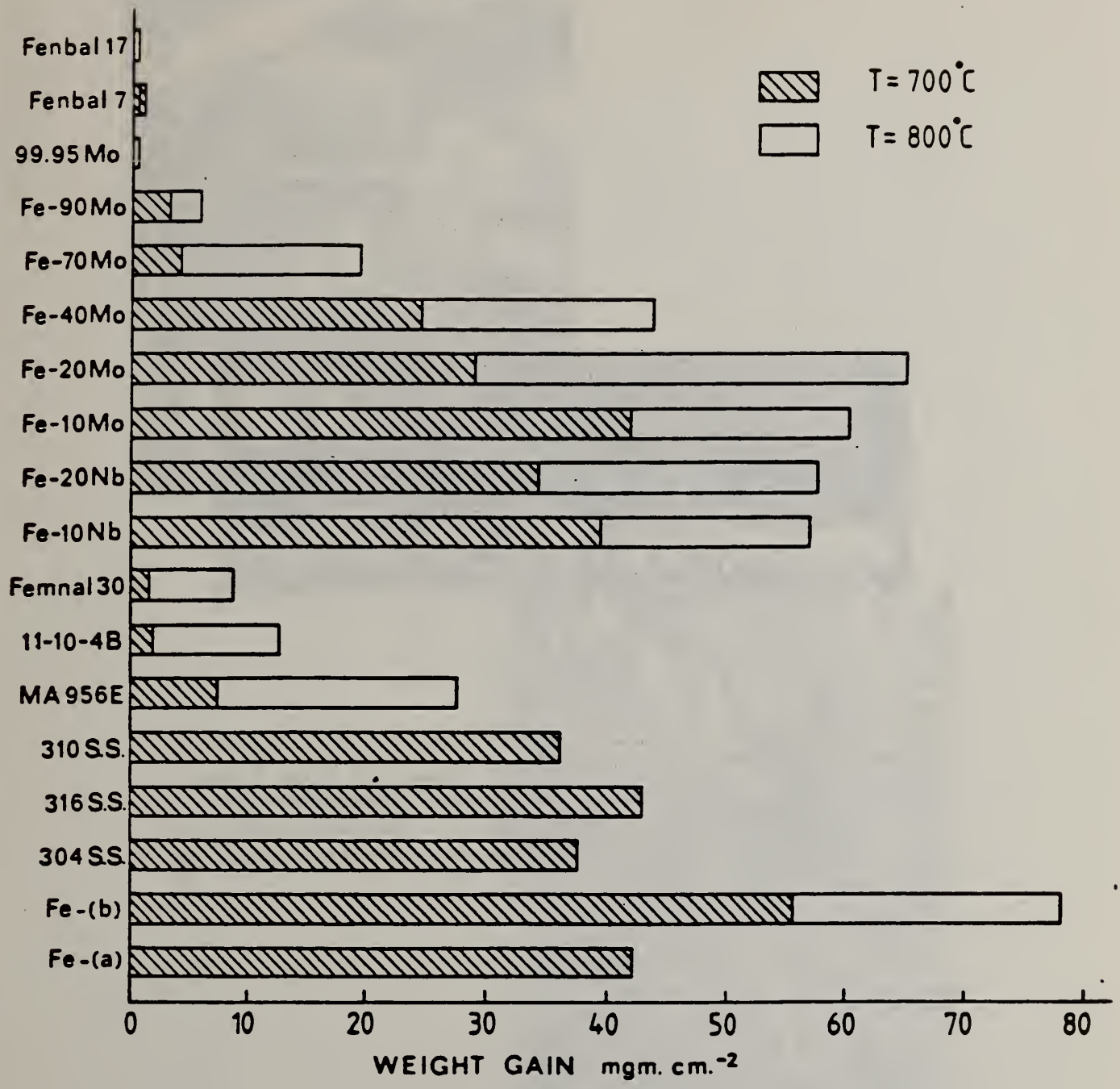

Fig. 13. A compilation of the weight gain data after 9 hours reaction in a gas mixture of hydrogen plus 1 volume % hydrogen sulphide; $pS_2 = 3 \times 10^{-9}$ Atm at 700°C and $pS_2 = 2.4 \times 10^{-8}$ Atm at 800°C. (ref. 14, 17)

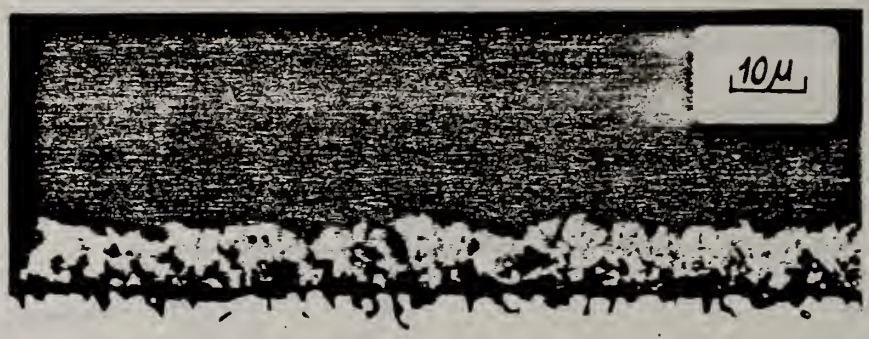

Fig. 14. Duplex Scale formation on Femnal 30 after 9 hours in H_2/1 vol. % H_2S at 700°C. Cross section of scale showing duplex layers. The outer layer is predominantly MnS and the peg-like inner layer is aluminum sulphide. (ref. 14)

(a)

(b)

Fig. 15. A comparison of the scale topographies present on two different Fe-Al-Mn-C alloys, (a) Femnal 30, and (b) 11-10-4B; 9 hours at 800°C in H_2 - 1 vol. % H_2S. (ref. 17)

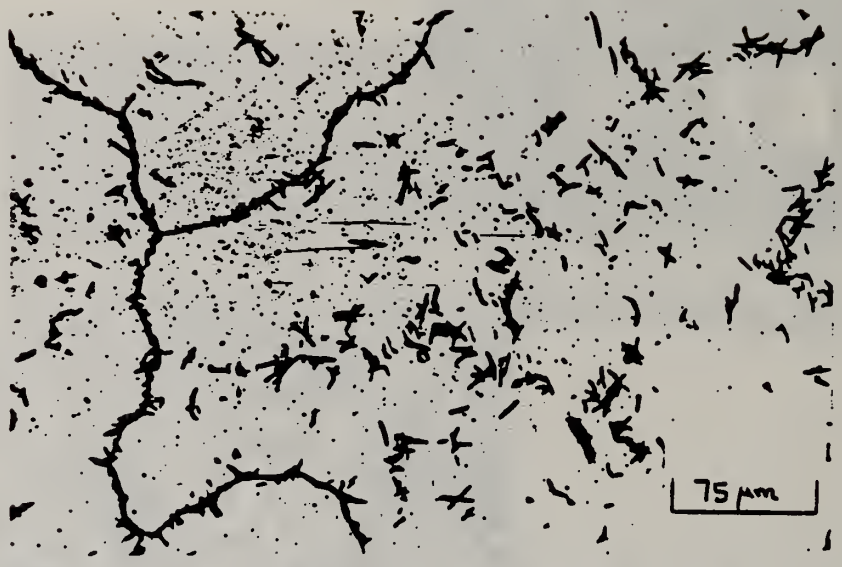

Fig. 16. Ferritic Alloy No. 4 (9Mn/7Al/.07C/Fe) - as cast state. (ref. 19)

Fig. 17. AGEING CURVES FOR AN Fe-30.4Mn-7.6Al-0.81C ALLOY (No. 2) AFTER SOLUTION TREATMENT AT 1050°C FOR ONE HOUR FOLLOWED BY WATER QUENCHING. (ref. 19)

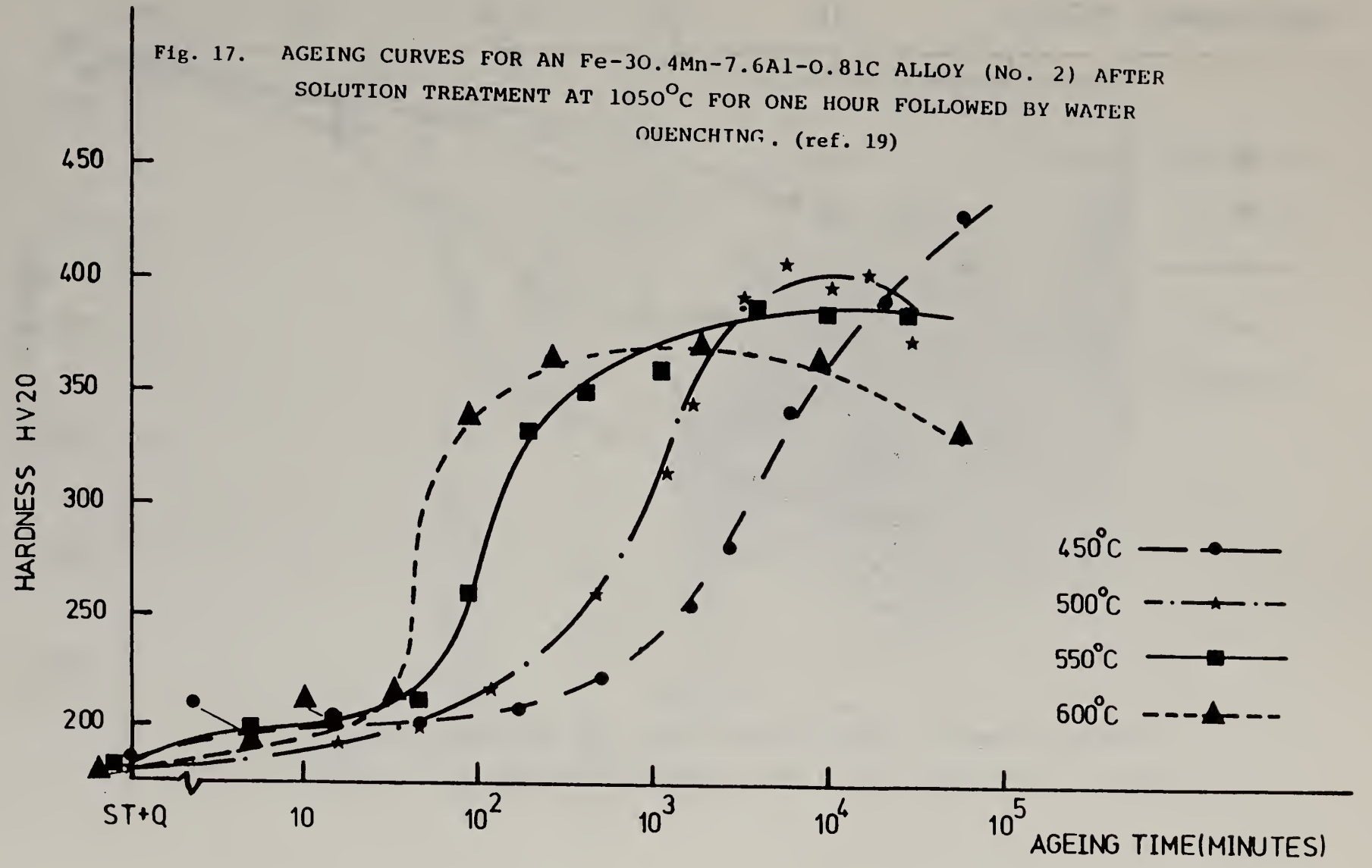

Fig. 18. AGEING CURVES FOR AN Fe-30.9Mn-8.0Al-0.97C ALLOY (No. 5) AFTER SOLUTION TREATMENT AT 1050°C FOR ONE HOUR FOLLOWED BY WATER QUENCHING. (ref. 19)

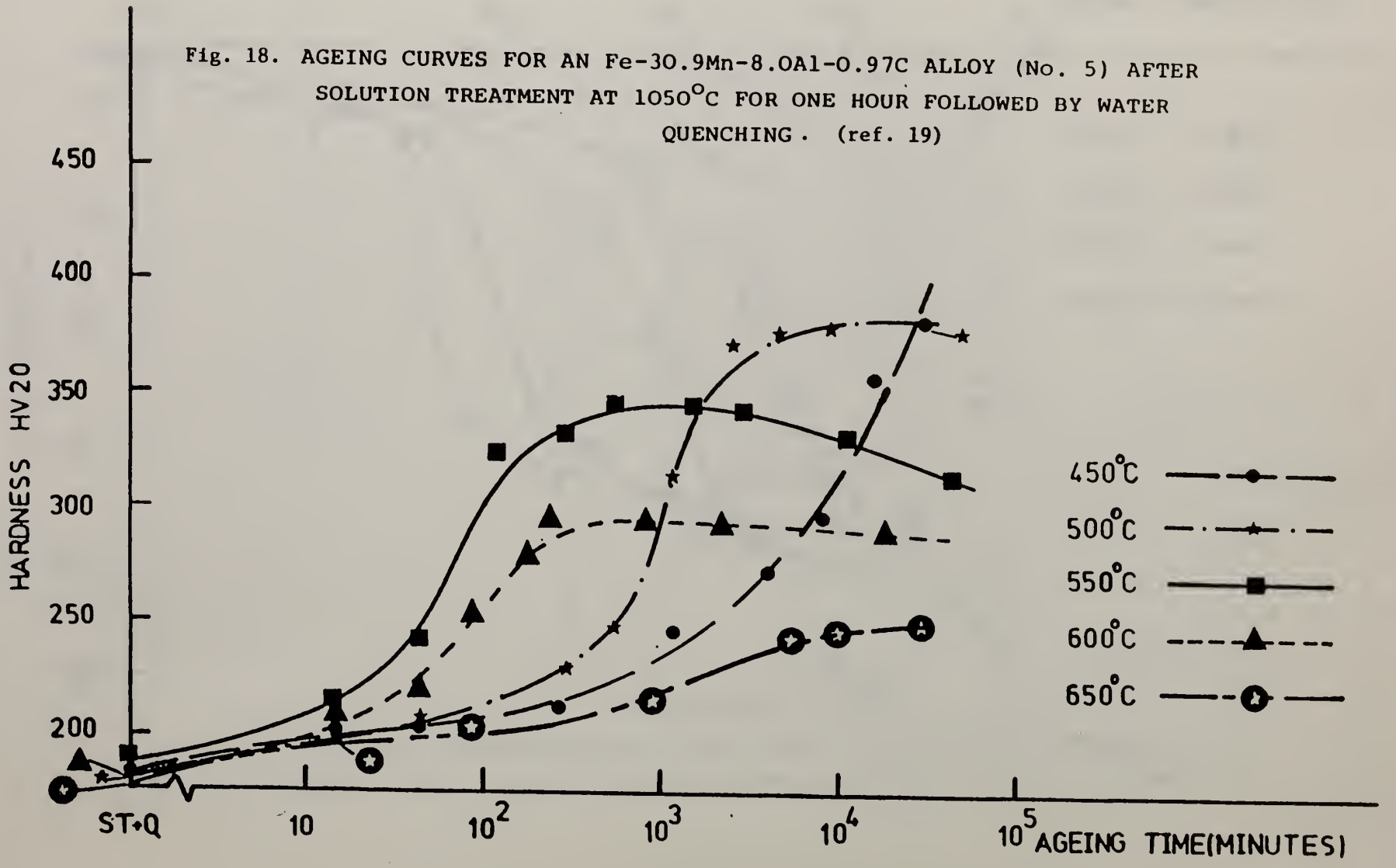

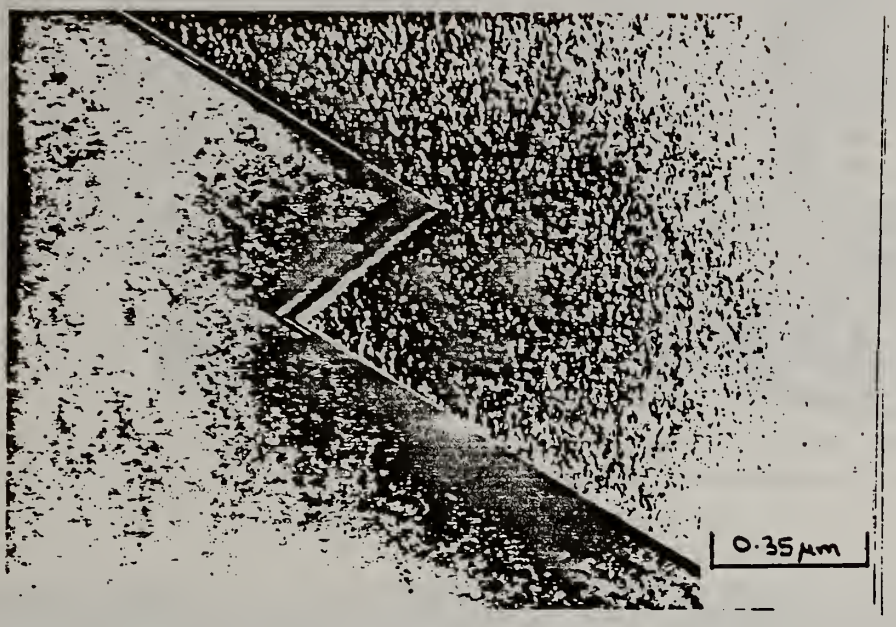

Fig. 19. Alloy No. 2.

Hot rolled bar - ST 950°C/30 mins/water quench (WQ)
Cold rolled 90%
ST 950°C/1 hr/WQ
Age 600°C/3 mins/WQ

Note the presence of very fine precipitation after aging for only three minutes. (ref. 19)

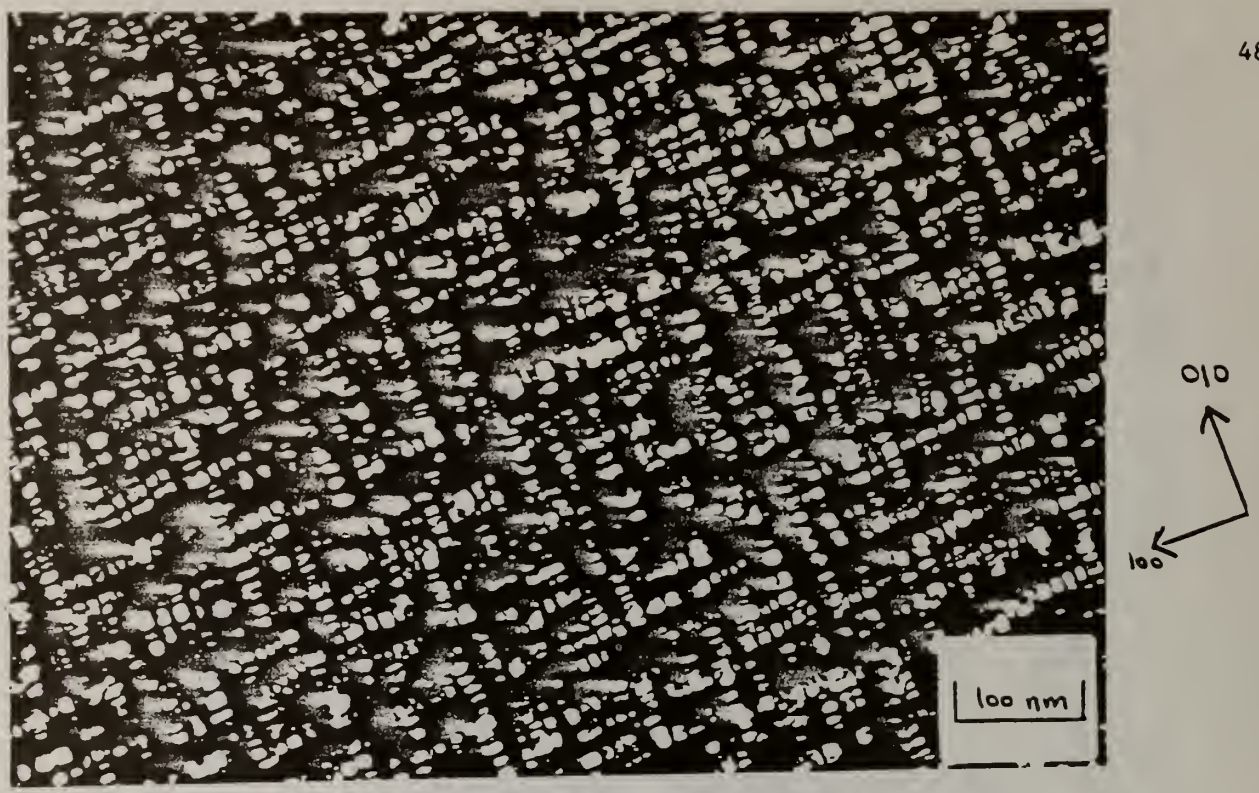

Fig. 20. Alloy No. 2. Treatment as in Fig. 19 but aged at 600°C for 30 minutes and water quenched.

Dark field micrograph from (010) precipitate spot in Fig. 21. (ref. 19)

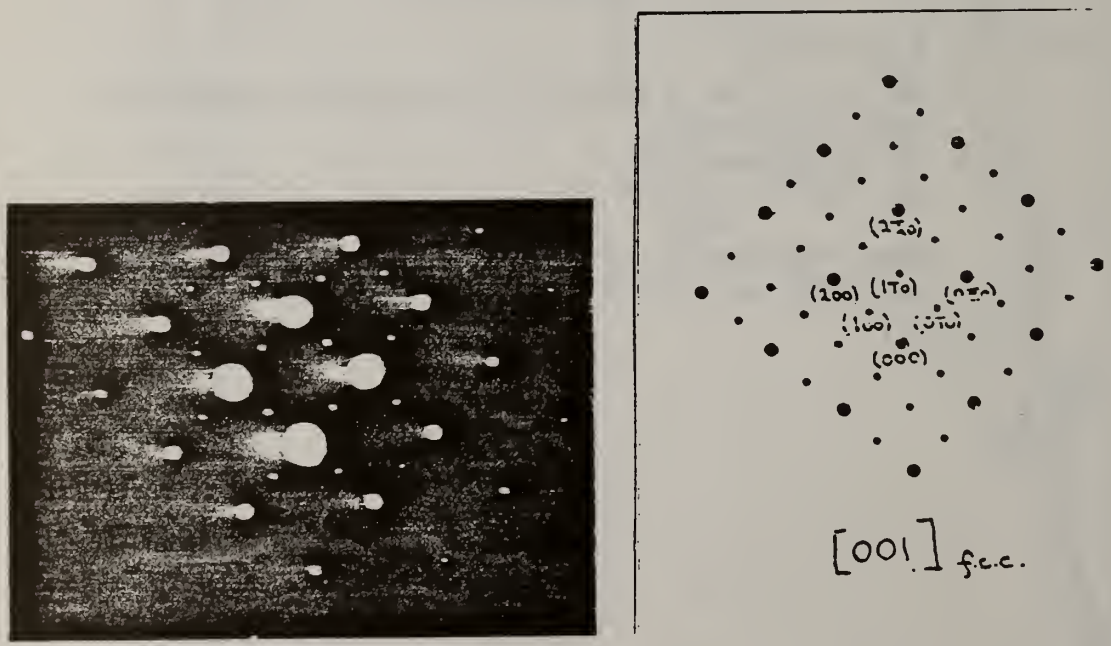

Fig. 21. Alloy No. 2. Selected area diffraction pattern from area seen in Fig. 20 showing superlattice spots intermediate between the austenite matrix spots. (ref. 19)

Fig. 22. Alloy No. 2. Treatment as in Fig. 19 but then aged at 600°C for one hour and water quenched. Bright Field Micrograph. (ref. 19)

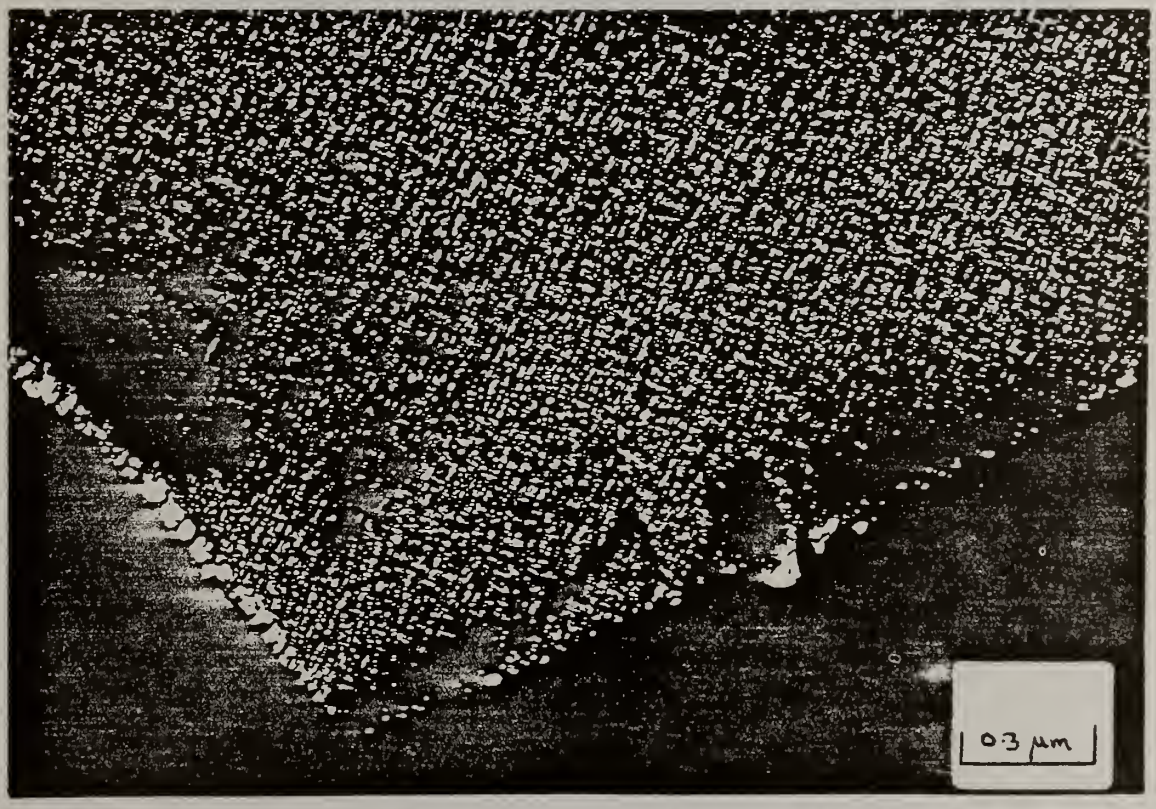

Fig. 23. Alloy No. 2. Dark Field Micrograph of area seen in Fig. 22. Zone axis just of [001]γ. Operative reflection is a (100) precipitate spot. (ref. 19)

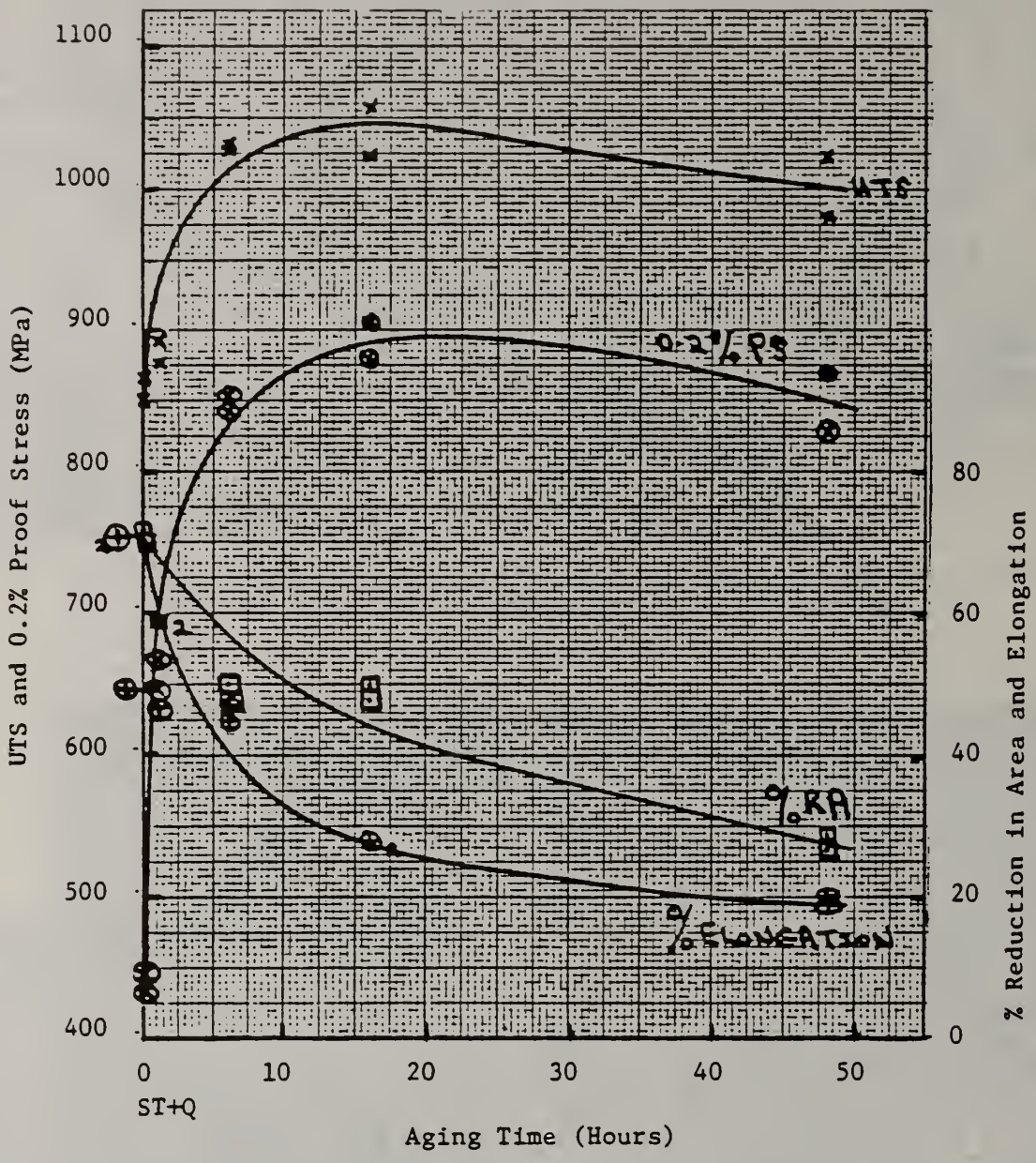

Fig. 24. The effect of aging time (at 550°C) on the tensile properties of Alloy No. 5 after ST 1050°C/1Hr/WQ. (ref. 19)

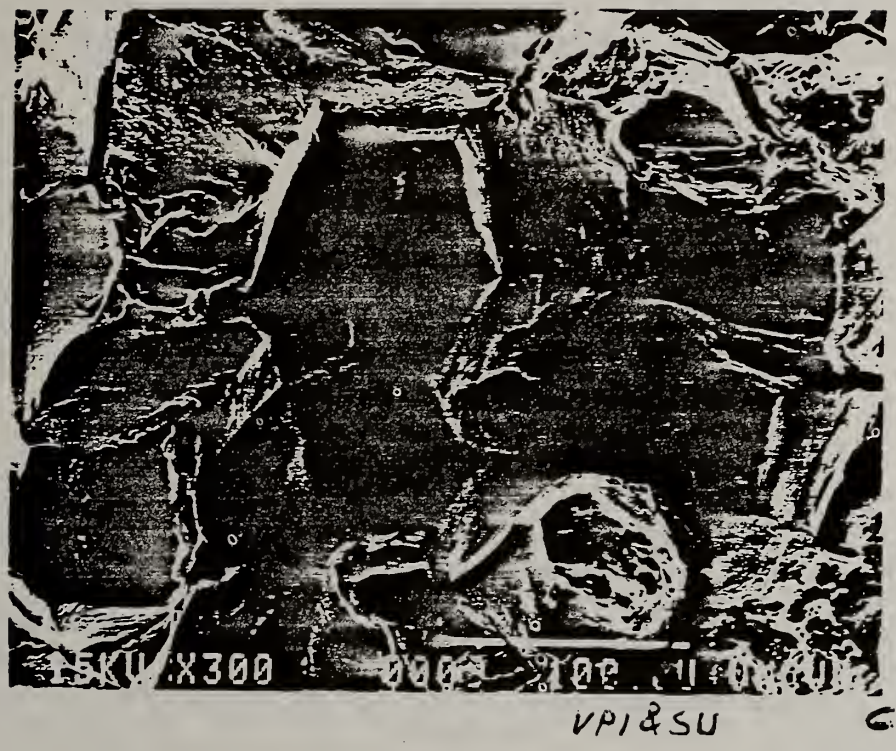

Fig. 25. Hydrogen-induced intergranular cracking in an Fe-Mn-Al alloy. (ref. 21)

THE DEVELOPMENT OF NEW ALLOYS

TO REPLACE CHROMIUM IN CARBURIZING STEELS FOR GEARS AND SHAFTS

CARL J. KEITH AND V. K. SHARMA
Materials Engineering and Technology
International Harvester Company
Hinsdale, Illinois

ABSTRACT

A status report on the Bureau of Mines sponsored research to develop a new series of cost-effective chromium-free steels is provided. These new steels will be capable of adoption by a broad range of industry as a substitute for the chromium-containing 8600 and 4100 standard grades of heat treated constructional alloy steels. Based upon several socio-economic scenarios and their projected impact on alloying element cost and availability in 1985, International Harvester's computerized metallurgical design system has been used to design two substitute steels. Both steels, a manganese-molybdenum substitute and a manganese-nickel-molybdenum substitute, are expected to provide microstructure, heat treat response, and mechanical properties equivalent to the 8600 and 4100 steels. Small experimental heats of both chromium-free replacement steels were prepared and their hardenability response and mechanical properties were evaluated and compared to the base line 8620 steel.

INTRODUCTION

Chromium is both a critical and strategic alloy element. With the exception of approximately 8 percent chromium recycled from stainless steel scrap, the U.S. relies totally on imports. Chromium resources in the Western Hemisphere are limited to about three-tenth of one percent of the world resources of chromite ore. Identified world supplies of chromium are sufficient to meet conceivable demand for many centuries, however 97 percent of the world's chromite reserves and 98 percent of its identified resources are located in Rhodesia (Zimbabwe) and South Africa[1]. This very high concentration of world reserves in a politically unstable area, coupled with the relatively rapid rise in world demand and limited substitution potential, creates a potentially dangerous situation. The National Materials Advisory Board in their report on contingency plans for chromium utilization points out that "at some future time the major source of chromite could become inaccessible to the United States as a result of political action."[2]

Depending on the level of economic activity, sixty-to-seventy percent of chromium consumed annually in the United States is used for metallurgical purposes. The bulk of this usage is in the production of heat resistant steels, superalloys, and corrosion-resistance stainless steels. At the present time there exists no viable substitute for chromium as used in these heat and corrosion resistant applications. However, approximately 17 percent of the chromium consumed annually is used in the production of the constructional alloy steels. In these applications chromium is used primarily for its effect on hardenability and, while its use is both highly efficient and cost-effective, it can be substituted for. Two particular grades of constructional alloy steel, chromium-molybdenum (4100) and nickel-chromium-molybdenum (8600), account for 60 percent of the chromium used in the constructional alloy steels and thus approximately 10 percent of the total U.S. demand. Conservation by substitution of this chromium could reduce demand by 10 percent or alternatively expand existing supply thereby extending the supply for those heat- and corrosion-resistant applications for which there is currently no viable substitute for chromium.

The purpose of the Bureau of Mines sponsored research described in this paper is to develop a new series of chromium-free constructional alloy steels capable of replacing the two chromium-containing AISI 8600 and 4100 steels. The goal is to substitute for the chromium in these two steels other cost-effective alloying elements in which the U.S. is self-sufficient or for which a more secure and stable source of supply exists. In the event of a chrome supply disruption or significant price escalation in the time period 1985-1995, the new chrome-free compositions can be adopted by a broad range of U.S. industry without significant testing and development effort. To be readily acceptable to domestic steel producers, the new chrome-free steels have been designed to avoid the necessity for special production practices which are not currently required for the production of the standard grades. For example, although it is more cost-effective to design chrome-free steels with manganese level exceeding 1.30 percent, the manganese range was limited to 1.00 - 1.30 percent because a broad range of domestic steel producers are not accustomed to producing higher manganese steel on a commercial basis.

SUBSTITUTE STEELS

The acceptance and adoption of new steels as standard grades is a relatively lengthy process requiring many years. Most of the currently used constructional alloy steel grades were developed in the late 1930s and adopted in the early 1940s as National Emergency Steels during World War II. Engineering design of parts and components, using these steels is well advanced, and manufacturing methods rely on process control parameters developed only after long and painful experience. It would be very difficult to replace parts made from these standard steels with parts made from new alloy compositions having different hardenability, heat treat response, and mechanical properties without redesigning the parts. Redesign of the parts would involve extensive engineering and manufacturing test programs. Engineering test programs would be required to ensure achievement of required engineering performance, and reliability and manufacturing test programs would be required to establish new process control parameters to enable consistent production of parts within required tolerance levels.

However, experience has shown that standard steels can be replaced by new steels of different alloy composition provided that the new steels exhibit the same hardenability, heat-treat response and mechanical properties. By careful control and balance of the composition, new steels can be developed to replace the standard steels in current parts without the need for redesign of the parts and with only nominal changes in process control parameters. Basic assumption in the development of such substitute steel is that the engineering performance of a heat treated component is controlled by the carbon content, microstructure, and residual stresses. The microstructure and residual stresses are governed by the carbon content, hardenability, and martensitic start-and-finish transformation temperatures. Alloy composition controls hardenability and transformation temperatures. Opportunities, therefore, exist to develop substitute steels composed of alternate cost-effective and/or readily available non-strategic alloy elements provided the new steels have the same carbon content, hardenability, and martensitic transformation temperatures.

The use of substitute steels as replacements for the standard steel grades is not a new concept. The SAE specification J1081 was developed to provide a uniform means of designating new steels during a period of usage prior to their acceptance as standard steel grades. Beginning in the early 1960s, new replacement steel grades developed by industry have been listed in this specification as EX steel grades. At International Harvester a computerized metallurgical design system has been used successfully over the past ten years to develop a number of proprietary, minimal cost, alloy compositions which are presently widely used in the production of IH products. None of these new steels is a chromium-free steel. At the present time, the use of chromium to enhance hardenability is highly cost-effective and the wide spread implementation of chromium substitution would not be in the economic best interest of the nation. As noted earlier, in the design of new chromium-free steels alloy costs have been minimized within the constraints of self-sufficiency and/or availability considerations.

Computer-harmonizing or the CH portion of International Harvester's metallurgical alloy steel design system CHAT (Computer Harmonized Application Tailored) was used to design new chromium-free steels. The IH CHAT system has been fully described elsewhere (3,4). The CH portion of the system is a computer program which uses linear and separable programming to optimize a primary or objective function while at the same time satisfying a series of additional functions. When the CH program is used to design replacement steel grades, the primary or objective function is described as the total cost of the alloy additives required to make the steel. This primary function is

minimized, while at the same time a series of restrictive functions embodying minimum and/or maximum base and case hardenability requirements, transformation temperature requirements, and additional limitations aimed at controlling intergranular oxide penetration during heat treatment and carbide formation during carburizing are all simultaneously satisfied.

ALLOY STEEL COST FACTORS

One of the key pieces of information required in designing a cost-effective replacement steel is the alloy steel cost factors. The cost factors used in the CH portion of the CHAT system are the raw material costs to the steel mill to add one percent of the alloy element to a full heat of steel. These cost factors are modified for the size of the heat and, the yield and recovery factors which account for oxidation, metal slag reactions, etc. and affect the efficiency of the alloy element additions. The CHAT system selects the optimized combination of alloy elements (minimized cost) meeting the input requirements and limitations. The resulting CHAT composition is then modified to provide an optimum price in terms of its "chemistry grade extra" as determined by commercial steel product price books. This difference between steel cost and steel price must be clearly appreciated. Although there is a close correlation between steel mill cost and steel product price, there is not always a one-to-one correspondence.

In designing the chromium-free steels, the 1981 alloy cost factors were projected to 1985 and then modified to reflect the following four future chromium supply scenarios considered probable in 1985:

Scenario A: Chromium supply will remain stable with prices rising in a steady manner as world economic and political conditions continue to evolve in a relatively orderly fashion. Based upon world conditions existing at this time, this scenario appears to be the most likely and is estimated to have a relatively high 75 to 80 percent probability.

Scenario B: Chromium remains available but supply and price fluctuate as the principal African producers seek to form an OPEC-like cartel and attempt to control pricing. This scenario is considered to be eminently possible due to the concentration of resources in southern Africa. However, this scenario is assigned a relatively low probability of 15% because of the high dependency of that area on export of minerals for foreign trade; the relatively low economic development of the area; and the reasonable availability of lower grade ores from other sources (including industrial and governmental stock piles) for both alloy element and ferro alloys.

Scenario C: Chromium supply from African sources is cut off as a result of a regional war or other occurrences causing a complete breakdown of export capability from the South African sources. As a result of political unrest, the potential for insurrection and/or war in this area is very real. The relative isolation of South Africa in the United Nations and world community and the active support of Soviet Bloc nations for the South African opposition groups are destabilizing factors. However, the interest of the major western powers in the mineral resources of the area and the relative economic and military strength of the nation of South Africa in relation to its own neighbors indicate that a war could probably be contained without seriously affecting export. The probability of a complete breakdown of South African production and export potential is therefore considered to be relatively low, i.e. 5 percent.

Scenario D: This scenario assumes the breakdown of African chromium supply as in Scenario C above, but then further assumes that at the same time Soviet and Albanian sources of chrome supply would also be cut off. This fourth scenario D is assigned a very low probability of 1 percent.

The costs for the alloy elements developed from various scenarios are shown in Table I. The cost forecasts, developed by the Resources and Technology Forecasting Group of IHC Corporate Technology as a part of an ongoing study, are intended to represent long-term trends rather than short-range fluctuations.

TABLE I - STEEL ALLOY COST FORECAST FOR 1985
Unit = $/ton (2,000 lbs)

Scenario	Ni* as NiO	Mo* as MoO_2	Cr* as Cr_2O_3	Mn* as MnO	Ferroalloys		
					FeCr	FeMn	FeSi
Scenario A	9,760	31,240	489	97.2	1,431	750	1,240
Scenario B	10,736	34,364	562	107.0	1,646	862	1,302
Scenario C	11,712	37,488	3,600	116.6	3,856	937	1,364
Scenario D	11,712	37,488	3,960	116.6	4,242	937	1,364
1981 Prices (Nov-Dec 1981)	7,160	21,340	360	71.5	1,067	538	900

* Price per ton of Contained Metal:
Scenario A: Stable world conditions, 75-80% probability
Scenario B: Producers' Cartel, 15% probability
Scenario C: South African Breakdown, 5% probability
Scenario D: Scenario C plus Soviet and Albanian sources cut off, probability 1%

The alloy element cost forecasts were reviewed with a number of experts in various areas of alloy availability. Of particular interest were comments from Climax Molybdenum Corporation regarding the projected costs for molybdenum oxide. The forecasts, conducted at a time when molybdenum was still considered to be in short supply, projected a 1985 molybdenum price tending toward $16/lb under stable world conditions of Scenario A. The Climax Molybdenum representatives suggested that the existing 1981 producer price of $6.85/lb would prevail throughout 1982 and would not exceed $10/lb by 1985. It was pointed out that the continuing economic recession, depressed steel market demand, and increased world production had affected producer inventory levels to a point where they could not be adjusted in the near-term future. Figure 1 and Table II reported in American Metal Market, July 1982,[5] tend to confirm this outlook.

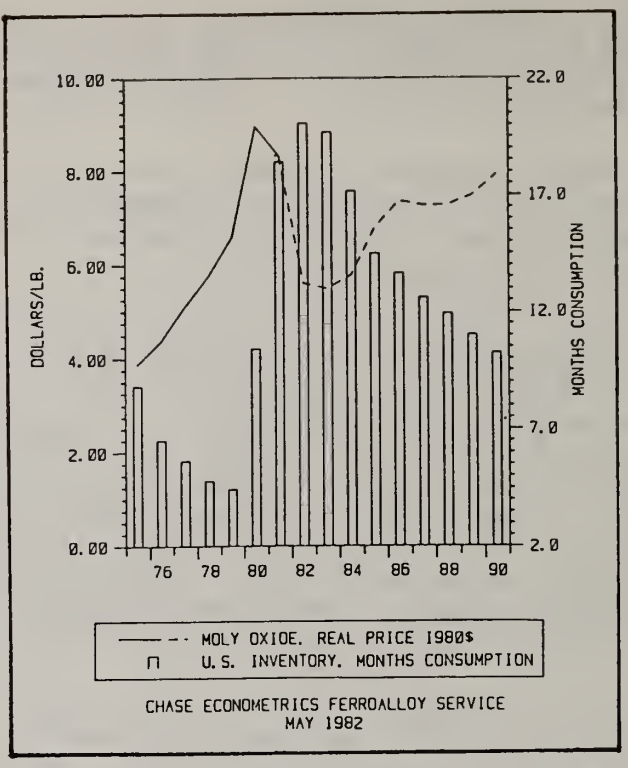

Figure 1 - Molybdenum Price and U.S. Inventory[5]

TABLE II - THE OUTLOOK FOR MOLYBDENUM[5]
(in thousands of metric tons)

	1982	1985	1990
Consumption			
United States	25.4	34.7	36.5
Other Countries	43.6	60.0	80.8
TOTAL	69.0	94.7	117.3
Supply (Mine)			
Capacity	117.5	140.3	156.2
Operating Rate	.69	.74	.84
Production	81.7	103.7	131.6
Price of Oxide ($/lb) 1980 $	$ 5.60	$ 6.80	$ 7.93

The cost factors used in the CH computer program significantly affect the selection of the optimum composition. To more fully evaluate the problems of cost projections, a cost sensitivity analysis for two competitive alloying elements, nickel and molybdenum, was performed. This cost sensitivity study included the constraints imposed in matching the metallurgical characteristic base and case hardenability of the 8600 and

4100 series steels, and is not applicable to other steel grades having different metallurgical characteristics. The results indicate that for the 8600 and 4100 series steels a Mo/Ni cost ratio of 2.4 is a critical point. Above this ratio (i.e., Mo cost greater than 2.4 times Ni cost), nickel substitutes to reduce Mo content; below this ratio, nickel does not substitute for Mo. A review of the history of alloy costs over the past 20 years indicates that the Mo/Ni cost ratio has existed on both sides of the 2.4 critical ratio. As it will be seen later, it is precisely for this reason that two different chrome-free compositions, a manganese-nickel-molybdenum and a manganese-molybdenum steel, have been developed in this program.

COMPOSITION OF CHROMIUM-FREE STEELS

Manganese, nickel and molybdenum, are three possible elements which can compensate for the base and case hardenabilities lost due to the removal of chromium in the chrome-free steels. Increasing the base carbon can increase the base hardenability, but in designing substitute steel only a minimal change in the base carbon is permitted. Obviously a change in the base carbon will have no effect on the case hardenability. Silicon contributes to case hardenability significantly but has no significant effect on base hardenability unless increased beyond approximately 0.60%. Silicon range in standard AISI steels is 0.15 to 0.35%. Producers and users of carburizing steels do not have experience with higher silicon carburizing grades of steels. Therefore, three key elements which can be effectively used to replace chromium are manganese, nickel, and molybdenum.

Although manganese is a relatively inexpensive alloying element, consideration was given to the use of both high and low manganese in the computer design of the chromium-free replacement steels. South Africa currently supplies approximately 35% of the Western demand for manganese[6], and the formation of a producer cartel for chromium which included the South African sources for chromium would in all probability affect manganese also. A breakdown of the African export capability for chromium would also involve export capability for manganese. These factors, and their effects on manganese costs, are included in Table I, Steel Alloy Cost Factors, under Scanarios B, C, and D. However, it is assumed that short-term manganese shortages could be offset by increased production from other western suppliers (primarily Australia and Brazil).

Four different manganese ranges varying from 0.40 to 1.50 percent Mn were considered. These four manganese ranges, along with additional restrictions of fixed silicon range, no chromium, and metallurgical base and case hardenability requirements for 8622 and 4118 steels, were included as input to the CH program. Using the 1985 alloy steel cost factors for various scenarios, the computerized alloy steel design system provided optimal chromium-free compositions for each manganese range. Chromium-free replacement steel compositions developed for the AISI 8620 steel are shown in Table III. The CH program first provided only the -1/4 chemistry. The +1/4 chemistry was established after a due consideration to the chemical range limits (tolerances) for the various alloying elements established by the American Iron and Steel Institute (AISI). This was accomplished within the CHAT system by varying the input requirements. Input requirements representing the minimum, maximum, and/or median values of the metallurgical characteristics describing the steel were varied systematically until the resulting new composition met AISI range tolerances and the primary objective function was optimized. Notice that the chromium-free chemistries in Table III are applicable to all four scenarios. Changes in the alloy cost factors resulting from various scenarios did not alter the composition. The computer selected the same cost-effective chemistry irrespective of alloy cost factors in Scenarios A to D, which indicates that

TABLE III
COMPOSITIONS OF CHROME-FREE REPLACEMENTS FOR AISI 8620 STEEL

ITEMS	AISI 8620		CH' VERSION SELECTION - STANDARD RANGES							
			.40-.60% Mn		.70-.90% Mn		1.00-1.30% Mn		1.20-1.50% Mn	
	-1/4	+1/4	-1/4	+1/4	-1/4	+1/4	-1/4	+1/4	-1/4	+1/4
C	.18	.23	.18	.23	.18	.23	.18	.23	.18	.23
Mn	.75	.85	.45	.55	.75	.85	1.07	1.23	1.27	1.43
Si	.20	.30	.20	.30	.20	.30	.20	.30	.20	.30
S	.03	.05	-	-	-	-	-	-	-	-
Cr	.45	.55	.02	.08	.02	.08	.02	.08	.02	.08
P	.01	.03	-	-	-	-	-	-	-	-
Ni	.47	.63	.01	.05	.35	.55	.35	.55	.25	.35
Mo	.17	.23	.72	.83	.42	.48	.27	.33	.27	.33
D_{Ib} Min	1.42		1.30		1.41		1.53		1.71	
D_{Ib} Max		2.33		2.06		2.19		2.45		2.64
D_{Ic} Min	4.31		5.03		4.15		4.09		4.39	
D_{Ic} max		6.45		7.08		5.83		6.21		6.23
M_s Base	797°	745°	830°	782°	807°	755°	791°	736°	784°	731°
M_{10}	779°	727°	812°	764°	789°	737°	773°	718°	766°	713°
M_{50}	712°	661°	745°	698°	722°	670°	707°	651°	699°	647°
M_{90}	612°	560°	645°	597°	621°	569°	606°	551°	598°	546°
M_f	410°	358°	443°	395°	420°	368°	404°	349°	397°	344°
M_s Case	305°	287°	343°	330°	321°	304°	305°	284°	296°	278°
A_{c1}	1329°	1330°	1336°	1339°	1319°	1318°	1313°	1311°	1312°	1313°
A_{c3}	1528°	1515°	1572°	1565°	1545°	1531°	1537°	1523°	1540°	1528°
A_{e3}	1493°	1477°	1516°	1504°	1498°	1481°	1490°	1471°	1488°	1473°
Cost Factor $ - 1981	$9.50/cwt		$19.50/cwt		$14.85/cwt		$10.85/cwt		$10.05/cwt	
$ - 1985A	$12.10/cwt		-		-		$13.20/cwt		$12.60/cwt	
$ - 1985B	$14.90/cwt		-		-		$15.25/cwt		$13.85/cwt	
$ - 1985C	$17.80/cwt		-		-		$15.90/cwt		$15.30/cwt	
$ - 1985D	$22.40/cwt		-		-		$15.90/cwt		$15.30/cwt	

Note: D_I values calculated from ±1/4 chemistry.

under the constraints imposed relative per dollar contributions of various alloying elements to hardenability does not change with the increase in the alloy cost factor from Scenario A to D.

Table III shows $\pm 1/4$ chemistries, characteristic hardenabilities, and various transformation temperature for the 8620 and the computer harmonized replacement versions for the four manganese ranges. Present and 1985 estimated prices under the four scenarios are given in the last column. The .40 - .60 Mn range results in the development of a Mn-Mo steel with a .70 -.85 percent molybdenum range. It would be a costly steel, and its use would require more extensive testing. The .70 - .90 Mn range results in the development of a Mn-Ni-Mo steel, which again is relatively costly. The 1.20 - 1.50 Mn range results in the development of the most cost-effective compositions. However, in current steel production practice, the use of manganese above 1.20 to 1.30 percent involves additional problems in ingot casting practice due to a tendency of the high manganese steel to cause cracking if allowed to cool in the ingot. This problem can be avoided by vacuum degassing and/or by controlled processing in the steel mill. Since the chromium-free steel to be developed in this project is intended for use by a broad range of industry, without a significant change in current production practices, the 1.20 - 1.50 percent Mn range is rejected, as are the .40 - .60 percent Mn and .70 - .90 percent Mn ranges, because they are too expensive. Based on these reasons, the 1.00 -1.30 percent Mn range which results in a replacement steel slightly more expensive than the 1.20 - 1.50 percent Mn steel, is selected as the optimal manganese range.

The 1.00 - 1.30 percent Mn steel CH composition was further refined to provide an optimum price in terms of the chemistry grade extras and to reproduce all metallurgical requirements of hardenability and transformation temperatures of the parent 8620 steel as closely as possible. Table IV shows the revised Mn-Ni-Mo composition. In Table III, for the 1.00 -1.30 percent manganese steel, the computer indicates an optimal cost with a steel containing nickel at a range of .35 - .55 percent. However, commercial practice does not distinguish (provides no price break) a difference on nickel content below a value of 0.7 percent. Therefore the nickel content in Table IV was increased to a range of .55 - .65 percent without affecting cost. This increase enhances case hardenability without significant increase in the base hardenability. Another modification in the chemistry is a decrease in the carbon range from 0.18 - 0.23 percent to 0.16 - .21 percent. Examination of the output of the CH program, Table III, indicates that the high carbon, case hardenability (D_{IC}) is the primary factor influencing the alloy composition. In order to meet the minimum D_{IC} requirement, the base hardenability, D_{Ib}, is being exceeded. Experience has shown that although the increased base hardenability does not affect the engineering performance of the new steel, manufacturing process problems are sometimes encountered as a result of increased core hardness in comparison to the previously used standard steel. The problem of increased core hardness or base hardenability can be ameliorated by a slight reduction in the carbon content. This reduction in the carbon content reduces the base hardenability without affecting the case hardenability. The resulting calculated Jominy hardenability band for the chrome-free steel matches the standard 8620 very closely, as shown in Figure 2.

TABLE IV
COMPOSITIONS OF CHROME-FREE REPLACEMENTS FOR AISI 8620 STEEL

Items	AISI 8620		CH" - REVISIONS			
			1.00-1.30% Mn Mn-Ni-Mo		1.00-1.30% Mn Mn-Mo	
	-1/4	+1/4	-1/4	+1/4	-1/4	+1/4
C	.18	.23	.16	.21	.16	.21
Mn	.75	.85	1.07	1.23	1.07	1.23
Si	.20	.30	.20	.30	.20	.30
S	.03	.05	-	-	-	-
Cr	.45	.55	.02	.08	.02	.08
P	.01	.03	-	-	-	-
Ni	.47	.63	.55	.65	.01	.05
Mo	.17	.23	.27	.33	.37	.43
D_{Ib} Min	1.42		1.55		1.52	
D_{Ib} Max		2.33		2.28		2.19
D_{Ic} Min	4.31		4.42		4.43	
D_{Ic} Max		6.45		6.41		6.11
M_s Base	797°	745°	800°	748°	816°	766°
M_{10}	779°	727°	782°	730°	798°	748°
M_{50}	712°	661°	716°	663°	731°	681°
M_{90}	612°	560°	615°	563°	631°	580°
M_f	410°	358°	413°	361°	429°	379°
M_s Case	305°	287°	299°	299°	313°	297°
A_{c1}	1329°	1330°	1307°	1307°	1324°	1326°
A_{c3}	1528°	1510°	1540°	1540°	1561°	1550°
A_{e3}	1493°	1477°	1490°	1490°	1507°	1494°
Cost Factor						
$ - 1981	$9.50/cwt		$10.85/cwt		$9.60/cwt	
$ - 1985A	$12.10/cwt		$13.20/cwt		$11.85/cwt	
$ - 1985B	$14.90/cwt		$15.25/cwt		$12.95/cwt	
$ - 1985C	$17.80/cwt		$15.90/cwt		$14.30/cwt	
$ - $1985D	$22.40/cwt		$15.90/cwt		$14.30/cwt	

NOTE: D_I values calculated from $\pm$1/4 chemistry.

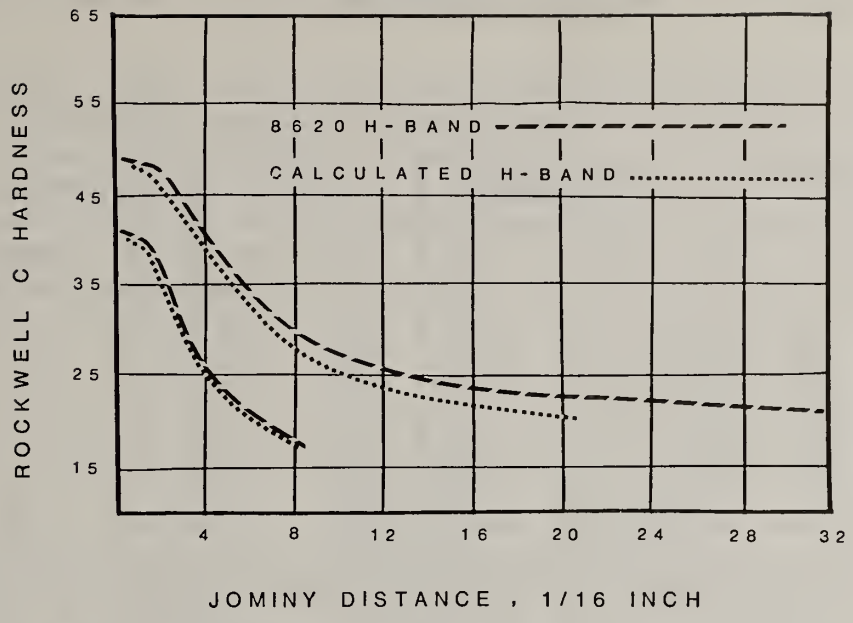

Figure 2 - Standard Jominy hardenability band for AISI 8620 steel compared to the calculated hardenability band for the chrome-free replacement steels.

It should be pointed out that the Mo/Ni price ratio used in this portion of the CH development program is approximately 3.2, as shown in Table I. Consideration of a Mo/Ni price ratio below 2.4, which actually exists at the time of writing this report, results in the development of the manganese-molybdenum composition shown in Table IV as the most cost-effective replacement steel. Since the Mo/Ni price ratio has historically varied on both sides of the critical ratio of 2.4, both the Mn-Ni-Mo and the Mn-Mo chromium-free steels are considered as future replacement compositions. The selection of the most cost-effective replacement will depend upon the relative costs of nickel and molybdenum at that future time when the need for the chromium-free steel occurs. The calculated Jominy hardenability band for the Mn-Ni-Mo and for the Mn-Mo steel is represented by the same curves in Figure 2.

Similar to the 8620 steel, CH development of chromium-free replacements for a representative 4100 series steel (4118) is given in Tables V and VI. The ladle chemical analysis ranges for the chromium-free replacement steels are summarized in Table VII. The calculated hardenability band for the Mn-Ni-Mo and Mn-Mo chromium-free replacement steels are compared to the standard AISI 4118 steel hardenability band in Figure 3.

In the development of the replacement steels, it is assumed that the chromium-free steels will be produced using essentially BOF practice and that the steels will be ingot cast rather than strand cast. If electric steel practice is used, the melt composition can be modified to account for the high residual element content normally present in the scrap charge. For the steel users, the chromium-free steels will have to be provided in a fully-killed fine grain condition with a standard silicon range, since the 8600 and 4100 steels used domestically in carburizing applications are generally specified to be fully-killed fine grain steels.

TABLE V
COMPOSITIONS OF CHROME-FREE REPLACEMENTS FOR AISI 4118 STEEL

ITEMS	AISI 4118		CH' VERSION SELECTION - STANDARD RANGES							
			.40-.60% Mn		.70-.90% Mn		1.00-1.30% Mn		1.20-1.50% Mn	
	-1/4	+1/4	-1/4	+1/4	-1/4	+1/4	-1/4	+1/4	-1/4	+1/4
C	.18	.23	.18	.23	.18	.23	.18	.23	.18	.23
Mn	.75	.85	.45	.55	.75	.85	1.07	1.23	1.27	1.43
Si	.20	.30	.20	.30	.20	.30	.20	.30	.20	.30
S	.03	.05	-	-	-	-	-	-	-	-
Cr	.45	.55	.02	.08	.02	.08	.02	.08	.02	.08
P	.01	.03	-	-	-	-	-	-	-	-
Ni	.01	.05	.01	.05	.35	.55	.01	.05	.01	.05
Mo	.10	.13	.52	.63	.27	.33	.17	.23	.15	.18
D_{Ib} Min	1.15		1.05		1.17		1.22		1.37	
D_{Ib} Max		1.76		1.68		1.83		1.87		1.99
D_{Ic} Min	3.17		3.75		3.18		3.02		3.30	
D_{Ic} Max		4.29		5.25		4.58		4.27		4.19
M_s Base	813°	765°	833°	785°	809°	757°	804°	753°	793°	743°
M_{10}	795°	747°	815°	767°	791°	739°	786°	735°	775°	725°
M_{50}	728°	681°	748°	701°	724°	672°	719°	669°	708°	658°
M_{90}	627°	580°	647°	600°	623°	571°	618°	568°	607°	558°
M_f	426°	378°	446°	398°	422°	370°	417°	366°	406°	356°
M_s Case	321°	307°	347°	334°	324°	307°	317°	301°	306°	290°
A_{c1}	1343°	1348°	1336°	1339°	1319°	1318°	1324°	1326°	1320°	1322°
A_{c3}	1536°	1525°	1560°	1553°	1537°	1523°	1540°	1531°	1539°	1528°
A_{e3}	1507°	1495°	1516°	1504°	1498°	1481°	1501°	1487°	1496°	1482°
Cost Factor										
$ - 1981	$4.90/cwt		$12.10/cwt		$10.75/cwt		$6.10/cwt		$5.65/cwt	
$ - 1985A	$5.95/cwt		-		-		$8.00/cwt		$7.00/cwt	
$ - 1985B	$7.65/cwt		-		-		$8.95/cwt		$7.70/cwt	
$ - 1985C	$10.50/cwt		-		-		$9.90/cwt		$8.45/cwt	
$ - 1985D	$15.10/cwt		-		-		$9.90/cwt		$8.45/cwt	

NOTE: D_I values calculated from ±1/4 chemistry.

TABLE VI
COMPOSITIONS OF CHROME-FREE REPLACEMENTS FOR AISI 4118 STEEL

ITEMS	AISI 4118		CH" - REVISIONS			
			1.00-1.30% Mn Mn-Ni-Mo		1.00-1.30% Mn Mn-Mo	
	-1/4	+1/4	-1/4	+1/4	-1/4	+1/4
C	.18	.23	.16	.21	.16	.21
Mn	.75	.85	1.07	1.23	1.07	1.23
Si	.20	.30	.20	.30	.20	.30
S	.03	.05	-	-	-	-
Cr	.45	.55	.02	.08	.02	.08
P	.01	.03	-	-	-	-
Ni	.01	.05	.25	.35	.01	.05
Mo	.10	.13	.17	.23	.22	.28
D_{Ib} Min	1.15		1.26		1.25	
D_{Ib} Max		1.76		1.85		1.81
D_{Ic} Min	3.17		3.17		3.33	
D_{Ic} Max		4.29		4.74		4.70
M_s Base	813°	765°	811°	759°	818°	768°
M_{10}	795°	747°	793°	741°	800°	750°
M_{50}	728°	681°	727°	674°	734°	683°
M_{90}	627°	580°	626°	574°	633°	582°
M_f	426°	378°	424°	372°	431°	381°
M_sCase	321°	307°	310°	292°	316°	300°
A_{c1}	1343°	1348°	1310°	1317°	1324°	1326°
A_{c3}	1536°	1525°	1543°	1530°	1552°	1541°
A_{e3}	1507°	1495°	1500°	1484°	1507°	1494°
Cost Factor						
$ - 1981	$4.90/cwt		$7.50/cwt		$7.10/cwt	
$ - 1985A	$5.95/cwt		$9.30/cwt		$8.85/cwt	
$ - 1985B	$7.65/cwt		$10.25/cwt		$9.80/cwt	
$ - 1985C	$10.50/cwt		$11.30/cwt		$10.65/cwt	
$ - 1985D	$15.10/cwt		$11.30/cwt		$10.65/cwt	

NOTE: D_I values calculated from $\pm$1/4 chemistry.

TABLE VII
CHROME-FREE REPLACEMENT COMPOSITIONS FOR STANDARD 4118 AND 8620 STEELS
LADLE ANALYSIS RANGES

Chemistry Ladle Range, Percent	4100 TYPE STEEL*			8600 TYPE STEEL*		
	AISI-4118 Steel	Mn-Ni-Mo Replacement	Mn-Mo Replacement	AISI-8620 Steel	Mn-Ni-Mo Replacement	Mn-Mo Replacement
Carbon	.18 - .23	.16 - .21	.16 - .21	.18 - .23	.16 - .21	.16 - .21
Manganese	.70 - .90	1.00 - 1.30	1.00 - 1.30	.70 - .90	1.00 - 1.30	1.00 - 1.30
Chromium	.40 - .60	r	r	.40 - .60	r	r
Nickel	r	.20 - .40	r	.40 - .70	.40 - .70	r
Molybdenum	.08 - .15	.15 - .25	.25 - .35	.15 - .25	.25 - .35	.35 - .45
D_{Ib}**,min,in	1.15	1.25	1.25	1.40	1.55	1.50
D_{Ib}**,max,in	1.75	1.85	1.80	2.35	2.30	2.20
D_{Ic}**,min,in	3.15	3.15	3.30	4.30	4.40	4.45

* The carbon content of the Mn-Ni-Mo and Mn-Mo replacements for the 8620 and 4118 steels is 0.02% lower than the standard grades. It is anticipated that this 0.02 % reduction in carbon content would be maintained throughout the entire replacement series.

** D_I values calculated from chemistry $\pm 1/4$ range.

r = residual level; Si range = .15-.35%; S = .05% max; P = .04% max.

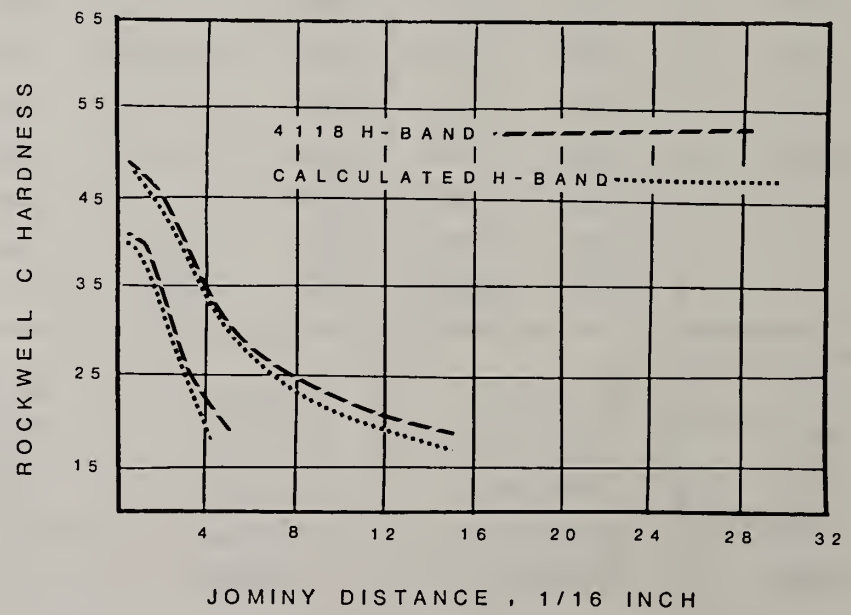

Figure 3 - Standard Jominy hardenability band for AISI 4118 steel compared to the calculated hardenability band for the chrome-free steels.

EXPERIMENTAL RESULTS

Small, 100 lbs, experimental heats of the chromium-free replacement steels were produced in order to experimentally confirm that hardenability, microstructure, and properties predicted for the chrome-free steels correlate with measured values. The experimental heats were produced at Climax Molybdenum and processed into forged bars or plate samples. Jominy hardenability tests were performed on the base composition, and carburized Jominy hardenability tests were performed to evaluate the high carbon hardenability of the chromium-free steels. Fracture toughness tests on specially prepared high carbon heats of the chromium-free replacement steels were conducted in accordance with procedures outlined in ASTM E-399. Six experimental heats were produced. The chemical analysis of the six heats is shown in Table VIII.

TABLE VIII - CHEMICAL ANALYSIS OF EXPERIMENTAL HEATS OF REPLACEMENT STEEL FOR THE AISI 8600 SERIES

Chemical Analysis % by Weight	SAMPLE IDENTIFICATION					
	8620 Base Line Heat	Mn-Ni-Mo Lo-Side Heat #41	Mn-Ni-Mo Hi-Side Heat #38	Mn-Ni-Mo Hi-Carbon Heat #39	Mn-Mo Mid- Heat #47	Mn-Mo Hi-Carbon Heat #70
Carbon	.21	.19	.23	.91	.21	.93
Manganese	.85	.86	.97	1.21	1.12	1.14
Silicon	.23	.18	.35	.32	.21	.31
Sulfur	.03	.03	.03	.03	.03	.02
Phosphorus	.02	.02	.03	.02	.02	.01
Nickel	.47	.55	.68	.58	.04	.04
Chrome	.46	.03	.11	.05	.05	.05
Molybdenum	.20	.21	.26	.34	.30	.40
Aluminum	.053		.071	.085	.09	.082
Nitrogen	-	.009	.015	.012	.019	.011
D_{Ib}, inch	1.75	1.35	3.05	-	1.75	-
D_{Ic}, inch	5.15	3.95	7.25	6.35	5.10	6.20

Jominy hardenability test results conducted on the low side heat of the Mn-Ni-Mo steel (heat #41) are shown in Figure 4. The measured curve falls below the standard curve and exhibits lower than the expected results. Investigation revealed that the grain size in this heat (ASTM #9) was finer than anticipated. In general, in hardenability calculations an ASTM grain size of No. 7 is assumed. The measured curve is compared to calculated Jominy curves assuming grain sizes of ASTM #7 and ASTM #9 in Figure 5. Note that the calculated hardenability curve assuming grain size of ASTM #9 falls closer to the experimental curve.

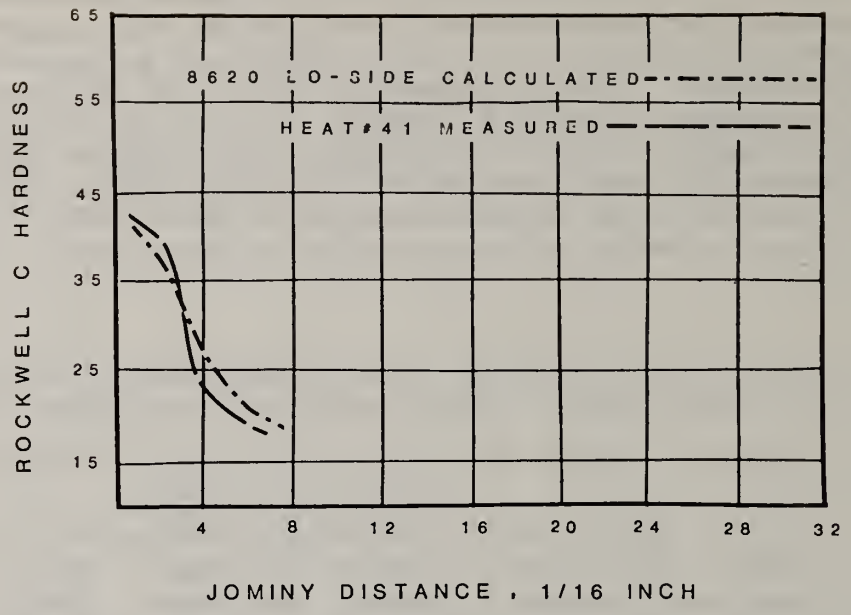

Figure 4 - Hardenability curve measured for the Mn-Ni-Mo low side heat #41 compared to the calculated 8620 low side hardenability curve.

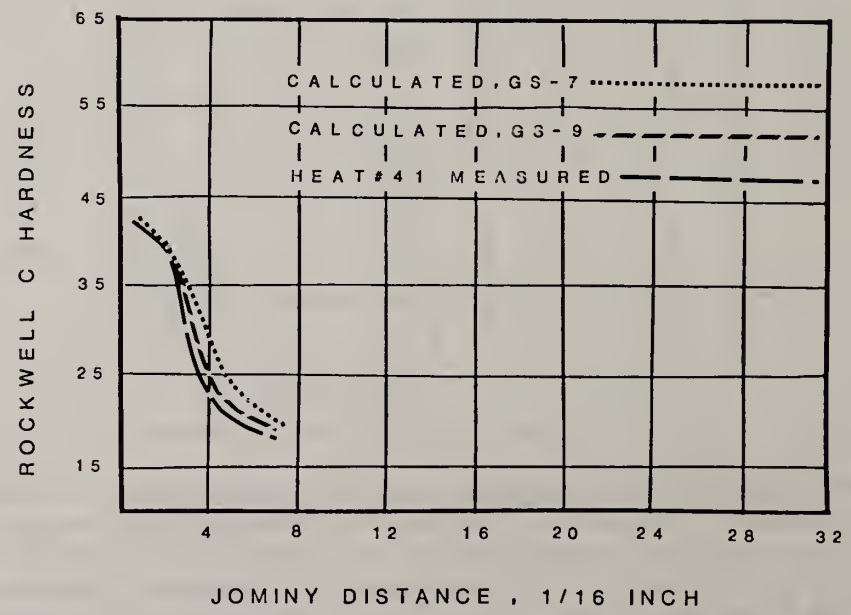

Figure 5 - Comparison of the measured low side hardenability to calculated hardness curves for different grain sizes.

The Jominy curve for the high side heat of the Mn-Ni-Mo steel is compared to the high side curve for the standard 8620 steel in Figure 6. The chemical analysis of the high side heat exceeds the desired analysis resulting in a higher hardenability and, hence, a higher measured curve. In producing experimental heats, it is very difficult to obtain exactly the analysis desired.

Jominy hardenability tests conducted on the mid-band heat of the Mn-Mo chromium-free steel are shown in Figures 7 and 8. This steel also exhibited a finer than expected grain size, and Figure 8 demonstrates that when the calculation is adjusted to include the finer grain size the measured and calculated curves correlate very well.

The occurrence of finer grain size in the experimental heats is related to a high aluminum content (.07 - .09 percent) and a high nitrogen content, which provides a larger number of AlN particles to affect the nucleation and growth of austenite.

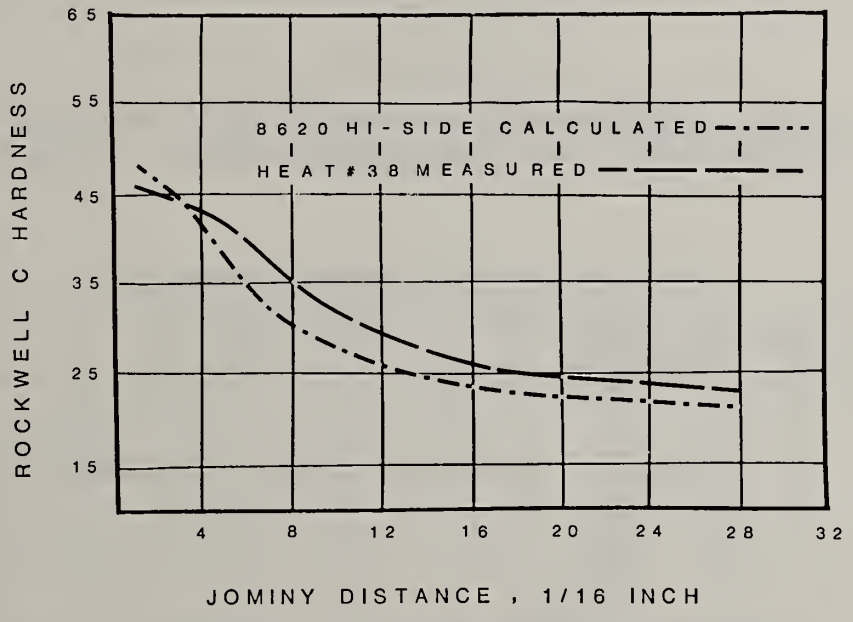

Figure 6 - Comparison of the high side Mn-Ni-Mo heat #38 to the calculated 8620 high side hardenability curve.

Carburized Jominy hardenability tests were performed on the three sample heats and results are shown in Figures 9 through 12. Figure 9 shows the 8620 standard steel base line test. All tests were pack carburized in new carburizing compound and heated at 1700° F for eight hours, and direct quenched using a standard Jominy bar quench fixture. The surface carbon content in the chromium-free steels was in general reduced, as compared to the 8620 standard sample. This reduction indicates a reduced tendency to form carbides as a result of the elimination of chromium, and implies that these steels would tolerate a greater variation in carbon potential in the furnace than the standard chromium containing steels.

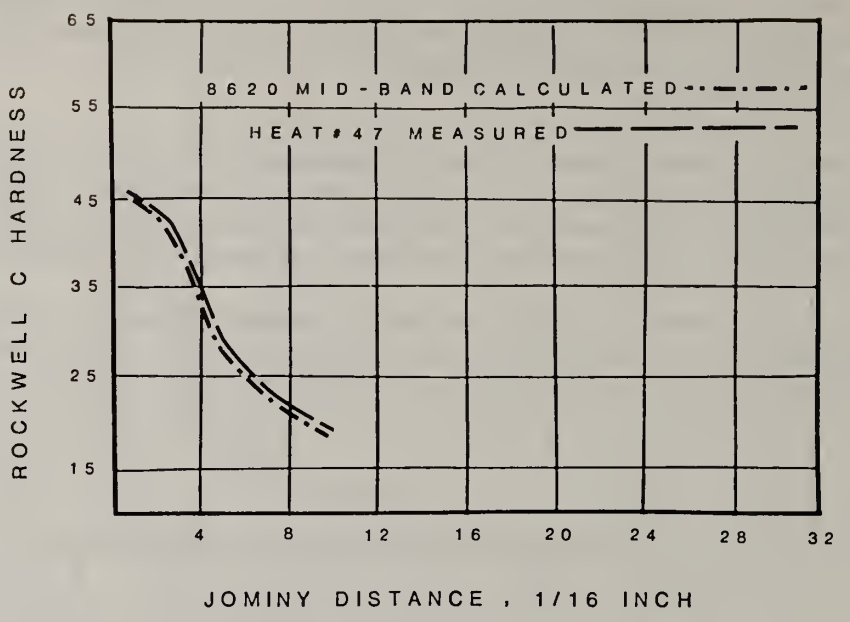

Figure 7 - Comparison of the mid-band Mn-Mo heat #47 to the calculated 8620 mid-band hardenability curve.

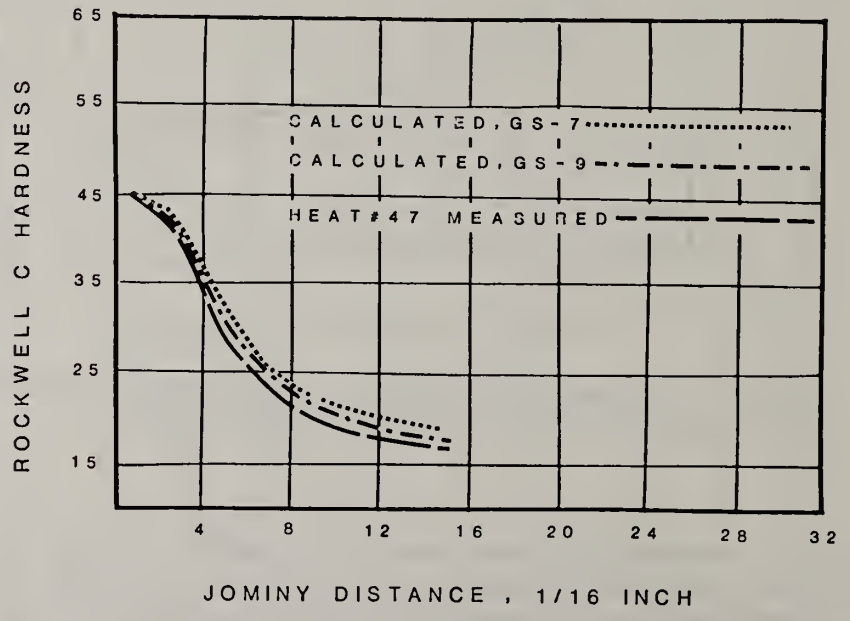

Figure 8 - Comparison of the measured hardenability were for heat #47 to calculated hardness curves for different grain sizes.

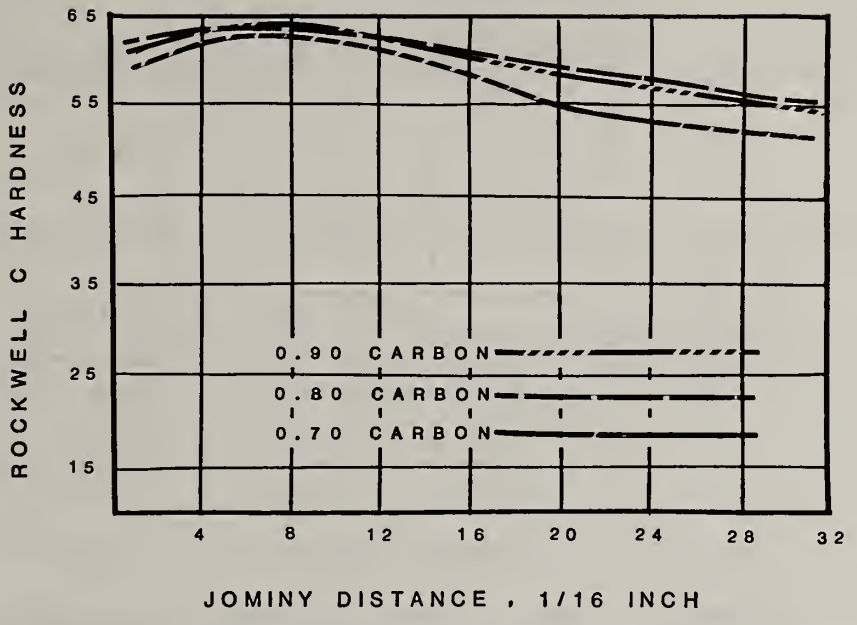

Figure 9 - High carbon (carburized) hardenability curves developed in the 8620 base line steel.

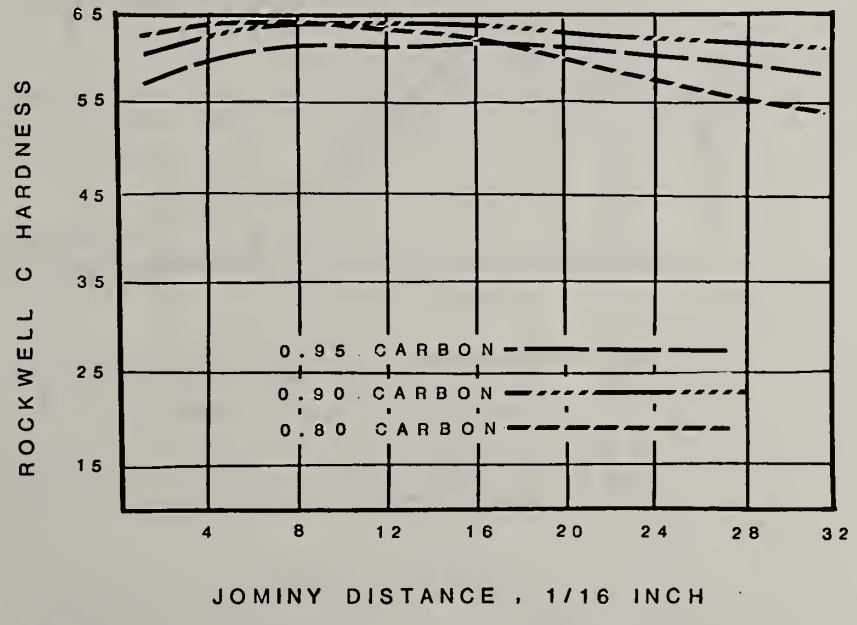

Figure 10 - High carbon (carburized) hardenability curves developed in the Mn-Ni-Mo high side heat #38.

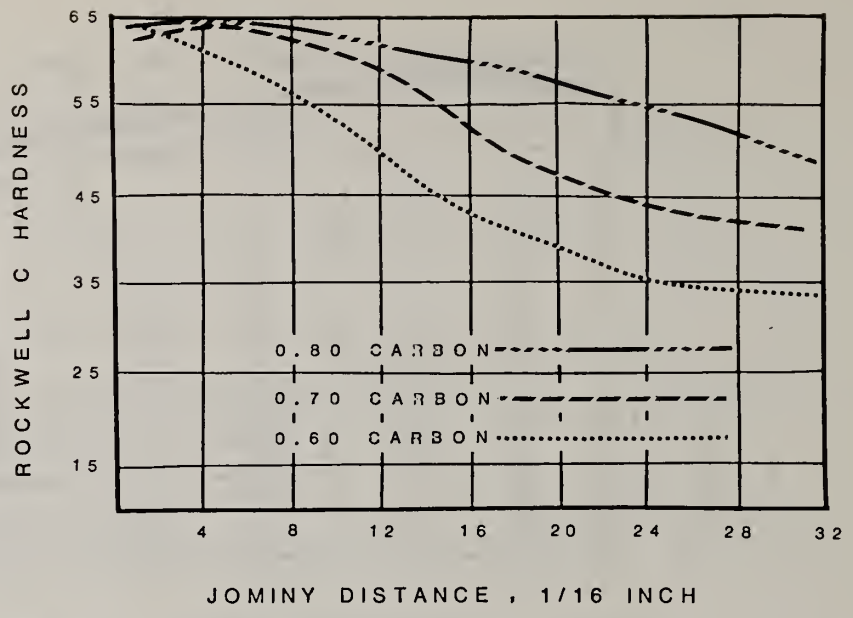

Figure 11 - High carbon (carburized) hardenability curves developed in the Mn-Mo mid-band heat #47.

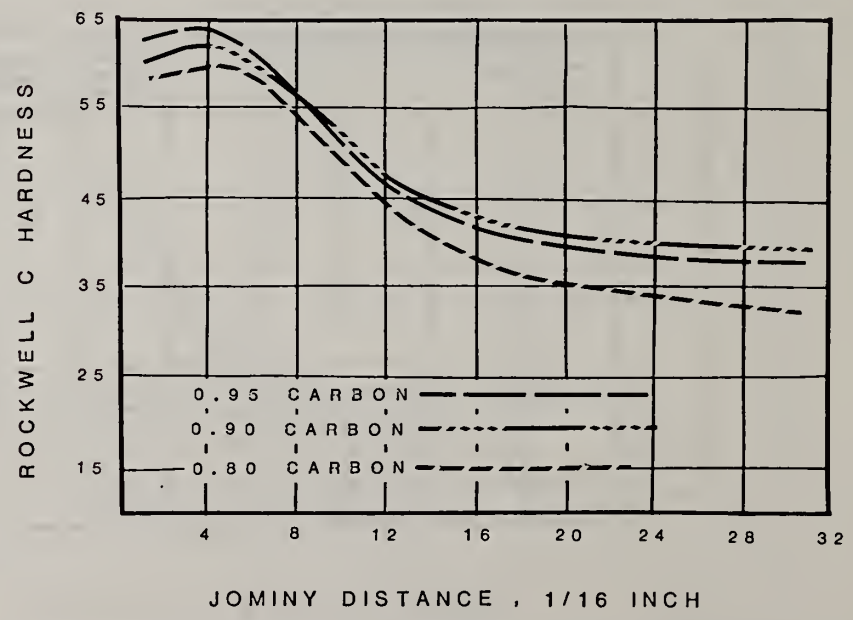

Figure 12 - High carbon (carburized) hardenability curves developed in the low side Mn-Ni-Mo heat #41.

Results of the fracture toughness studies performed on high carbon steels to simulate case microstructure are given in Table IX. High carbon chrome-free replacement steels were poured especially for this program. The data for 8695 steel, included for comparison, was obtained at IH under another in-house program. K_{1C} values are averages of at least three measurements. X-ray retained austenite (RA) measurements given in the table were made using a rotating and tilting stage[7] to compensate for the texture in the specimens.

TABLE IX
PLANE STRAIN FRACTURE TOUGHNESS VALUES FOR HIGH CARBON STEELS

Sample	%C	Rc	RA	K_{1C}, Ksi $\sqrt{in.}$
Mn-Mo	0.93	60.5	22%	16.2
Mn-Ni-Mo	0.91	60.5	23%	16.1
8697	0.97	60.0	23%	15.2

Fracture toughness values for all three steels are essentially the same. A slightly lower value for 8697 steel may be attributed to a slightly higher carbon content of 8697 steel.

COST BENEFIT OF THE CHROMIUM-FREE STEELS

The cost benefit to be derived from the development of chromium-free replacement steels for the 8600 and 4100 standard steels may be estimated as the difference in the costs required to purchase the chromium-containing standard steels vs. the costs required to purchase the chromium-free replacement steels, assuming that a chromium supply interruption has occurred in 1985.

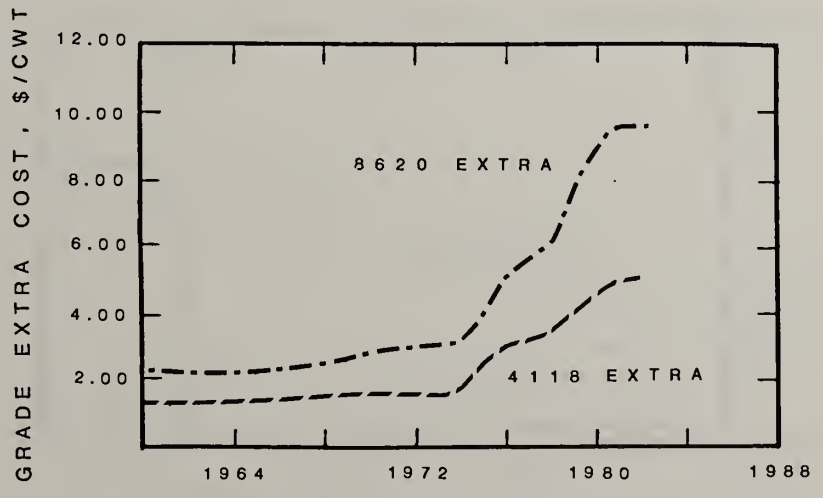

Figure 13 - Chemistrys grade extras for AISI 8620 and 4118 steels: 1960 to 1982

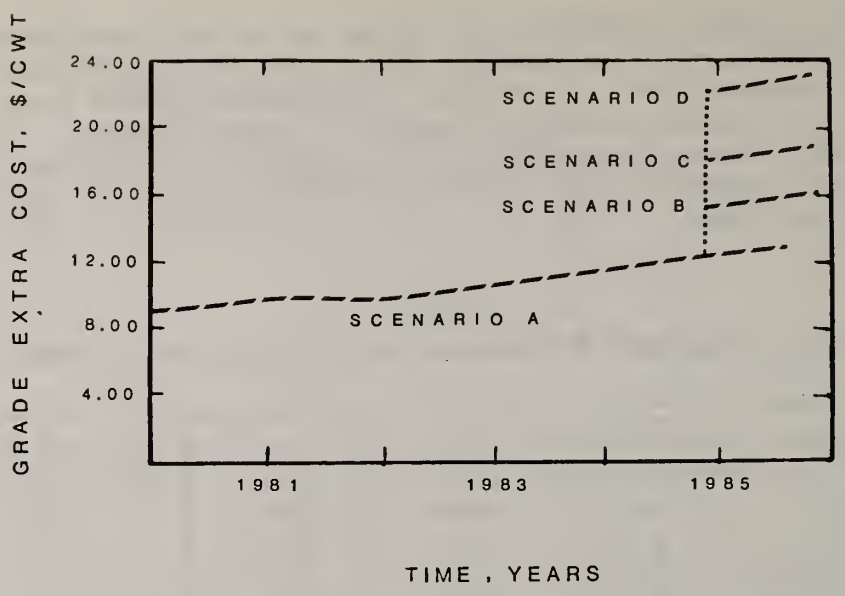

Figure 14 - Predicted effect of the various 1985 chrome supply scenarios on the 8620 steel grade extra.

The cost of the two AISI standard grades of steels in terms of their grade extras is shown for the time period of 1960 to 1982 in Figure 13. The effect of the various chromium supply scenarios on the 8620 steel grade is projected to 1985 in Figure 14.

The 8620 steel grade extra increases from $12.10/cwt in Scenario A to $22.40 in Scenario D. The steel grade extras for the corresponding Mn-Ni-Mo and Mn-Mo chromium-free replacement steels are shown in Figures 15 and 16 respectively. Both of the replacement steels at a 1981 grade extra are more expensive than the AISI 8620 steel. In 1985 the Mn-Ni-Mo replacement steel becomes cost-effective only under the

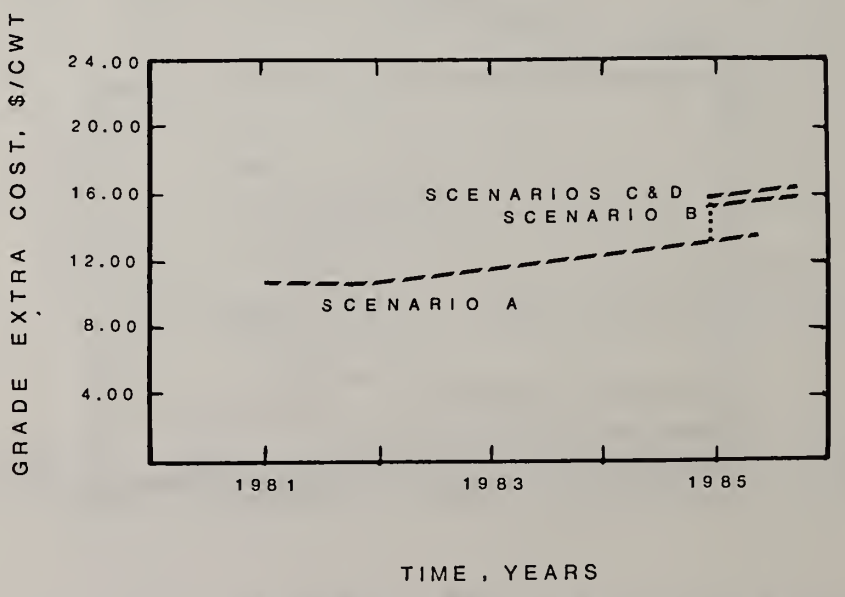

Figure 15 - Predicted effect of the various 1985 chrome supply scenarios on the Mn-Ni-Mo (replacement for 8620) grade extra.

chromium supply Scenarios C and D. The Mn-Mo replacement for the AISI 8620 at a 1981 grade extra is slightly more expensive ($9.50/cwt vs. $9.60/cwt), but it becomes cost-effective under all scenarios in 1985. Based on the 1978 domestic production of 2,042,176 tons of 8600 type steel, the Mn-Ni-Mo and Mn-Mo steels provide an annual cost advantage of 257.3 and 322.6 million dollars, respectively, in Scenario D.

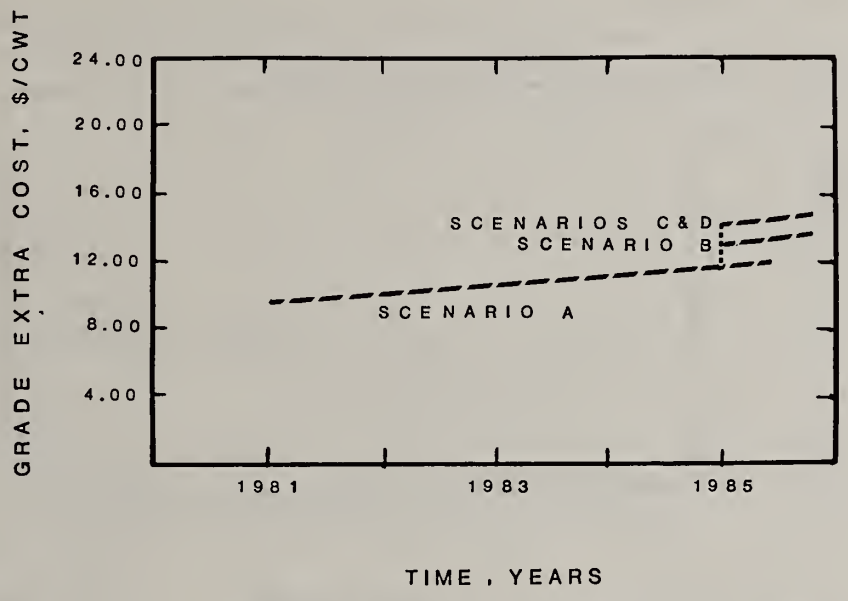

Figure 16 - Predicted effect of the various 1985 chrome supply scenarios on the Mn-Mo (replacement for 8620) grade extra.

A similar cost analysis for the AISI 4188 and its two chromium-free replacement steels is shown in Figures 17 to 19. Projected 1985 steel grade extra cost for 4118 steel increases from $5.95/cwt, Scenario A, to $15.00/cwt under the conditions of Scenario D. These chrome-free steels, however, are not cost-effective in Scenario A,

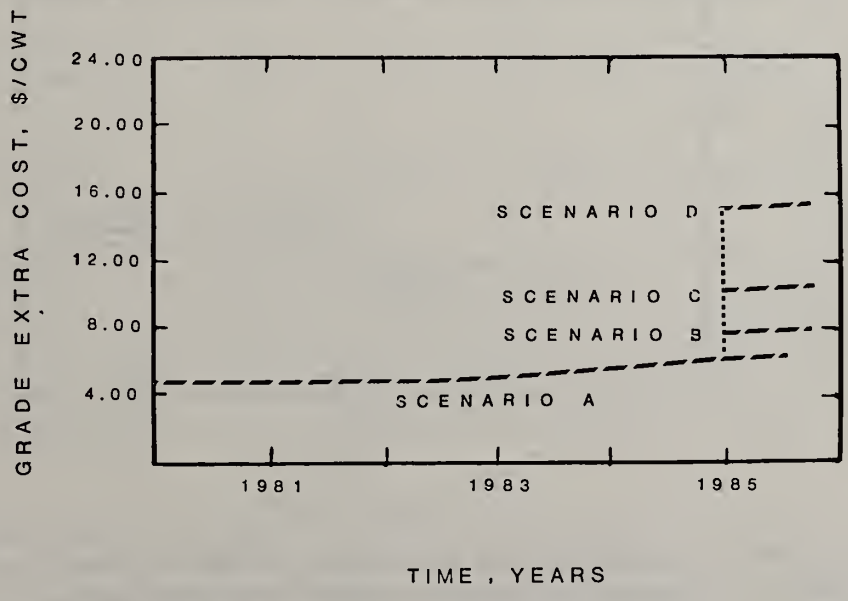

Figure 17 - Predicted effect of the various 1985 chrome supply scenarios on the 4118 steel grade extra.

B and C. Under the 1985 chromium supply Scenario D, the Mn-Ni-Mo and Mn-Mo replacement steels for 4118 steel provide an annual cost advantage of $198.5 and $233.8 million dollars, respectively. This cost savings is based on 1978 domestic production of 2,687,512 tons of AISI 4100 series steel.

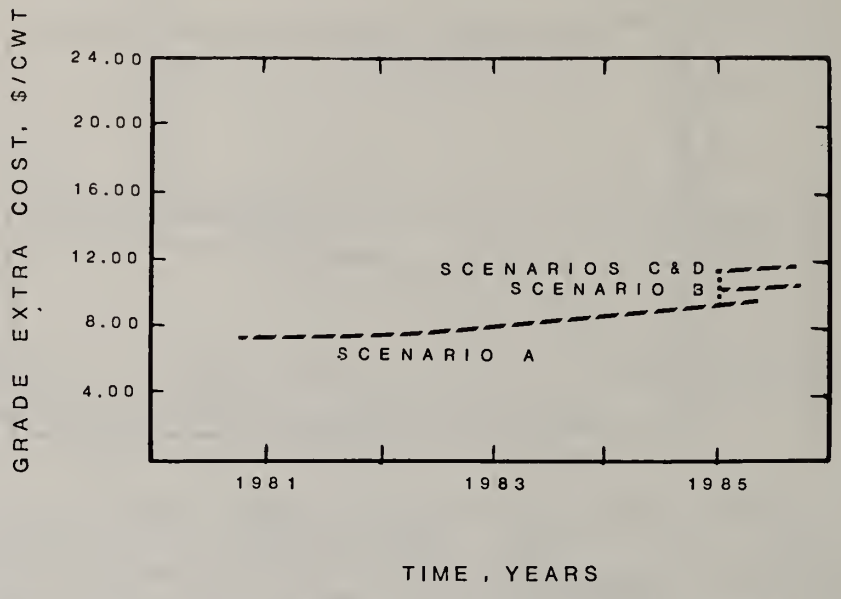

Figure 18 - Predicted effect of the various 1985 chrome supply scenarios on the Mn-Ni-Mo (replacement for 4118) grade extra.

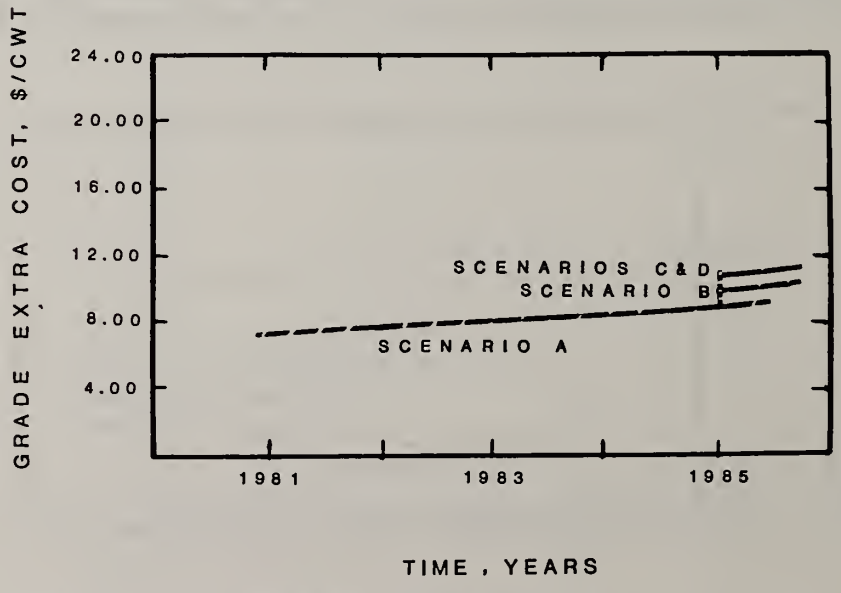

Figure 19 - Predicted effect of the various 1985 chrome supply scenarios on the Mn-Mo (replacement for 4118) grade extra.

The economic advantages of using chrome-free steels under various scenarios is summarized in Table X. The replacement of both 8600 and 4100 types steels with the Mn-Ni-Mo and Mn-Mo steels, under conditions of Scenario D, will result in a combined cost advantage of $455.8 and $556.4 million, respectively.

TABLE X - ECONOMIC ADVANTAGE OF CHROME-FREE STEELS

Steel Type	Grade Extra Cost for Each Scenario, $/cwt				
	1981	1985A	1985B	1985C	1985D
AISI 8620 Steel	9.50	12.10	14.90	17.80	22.20
Mn-Ni-Mo 8600 Replacement	10.85	13.20	15.25	15.90	15.90
Mn-Mo 8600 Replacement	9.60	11.85	13.15	14.30	14.30
AISI 4118 Steel	4.90	5.95	7.65	10.50	15.00
Mn-Ni-Mo 4100 Replacement	7.50	9.20	10.25	11.30	11.30
Mn-Mo 4100 Replacement	7.10	8.80	9.80	10.65	10.65
Annualized Cost Advantage (Penalty)* - Millions of Dollars					
Mn-Ni-Mo 8600 Replacement	(55.2)	(44.9)	(14.3)	159.3	257.3
Mn-Mo 8600 Replacement	(4.1)	10.2	71.4	224.6	322.6
Mn-Ni-Mo 4100 Replacement	(139.8)	(174.7)	(139.7)	(42.9)	198.5
Mn-Mo 4100 Replacement	(118.3)	(153.2)	(115.6)	(8.0)	233.8
Combined Cost Advantage (8600 and 4100 Steels) - Millions of Dollars					
Mn-Ni-Mo Replacement	(195.0)	(219.6)	(154.0)	116.4	455.8
Mn-Mo Replacement	(122.4)	(163.4)	(44.2)	216.6	556.4

* Annualized cost advantages based upon 1978 domestic steel production of 2,042,176 tons of 8600 type steels and 2,687,512 tons of 4100 type steels.

The Mn-Mo replacement steels provide approximately a 22 percent additional cost advantage over the Mn-Ni-Mo steels. This is correct only under the assumption that the molybdenum market will be capable of absorbing the additional increased demand without increasing the molybdenum price above the critical ratio of 2.4. Based upon the 1978 production volume of 4,727,000 tons (combined) of 8600 and 4100 series steels, 17.5 million lbs of molybdenum were required to produce the standard steels. In eliminating chromium to develop the new chromium-free replacement grades, an increase in molybdenum content is required. The manganese-nickel-molybdenum steel grade would require 27 million lbs of molybdenum to produce 4,727,000 tons of steel. This is an increase of approximately 10 million lbs of new molybdenum demand. The manganese-molybdenum steel grade would require 35 million lbs of molybdenum, an increase of 18 million lbs of new demand. The selection of either the manganese-nickel-molybdenum grade or the manganese-molybdenum grade as the most cost-effective replacement for the 8600 and 4100 standard steels is dependent upon the ability of the molybdenum market to accept and accommodate a rapid increase in new domestic demand at the time the chromium supply interruption occurs. If the molybdenum market is capable of accepting 18 million lbs of new demand without raising the price of molybdenum above the critical ratio of 2.4, then the manganese-molybdenum replacement is the most cost-effective. Based upon current evaluation of the molybdenum market, it seems that the molybdenum market will be able to absorb the additional demand and the manganese-molybdenum replacement steel would be the most cost-effective chromium-free replacement steel.

CONCLUDING REMARKS

Based upon the several socio-economic scenarios and their projected impacts on alloying elements cost and availability in 1985, two chromium-free substitute steels have been designed. Both steels, a manganese-molybdenum substitute and a manganese nickel-molybdenum substitute, are expected to provide microstructure, heat treat response, and mechanical properties equivalent to the 8600 and 4100 steels. The use of chromium at the present time is highly cost-effective and the implementation of the chromium-free steels under the present conditions would not be in the best economic interest of the nation. However, the development of the two chromium-free steels provides materials information which can be saved or stored in a "National Substitution Data Bank" against a future time when an interruption in the chromium supply occurs. Under the worst case scenario - breakdown in South African chromium supply and at the same time, cut-off of Soviet and Albanian sources - the use of chromium-free steels is expected to provide savings of over half a billion dollars annually. It is also possible that the existence of chromium-free substitute steels could moderate future chromium producer supply and pricing policies. Thus, the development of these substitute steels significantly enhances the National "substitution preparedness" with regard to chromium as used in the constructional alloy steels. Obviously, additional testing is required to develop engineering design data and to confirm equivalency of at least one of these chromium-free steels under production conditions prevalent in U.S. industry. Availability of this data will further encourage the ready adoption and widespread use by industry of the new chromium-free steel in the event of a shortage in the supply of chromium.

ACKNOWLEDGMENT

This project was sponsored by the United States Department of the Interior, Bureau of Mines under Contract No. JO 113104. The support of Messrs. J. T. Dunham and K. W. Mlynarski of the Bureau of Mines, Washington Office, in developing the project is sincerely appreciated. The contract was administered through the Materials Section of the Bureau of Mines, Albany Research Center, under the direction of Mr. H. W. Leavenworth with Mr. Max L. Glenn serving as technical project officer. The assistance of Mr. Glenn in providing technical and administrative assistance is gratefully acknowledged.

REFERENCES

1. Morning, J. L., Mineral Commodity Profiles, Chromium - 1977, Bureau of Mines, U.S. Department of Interior, May 1977.

2. Contingency Plans for Chromium Utilization, NMAB Commision on Sociotechnical Systems, National Research Council, National Academy of Sciences, Washington, D.C., 1978 - NMAB - 335.

3. Breen, D. H., Walter, G. H., Keith, C. J., and Sponzilli, J. T., "Computer Based System Selects Optimum Cost Steels," Metal Progress, November 1973.

4. Keith, C. J., Sponzilli, J. T., Sharma, V. K., and Walter, G. H., "International Harvester's CHAT System for Selecting Optimum Compositions for Heat Treated Steels," Hardenability Concepts with Applications to Steel, edited by Doane, D. V. and Kirkaldy, J. S., published by AIME, 1978.

5. Ralph, W. L., "Lessons from Nickel," Molybdenum Supplement, American Metal Market, July 1982.

6. U.S. Bureau of Mines, Mineral Commodity Summaries 1980, Washington, D.C., Government Printing Office, 1980.

7. Shin, S. W., and Sharma, V. K., "Application of A Tilting and Rotating Specimen Stage to X-Ray Retained Austenite Measurement in Textured and Coarse Grained Steels," SAE Trans., Paper 800428.

CHROMIUM-FREE STEELS FOR CARBURIZING

D. E. Diesburg, G. T. Eldis and H. N. Lander*

INTRODUCTION

Despite the fact that most commonly used carburizing steels contain on the order of 0.5 to 1% chromium, the prospect of a restriction or total cut-off of chromium supply is not terribly troubling to the carburizing steel metallurgist. There already exist several standard chromium-free carburizing grades. The general methodology of developing new carburizing steels to replace existing grades, substituting more abundant and less expensive alloying elements to reduce overall steel cost while maintaining desired properties, is well developed, thanks to past materials shortages of one kind or another. And especially over the last five years or so, we have gained a great deal of knowledge concerning the effects of all the commonly used elements, individually and in combination, on the critical properties of carburized components, so that designing chromium-free steels to meet the requirements of typical carburizing steel applications should pose very little difficulty. Indeed, the only area in the realm of carburizing steels where the prospect of a chromium shortage gives us pause is the relatively specialized application of elevated temperature service. At present, all elevated temperature carburizing steels contain chromium, and the steel properties are heavily dependent on a dispersion of alloy carbide precipitates. However, the authors are confident that, if work is begun now, we can be ready to meet any future chromium shortage with a suitable low-chromium or chromium-free steel for this application, too.

---

* D. E. Diesburg, G. T. Eldis and H. N. Lander are Research Supervisor, Research Manager, and Sr. Vice President, Research and Development, respectively, Climax Molybdenum Company of Michigan, Division of AMAX of Michigan, Inc., Ann Arbor, Michigan.

In the discussion which follows, we will first look at existing standard carburizing steel grades to get an indication of the economic impact of a chromium shortage. We will then consider the effects of various alloying elements on hardenability and on the mechanical properties critical to carburizing steel performance, to show the directions we are likely to follow in our pursuit of new chromium-free carburizing steels and the properties these steels are likely to possess. Lastly, we will look briefly at the most critical problem for chromium-free carburizing steels, namely, elevated temperature service.

EXISTING STANDARD GRADES

In any discussion of carburizing steels, we usually find it convenient to classify the steels into one of three core hardenability ranges, low, medium or high. Figure 1 illustrates these three ranges as schematic hardenability bands showing the depth of hardening in an end-quench test to be expected for each range. Table I catalogues various domestic (SAE standard) and European grades in the respective groupings.

The low-hardenability grades consist of those steels used for relatively small carburized components, specified by the U.S. automotive industry as SAE 4000, 4100, 4400, 4600, 5100, 8600 and 8700. The SAE 8600 and 8700 grades have the highest alloy hardenability and represent the hardenability most often required for such components. SAE 4028 has a hardenability similar to that of SAE 8617; however, a substantial amount of the hardenability comes from the carbon content. This is an important point. Carbon is a very potent element in increasing hardenability, and as such is about the most cost-effective

"alloying" element. But higher core carbon contents generally lead to relatively inferior bend strength properties.[1,2] Thus, the SAE 4028 grade would be used primarily in those applications where specific bending stresses are relatively low. Of the low-hardenability grades, SAE 4000, 4400 and 4600 are chromium-free steels. The other grades contain nominal chromium contents ranging from 0.5 to about 1.0%. In general, the alloy cost of the chromium-free grades is higher.

The medium-hardenability steels are represented by grades such as SAE 4300 and 8800, both containing 0.5% Cr. These grades are used when the section sizes being quenched are too large for the low-hardenability steels to maintain an adequate core hardness. At present, there are no standard chromium-free steels that fall into the medium-hardenability classification.

The high-hardenability grades include such steels as SAE 4815, 3310 and 9310. The SAE 4800 grade is a chromium-free Ni-Mo steel while the SAE 9310 and 3310 steels are Ni-Cr steels containing 1.2 and 1.6% Cr, respectively. These steels are used to produce large components with tough martensitic cores and also for smaller components expected to encounter service too severe for the low- or medium-hardenability steels. In this respect, these grades are often considered to be high performance grades.

Within the various core hardenability ranges, there are several new grades which have been proposed and made commercially available which represent more economical alloy compositions than existing standard grades. These proposed alternates have been assigned SAE EX (or PS) numbers. Table II shows a few examples of EX steels designed by the Climax Molybdenum Co. and compares them with the SAE grades they were designed to replace. All of these alternate

steels* contain higher levels of chromium, manganese and molybdenum than the corresponding SAE grades, illustrating a principal reason for the frequent use of chromium in carburizing steels: At today's availability and price, chromium provides an economical source of alloy hardenability.

But what of the technical merits of chromium? Cost factors aside, can we achieve desired properties without this alloying element? Let us consider various attributes of carburizing steels and what we know about the effects of alloy additions.

HARDENABILITY

We normally subdivide hardenability into two categories. Core hardenability is a measure of the ability to achieve hardness at depth in the low carbon core of the carburized component. It is the hardenability of which we've been speaking in the discussion thus far of hardenability ranges. Case hardenability is a measure of the ability to achieve martensitic microstructures, free of softer pearlitic and bainitic transformation products, in the high carbon case of the carburized component.

Figure 2 illustrates the effects of the common alloying elements on core hardenability.[3] Molybdenum and manganese are, individually, of comparable effectiveness, although molybdenum is substantially more effective if the steel

---

*There is no standard grade with a hardenability range similar to EX55. Its hardenability exceeds that of SAE 9310 and SAE 3310, but with a nominal carbon content of 0.17% and a rather low chromium level of 0.55%.

contains a minimum of about 0.75% Ni. Chromium is somewhat less effective than manganese or molybdenum, and nickel is relatively ineffective by itself. Silicon has no effect on core hardenability at the levels typically found in carburizing steels. If we included a cost factor into these data, turning the abscissa into "alloy cost," the order of the elements would be reversed with manganese being by far the most effective alloying addition, followed by chromium, molybdenum and nickel. That is at current prices and availability, of course. From the core hardenability standpoint, elimination of chromium poses no major difficulties. The hardenability decrease resulting from elimination of, say, 1% Cr from the steel could be readily recovered by an increase of 0.6% in the combined Mn + Mo content. The ratio of manganese to molybdenum selected for such a substitution would depend upon several factors, among them the overall level of those elements already present in the steel, since excessive use of any one element can aggravate the problems of alloy segregation during solidification. Other factors to be considered will be discussed later.

Figure 3 shows the influence of molybdenum, manganese, chromium and nickel on case hardenability, in the carburized areas of the component where carbon content is usually on the order of 0.8 to 0.9%.[4] The relative effectiveness of the elements is quite different than for core hardenability. In addition, molybdenum and nickel share a common attribute which makes them, relative to manganese and chromium, even more effective than Figure 3 implies. These elements are immune to depletion from the matrix by the mechanism of surface oxidation. During normal carburizing in endothermic atmospheres, the oxygen potential is high enough to induce oxidation of chromium, manganese and silicon.[5] These elements are depleted from the matrix at the surface of the

specimen, as illustrated in Figure 4 which shows the results of electron probe microanalysis on a 1.1%Mn - 1.1%Cr steel carburized in an endothermic atmosphere.[6] Figure 5 shows the microstructural effects of this surface oxidation, a decrease in hardenability at the surface and transformation to pearlite and bainite rather than martensite. Depending on depth of oxidation/depletion, size and quenching rate of the component, subsequent surface treatment (lapping, shot peening) and in-service loading experienced by the component, these non-martensitic transformation products at the surface could ultimately prove detrimental to performance.

Turning back to Figure 3 and our example of removing 1% Cr from the steel composition, we could maintain the same level of case hardenability by simply adding 1% Mn. (Note that this is substantially more than the 0.6% Mn required to maintain a constant level of core hardenability, as discussed before.) However, given that the steel will most probably already contain at least 0.5% Mn, a full manganese-for-chromium substitution would not be a good choice. It would result in an "excessive" level of manganese (1.5% or more), and would only aggravate the surface oxidation problem (Figure 4). A more suitable substitution might be, say, 0.4%Mn + 0.2%Mo, which would maintain both the case and core hardenability lost by the removal of 1% Cr. Regardless of the exact combination of elements chosen to substitute for the chromium, it is quite clear that the substitution can be made without experiencing any reduction of steel performance from the hardenability standpoint.

MECHANICAL PROPERTIES

There are two rather independent mechanical properties of carburizing steels that determine their overall performance: (1) the ability to resist pitting and (2) the ability to resist bending. In most applications, carburized components are overdesigned with respect to bending fatigue simply because complete fracture is a less tolerable situation than is surface degradation such as pitting, although severe pitting also can eventually lead to complete fracture.

Pitting Fatigue

Factors influencing pitting fatigue are more difficult to evaluate experimentally than are the factors influencing bending fatigue. Although it is generally believed that pitting behavior is dependent on hardness and microstructure, at times it has been difficult to confirm this experimentally.[7,8] Recent research has shown pitting to be associated with inclusions.[9] Pitting resistance has also been shown to be dependent on the lubricant.[10] A proper lubricant can maintain a film between the contact surfaces and significantly improve the pitting fatigue lives of carburized components. Soft microstructures are generally accepted as having poor resistance to pitting, although hard microstructures can also exhibit pitting. Surface decarburization, the presence of a large amount of retained austenite, and the transformation of austenite to pearlite or bainite during quenching can cause soft regions to occur in a carburized case and thus are believed to lead to an eventual pitting failure. Figure 6 shows pitting damage as revealed in the scanning electron microscope.

All common alloying elements used in carburizing steels, namely chromium, manganese, nickel and molybdenum, are added to obtain the required hardenability. In this respect, the elements are interchangeable as already discussed. However, there are independent limiting factors that determine the maximum amount of each element that should be added, in addition to the segregation and surface oxidation problems already mentioned, which could affect pitting resistance. Nickel and manganese are both austenite stabilizers and therefore must be used in moderation if retained austenite in the carburized case is expected to be a problem. Chromium also has a carbide formation limitation. High chromium contents are believed to promote the formation of large carbides in the case during carburizing, thus steels such as SAE 3310 and SAE 9310 generally require extra care during carburizing and heat treatment.

Reducing or eliminating the chromium contents in carburizing steels is not expected to have a strong effect on the pitting resistance, provided the corresponding loss in hardenability is regained by adding manganese, nickel or molybdenum and retained austenite content remains under control. In support of the contention that chromium-free steels will offer adequate pitting resistance compared to chromium-containing steels, one can look at the current successful use of existing grades of chromium-free steels such as SAE 4000, 4400, 4600 and 4800. There are no reported indications that these grades are any more prone to pitting than the chromium-containing steels.

Bending Fatigue and Impact

Bending fatigue properties of carburized steels are highly dependent on the compressive residual stress that develops at the carburized surface during

quenching.[11,12] This is illustrated nicely by the improvement in high cycle fatigue limit resulting from shot-peening, shown in Figure 7.[13] Shot-peening prior to carburizing does not provide a similar improvement in fatigue behavior (Figure 8).[14] Altering the residual stress at the surface so as to make it less compressive, as by improper heat treatment or other processing, can have a dramatic negative effect on fatigue behavior. This is illustrated in Figure 9 by the data for EX55 subjected to a carbonitriding treatment.[13] The particular cycle employed resulted in a very high (70%) retained austenite content at the specimen surface. Despite this high austenite content, the bulk residual stress at the surface was compressive and the fatigue properties quite good. A refrigeration treatment reduced the austenite content to 40%, but also resulted in a net bulk tensile residual stress at the surface. The effect on fatigue properties was disastrous.

The only expected effect of chromium per se on constant load amplitude high-cycle fatigue behavior would be the result of chromium depletion from the surface, either by severe oxidation or by massive carbide formation. This could allow pearlite or bainite to form at the surface, thus causing the surface to have less compressive residual stress, perhaps even a tensile stress.[15] Figure 10 illustrates the theoretically calculated effect of compressive residual stress on fatigue limit for various assumed degrees of surface oxidation.[16] Here, the oxidation product is assumed to act as an internal defect (stress concentrator) which intrinsically reduces fatigue limit. The importance of maintaining a substantial compressive residual stress at the surface is quite clear. Reducing or eliminating chromium in carburizing steels is thus expected to have no detrimental effect on high-cycle fatigue behavior,

provided the lost case hardenability is replaced with other alloying elements to ensure the surface microstructure remains martensitic. Indeed, to the extent that chromium-free alternate steels might be less susceptible to surface oxidation effects, an improvement in properties might be expected.

The apparent sole dependence of bending fatigue performance (fatigue limit) on the surface residual stress is true when the applied loads are rather low, with maximum loading in the vicinity of the laboratory-measured fatigue limit. However, most carburized parts in service are subjected to a wide spectrum of loading, and the infrequent occurrence of loads well in excess of the fatigue limit must be anticipated. Such overloading can result in material damage, so that the effective fatigue limit after the overload is reduced.[17] The magnitude of overload that can be tolerated before significant damage occurs can simply be referred to as "toughness," and <u>is</u> highly dependent on alloy content as well as the fracture toughness and residual stress further away from the carburized surface.[14] The relative ability of the steels to resist overloading can be evaluated by measuring the impact fracture strength of the carburized component, that is, the load required to fracture the component in a single blow. Climax has been evaluating the effect of various alloy combinations on the impact fracture strength for several years and has published some generalizations that can be used to assess the contribution of chromium to bending fatigue life when random high and low loadings are encountered.[18]

For low-hardenability steels, Figure 11 indicates that chromium generally has a negative effect on impact fracture strength over the range of 0.2 to 1.2%. Thus, no <u>detrimental</u> effect on impact fracture strength or "toughness" is

expected if chromium is eliminated from carburizing steels, provided adequate alloy substitution is made to maintain hardenability.

In the medium-hardenability range, the steel compositions generally include various nickel-chromium-molybdenum combinations. The influence of chromium on impact fracture strength is dependent on the nickel content of the steel. Combined with nickel contents of 1% or less, chromium shows a negative effect on impact fracture strength similar to that experienced in the low-hardenability steels. In combination with nickel contents exceeding 1.0%, chromium has no influence. So again, using chromium-free steels for medium-hardenability should have no detrimental effect on "toughness."

All high-hardenability steels contain more than 1.5% Ni, and as might be expected from the trends in low- and medium-hardenability steels of various chromium and nickel contents, chromium content has no effect on impact fracture strength in the high hardenability steels. The excellent performance of SAE 4800 steels provides ample evidence of the toughness of chromium-free high-hardenability steels. EX55 contains 0.55% Cr, and it has exhibited even better performance than SAE 4817 (other factors, such as the higher hardenability of EX55, are partly responsible for this). A chromium-free version of the EX55 composition, containing 2% Ni and 1% Mo, has been evaluated in the impact fracture test and has exhibited similar behavior to that of EX55. Therefore, in all three hardenability ranges, chromium-free steels are expected to have a toughness equal to or better than currently used chromium-containing steels.

ELEVATED TEMPERATURE SERVICE

Special steel compositions are available for carburized components to be used at temperatures up to 315 C (600 F). Table III gives some examples. Such steels are required to retain adequate case hardness and toughness at these elevated service temperatures. Typical requirements might include a minimum case hardness of 58 HRC after 1000 hours exposure at 315 C (600 F), along with a minimum fracture toughness specification.

To a large extent, these properties are dependent upon precipitation of various alloy carbides during tempering at temperatures above the intended service temperature, to form a strengthening dispersion stable at the operating temperature with a morphology not overly detrimental to fracture toughness. A variety of alloy carbides have been identified after heat treatment of such materials, including M_6C in the lower carbon core regions of the samples, and $M_{23}C_6$, M_2C and MC in the carburized case, depending on the exact steel composition and heat treatment temperatures used.[19] The extent to which chromium enters into these various carbides is not well defined, and its necessity from the standpoint of precipitation kinetics and precipitate stability is even less well defined. Thus, at present, we can't be certain how successful we would be in meeting the requirements of elevated temperature service with a chromium-free composition. The authors are optimistic, however. From the standpoint of "carburizability," the lower the chromium content the better.[20] Carbide precipitation and secondary hardening certainly do occur in vanadium, molybdenum and tungsten alloyed steels without chromium additions,[21] and such precipitation is the major prerequisite for good elevated temperature properties. The comparably good performance of X-53 and X-2M, with 1 and 5% chromium,

respectively, also bodes well for the development, if eventually necessary, of chromium-free compositions. CBS 1000, with only 1% Cr, has performed even better in Climax laboratory tests than X-53 and X-2M, and X-ray diffraction studies have shown it contains no $M_{23}C_6$, the chromium-rich carbide. Indeed, the main difficulty in developing chromium-free steels for elevated temperature service may have nothing to do with service performance at all, but rather be related to slight atmospheric corrosion of components in inventory. Rather remarkably, it was found in developing the CBS 1000 steel that nominally 1% Cr was the minimum amount necessary to avoid problems of component degradation in storage.[19]

SUMMARY

Although chromium is a common alloy addition to carburizing steels, all the evidence indicates it is not necessary for performance in typical (ambient temperature) carburizing steel applications. Chromium is currently added to low-, medium- and high-hardenability steels for economic reasons. Chromium-free steels are expected to perform equally well and, in many situations, may even provide better performance than currently used chromium-alloyed grades. Additional work is necessary to determine the full potential of chromium-free carburizing steels to meet the requirements of elevated temperature service, but the prospects appear promising.

REFERENCES

1. V. S. Sagaradze, "Effect of Carbon Content on the Strength of Carburized Steel," Metal Science and Heat Treatment, March 1970, No. 3, pp. 198-200.

2. C. Kim and D. E. Diesburg, "Fracture of Case-Hardened Steel in Bending," submitted for publication in the Journal of Engineering Fracture Mechanics.

3. C. A. Siebert, D. V. Doane and D. H. Breen, The Hardenability of Steels, American Society for Metals, Metals Park, Ohio (1977), p. 101.

4. C. F. Jatczak, "Hardenability in High-Carbon Steels," Met. Trans., 4 (1973), pp. 2267-2277.

5. I. Kirman, G. Mayer and F. W. Strassburg, "Einfluss von Nickel and Randge füge auf die Brucheigenschaften einsatzgehärteter Stähle," Härterei-Techn. Mitt. 29 (1974), pp. 88-94.

6. Y. E. Smith and G. T. Eldis, "New Developments in Carburizing Steels," Met. Engr. Quarterly, 16, No. 2 (1976), pp. 13-20.

7. J. S. Learman and G. T. Eldis, "Effect of Bainite in the Outer Carburized Case on Rolling Contact Fatigue Life," SAE Paper No. 760665.

8. S. L. Rice, "Pitting Resistance of Some High Temperature Carburized Cases," SAE Paper No. 780773.

9. D. H. Breen, formerly with International Harvester, currently with the Gear Research Institute, unpublished research.

10. J. P. Sheehan and M. A. H. Howes, "The Role of Surface Finish in Pitting Fatigue of Carburized Steel," SAE Paper No. 730580.

11. D. A. Sveshnikov, I. V. Kudryartsev, N. A. Gulyaeva and L. D. Golubovskaya, Chemicothermal Treatment of Gears," Metal Science and Heat Treatment, No. 7, July 1966, pp. 527-532.

12. Chongmin Kim, D. E. Diesburg and G. T. Eldis, "Effect of Residual Stress on Fatigue Fracture of Case-Hardened Steels," ASTM STP 776 (1981) pp. 224-234.

13. Chongmin Kim, D. E. Diesburg and R. M. Buck, "Influence of Sub-Zero and Shot-Peening Treatments on Impact and Fatigue Fracture Properties of Case-Hardened Steels," Journal of Heat Treating (3), 1 (1980), pp. 3-13.

REFERENCES (Continued)

14. R. W. Buenneke, C. R. Dunham, M. P. Semenek, M. M. Shea, M. B. Slane and J. E. Tripp, "Gear Single Tooth Bending Fatigue Test," SAE Paper No. 821042.

15. B. Hildenwall and T. Ericsson, "Residual Stresses in the Soft Pearlitic Layer of Carburized Steel," Journal of Heat Treating (3), 1 (1980), pp. 3-13.

16. D. E. Diesburg, C. Kim and W. Bulla, "Impact and Fatigue Fracture of Carburized Cases Related to Fracture Toughness and Residual Stress," Presented at Heat Treaters Conference, Wiesbaden, West Germany, 1981, proceedings to be published.

17. T. B. Cameron and D. E. Diesburg, "The Significance of Impact Fracture Strength of a Carburized Steel," to be presented at the Spring Meeting of TMS-AIME in Atlanta, March 6, 1983 (to be published).

18. D. E. Diesburg and Y. E. Smith, "Fracture Resistance in Carburizing Steels Part II: Impact Fracture," Metal Progress, 115 (6), June 1979, pp. 35-39.

19. C. F. Jatczak, The Timken Co., private communication.

20. C. F. Jatczak, "Specialty Carburizing Steels for Elevated Temperature Service," Metal Progress 113, No. 4 (1978), pp. 70-78.

21. G. A. Roberts, J. C. Hamaker and A. R. Johnson, Tool Steels, American Society for Metals, Metals Park, Ohio (1962), pp. 215-218.

Table I

COMPOSITION, HARDENABILITY AND COST OF COMMERCIALLY AVAILABLE STANDARD CARBURIZING STEELS

	Nominal Composition, Wt – %					Hardenability,[b]	
Steel[a]	C	Mn	Cr	Ni	Mo	D_I, mm	$/ton[c]
Low Hardenability							
4028	0.28	0.80	–	–	0.25	40	157
4118	0.20	0.80	0.50	–	0.10	36	98
4422	0.22	0.80	–	–	0.40	39	184
4617	0.17	0.55	–	1.80	0.25	37	323
5120	0.20	0.80	0.80	–	–	41	55
8620	0.20	0.80	0.50	0.55	0.20	48	189
8720	0.20	0.80	0.50	0.55	0.25	50	208
*18CrMo4	0.18	0.65	1.05	–	0.25	53	163
*20NiCrMo2	0.20	0.75	0.50	0.55	0.20	45	189
*20MoCr4	0.20	0.75	0.40	–	0.45	48	253
*16MnCr5	0.16	1.15	0.95	–	–	52	97
Medium Hardenability							
4320	0.20	0.55	0.50	1.80	0.25	60	327
8822	0.22	0.85	0.50	0.55	0.35	62	252
High Hardenability							
4815	0.15	0.50	–	3.50	0.25	66	512
3310	0.10	0.55	1.60	3.50	–	>127	499[d]
9310	0.10	0.55	1.20	3.25	0.10	89	530[d]
*14NiCrMo13	0.14	0.45	0.95	3.25	0.25	99	559
*17CrNiMo6	0.17	0.50	1.65	1.50	0.30	>127	431
*20NiMoCr6	0.20	0.75	0.40	1.60	0.45	87	436

[a]Asterisk denotes European standard. Others are SAE grades.

[b]Calculated from composition assuming ASTM grain size No. 7.

[c]Grade extra charge based on U.S. industry pricing.

[d]Does not include $25/ton electric furnace extra, which is required.

Table II

COMPOSITION, HARDENABILITY AND COST OF SEVERAL SAE GRADES AND THEIR EX ALTERNATES

	Nominal Composition, Wt – %					Hardenability,[a]	
Steel	C	Mn	Ni	Cr	Mo	D_I, mm	$/ton[b]
SAE 8620	0.20	0.80	0.55	0.50	0.20	48	189
EX 24	0.20	0.87	–	0.55	0.25	48	154
SAE 4320	0.20	0.55	1.85	0.50	0.25	60	327
EX 29	0.20	0.87	0.55	0.55	0.35	63	256
SAE 4815	0.15	0.50	3.50	–	0.25	66	512
EX 30	0.15	0.80	0.85	0.55	0.52	80	357
EX 55	0.17	0.87	1.80	0.55	0.75	>127	528

[a]Calculated from composition assuming ASTM grain size No. 7.

[b]Grade extra charge based on U.S. industry pricing.

Table III

CARBURIZING STEELS FOR ELEVATED TEMPERATURE SERVICE

	Nominal Composition, Wt – %							
Steel	**C**	**Mn**	**Cr**	**Ni**	**Mo**	**W**	**V**	**Cu**
CBS 1000	0.14	0.5	1.15	2.9	4.7	–	0.3	–
X-53	0.18	0.4	1.05	2.1	3.3	–	–	2.0
X-2M	0.15	0.3	4.90	–	1.4	1.4	0.4	–

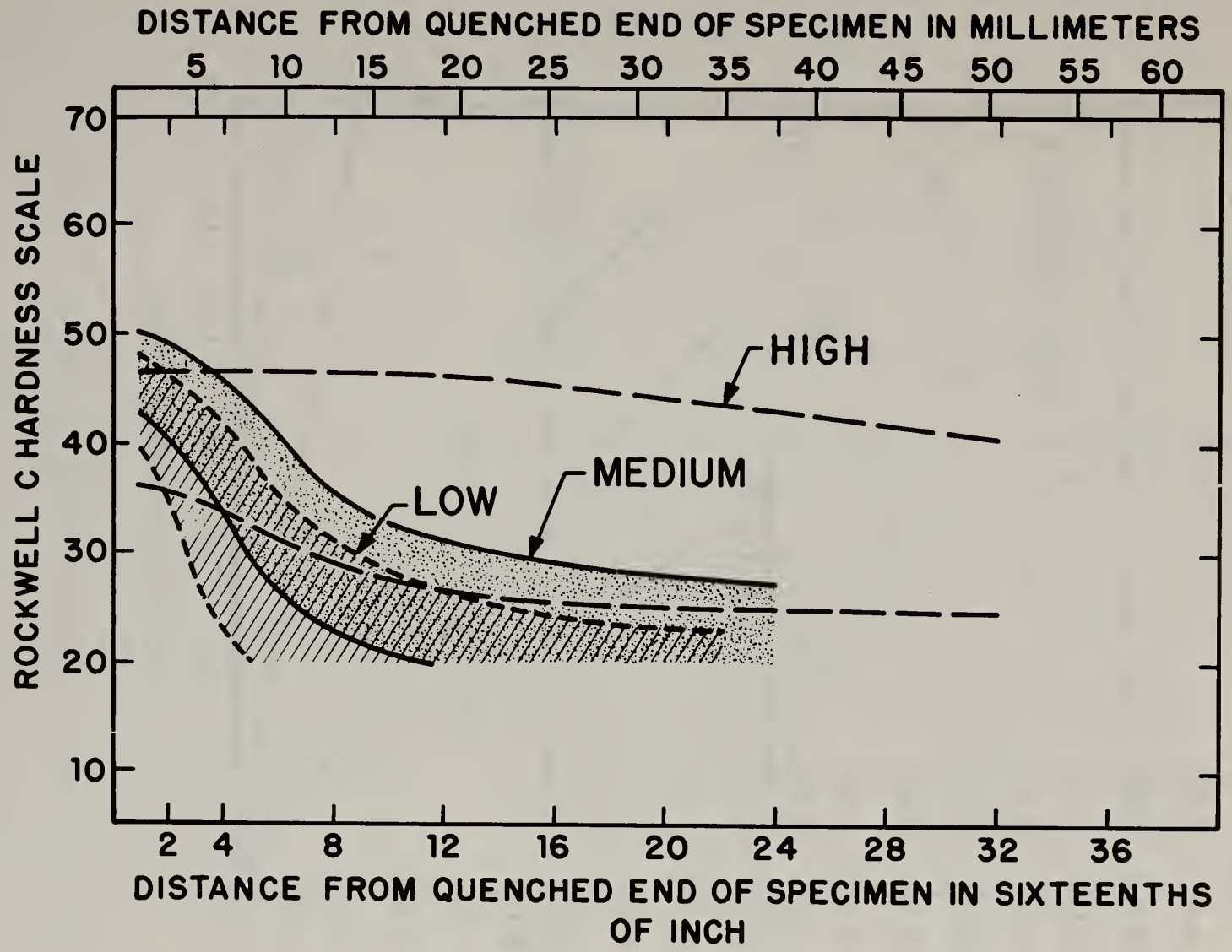

Figure 1 Schematic End-Quench Hardenability Bands Illustrating Depth of Hardness Expected in Steels of Low, Medium and High Hardenability

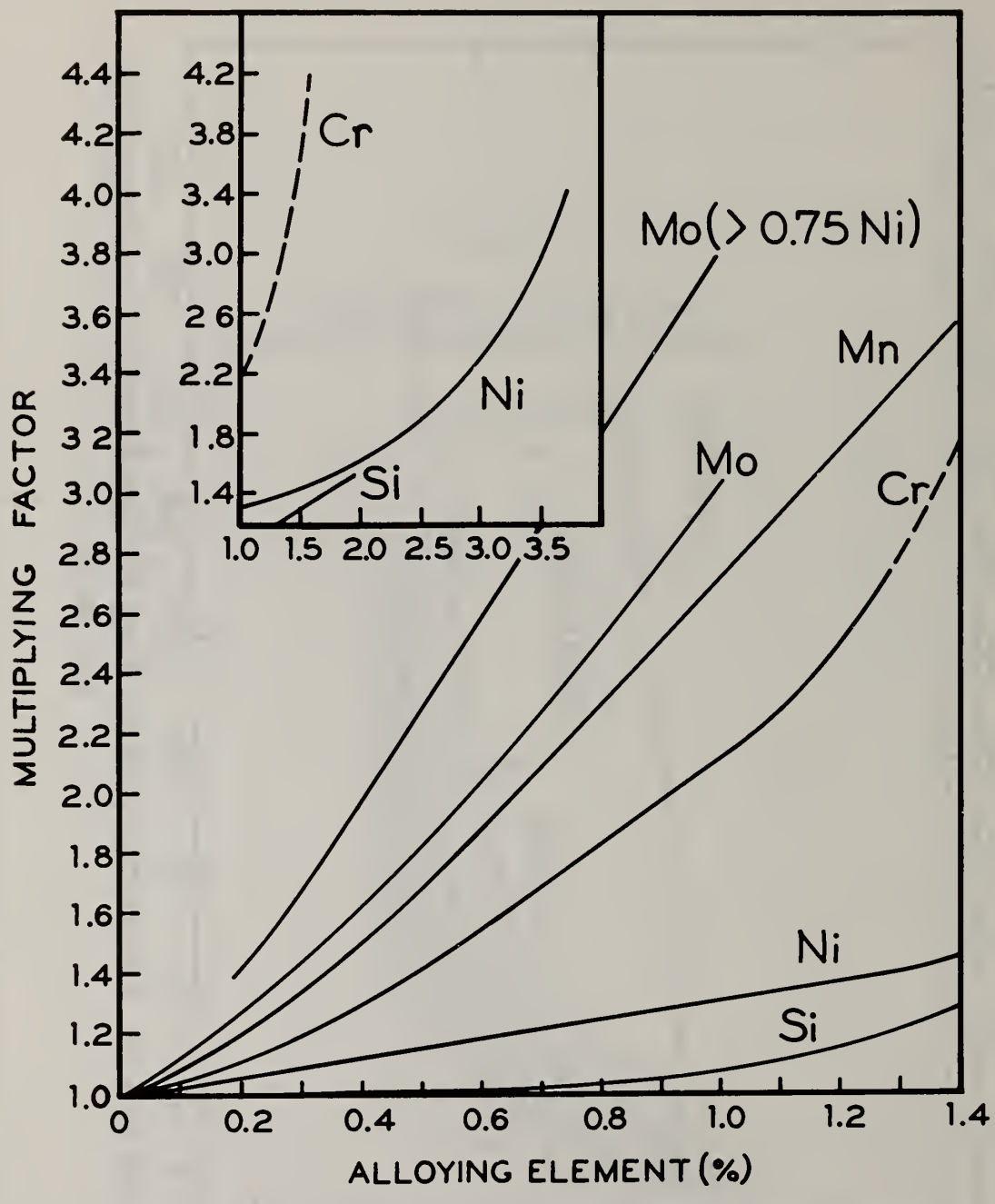

Figure 2 Effect of Various Elements on Hardenability at 0.2% Carbon Content (Reference 3)

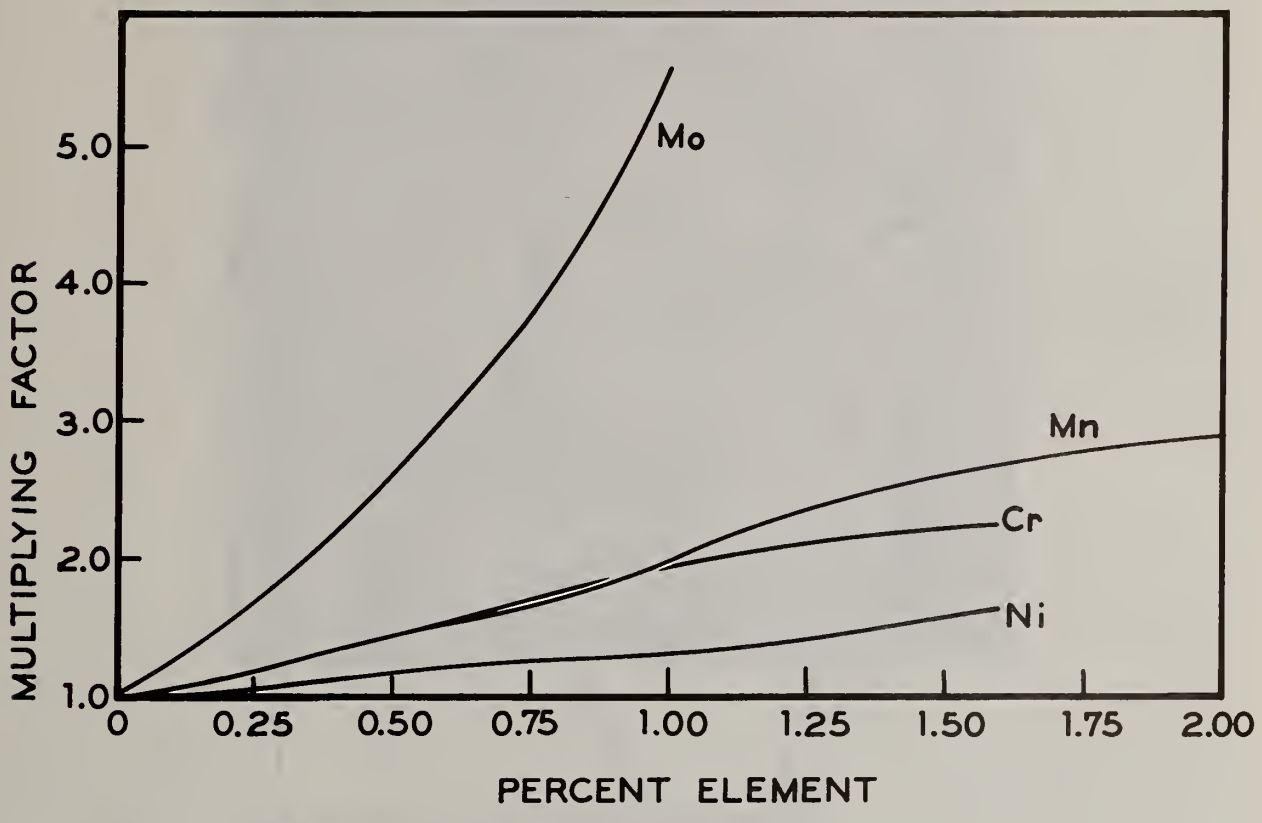

Figure 3 Effect of Various Elements on Hardenability at 0.85% Carbon Content (Reference 4)

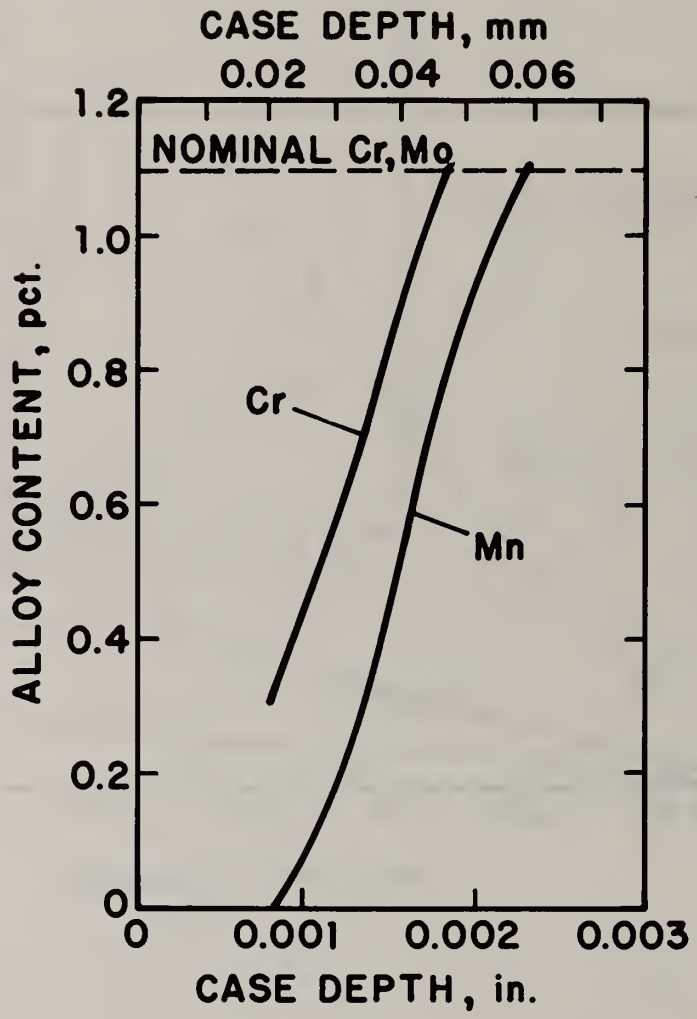

Figure 4 Chromium and Manganese Concentration Profiles Developed in the Specimen Case During Carburizing of a 1.1%Mn - 1.1%Cr Steel (Reference 6)

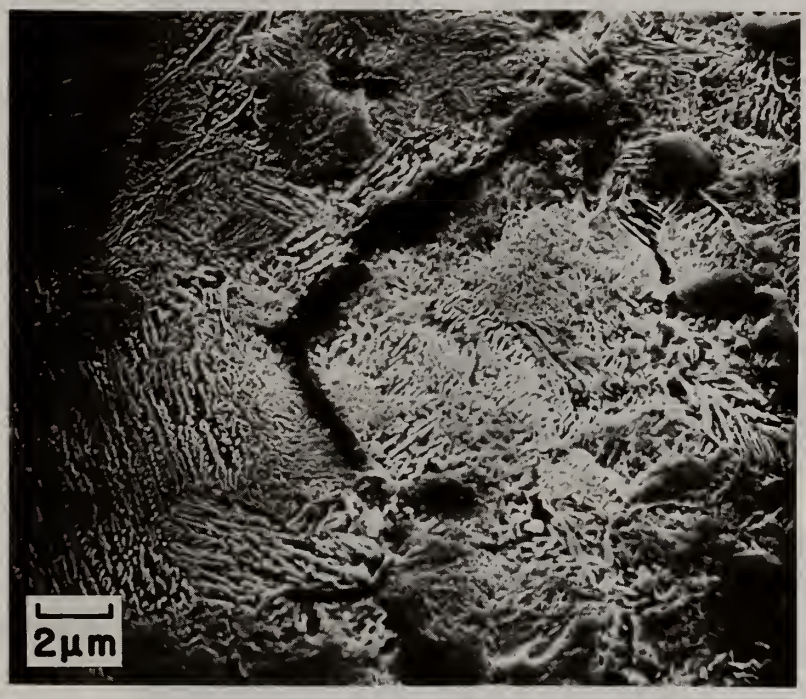

Figure 5 Scanning Electron Micrograph of Carburized Case in 1.1% Mn - 1.1% Cr Carburizing Steel

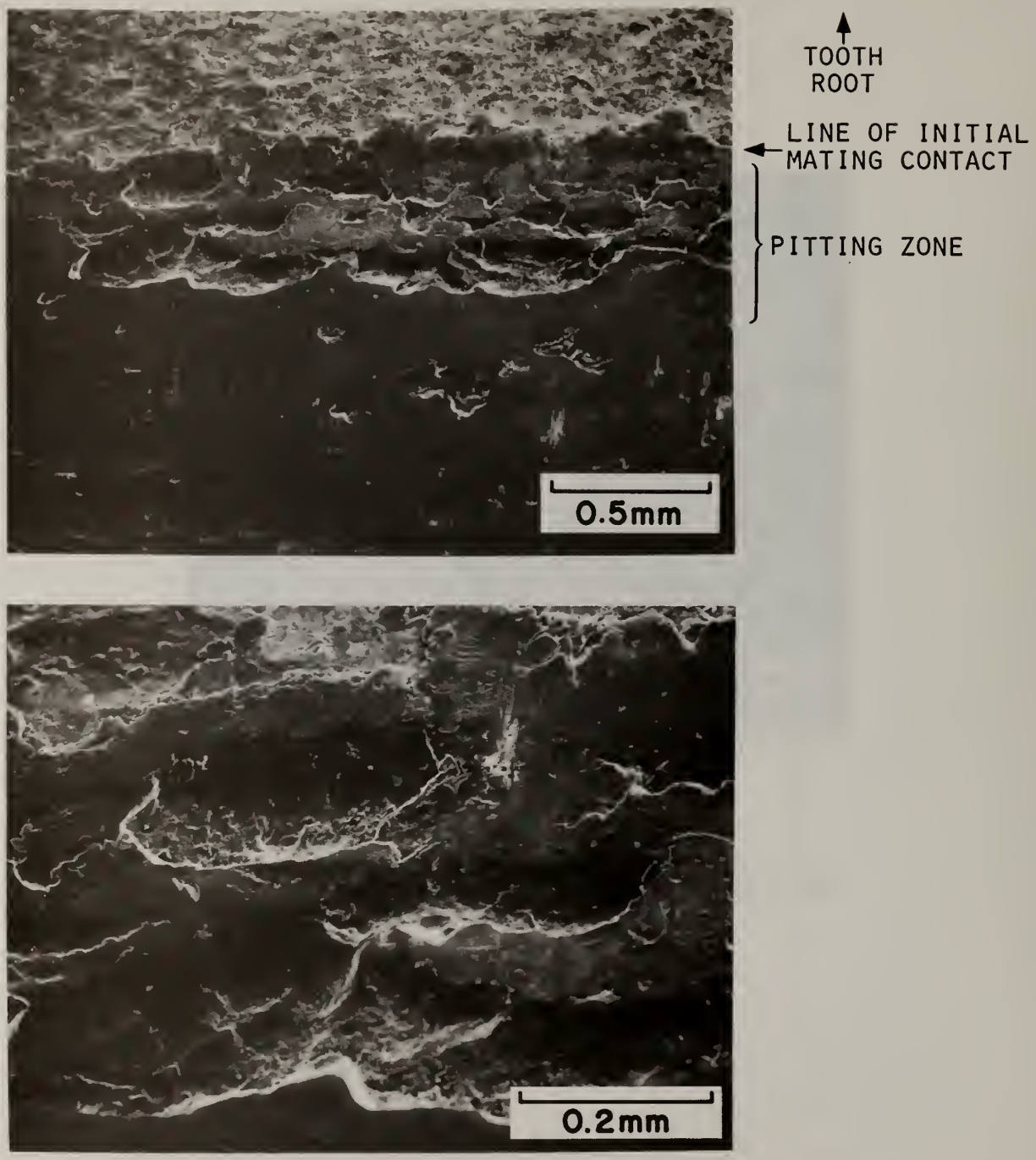

Figure 6 Scanning Electron Micrographs of the Heavily Pitted Region on the Compression Face of a Driven Gear

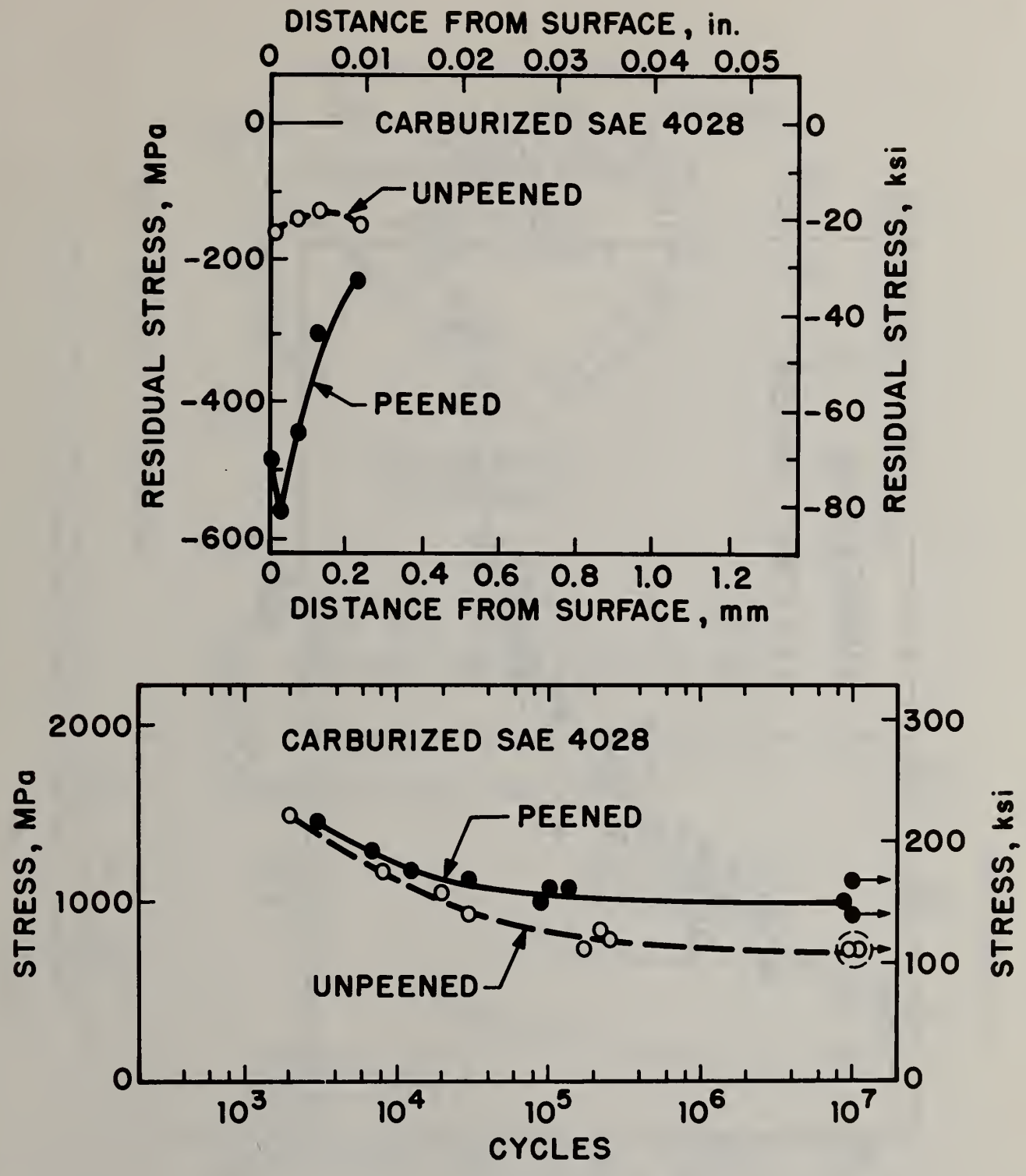

Figure 7 Residual Stress Profiles and Stress-Life Curves for Carburized SAE 4028, Before and After Shot-Peening (Reference 13)

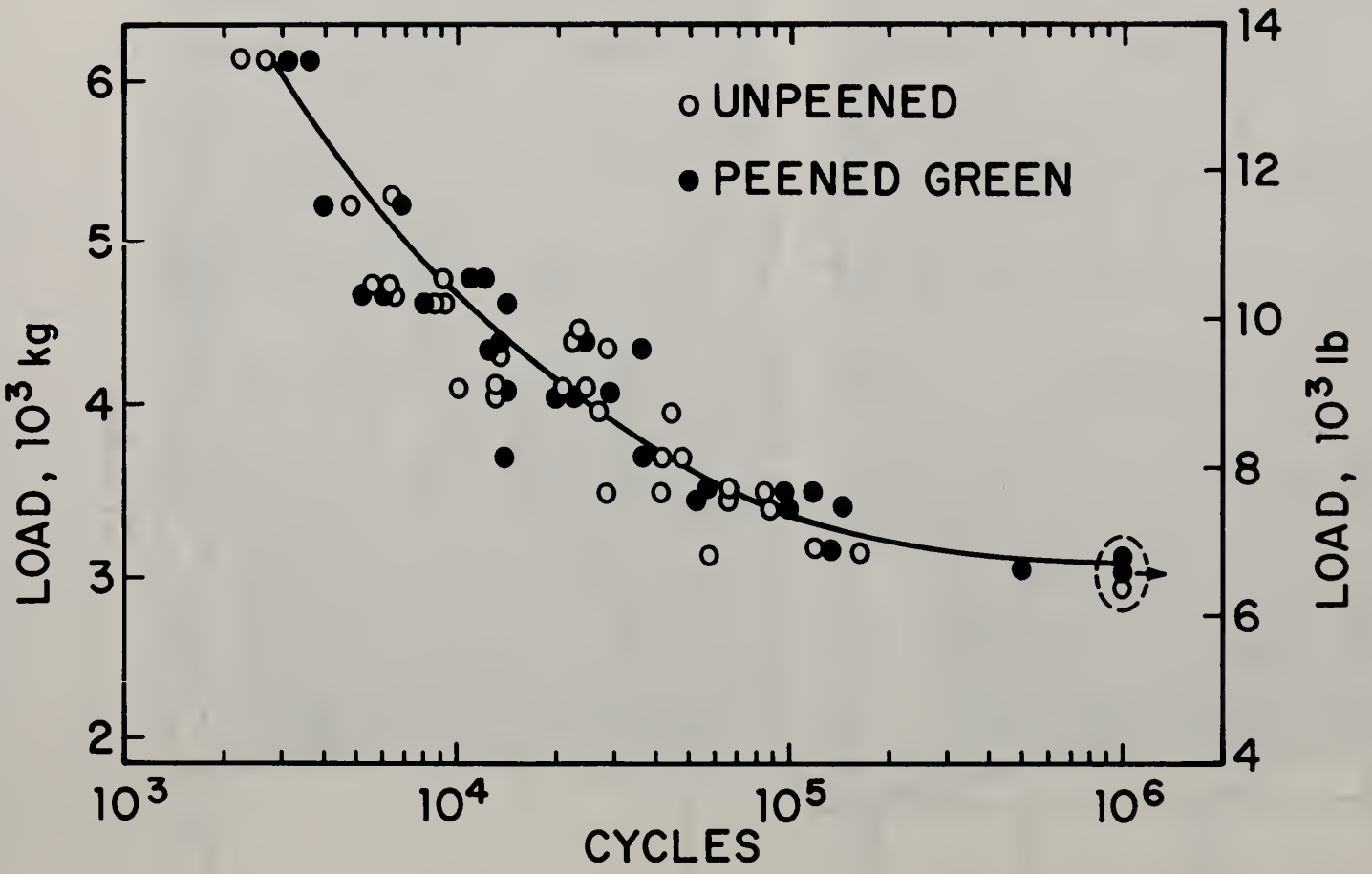

Figure 8 Load-Life Data for Carburized 8620, With and Without a Shot-Peening Treatment Prior to Carburizing (Reference 14)

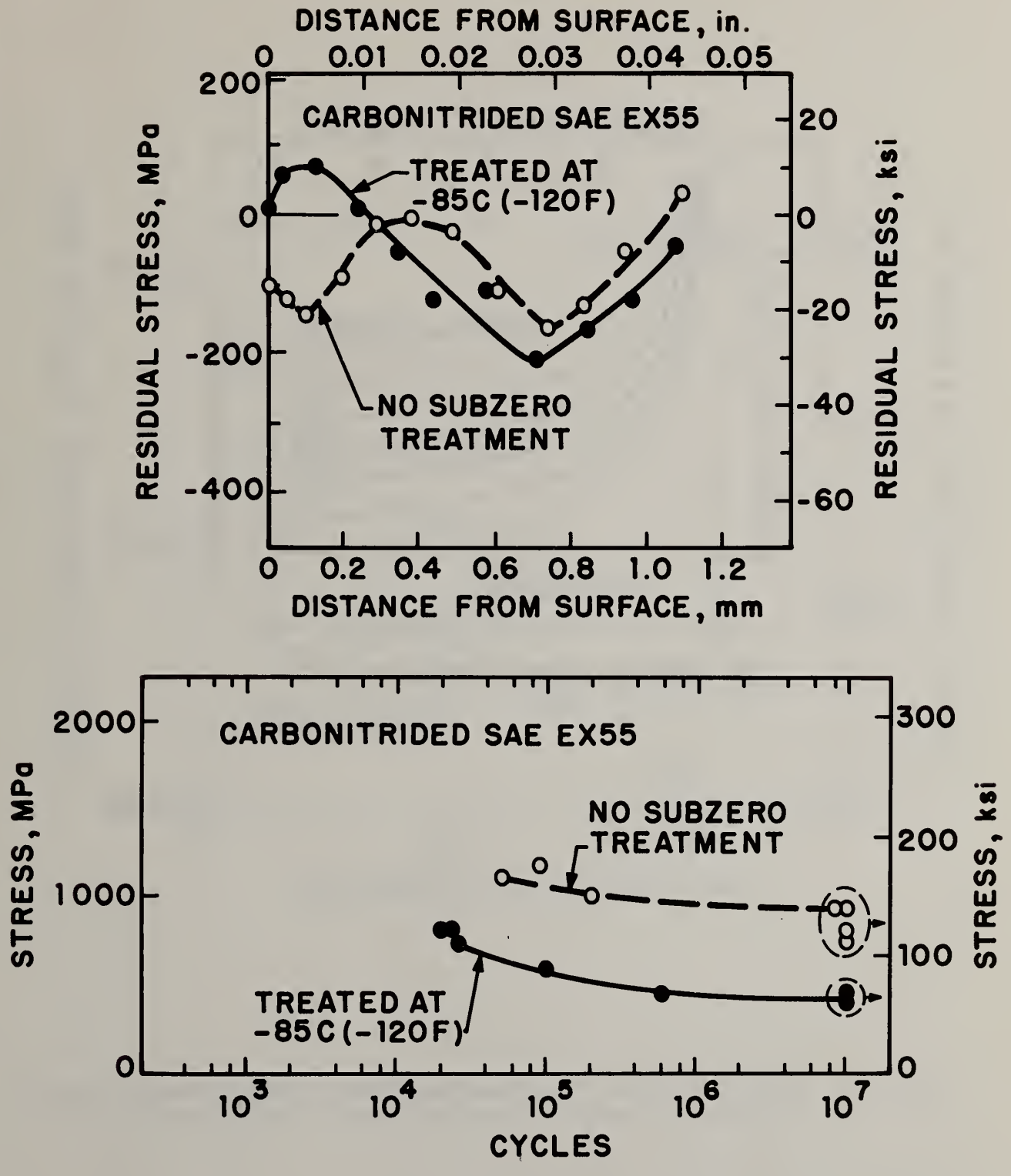

Figure 9 Effect of Refrigeration Treatment on Residual Stress and Stress-Life Behavior of Carbonitrided EX55 (Reference 13)

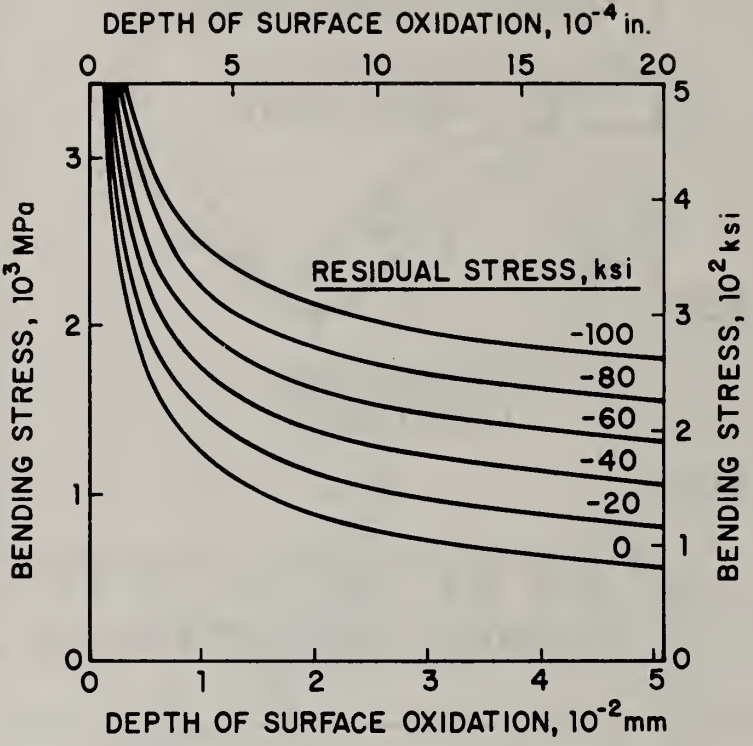

Figure 10 Predicted Effect of Surface Oxidation on Bending Fatigue Limit for Various Levels of Residual Strength (Reference 16)

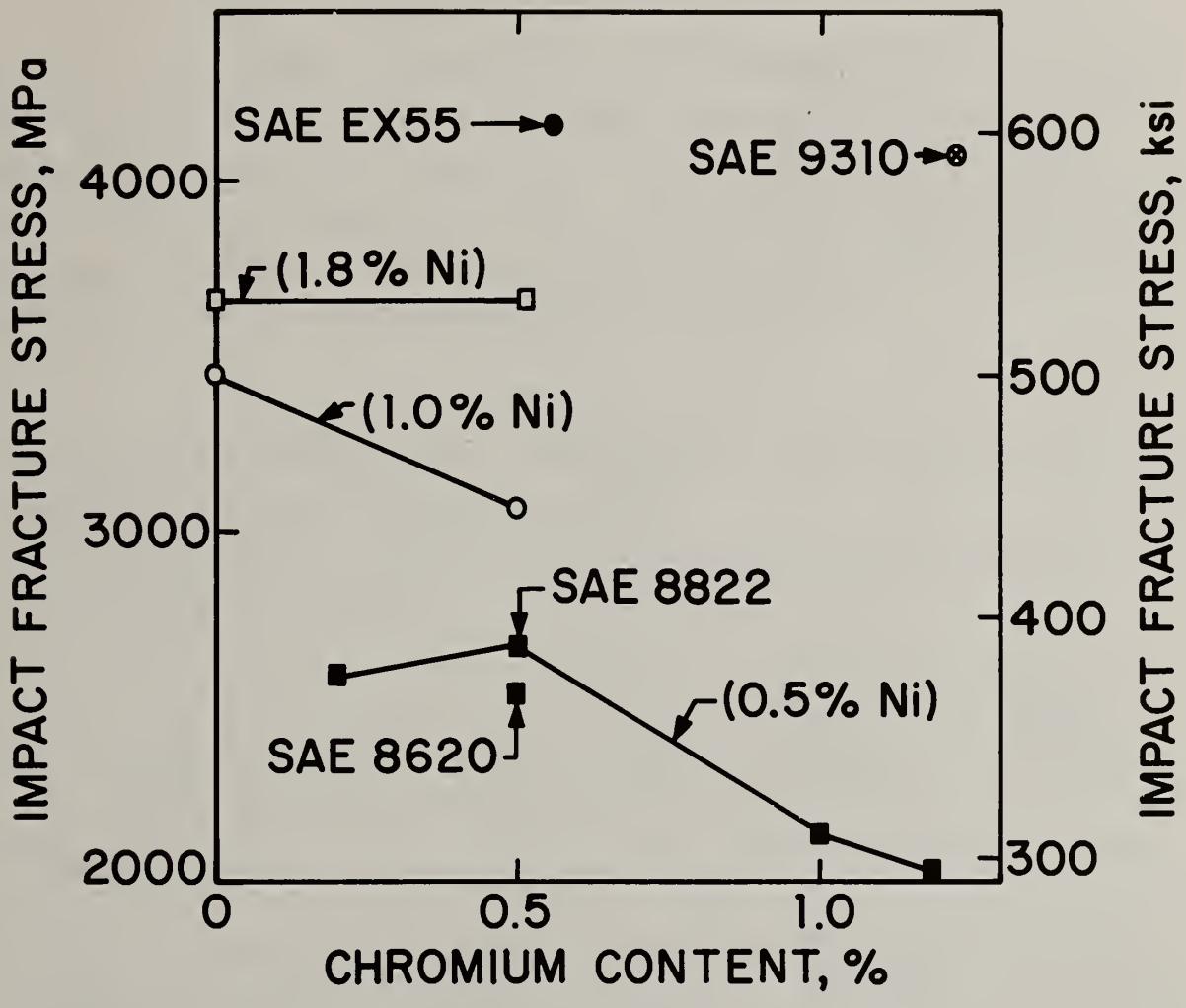

Figure 11 Influence of Chromium and Nickel Contents on Impact Fracture Strength of Carburized Steels (Reference 18)

Report from Nachang Gear Plant, Beijing, China

RARE EARTH BORON STEEL (25 Mn-Ti-B) GEARS

Presented by
Dale H. Breen and Allen G. Gray

Rare Earth Boron Stee (25 Mn-Ti-B) is a chromium free carburized steel developed jointly by 20+ plants, research institutes and colleges in China. This new steel is based on utilizing the material that is abundant in China. The outstanding features of this steel are that it has good properties, is based on mature technology, and has high reliability and low cost.

I. The Chemical Composition, Fundamental Properties and the Refining of Rare Earth Boron Steel.

1. The chemical composition of rare earth boron steel in weight percentage.

C	Mn	Si	Ti	B	Rare Earth
0.22 -0.28	1.30 -1.60	0.20 -0.45	0.06 -0.12	0.001 -0.004	20.05

2. The mechanical properties of the rare earth boron steel.

Heat Treat	Tensile Strength (kg/mm^2)	Ultimate Yield (kg/mm^2)	Elongation (%)	Reduction of Area (%)	Impact Strength ($kg.m/cm^2$)
850 C Oil Quench 200 C Anneal	$^{2}140$	$^{2}110$	$^{2}10$	$^{2}40$	$^{2}6$

3. The refining of the rare earth boron steel. In the past 10 years, steel plants throughout China such as Dayie Steel Plant, Nanchang Steel Plant, and Peking Specialty Steel Plant, have produced over 10,000 tons of rare earth boron steel. Among those plants, the Dayie Steel Plant has the highest capacity for producing the rare earth boron steel.

Rare earth boron steel can be refined by using electric furnace, a combination of electric furnace and converter, or simply converter. Regardless of the refining method, the processing is simple, the quality of the product is good, and yield is high (according to the tabulation by Dayie Steel Plant, the yield by using any of the three refining methods is about 97%). Therefore, this type of steel can be produced in many steel plants in large quantity.

4. Cost. According to the calculation made by Dayie Steel Plant, the price of the different kinds of rare earth boron steels when compared to 18 chrome-manganese-titanium steel is about 140 yuan lower per ton. That is to say the price of rare earth boron steel has a cost of about 15% lower than the 18 chrome-manganese-titanium steel. Therefore, wide application of rare earth boron steel can lead to lowering the cost of production of finished product.

II. Review of Plant Experiment and Application of Rare Earth Boron Steel.

Our plant has participated in the development, trial application and promotion of the rare earth boron steel since 1964. Starting November of 1974, we have been substituting 18 chrome-manganese-titanium steel and 22 chrome-mangenese-moly steel with the rare earth boron steel in the manufacturing of shift gears for tractors and automobiles. In October of 1975 in a meeting called "The 25 Manganese Titanium Boron Rare Earth Steel Application, Exchange, Promotion and Testing" sponsored by the Ministry of Metallurgical Industries and the Number One Ministry of Machinery, we have reported in conjunction with other

organizations the complete technical evaluation of the rare earth boron steel. After that, we have expanded the application of the rare earth boron steel to other types of complicated gears for tractors and automobiles. Thus the rare earth boron steel has now become one of the major carburized gear steel in our plant.

To date, we have applied the rare earth boron steel in the making of 76 types of gears in 7 different types of machineries.

Machine Design-nation	45(55)	54	27	12	NJ-130	CA-10B	750
Number of gears	32	2	22	6	4	6	4

From 1966 to September 1981, we have used over 12,000 tons of rare earth boron steel. If we take the price difference between rare earth boron steel and the chrome steel of 140 yuan, we have saved so far in the cost of material alone about 1.8 million yuan.

III. The Technical Properties of the Rare Earth Boron Steel.

1. The production of forged gear blank.

a. In the production of this material no matter whether saw or shear is applied, there is no abnormal phenomena. The properties are comparable with 18 chrome-manganese-titanium and 22 chrome-manganese-moly steel.

b. The forging temperature range of rare earth boron steel is 1250°C maximum and 900°C minimum. Because of the good hot workability of the steel, it is easy to form in a closed die forging operation. The oxide layer on the forged blank is thicker but it is also fragile and loose. Therefore it is easy to remove.

c. Normalization temperature for the forged gear blank is 960°C. Usually we use air cooling. After normalization, the hardness is HB156 to HB207 and 80% of the blank has a hardness of about HB163 to 187.

2. Machineability. The machineability of the rare earth boron steel is good. The chips are easy to break and there is no tangling phenomena. The machineability is comparable with chrome steel. The cleanness of the product after the machining operation is similar to those of the chrome steel and can therefore satisfy the product design demand completely. In our production, it was discovered that when machining the center hole of a gear blank of rare earth boron steel the machining speed has to be reduced. This could be due to the higher strength and higher toughness of this particular steel.

3. Heat Treating of Gears. The rare earth boron steel has a structure of fine grain and a direct quenching process can be used after carburization. The features of the process are as follows.

a. Carburization Speed. The speed of carburization for both rare earth boron steel and chrome steel is basically the same. There is no difference in the carburization production rate.

b. The Carbon Concentration in the Carburized Layer. The diffusivity of carbon in rare earth boron steel is lower than 18 chrome-manganese-titanium steel, therefore there is a more uniform concentration of carbon in the carbon diffusion layer compared to chrome steel. Therefore better metallographic structure could be obtained.

c. Grain Size Classification. After carburization and quenching, 82% of the Martensite structure on the surface diffused layer has a grain size of 2-4, the other being 1 and 5. 86.5% of the residue Austenite structure has a grain size of 2-4 and the remaining being 1 and 5. 98% of the core Ferritic structure has a grain size of 1, the remaining being 2.

Because rare earth boron steel does not contain strong carbide formers, the amount of carbides in the diffused layer is not very high. The above described metallographic structure is superior to the chrome steel. Rejection rate due to inferior metallographic structure of the rare earth boron steel carburized quenched gear is very low. On the other hand, the gear made of chrome steel after carburization heat treating, the rejection rate sometimes is as high as 1.5% due to simply the carbide being out of spec.

d. Hardness. The surface hardness of rare earth boron steel after carburization, quenching, and annealing is generally around RC59 to 62 which is comparable to chrome steel gears. We therefore can meet the desired requirement.

Due to the higher quenchability of the rare earth boron steel after quenching of the carburized gear the hardness in the center part of the gear is also higher. Take for example, the 5/3.75 gear, the hardness in the center of a 18 chrome-manganese-titanium gear after carburization and quenching is around RC35-39 while that of the rare earth boron steel gear is around RC40 and above. This resulted in a stronger base metal for the rare earth boron steel gear.

c. Distortion of Gear During Carburization and Quenching.

Based on long term production experiences, the distortion of the teeth of gear made by rare earth boron steel after heat treating is very close to that of the chrome steel however, the distortion of the keyholes of the rare earth boron steel is higher than the chrome steel in general. But through better data gathering and statistical analysis, we conclude that for the same kind of gear, the fundamental trend of distortion is basically the same for both rare earth boron steel and chrome steel. The distortion direction is the same, basically shrinkage. The standard deviation of the amount of distortion is about the same. The average amount of distortion is usually higher in the rare earth boron steel so it is concluded that we have a handle on the trend of distortion in a rare earth boron steel gear.

IV. Machine Testing the Machine Application of the Gear and the Effect of Rare Earth and Boron in the Steel

1. Machine Testing. The third shift gear of #27 tractors gear box is a typical example. The wall of the gear is very thin. It has four 2.3 mm diameter oil hole and the inner wall is cladded with copper bushing. The load is also applied on the gear when the tractor is in the reverse shift. The original material for this gear was 18 chrome-manganese-titanium steel. In order to increase the strength, it was later modified to use 22 chrome-manganese-moly steel. Now the gear is made using 25 manganese-titanium-boron and rare earth steel.

A machine testing of four different kinds of steels was performed in Jiangxi Tractor Plant to compare their relative lives. The testing specification is as follows: the load is 58.7 kg-meter (this is in equivalent to 2.19 times the load the third gear will take). The speed is about 727 rpm. The following table tabulates the results of the test.

Results of Test Rigs

Materials	Time to Crack Formation (hr)	Time to Fracture (hr)	Metallographic Structure Surface	Metallographic Structure Center	Hardness RC Surface	Hardness RC Center	Carbon Diffusion Layer (μ)	Damage Condition
18 CrMnTi	325	616	Fine M +	Low	61.5	40	0.76-0.85	Broken at
	357	776	Some A	Carbon M	60	42	0.9-0.98	oil tap
	365	825	-	-	-	-		(same)
22 CrMnMo	195	626	Fine M + Some A	Low Carbon M + Some F	62	39.5	0.67-0.76	(same)
	323	708	(same)	Low Carbon M	64	41.5	0.86-0.95	(same)
	366	1000	(same)	(same)	62	42	0.67-0.76	unbroken
25 MnTiB	203	864	(same)	Low Carbon M + Some F	60	43.5	0.72-0.8	Broken at oil tap
	229	1120	-	-	--	--	0.72-0.8	(same)
25 MnTiB	419	1175	Fine M + Large Amt A	Low Carbon M + Some F	57.5	46		Broken Somewhere Else
	415	1329	-	-	--	--		(same)

M = Martensite F = Ferrite A = Austenite

JHC/cas
1/7/82

In our plant, we have done similar tests of a third shift gear with a load of 29.4 kg meter, a speed of 1450 rpm. After over 15,000 hours, the gear is still in good shape and the test is continuing.

2. Actual Application. The main rear shaft cone gear of a #7 tractor is one of the gears that sustains the largest load. Originally 18 chrome-manganese-titanium steel was used and the life of the gear is about 2000 hours. Later on, 22 chrome-manganese-moly steel was used and 52.5% of the gears lasted less than 5000 hours. After switching to 25 mangenese-titanium-boron rare earth steel, according to a survey in 1977, 43% of the gears has reached the life of 10,000 hours. In three communes in several provinces, the application lives for that part are 13,040 hours, 11,420 hours, and 13,560 hours respectively. More than half of the time, their tractors were used in a rice paddy. In May of 1981, we made a survey of our users who reported their 25 manganese-titanium-boron rare earth steel central transmission gear after 16,070 hours and 10,000 hours respectively are still in good shape. The teeth still shine and in perfect shape. Also, in one of the applications in automobile, rare earth transmission gear after 200,000 km of traveling, the face of the gear is still in good shape and shining. Another survey made on a East-Is-Red 54 tractor, one gear on that tractor lasted about 4,000 hours and the wear value of the face of the gear is about .08 to .102 mm. Another test was done on a transmission gear that was carburized and also nitrided. The test results show that after 8,000 hours of application, the maximum wear is about .05 mm. On the tractors produced by our plant namely #12, #27, #55, and #54, the main transmission gears all lasted more than 6,000 hours.

Since 1969 to date, we have conducted seven users survey in conjunction with personnel of research institute and technical school and have conducted visits to the customers. It is clear that from these results not only the 25 manganese titanium boron rare earth steel has a higher bending fatigue resistance strength, it also has a higher bending strength, a higher contact fatigue strength, and a lower crack sensitivity. The results from test rig and on-site application are consistent.

3. The Effect of Rare Earth and Boron in the Steel.
To answer the question why 25 manganese-titanium-boron rare earth steel gear is better than the original steel gear, we have conducted a research in conjunction with the Peking University of Iron and Steel Technology and here are the results:

   a. Proper addition of rare earth in the steel apparently can have a desulfurization effect and it can also change the property of the inclusions. The rare earth converts the elongated manganese sulfide into spherical rare earth sulfide (Re_2S_3) or oxysulfide (Re_2O_2S). The elongated inclusion of manganese sulfide apparently lowers the transverse ductility of the steel and also its toughness. The coversion effect of the rare earth on the sulfides thus eliminated the detrimental effect of elongated shape manganese sulfide. As a result, the strength of the 25 manganese-titaniun-boron rare earth steel gear is increased. In the meantime, the rare earth in the steel converts the aluminum oxide or aluminum compounds which have higher hardness to a rare earth aluminum compound inclusion which has a lower hardness. Through this process, the fatigue strength of the gear was increased.

b. The rupture strength and toughness of the carburized layer of the 25 manganese-titaniun-boron rare earth steel gear are raised by the rare earth addition.

c. The gear has a higher carbon concentration (.25%) in its inner part. The boron raises its quenchability. After quenching the inner strength of the gear is subsequently raised. Therefore, in gears having identical carburized layer thickness, the 25 manganese-titanium-boron rare earth steel has a deeper effective hardened layer therefore a longer application life for the gears.

At the present, our plant is mass producing gears for tractors and automobiles by using the rare earth boron steel and these gears have received good rating and are warmly welcome by the users.

This report was prepared in October 1981 by the Nanchang Gear Plant.

JHC/cas
1/7/82

POTENTIAL FOR SELECTIVE HARDENING BY INDUCTION IN CHROMIUM FREE STEELS

By
Peter A. Hassell
Ajax Magnethermic Corp.

"Electromagnetic Induction," "Faraday's Law," "Transformer Effect," in electrical jargon describe the single basic principle which makes it possible to heat any electrical conductive material in an alternating or changing magnetic field. This is the basis for all induction heating, a process which is very much akin to I_2R or the resistance heating of an electric furnace, toaster or hair dryer--electric current flowing against the inherent resistance of the metal being heated. Losses considered undesirable in transformers, motors and other electric induction devices are accentuated to heat and melt metals. Inductive coupling is the key to some of the very unusual ways in which electromagnetic induction can be applied for heating. No physical contact is required nor is any sensible heat a part of the energy transfer system. With heat generated in the charge proper, and surface energy transfer problems eliminated, opportunities exist to apply large amounts of heating energy, very high energy densities, and in controlled patterns where heating currents are the image of the heating inductors.

One should not exclude low power, low energy induction heating, because in specific uses, it can be an economically attractive method for heating various products, where the process dictates this kind of treatment. Any reasonable electrical conductor can be inductively heated, but in the manufactured product world of today, metals by far predominate the electrical conduction material category. In general, metals require considerable process heating, and this was emphasized in a study which indicated an average of

nine separate heating operations used in the manufacture of a typical steel part. Recent efforts to more efficiently use energy are tending to reduce this number, and induction heating is making some noteable contribution to this endeavor.

Induction heating as a metalworking tool has application in many basic metalworking processes. Some of these are melting, heating for hot working, heat treating, joining, and a host of other miscellaneous uses in which shape or metallurgical structure does not change. The latter include, shrinking, applying metallic and organic coatings, stress inducement, sintering and others which utilize the unique application capabilities of electromagnetic induction. Alloy conservation possibilities certainly exist in induction hardening, but other induction applications also provide potential to enhance this effort.

Metal heat treating is certainly one of the major uses for the induction heating technique. Today, in the various metalworking industries, most engineering and production people are exposed to some form of induction heating, very likely for one of their own manufacturing processes. Very often it is one of the heating methods considered for a new application or a new facility. At this time, induction heat treating of non ferrous metals seems to be limited to annealing, mostly continuous annealing in uniform sections. On the other hand, induction is broad in its use for heat treating ferrous metals. Localized and surface hardening, through hardening and tempering, normalizing and annealing, solution annealing and stress relieving are some of the types of heat treatment performed by the induction method. All types of steel and cast irons are candidates, and most every type of ferrous metal is in some place or in some way now being induction heated.

Some shape and part configurations offer limitations to uniform heating; and for this reason, the induction method should not be considered a cure for all metal heating problems. It is, however, being successfully applied to parts and metal sections too numerous to mention, in thousands of installations all over the world. In addition, new uses are continually being developed, particularly where one or more of its unique capabilities can be put to work.

Induction hardening in this country first became visible in the early 1920's when a motor generator frequency converter, used in melting high grade steel, was connected to a second station and ultimately used to surface harden mill rolls for use in the production of cold rolled steel. The tendency of alternating currents to travel in the surface layers of a conductor was recognized as a contributor to the desired surface heating and hardening. Coupled with what was then considered high power density, the skin effect and tendency to surface heat produced a roll with somewhat greater depth of hardness as compared with the same alloy steel quenched from furnace heating.

Later, in about 1932, crankshaft hardening was tried by a manufacturer of melting furnaces, using a high frequency converter which powered one of his small furnaces. The real value of a very pronounced skin effect at higher frequencies was recognized as a means for producing localized surface heating. This test also revealed the potential for high frequency inducation to produce wear resistant surfaces on cast iron and steel parts. Moreover, this treatment could be confined to specific areas where required. Beyond the value of a single stage, short cycle, low distortion, case hardening treatment, an additional economic advantage was recognized by progressive metallurgical thinkers--elimination of expensive alloy extras in the purchased steel.

Internal hardening of engine cylinder liners was developed later to provide long life, wear resistant surfaces for use in heavy duty engines. Axle shafts and other overall surface hardening applications must be included as part of induction's role in reducing the need for critical alloys. Many tons of now critical alloys have been saved in the manufacture of parts which are locally heat treated, in the sense of controlled depth only. High density surface heating, or controlled depth heating with induction does much to eliminate the need for alloys in heat treating steel; when one considers the primary role of alloys is to improve hardenability. Furthermore, typical short induction heating cycles, with zero time at temperature, have been found to render most carbide forming alloys ineffective; at least when conventional heat treating temperatures are used.

In the late 30's, induction heat treating was primarily seen as an innovative, localized surface hardening technique, which could take the place of lengthy surface addition case hardening treatments, such as carburizing and nitriding. Selective heating not only saved time and energy, it was also touted for reduced distortion, and some saw the potential for use of leaner, less expensive steels.

World War II and its concerted effort to improve ordnance components, armor piercing shot, gun parts, tank and military vehicle engine and drive components, all provided impetus to the increasing use of induction hardening. Metalworking industries came out of the war with considerably more knowledge of induction heating, however, not necessarily directed to any kind of conservation.

Ultimate hardness was one of the prime objectives sought in making armor piercing shot; an extremely hard nose, tapering into a more ductile structure. In test after test, induction heating and quenching provided hardness a few points higher on the Rockwell "C" scale as compared with identical shot similarly quenched after heating in a fuel fired or electric furnace. Simultaneously, this phenomena was observed in other parts, and subsequently dubbed "Superhardness." Conservative metallurgists called it a figment of the induction hardeners imagination, but it was there and measureable in many hardened parts. Later investigation indicated the added hardness was a result of rapid heating, which engendered a condition of higher stress in the hardened martensitic structure. Some studies indicated part of the increased hardness was due to less retained austenite in the hardened structure, when quenched from a rapidly produced, non-homogeneous austenite.

Analysis of the forces applied in high differential induction heating and quenching is difficult. Involved is differential thermal expansion; a layer of plastic metal upsetting over colder hard metal, cooling in two directions; to the quench and to the core, and all this coupled with increased volume in the final hardened structure. Residual stresses from induction hardening can be significant, can be beneficial; and properly applied, they can very materially improve the fatigue strength and life of parts subjected to torsional and bending loads. Coupled with a higher case hardness, in which depth exceeds the applied stresses, residual compressive stresses will do a great deal to increase endurance limits performance capabilities of a part.

Short cycle induction heating was difficult to understand, and early users tended to treat this type of heating as furnace heating without regard for time. In the late 1940's and early 1950's, with considerable interest in induction hardening, the effects of short cycle, zero time at temperature reactions were the subject of many metallurgical investigations. A great deal was learned to provide a substantial base, but this kind of knowledge is never complete, and we are still on a learning curve to fully utilize the advantages offered by extremely fast controlled heating that can also be applied in well defined patterns.

To gain some perspective on how induction heating can reduce the need for alloys in steel, and particularly chromium, we know hardenability improvement is the primary function of most alloys used in hardenable steels. Other than induction or direct flame hardening, furnace hardening treatments for steel involve surface additions to case harden, i.e., carburizing, nitriding, carbonitriding, or bulk quenching and tempering Carbon and nitrogen surface additions produce a hard wear resistant surface, and quench and temper offers some wear resistance, but primarily it is a process for increasing tensile strength with some compromise in ductility. Both are candidates for, and both have been widely applied to alloy steels, where the primary function of alloy is to improve hardenability; increasing the depth to which quenching is effective.

The mechanics of adding carbon or nitrogen involve placing these elements in contact with the surface of the metal; atoms are exchanged and a process of diffusion carries the added elements into the surface layers. Carburizing,

nitriding and carbonitriding are processes which require considerable time, measured in hours, depending upon the depth required. For this reason, there are economical and practical limits to the maximum depth of hardend layers produced by carbon or nitrogen addition. An increased carburizing temperature can be used to accelerate the diffusion rate, but the process is normally carried on a temperatures where added time or temperature may cause undesirable grain growth.

Case depth limitations in parts hardened by carburizing or nitriding often dictate the need for strengthening of support metal under the case. Hardenability alloys are generally specified to insure transformation at the required depth. If a part is to resist bending or torsional loads, this again may call for alloys to develop core properties to an adequate depth. Alloys will be used to improve hardenability so the effect of quenching can reach the sub case or core metal. For this reason, many carburizing and most nitriding grades of steel are alloy steels.

Other than electron beam or laser hardening, induction heating can provide the highest energy density for controlled depth heating. Skin effect is ever present because it makes the induction process work. Increasing frequency tends to promote surface layer heating, and this is another element which can be used to selectively heat only the metal required to produce desired results.

Controlled depth heating dramatically reduces the need for hardenability enhancing alloys simply by reducing the amount of heat that must be removed in the quenching process. In the critical early stages of quenching, heat moves

in two directions: to the quench and to the core, even in a part surface heated overall. For example, in a deep induction case hardened, 2" diameter shaft with 3/16" effective hardened depth, the total heat content is less than one half that of the same part out of a furnance at 1650°F.

When a shaft is locally heated, for example, in a bearing area, the heat also moves axially, and the cooling effect with added adjacent colder metal is even more dramatic. Scan or progressive induction hardening, widely used in heat treating shafts, gears, machine tool ways and other parts, in effect is a continuous incremental heating and cooling process where heat conduction of quenching takes place in all directions. Critical cooling rates to substantial depths are easily achieved for austenitized low hardenability steels--depths which will support reasonabily hgih loads in pressure or brinelling, torsion or bending.

Alloying elements are not always effective in induction hardening cycles. This is particularly true of carbide formers such as chromium, molybdenum, vanadium and tungsten, which in short induction heating time (unless abused) precludes any appreciable grain growth. In most induction heat treating cycles, the time at grain coarsening temperatures is such that no noticeable growth occurs. This has been demonstrated in steel where the surface has been close to the melting point.

Abrasion resistance imparted by undissolved carbides in hypoeutectoid steel is know, and this may be reason to use some carbide forming alloys; however, if higher hardness is obtainable with induction heating and quenching, the use of hardness rather than alloy carbides might be considered in a materials conservation program.

The other beneficial effects cited for carbide forming alloys, including resistance to softening and loss of strength on heating and a better balance between strength and toughness, are not fully realized in the critical hardened metal, unless the carbides are dissolved in the austenite prior to quenching. This thought might be useful when considering induction hardened alloy steels, and help in the conservation of critical category alloys, of which chromium is a prominent member.

Like most metallurgical reactions, carbide dissolution is effectively accelerated by increasing the austenitizing temperature. Measures induction heat treating temperatures of 150 to 300 degrees F above furnance temperatures are commonly used to increase carbide solution in the austenite. Grain enlargment, largely detrimental to physical properties in steel, including notch toughness and transition temperatures previously indicated, is very substantially elevated temperatures, the time element for any measurable grain growth does not exist. This has been well proven in extremely short heat cycles with measured surface temperatures will over 2000°F. The time-temperature relationship of metallurgical reactions is vividly demonstrated in almost all induction heating applications for metal working, in particular selective surface hardening.

In reality, where heat is localized in depth or in area, the induction hardening process is capable of providing, without presence, the benefits of most commonly used alloys of engineering steels. Potential benfits on a comparable basis include increased hardenability and improved physical properties to meet the application demands of products requiring resistance to failure from abrasion, brinelling, torsion, bending and low temperature

impact. The ability to develop desirable residual stresses must be recognized because, properly applied, these can substantially improve the performance of heavily loaded parts. In some applications, fully utilized on an educated basis, the total metal in a part can be reduced, and alloy conserved as well.

The potential use of induction hardening to reduce critical alloy consumption within its scope is real, but the net contribution will depend upon how seriously metalworking industries consider this a need, either for economic reasons or survival. If the philosophy becomes pervasive, the savings can be substantial. This has been proven by some of the more dedicated, progressive metallurgical thinking companies who are substantial users of steel. Induction hardening has played a major role in some long term programs for better utilization of materials.

Many products made of chromium containing alloy steels can be relegated to grades using other alloying elements for hardenability or abrasion resistance. Manganese, molybdenum and boron are useful substitutes where alloy is needed, but induction has turned many alloy steel parts to plain carbon grades without sacrificing physical properties, consuming more energy or adding to manufacturing cost. Material and heat treatment should be considered when a part is in the development stange to determine how it can be designed to best utilize materials and processes. In a dedicated materials conservation philosophy, material is the first consideration, followed by an intensive search for the best process to develop needed performance properties.

In this country, an abundance of materials and energy has made us somewhat complacent about conservation; and now our friends from countries where resources have been limited, are showing us how to use methods we developed

to produce higher quality products with less critical materials. Fortunately, we have a few outstanding examples of industries with foresight who are ahead in the material and process technologies. They are very observant, international in their outlook, and have a solid philosophy, developed over many years. We can all take lessons for the future from those outstanding examples.

Briefly we have shown how some selective induction hardening can reduce or eliminate the need for critical alloys in heat treating engineering steels. We haven't begun to scratch the surface, and a good start is to look at every existing induction hardened part made of alloy steel. Beyond that, no one should write a specification calling for alloy induction hardened steel, and particularly those containing chromium, without asking if the alloy is needed, or more importantly, will it be useful induction hardened. Outmoded material specifications should be examined, and standards should be opened up for intelligent evaluation of new knowledge on processes affecting metals and alloys. We can no longer stand extreme conservatism in government and military specifications or in engineering materials codes.

Induction heating can undoubtedly contribute much to conserve or eliminate chromium in applications other than hardening. Many of these possibilities are fact and have been proven in laboratory or behind the scene uses, ready to be applied to products in which alloys and critical materials are being wasted.

Some possibilities are in unsuspecting areas, such as an induction treatment to impart corrosion resistance. Will we let others find the needs of the future, and if profitable and advantageous to them, show us; or do we have the foresight and the desire to properly use what has been generously provided in this finite world?

BEARING STEELS OF THE 52100 TYPE WITH REDUCED CHROMIUM

by C. F. Jatczak, The Timken Company

The Timken Company is primarily a manufacturer of tapered roller bearings which are made from carburizing steels that generally contain low amounts of chromium - typically between 0.25 and 0.50%. At the same time, however, the Company is a major supplier of 52100 high carbon steels to various ball bearing manufacturers. By contrast with the carburizing grades, the 52100 steel contains 1.5% Cr. This makes our job of supplying it without interruption very vulnerable to chromium shortages.

In anticipation of a possible Cr shortage in the early 1970's (which later did occur), we set out to apply our combination of steel and bearing knowledge to develop a suitable low Cr alternate which would satisfy all of the technical and bearing performance requirements of standard 52100 ball bearing components. A secondary aim was to make the new composition so economically attractive that our customers would be willing to evaluate its performance as soon as possible.

The resulting composition, designated TBS-9, is shown in Figure 1. A savings of 1% Cr was achieved. Test results to date indicate that TBS-9 offers processing characteristics and service performance which are in fact superior to those of 52100 at a lower cost. For example, the metallurgical characteristics of the steel are such that its annealing times are much shorter, thus lowering our costs. We were able to pass these savings on to our customers, which in 1971 amounted to $60/70 per ton for steel in tubular form furnished with a spheroidized microstructure. Today this savings is not as lucrative as it was in 1971, due largely to a large increase in the price of Mo; nevertheless it is still significant.

From the Cr conservation standpoint, the 1% lower Cr content in TBS-9 amounts to a rather modest but important savings of 20#/ton. Based on AISI data for 1981, in which approximately 91,000 tons of high carbon bearing steels were sold domestically, the bulk savings in Cr could amount to 910 tons annually if TBS-9 were substituted across the board.

Since 1971, TBS-9 has received wide acceptance as an alternate for 52100. About one-third of Timken's high carbon steel business is now TBS-9 steel.

Hardenability played an important role in the development of this grade. The steel was designed to meet the hardenability specifications of the 52100 grade. This was easily accomplished

as shown in Figure 2, because of extensive prior work conducted by Timken on the influence of the various alloying elements on hardenability of high carbon steels.* The process was simply one of substitution of Mn and Mo for Cr based on the data shown in Figure 3.

Metallurgical and processing characteristics were also designed to be at least equivalent. The results were equivalent forging and tube piercing characteristics and as already noted superior annealing behaviour, because less time is required to produce the spheroidized structure which provides ease of machining. The maximum as annealed hardness is BHN 207; however, the typical range is 179/192 Brinell.

The effects of various austenitizing and tempering temperatures on hardness of TBS-9 are illustrated in Table 1.

The ultimate criterion for a ball bearing steel is its resistance to rolling contact fatigue. The fatigue resistance of TBS-9 was compared with 52100 and lower carbon version 5160 in our laboratories - our fatigue machines provide a rolling contact test that controls all variables except the material itself. Contact geometry is very similar to a ball bearing. The test conditions employed were: specimen, 4 by 5/8 in. diameter cylinder; load rings, 1 in. crown radius on an 8½ in. diameter; speed, 9000 rpm; load, 1680 lb.; maximum Hertz stress, 700 ksi; lubricant, SAE 20 oil; temperature, 175°F.

The results are shown in Figure 4. The contact resistance of TBS-9 is superior to that of 5160 and similar to that of 52100. Actual bearing field tests conducted by our customers since these RCF tests have confirmed the equality of TBS-9 with 52100 with respect to bearing life. As was noted earlier, TBS-9 has replaced at least 1/3 of our high carbon bearing steel orders. This is the best confirmation of its viability as a ball bearing steel.

To summarize, it is clear that a reduction in Cr in high carbon bearing steels need not cause any consternation in the industry at all. Simple substitution of the TBS-9 should provide uninterrupted production of ball bearing races even during drastic shortages of the element chromium.

---

* See "Determining Hardenability from Composition," by C. .F. Jatczak, Metal Progress, September, 1971, p. 60.

FIGURE 1

COMPARISON OF 52100 AND TBS-9 CHEMISTRY

Type	C	Mn	Si	Cr	Mo
52100	.95/1.10	.25/.45	.20/.35	1.30/1.60	-
TBS-9	.89/1.01	.50/.80	.20/.35	.40/.60	.08/.15

Table I — Effects of Austenitizing and Tempering Temperatures on Hardness of TBS-9

Temperature, F	Hardness, Rc	
Austenitizing	As Quenched	After 300 F Temper
1,475	66.0	63.5
1,500	65.0	64.0
1,525	66.0	63.5
1,550	66.0	63.5
1,575	65.0	63.0
Tempering (1,550 F Quench)	**After 1 Hr Temper**	**After 2 Hr Temper**
200	65.0	65.0
300	64.0	63.5
400	60.5	60.0
500	58.5	58.0
600	55.5	55.5
700	52.5	52.0
800	49.0	49.0
900	45.0	45.0
1,000	40.0	39.0
1,100	36.0	35.0
1,200	32.0	30.0
1,300	26.0	24.0

Typical Rockwell C hardness (normalize 1,650 F, anneal, quench 1,550 F): J1 position (1/16 in. Jominy distance), 65; J2, 65; J3, 65; J4, 61; J5, 47; J6, 43; J7, 43; J8, 43; J10, 43; J12, 41.

TYPE	HEAT NO.	C	Mn	Si	Cr	Mo	NORM. TEMP. °F	QUENCH TEMP. °F
52100	Avg 16 hts.	.98/1.10	.25/.45	.20/.35	1.30/1.60		1650	1500
TBS-9	Avg 35 hts.	.89/1.01	.50/.80	.15/.35	.40/.60	.08/.15	1650	1500

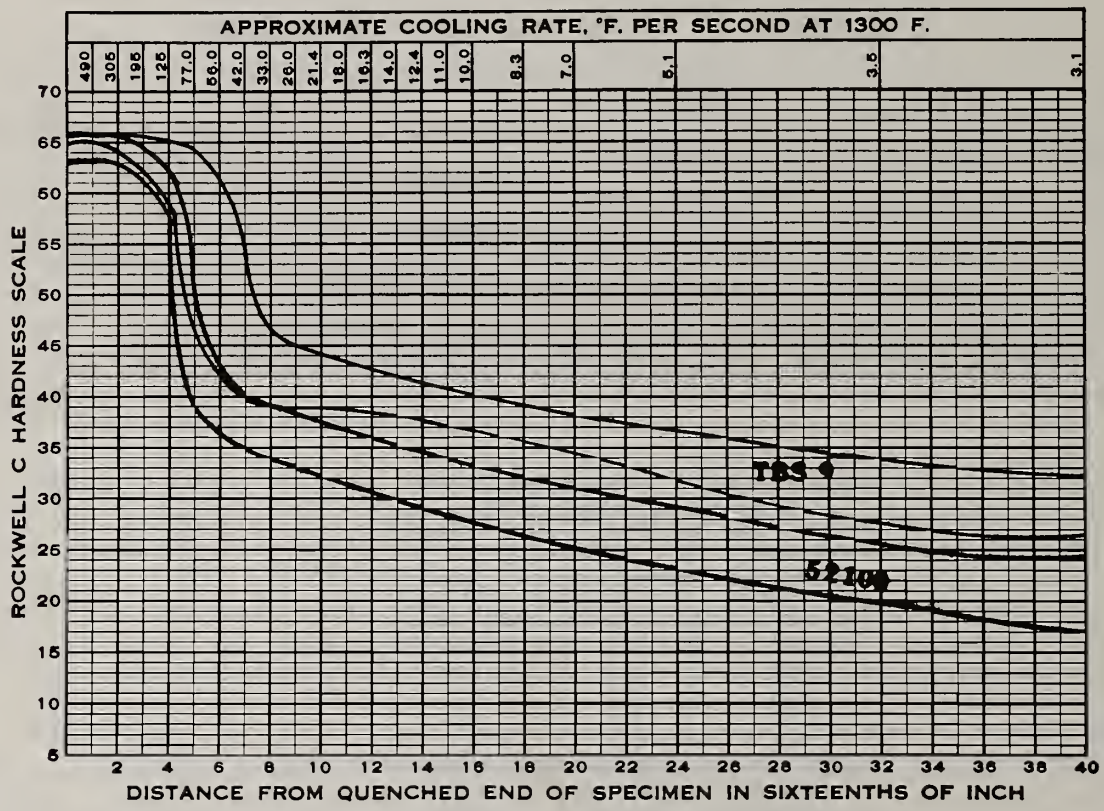

Figure 2. Comparison of Hardenability of TBS-9 versus 52100.

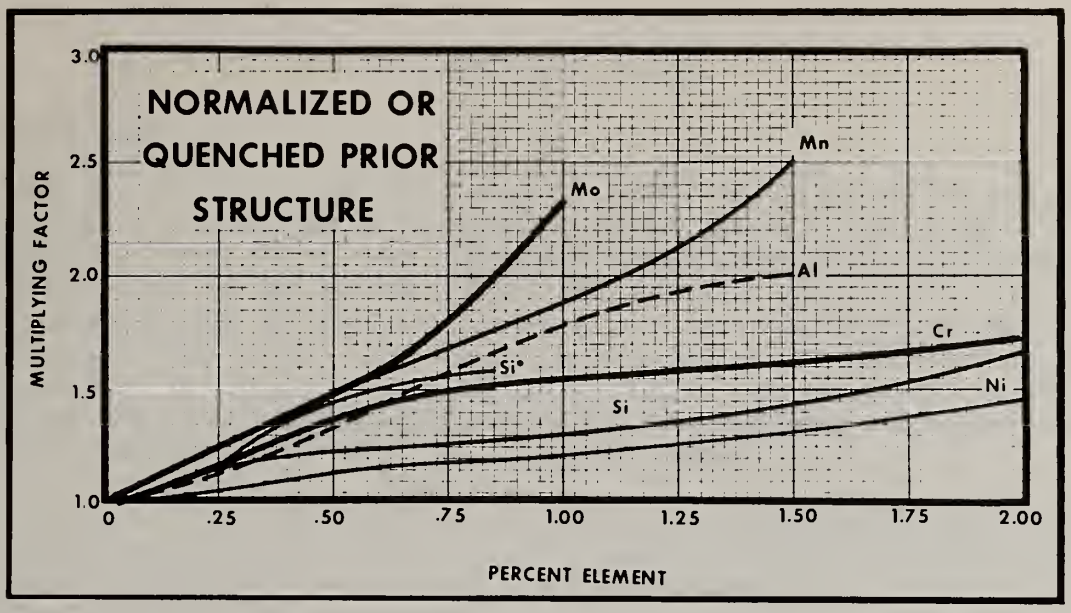

Figure 3. Multiplying factors for the calculation of hardenability in high carbon quenched from 1525°F (830C), see reference indicated below.

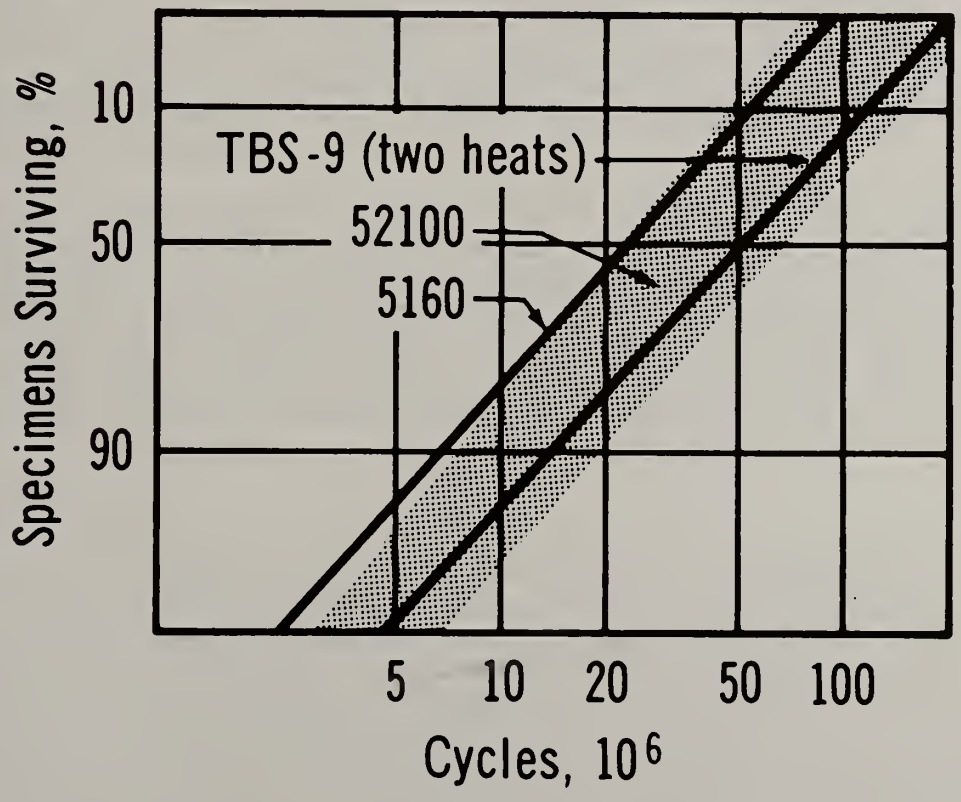

Figure 4. Comparison of rolling contact fatigue life.

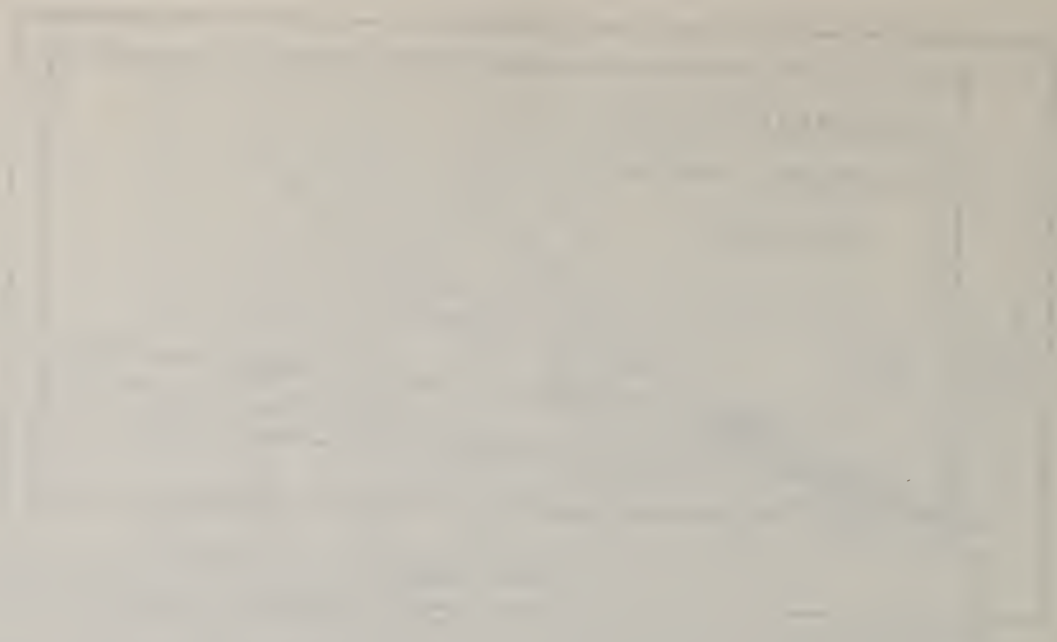

I. STRUCTURAL ALLOYS

A. Bar Products

To begin I would like to first briefly review the state-of-the-art in conservation and substitution technology for structural alloy bars. This subject has been one of deep concern and some considerable research at Republic Steel as we are the largest bar producer in the U. S. In a typical business year an analysis of Republic's consumption of raw materials by product line reveals that approximately 80% of our purchased chromium is consumed in the production of bar products. Our stainless operations utilize 11% of the purchased chromium and the remaining 9% is divided evenly between tubular and flat rolled products.

As a result of this consumption distribution of chromium we have focused our alloy substitution research on bar products and have emphasized research to utilize substitutes with wide distribution and domestic sources such as vanadium and molybdenum.

Alloy Substitution -- The Current State-Of-The-Art

Alloy substitution in steels is not a new endeavor and in recent history dates back to World War II when 16 National Emergency Steels (N.E. Steels) were developed and introduced in 1944. As the nation was faced with shortages of critical alloying elements and of uncontaminated alloy scrap, the steel industry united together and developed in a relatively short period of time the N.E. Steels. The N.E. Steels were all fine-grain alloy steels produced by the best alloy practice known to the industry and they were developed on the basis of equaling the hardenability of the grades they were to replace.

The N.E. Steels were triple alloy steels (Cr-Ni-Mo steels, 8600 and 9400 series) which permitted greater recovery and utilization of alloys from scrap. They therefore aided in meeting mill production schedules as well as producing steels conforming to the specified chemical ranges which was a problem with the single or dual-alloy type steels such as 5100, 3100, 4100, and 4600. Many of these N.E. Steels such as 8620, 8630, and 8720 have been and are still the standards and "Work-horses" of industry.

The EX Steels

More recently there has been another example of large-scale alloy substitution as a result of raw material shortages. This example resulted from the nickel mining strike by INCO and Falconbridge Nickel Mines, Ltd., which occurred in 1969. The strike at the INCO mines lasted four months beginning on July 9, 1969, and ending on November 14, 1969. The resulting shortage in nickel manifested itself by an intense level of development activity on the part of two domestic steel companies and two ferroalloy suppliers to provide alternate steels with equivalent hardenability and mechanical properties with reduced nickel levels.

This development activity resulted in both Republic and International Harvester introducing new economical alternative steels (the SAE EX steels) to the marketplace by January 1970. Therefore, in about five months' time alternate materials had been developed in response to the raw materials shortage. By 1971, 52 EX steels had been developed and offered to the trade. Ten years later (1981) 30 EX steels remained in existance.

The significant point to be made is the development response time required to introduce substitute alloy grades as a result of a raw materials shortage. In the case of the nickel shortage in 1969 the steel industry and ferro alloy suppliers had alternate grades of alloy bar products on the market in five months time.

Today we have accurate computerized hardenability prediction systems to aid us in our alloy development work which enables us to shorten the development cycle of alloy bar products even further. The development of new grades of stainless steel is a different story and takes a considerably longer period of time to develop (usually several years).

Current Alloy Substitution Technology

In this section a brief description of existing alloy substitution technology will be presented. This information is intended to illustrate the current technolgoy and know-how that we have at our fingertips which allows us to respond to customer demands for alloy substitution or raw materials shortages as they arise.

Alloy Substitution Capabilities Within Current AISI-SAE Grades

Illustrated below are a few examples of where alloy substitution can readily take place by merely substituting one existing AISI-SAE grade for another based on equivalent hardenability bands. The first example illustrates how 8600 series steels (Ni-Cr-Mo grades) can be substituted for the 5100 series steels (straight Cr grades) and reduce the average Cr content from about 0.80% to about 0.50%. The second example deomonstrates how a C-Mn-Mo grade (4042) can be substitued for a C-Mn-Cr grade (5046) in the event of a Cr shortage. The third illustration shows how a C-Mn-B steel (15B37) can be substituted for a C-Mn-Cr steel (5132) in the event of a Cr shortage.

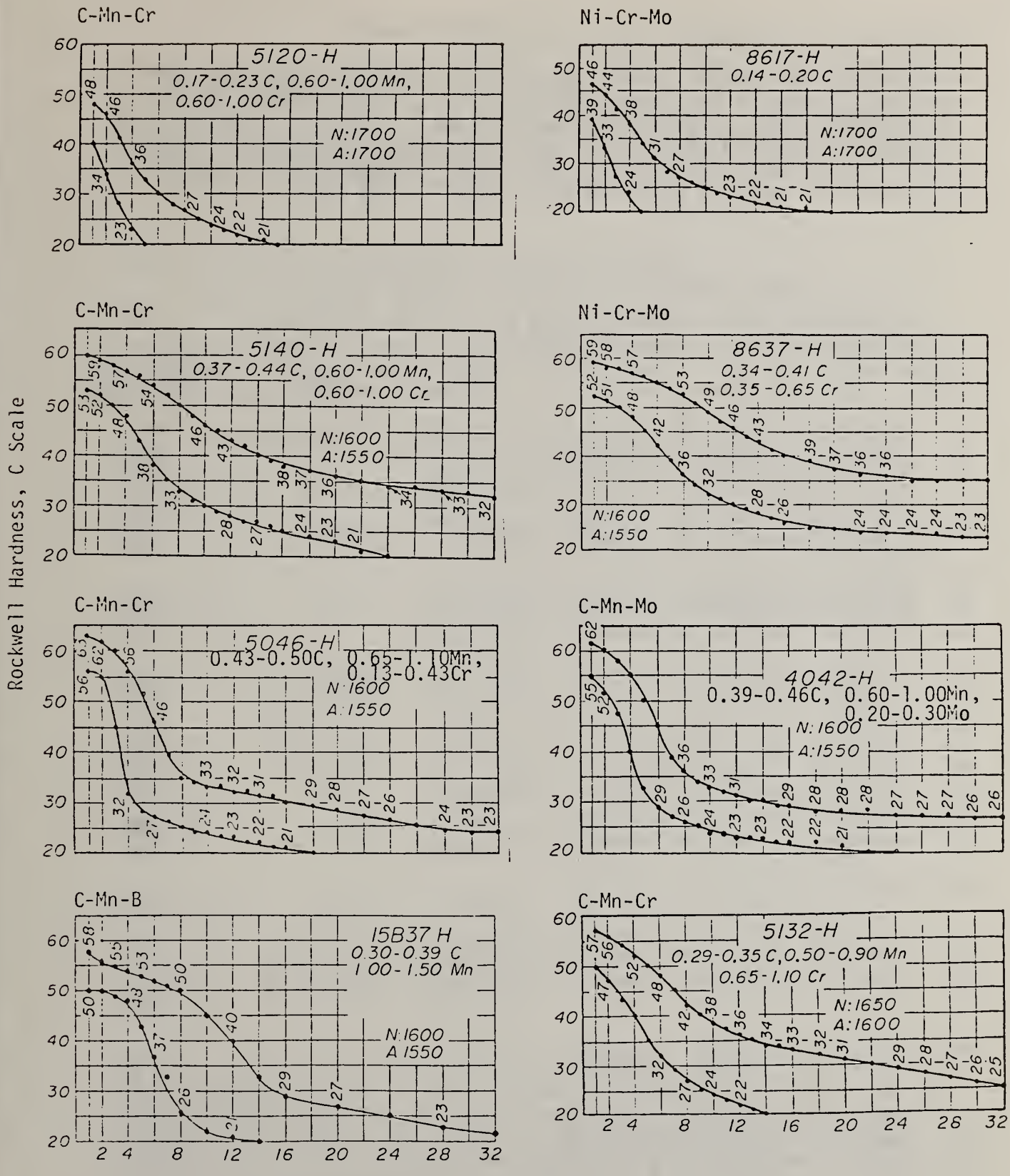

These few examples should suffice to illustrate how existing standard AISI grades of steel can be substituted for other existing grades in the event of a raw materials shortage.

Alloy Substitution Capabilities Via the SAE EX Steels

As mentioned previously, the SAE series of EX steels represent the SAE numbering system for new grades of alloy steels. As a function of time the EX steel either is dropped because of lack of interest in the alloy or it becomes a standard SAE grade if the alloy becomes popular and widely used. The currently available EX steels and the standard SAE grade for which they are normally substituted are shown in the list.

THE EX STEELS AND EQUIVALENT STANDARD GRADES

EX No.	Composition (%)					Equivalent SAE Grade
	C	Mn	Cr	Mo	Other	
10	0.19-0.24	0.95-1.25	0.25-0.40	0.05-0.10	0.20-0.40 Ni	8620
15	0.18-0.23	0.90-1.20	0.40-0.60	0.13-0.20	-	8620
16	0.20-0.25	0.90-1.20	0.40-0.60	0.13-0.20	-	8622
17	0.23-0.28	0.90-1.20	0.40-0.60	0.13-0.20	-	8625
18	0.25-0.30	0.90-1.20	0.40-0.60	0.13-0.20	-	8627
19	0.18-0.23	0.90-1.20	0.40-0.60	0.08-0.15	0.0005 B min	94B17
20	0.13-0.18	0.90-1.20	0.40-0.60	0.13-0.20	-	8615
21	0.15-0.20	0.90-1.20	0.40-0.60	0.13-0.20	-	8617
24	0.18-0.23	0.75-1.00	0.45-0.65	0.20-0.30	-	8620
30	0.13-0.18	0.70-0.90	0.45-0.65	0.45-0.60	0.70-1.00 Ni	4815
31	0.15-0.20	0.70-0.90	0.45-0.65	0.45-0.60	0.70-1.00 Ni	4817
32	0.18-0.23	0.70-0.90	0.45-0.65	0.45-0.60	0.70-1.00 Ni	4820
33	0.17-0.24	0.85-1.25	0.20 min	0.05 min	0.20 Ni min	4027
34	0.28-0.33	0.90-1.20	0.40-0.60	0.13-0.20	-	8630
36	0.38-0.43	0.90-1.20	0.45-0.65	0.13-0.20	-	8640
38	0.43-0.48	0.90-1.20	0.45-0.65	0.13-0.20	-	8645
39	0.48-0.53	0.90-1.20	0.45-0.65	0.13-0.20	-	8650
40	0.51-0.59	0.90-1.20	0.45-0.65	0.13-0.20	-	8655
54	0.19-0.25	0.70-1.05	0.40-0.70	0.05 min	-	4118
55	0.15-0.20	0.70-1.00	0.45-0.65	0.65-0.80	1.65-2.00 Ni	4817
56	0.08-0.13	0.70-1.00	0.45-0.65	0.65-0.80	1.65-2.00 Ni	9310
57	0.08 max	1.25 max	17-19	1.75-2.25	-	30303
58	0.16-0.21	1.00-1.30	0.45-0.65	-	-	4118
59	0.18-0.23	1.00-1.30	0.70-0.90	-	-	8620
60	0.20-0.25	1.00-1.30	0.70-0.90	-	-	8622
61	0.23-0.28	1.00-1.30	0.70-0.90	-	-	8625
62	0.25-0.30	1.00-1.30	0.70-0.90	-	-	8627
63	0.31-0.38	0.75-1.10	0.45-0.65	-	0.0005-0.003 B	-
64	0.16-0.21	1.00-1.30	0.70-0.90	-	-	-
65	0.21-0.26	1.00-1.30	0.70-0.90	-	-	-

Currently there are about 30 different EX steels which can be substituted for a large variety of standard SAE grades. Generally the use of an EX steel results in a reduction in either the Ni content or the Mo content compared to the standard SAE grade. As we have experienced both Ni and Mo shortages in the past 10 to 12 years the utilization of the SAE EX steels has been both industrially and technologically significant.

Alloys "On the Shelf" as a Result of Recent Research

Recent Republic Research efforts to develop bar products with reduced levels of critical alloying elements while maintaining the required heat treatment response and mechanical properties have resulted in a number of "on the shelf" alloys ready to go as demand arises. The table below summarizes some of these developments.

NEWLY DEVELOPED PRODUCTS WHICH ARE EXAMPLES OF MATERIALS SUBSTITUTION

Product Area	Old Grade	New Grade	Alloy Savings
Alloy Bar	3310	3120 Modified	Reduce Ni from 3.50 to 1.75% Reduce Cr from 1.50 to 0.60%
Alloy Bar	4815	3120 Modified	Reduce Ni from 3.50 to 1.75% Reduce Mo from 0.25 to 0%
Alloy Bar	4620 Modified	3120 Modified	Reduce Mo from 0.50 to 0%
Alloy Bar	4815	"2Ni-1Mo"	Reduce Ni from 3.50 to 1.75%
Alloy Bar	EX-55	"2Ni-1Mo"	Reduce Cr from 0.55 to 0%
Alloy Bar	4118	10B18 + V	Reduce Mo from 0.11 to 0% Reduce Cr from 0.50 to 0%
Alloy Bar	4027	C-Mn-Cr	Reduce Mo from 0.25 to 0%
Ultra-High-Strength Alloy Steel	HP 9Ni-4Co	"10Ni-1Mo"	Reduce Co from 4.5 to 0%

The first alloy shown (3120 Modified) is actually now off the shelf and in use in automotive steering gear systems. A second alloy "2 Ni - 2 Mo" is currently being evaluated for use in rock-drilling bits and would reduce Cr content from 0.55% to 0% compared to the currently used EX-55 steel. In the vacuum-melted specialty steel area "10 Ni - 1 Mo" steel is under development as a replacement for the HP 9 Ni - 4 Co steels in the event of a cobalt shortage.

Computer Prediction Capability as an Alloy Development Tool

In the past several years various hardenability prediction models have been developed. The most accurate computer prediction model is the Minitech hardenability and mechanical property predictor. This prediction system provides a rapid and highly accurate means of predicting hardenability, heat treatment response, and mechanical properties as a function of steel composition. This therefore provides a rapid and reliable means of designing alternate bar product alloys based on current alloy costs and availability without going through a lengthy program of melting and evaluating experimental steel compositions.

Examples of the type of information that the Minitech predictor can provide and the accuracy of the calculations are shown below. The first and most important information desired is the core hardenability of the steel. Shown in Figure 1 are comparisons of the experimental and Minitech predicted hardenability curves for a given composition of 8620 steel. The excellent agreement between experimental and predicted results in apparent.

For carburizing grade steels such as 8620 the next piece of information an alloy developer needs is the case hardenability or carburizing response of the alloy. Shown below in Figure 2 is an example of the ability of the Minitech system to calculate or predict the case hardenability for a given set of heat treatment conditions and steel composition. Again, excellent agreement is observed between experimental and predicted results.

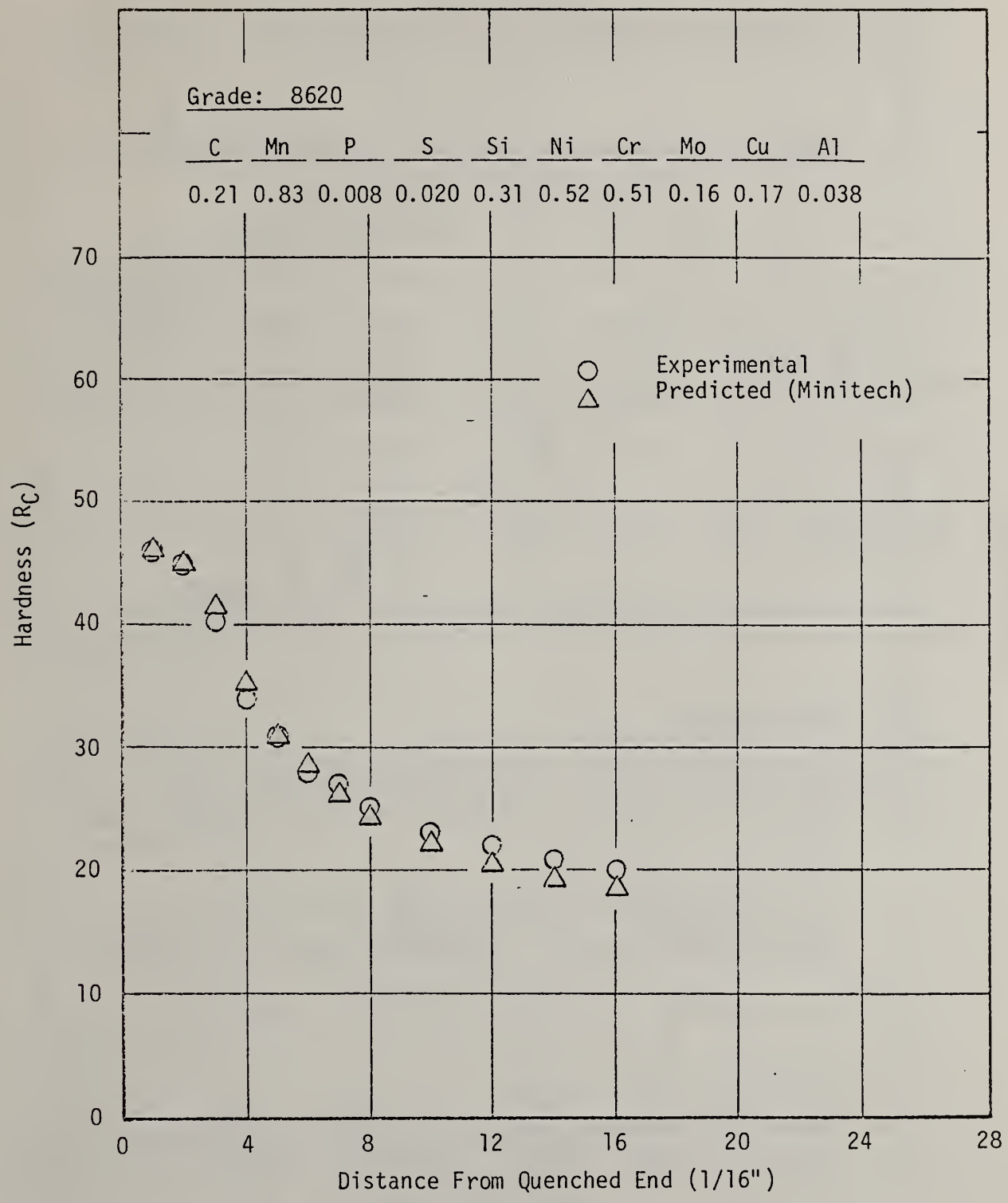

Figure 1. Comparisons of the Experimental and Minitech Predicted Hardenability Behavior for 8620 Steel.

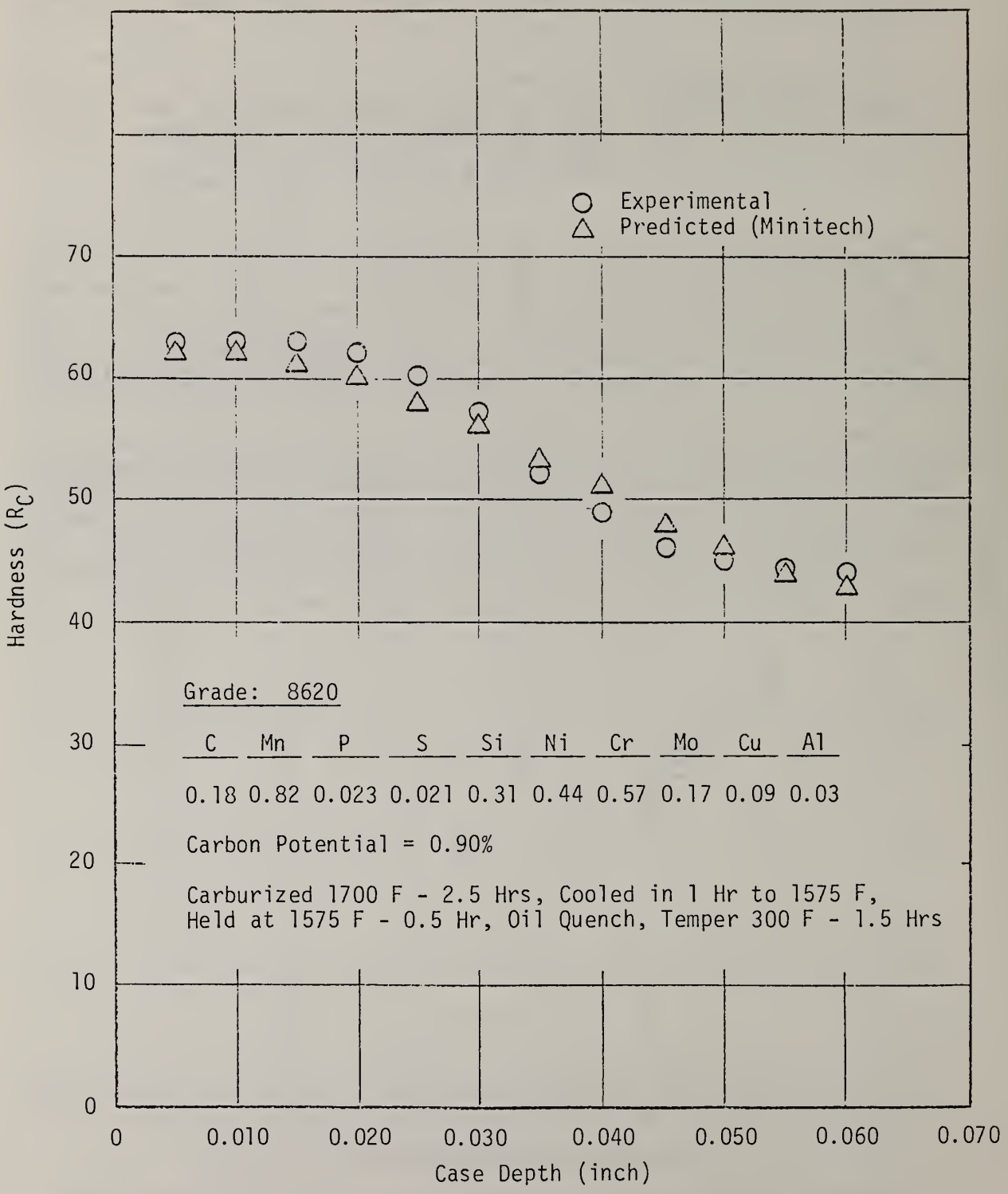

Figure 2. Comparisons of Experimental and Predicted Case Hardenability Response for 8620 Steel.

The next information that is desired, for a new alloy, are the mechanical properties of the heat-treated steel for various section sizes of bar products. Shown below are the calculated (Minitech) and experimental mechanical properties of pseudo-carburized (core properties) 8620 steel.

MECHANICAL PROPERTIES (EXPERIMENTAL VERSUS PREDICTED)

OF PSEUDO-CARBURIZED 8620 STEEL

(1700 → 1550 F, Oil Quench, 300 F Temper)

Bar Diameter (inch)	BHN	UTS (ksi)	YS (ksi)	% Elong	% RA	Method
1/2	388	199,500	157,000	13	49	Experimental
	399	199,000	181,000	14	47	Predicted
1	255	126,700	83,750	21	53	Experimental
	268	134,000	112,000	21	60	Predicted
2	235	117,200	73,000	23	58	Experimental
	235	118,000	96,000	24	64	Predicted

Considering the normal heat-to-heat variability this agreement between calculated and experimental mechanical properties is considered to be good.

For through hardening steels such as 4140, the quenched and tempered mechanical properties as a function of tempering temperature are of interest to the design engineer and the metallurgist. A comparison of the quenched and tempered mechanical properties (experimental versus predicted) are shown in the table below for two different grades of alloy steel.

QUENCHED AND TEMPERED MECHANICAL PROPERTIES

(EXPERIMENTAL VERSUS PREDICTED) FOR 4140 AND 8650 STEELS

Grade	Temper Temperature (F)	YS (ksi)		UTS (ksi)		% Elong		% RA	
		Exp	Pred	Exp	Pred	Exp	Pred	Exp	Pred
4140	400	238	235	257	247	8	11	38	38
	600	208	199	225	215	9	13	43	44
	800	165	169	181	188	13	15	49	49
	1000	121	128	138	149	18	19	58	57
8650	400	243	268	281	275	10	10	38	32
	600	225	221	250	235	10	12	40	41
	800	192	196	210	213	12	13	45	45
	1000	153	146	170	166	15	17	51	54
	1200	120	113	140	135	20	21	58	60

These data, generated for 1-inch round bar product, demonstrate good agreement between experimental and predicted values. In addition to the value of this powerful prediction tool to the alloy developer, the production metallurgist can use this computer program very successfully as a quality control tool and in heat disposition.

In summary, there exists today a very large body of knowledge concerning the metallurgy and application of carbon and alloy bar products. This knowledge bank includes, in part, the development, application and over 35 years of experience with the WWII National Emergency Steels, the SAE EX steels most of which originated from the 1969-1970 time period when there was a nickel shortage due to a strike, and for the last several years includes computerized hardenability prediction systems which are highly accurate and extremely fast and result in a significant shortening of the alloy development cycle time. With this knowledge base the steel industry is positioned to respond very rapidly to any possible raw materials shortage.

In terms of alloy bar steels there would not be a serious problem in the event of a chromium shortage. The technology is in hand to readily find alloy substitutes for Cr containing alloy steels through the judicious use of Mo, B, and V. Whether it is a carburizing grade such as 8620 or a through hardening grade such as 4140 there is not a problem in finding an adequate non-chromium containing substitute.

B. Structural Alloy Plate

Under the category of structural alloy plate materials we will briefly discuss the possibilities for chromium conservation and alloy substitution in the following classifications of plate materials.

1) Constructional Alloys

2) Abrasion-Resistant Alloys

3) Weathering Steels

4) Pressure Vessel Steels

1) Constructional Alloys

As shown in the table below, many of the high strength 80 to 100 ksi Y.S. structural, weldable plate steels contain Cr and Mo. These quenched and tempered plate materials (covered under ASTM Specifications No. A514 and A517) are produced in a variety of thicknesses up to 6" and are intended for use in welded bridges and other structures.

Constructional Alloys (High-Strength Plate)

Name	Composition							Y.S. ksi	ASTM Spec.
	C	Mn	Si	Ni	Cr	Mo	Other		
SSS-100	0.16	0.55	0.27	-	1.70	0.50	Cu,V,B	100	A514
RQ100 A	0.16	0.60	0.27	-	-	0.55	B	100	A514
N-A-XTRA-100	0.21	0.85	0.65	-	0.65	0.28	Zr,B	100	A514
T-1	0.15	0.80	0.20	0.85	0.55	0.55	Cu,B,V	100	A514
HY80	0.18	0.25	0.27	2.75	1.40	0.35	-	80	-
HY100	0.20	0.25	0.27	3.00	1.40	0.35	-	100	-
HY130	0.12	0.75	0.27	5.00	0.55	0.45	V	130	-

In ASTM Specification A514 there are fifteen different compositions or Grades listed (Grades A through Q) some of which are shown in the table above. Of these fifteen different grades there are four grades that do not contain chromium. One of these grades is shown in the table above and it can be seen that higher Mo levels and the addition of boron are utilized in order to meet the hardenability requirements. The different compositions indicate that the balance of alloying elements is primarily based on hardenability considerations and experience has indicated that the non-chromium containing grades meet the specification and customer requirements equally as well as the Cr-containing grades. Similar to the situation with heat treated bar products it is preimarily a matter of achieving hardenability most economically.

Therefore, if there were a chromium shortage there would not be a technical problem in the area of quenched and tempered constructional plate steels.

The situation with HY80, HY100, and HY130 steels for Naval ship applications is not as straight forward and adequate substitutes for these grades are not readily apparent at this time. Later in this session Dr. Brian Jones will have information to share concerning the possibility of substituting microalloyed HSLA plate materials for HY80 steel.

2) Abrasion-Resistant Plate Steels

A similar analysis of abarasion resistant plate steels shown by the compositions listed in the table below reveals that there is an ample choice of quenched and tempered (Q & T) abrasion resistant plate materials that are Cr free. The users can select from a variety of C-Mn, C-Mn-Mo-B, and C-Mn-Mo-Ni-B Q & T alloys. Therefore, chromium availability would not be a problem for abrasion resistant plate steels.

TABLE II

ABRASION-RESISTANT ALLOYS

Name	Composition, % C	Mn	P	S	Si	Cu	Cr	Mo	Other (a)	Hardness, Bhn
SSS-AR-321	0.25	0.40-0.70	0.04	0.05	0.20-0.35	0.20-0.40	0.85-2.0	0.15-0.60	Ti or V, B	321
SSS-AR-360	0.25	0.40-0.70	0.04	0.05	0.20-0.35	0.20-0.40	0.85-2.0	0.15-0.60	Ti or V, B	360
SSS-AR-400	0.25	0.40-0.70	0.04	0.05	0.20-0.35	0.20-0.40	0.85-2.0	0.15-0.60	Ti or V, B	400
RQAR-321	0.25-0.32	0.40-0.65	0.035	0.040	0.20-0.35	-	0.80-1.15	0.15-0.25	-	321
RQAR-340	0.25-0.32	0.40-0.65	0.035	0.040	0.20-0.35	-	0.80-1.15	0.15-0.25	-	340
RQAR-360	0.25-0.32	0.40-0.65	0.035	0.040	0.20-0.35	-	0.80-1.15	0.15-0.25	-	360
RQAR-400	0.25-0.32	0.40-0.65	0.035	0.040	0.20-0.35	-	0.80-1.15	0.15-0.25	-	400
RQC-321	0.28	1.50	0.040	0.050	0.20-0.60	-	-	-	B	321
RQC-340	0.28	1.50	0.040	0.050	0.20-0.60	-	-	-	B	340
RQ321A	0.12-0.21	0.45-0.70	0.035	0.04	0.20-0.35	-	-	0.50-0.65	B	321
RQ340A	0.12-0.21	0.45-0.70	0.035	0.04	0.20-0.35	-	-	0.50-0.65	B	340
RQ360A	0.12-0.21	0.45-0.70	0.035	0.04	0.20-0.35	-	-	0.50-0.65	B	360
RQ321B	0.12-0.21	0.45-0.70	0.035	0.04	0.20-0.35	-	-	0.45-0.60	1.20-1.50 Ni, B	321
RQ340B	0.12-0.21	0.45-0.70	0.035	0.04	0.20-0.35	-	-	0.45-0.60	1.20-1.50 Ni, B	340
RQ360B	0.12-0.21	0.45-0.70	0.035	0.04	0.20-0.35	-	-	0.45-0.60	1.20-1.50 Ni, B	360

3) Weathering Steels

Weathering steels are HSLA 50 ksi min Y.S. plates and shapes intended primarily for use in welded bridges and building were weight savings and durability are important. The ASTM A-588 standard specification covers ten different grades of weathering steels (Grades A through K) and three of these grades do not contain chromium. While most of these steels contain C-Mn-Si-Ni-Cr-Cu and V they can be made to have adequate atmospheric corrosion resistance, in the absence of Cr, by increasing the Ni and Cu levels. A second option would of course be to do without weathering steels and get out the bucket of paint and paint brush.

The bottom line with weathering steels is that an absence or shortage of Cr would not be a problem.

4) Pressure Vessel Plate Steels

ASTM Standard Specification A387 for pressure vessel plates, covers the Cr-Mo alloy steel plates intended primarily for boilers and pressure vessels designed for elevated temperature service. This specification covers the well known and widely used 2-1/4 Cr - 1 Mo and 1-1/4 Cr - 1/2 Mo steels.

The market for the ASTM A-387 grades (there are 8 different grades in this specification) is some 8,000 to 9,000 tons/year domestically and 15,000 to 20,000 tons/year worldwide. Concerning plate products there is only one major domestic producer (Lukens Steel) the remainder of the steel being foreign, primarily from Japan. The most popular grade is Grade 11 (1-1/4 Cr - 1/2 Mo) which is used extensively in process piping and heat exchanger tubing. The next most popular grade is Grade 22 (2-1/4 Cr - 1 Mo) which is primarily used as a plate product for pressure vessels and high temperature, high pressure hydrogen service for petrochemical applications.

In these grades if you lower Cr content you loose high temperature strength. As the writer understands the state of the art of technology in this class of steels there are no known substitutes for these grades and furthermore there is apparently no research work being done to find substitutes or reduce Cr levels in these pressure vessel steels. The current thinking is that there is no known substitute for Cr when it comes to resistance to hydrogen at elevated temperatures.

The Climax Molybdenum Company is doing research to develop an alloy which will have greater high temperature strength, greater hardenability and greater resistance to hydrogen. This has lead to the development of a 3 Cr - 1-1/2 Mo - .10 V steel. Unless the section sizes can be reduced significantly, this development, while technologically significant, will not be beneficial from a chromium conservation viewpoint.

In this product area the bottom line would appear to be that Cr substitution or conservation does not look favorable at this time and there is a real need for research in this area. As there are a limited number of domestic suppliers of A-387 plate steels this is an area where the Federal Government should step in and sponsor some R & D work.

II. HIGH STRENGTH LOW ALLOY STEELS

The high strength low alloy (HSLA) steels and their possible vulnerability to a chromium shortage will be reviewed in depth by the next two speakers on the program; Mr. Michael Korchynsky of Union Carbide Corporation and Dr. Brian Jones of Niobium Products Company. Their presentations will cover plate steels, skelp for line pipe applications, dual-phase steels HSLA microalloyed steels, weathering steels and HSLA steels in general. Dr. Koo from Exxon Research will discuss the optimization of alloying elements in low carbon dual phase steels and medium carbon structural steels.

III. ULTRAHIGH STRENGTH STEELS

The major use of ultrahigh strength specialty steels is in aircraft forging applications. These critical load bearing forgings are used in such applications as engine mounts, tail section forgings, wing mounts, flap tracks and landing gears to mention just a few. The landing gear typically comprises about 14% of the weight of the aircraft, therefore, high strengths and good fatigue resistance are mandatory.

The primary ultrahigh strength steels which have been used for landing gears over the past 30 to 40 years are shown in the table below. What is readily apparent from this list of steel compositions is that all of the alloys contain chromium. What is not nearly as readily apparent is whether a chromium-free steel could be developed for this very demanding high hardenability application.

Aircraft Landing Gear Steels

	Composition							
Alloy	C	Mn	Si	Ni	Cr	Mo	V	Other
98 BV 40	0.43	0.85	0.65	0.75	0.90	0.50	0.04	B
4330 M	0.30	0.95	0.27	1.80	0.85	0.40	0.08	-
4340	0.40	0.75	0.27	1.80	0.80	0.25	-	-
300M	0.40	0.75	1.65	1.80	0.80	0.40	0.80	-
HP 9-4-30	0.30	0.25	0.10	7.50	1.00	1.00	0.10	4.5 Co
HP 310	0.40	0.75	2.50	1.80	0.90	0.40	0.20	-

There is not currently any alloy development work in progress which has as its goal to develop a Cr-free steel for ultrahigh strength steel aircraft landing gear applications. As both military and commercial aircraft utilize the same alloys for landing gears (300M being the current work horse alloy for landing gears) this would appear to be another very appropriate and vital area for the Federal Government to sponsor alloy substitution research.

SUMMARY

In summary, the state-of-the-art of substitution for chromium in structural alloy, HSLA, and ultrahigh strength steels has been reviewed. With regard to heat treatable structural alloy bar products there are ample chromium-free substitutes for most grades and a high technology base for rapidly developing alternate chromium-free structural alloy bar steels. Concerning both structural alloy plate steels and abrasion-resistant plate steels there has been available, for a considerable period of time, adequate Cr-free steels in both of these categories of Q & T plate materials. Likewise for ASTM A-588 weathering steels, there are a number of existing Cr-free weathering plate steels. The as-hot rolled microalloyed HSLA plate, strip and skelp steels generally do not contain chromium and these steels would not appear to be a problem area in the event of a chromium shortage.

The two major alloy steel areas which would be severely crippled in the event of a chromium shortage, in the near future, are the ASTM A-387 pressure vessel plate steels and aircraft forging and landing gear steels. For both of these classes of steels there are no known Cr-free substitute alloys and there is no research in progress to develop such substitutes for either the pressure vessel steels or landing gear steels. Both types of steel are utilized in critically important applications and it is felt that these two areas should receive serious consideration by the Federal Government to sponsor research work to develop adequate chromium-free substitute materials.

Alternative Compositions for Future HSLA Steels

The technology of high strength low-alloy (HSLA) steels has made tremendous advances over the past decade. This has come about because of the development of controlled-rolling techniques and research into the benefits of microalloys. There now exists a family of micro-alloyed steels capable of providing high yield strength combined with low temperature toughness and weldability. They have been utilized primarily in the pipeline and automobile industries. The purpose of this paper is to illustrate the properties available from this class of steel and to suggest that their field of application be extended to include areas traditionally reserved for heat-treatable chromium-containing steels.

The Development of HY 80

In the mid 1950's, design requirements called for a steel with 80 ksi yield strength for use as plates and frames in submarine pressure vessels. This necessitated the steel to provide adequate strength, ductility and notch toughness together with good weldability under shipyard conditions. Strength and notch toughness were, of course, also required from the weld deposit and HAZ. In the USA, following a fairly exhaustive investigation of the alloy approaches then available, this led to the development of the heat-treatable Ni-Cr-Mo steels known as HY 80. These are fully-killed aluminum-grain-refined steels which develop the desired strength properties following water-quenching from 1650°F and tempering in the range 1200-1250°F. A specification[1] for chemistry and mechanical properties for HY 80 is given in Table 1.

The difficulty in alloy selection was in obtaining an approach which provided the high strength levels required together with acceptable low temperature toughness levels. To achieve this 25 years ago it was felt necessary to use heat-treatable nickel-containing steels which have a shallow-sloping brittle-ductile transition curve and therefore, retain respectable toughness at low temperatures. This however, in the steels concerned is achieved only at the expense of weldability. Due to what is now considered to be a relatively high carbon level and the chromium and molybdenum additions, HY 80 is a steel which can be very prone to hydrogen-cracking. Its carbon equivalent using the International Institute of Welding formula (see Table 2) is around 0.70. This means that successful welding requires the use of low-hydrogen techniques usually in conjunction with pre-heat to allow hydrogen escape during post-weld cooling. Three pre-heat calculation analyses are indicated in Table 2 all recommending levels of 150°C or 300°F minimum.

In the 1980's, however, we no longer need to use heat-treatable nickel steels to achieve good low temperature properties. Controlled rolling and microalloying have now produced materials sufficiently fine-grained to give the required strength levels and to push transition temperatures to extremely low temperatures. Since the pipeline industry for which these steels were primarily designed views field weldability as a primary requisite, there has been a great incentive in this direction and these properties are achieved with carbon equivalents below 0.35 indicating excellent material tolerance of hydrogen and resistance to HAZ cracking.

Low Transition-Temperature Micro-alloyed Steels

Table 3 shows typical compositions of several low-carbon microalloyed

steels which have been developed in recent years. Selection of microalloy approach is made on the basis of final property requirements, controlled-rolling schedules and mill capabilities.[2]

The versatility of microalloy approach can be best illustrated by considering the development of X70 grade (70 ksi yield strength) linepipe steels. A few years ago it was considered necessary in producing these materials at thicknesses of about 0.6 inches to use a Nb-Mo approach with about 0.04% Nb and 0.30% Mo. This led in Italy for instance to the development of the Molytar Steels.[3] In 1979, however, due to a temporary sharp rise in the molybdenum price, alternatives to the Mo addition were sought. In Italy, it was found expedient at that time to use Nb-Cr steels with 0.2% Cr. While this does not have the hardenability effect of Mo, suitable controlled rolling schedules were easily able to achieve X70 grade requirements. Further work, however, established that even the chromium addition could be replaced and that, with the correct heat-treatment and rolling methods, a dual micro-alloy addition of Nb and V could do the job.

The Northern Border Pipeline, therefore, which represented an order of more than 500,000 tons of mainline 0.6 inch wall X70 grade pipe, used no molybdenum, and more than 90% of it, from manufacturers across the world, used 0.04% Nb and 0.05-0.07% V as the microalloys. Some heats did utilize the Nb-Cr approach, however, and this allowed a direct comparison to be made of the tensile properties achieved by replacing 0.20% Cr by a much smaller vanadium addition. It can be seen from the distribution of values shown in Fig. 1 that no variation in yield strength attained was observed and only minor changes in ultimate tensile strength.

For plate of this gage and strength, therefore, there is no requirement to use chromium and a selection of microalloy approaches are available. For thicker grades, it is common to use molybdenum additions once again and for high toughness at severely low temperatures - the most stringent requirement of HY 80 specificaiton - several novel microalloy developments are being promoted.

Tables 4 - 6 illustrate a development by Nippon Steel known as ultra low carbon bainitic steel or ULCB.[4] Here a very small addition of boron (.001%) leads to a transformation from ferrite-pearlite to a bainitic structure. In order to utilize the effects of boron, nitrogen has to be fixed by a titanium addition and carbon reduced to very low levels (< .03%). In ultra-low carbon steels the role of niobium is also important since it can remain in solution additionally promoting the achievement of a super-fine bainite structure.

The properties achieved in this way are most impressive. It can be seen in Table 5 that yield strengths in the vicinity of 80 ksi can be attained in plates up to 22 mm thick with very low drop weight tear test transition temperatures. The more commonly specified 50% Charpy crystallinity temperature is in all cases less than -80°C.

For the alloy designated UB-5 it can be seen that a yield strength of 95 ksi is achieved due to the additions of Mo and Ni, in 20 mm plate. This excessive yield strength can in fact be traded off to allow X80 properties in plate greater than 1 inch in thickness.

Table 6 shows the obtained submerged-arc weld metal and HAZ properties. The high toughness is explained by the grain growth suppression effect of titanium nitride particles and the elimination of martensite formation due to te low levels of carbon.

The requirement for very low-temperature finish-rolling (controlled-rolling) can also be relaxed under certain circumstances. Recent research (5) investigations on an HSLA steel containing 0.5% Ni and 0.13% Nb has indicated properties in excess of X70 grade together with very good low temperature toughness in both base plate and submerged-arc weld. These were obtained in plate rolled to 0.6 inch thickness at a finishing temperature of 1400°F. Composition and properties of this steel are shown in Table 7 . The low temperature toughness characteristics are illustrated in Fig. 2 .

Conclusions

The microalloyed controlled-rolled steels developed mainly for line-pipe applications are able to develop 70 ksi and in certain instances, 80 ksi yield strength together with excellent low temperature toughness properties, both in the plate material and in submerged-arc weld metal and HAZ. They can be used in thicknesses certainly up to 1 inch and, with additions of molybdenum, to greater thicknesses. They need contain no chromium and offer very significant advantages in terms of weldability over the heat-treatable Ni Cr Mo HY 80 steel traditionally used for shipplate applications.

The microalloys involved are Nb, V, Mo and Ti. While niobium is currently obtained largely from Brazil and Canada, there are ample deposits in the USA, currently not regarded as commercially exploitable. The other microalloy elements are widely distributed thoughout the world including sources in the USA.

References

1. "The Metallurgy and Welding of QT 35 and HY 80 Steels", The Welding Institute. Research Report. 1974.

2. B. L. Jones, "Metallurgical Considerations in Linepipe Production", American Welding Society Conference on Pipeline Welding and Inspection, Houston, September 1982.

3. M. A. Civallero, C. Parrini and N. Pizzimenti, "Production of Large-Diameter High Strength Low Alloy Pipe in Itlay", Microalloying 75 Conference, Union Carbide, Washington, D.C. 1975.

4. H. Nakasugi, H. Matsuda and H. Tamehiro, "Ultra-Low Carbon Bainitic Steel for Linepipe", Conference on "Steels for Linepipe and Pipeline Fittings", Metals Society, London, 1981.

5. F. Heisterkamp and K. Hulka, Niobium Products Company Ltd., internal report, 1982.

TABLE 1.

Chemical composition and mechanical properties specification for HY80 steel plates (from MIL-S-16216G ships)

Chemical composition

Element	Per cent	
	Not less than	Not more than
Carbon	-	0.18
Manganese	0.10	0.40
Phosphorus	-	0.025
Sulphur	-	0.025
Silicon	0.15	0.35
Nickel	2.00	3.25
Chromium	1.00	1.80
Molybdenum	0.20	0.60
Residual elements		
Titanium	-	0.02
Vanadium	-	0.02
Copper	-	0.25
S + P < 0.045%		

Tensile properties

Thickness range mm (in.)	0.2 per cent proof stress, (ksi)		Elongation on 50mm (2in.) gauge length, %	Reduction in area, %
	Minimum	Maximum	Minimum	Minimum
Less than 16 (0.625)	80	100	19	-
16 (0.625) and over	80	95	20	55 longitudinal 50 transverse

Impact properties

i. Minimum energy absorption in Charpy V notch test

Plate 11.5mm (0.5in.) to 50mm (2.0in.) incl.	68J (50ft lb) at -84°C No single specimen < 61J (45ft lb)
Plate over 50mm (2.0in.)	41J (30ft lb) at -84°C No single specimen < 34J (25ft lb)

Table 2. Carbon equivalent, weldability and pre-heat calculations for HY 80 and similar steels (Ref. 1).

Preheat temperatures to avoid HAZ cold cracking (NCRE approach)

Carbon equivalent, %	Thermal severity number (TSN)					
	4	8	12	16	20	24
0.4	-	40°C	70°C	85°C	95°C	100°C
0.5	40°C	65°C	90°C	105°C	115°C	120°C
0.6	65°C	90°C	110°C	125°C	135°C	140°C
0.7	90°C	110°C	130°C	140°C	145°C	150°C
0.8	110°C	125°C	140°C	155°C	155°C	160°C

Comparison of hardenability of HY80, Q1 (N) and QT35 steels using carbon equivalent

$$CE\% = C + \frac{Mn}{6} + \frac{Ni + Cu}{15} + \frac{Cr + Mo + V}{5}$$

	HY80, %	Q1(N), %	QT35, %
Typical ladle analysis for plate less than 44mm (1.75in.) thick	0.71	0.71	0.64
Maximum specified ladle analysis for 44mm (1.75in.) thick plate	0.95	0.95	0.75

Calculated minimum preheat temperatures to avoid HAZ cold cracking in plates having typical analyses, assuming a restrained weld of thermal severity 18 and poor fit-up.

	Carbon equivalent, %	NCRE approach, °C	Welding Institute approach, °C	UK MOD (Navy) recommended pre-heating range, °C
QT35	0.64	136 ± 5	133 ± 10	120-150
HY80	0.71	144 ± 5	156 ± 10	120-150
Q1 (N)	0.71	144 ± 5	156 ± 10	120-150

Table 3. Typical Chemical Compositions of X-70 Pipe

Steel Type	Gage	C	Mn	Si	Mo	Ni	Cu	Cr	Nb	V	Ti	N	B
Nb-V	18	0.09	1.50	0.15	-	0.16	0.10	0.12	0.04	0.08	0.016	0.005	-
Mn-Mo-Nb	22	0.05	1.70	0.20	0.26	-	-	-	0.06	-	0.018	0.001	-
Mn-Nb-V	22	0.08	1.90	0.27	0.24	0.20	0.24	-	0.05	0.06	-	0.007	-
Nb-Ni (14)	18	0.07	1.60	0.20	-	0.55	-	-	0.11	-	0.019	0.004	-
Nb-V-Cr	15	0.09	1.52	0.22	-	-	-	0.35	0.04	0.08	-	0.008	-
Nb-Mo-Cr	15	0.08	1.50	0.20	0.18	-	-	0.30	0.05	-	-	0.010	-
Mo-Nb-Cu	15	0.06	1.45	0.20	0.25	-	0.30	-	0.025	-	-	0.009	-
Ti-Ni	15	0.08	1.58	0.30	-	0.26	-	-	-	-	0.070	0.004	-
Ti-Cu-Ni (10)	20	0.09	1.61	0.30	-	0.12	0.21	-	-	-	0.063	-	-
Low C-Nb	20	0.02	1.78	0.13	-	-	-	-	0.10	-	0.015	0.004	-
Low C-Nb-B (15)	20	0.02	1.89	0.13	-	-	-	-	0.05	-	0.016	0.002	0.001
Low C-Nb-Mo-B (15)	22	0.02	2.01	0.16	0.30	-	-	-	0.05	-	0.018	0.002	0.001
C-Mn-Nb (Q & T)	20	0.09	1.37	0.27	0.16	1.00	-	-	0.02	-	0.020	0.005	-
C-Mn-Nb (Controlled Cooled)	20	0.08	1.55	0.60	-	-	-	-	0.06	-	-	0.010	-

*0.25 for gages above 18-20 mm.

All Aluminum levels .02 - .05
All Sulfur levels .002 - .007

Table 4 Typical Chemical Compositions of ULCB Steel for Various Grades

(%)

Steel	Grade	C	Si	Mn	P	S	Ni	Mo	Nb	Ti	B	C_{eq} *1)	P_{CM} *2)
UB-1	X-65	0.02	0.14	1.59	0.018	0.003	-	-	0.04	0.017	0.001	0.29	0.11
UB-2	X-65	0.03	0.16	1.61	0.016	0.003	0.17	-	0.05	0.016	0.001	0.31	0.12
UB-3	X-70	0.03	0.14	1.91	0.018	0.003	-	-	0.05	0.018	0.001	0.34	0.14
UB-4	X-70	0.01	0.15	1.87	0.022	*3) 0.007	-	-	0.04	0.020	0.001	0.32	0.11
UB-5	X-80	0.02	0.26	1.95	0.022	0.003	0.38	0.31	0.04	0.019	0.001	0.43	0.16

*1) $C_{eq} = C + \frac{Mn}{6} + \frac{Cr+Mo+V}{5} + \frac{Ni+Cu}{15}$

*2) $P_{CM} = C + \frac{Mn+Cu+Cr}{20} + \frac{Si}{30} + \frac{V}{10} + \frac{Mo}{15} + \frac{Ni}{60} + 5B$

*3) High-sulfur content

Table 5 Mechanical Properties of Pipe Body

Steel	Grade	Pipe size (mm)	Direct. of test	Tensile properties				Charpy V-notch impact properties		BOWTT	
				Y.S. (MPa)	T.S. (MPa)	El. in 50.8mm (%)	Yield ratio (%)	Energy at -20°C (J)	50% Shear FATT (°C)	Shear fracture area at -20°C (%)	80% Shear FATT (°C)
UB-1	X-65	1420 OD x 16 WT	Trans-verse	500	583	42	85	369	< -80	100	-50
UB-2	X-65	1220 OD x 25 WT	Trans-verse	493	602	45	82	324	< -80	95	-30
UB-3	X-70	1420 OD x 20 WT	Trans-verse	542	641	42	85	206	< -80	100	-40
UB-4	X-70	762 OD x 22 WT	Trans-verse	551	622	41	89	159	< -80	98	-35
UB-5	X-80	1420 OD x 20 WT	Trans-verse	653	732	33	89	178	< -80	100	-50

Note : 70ksi ≡ 483 MPa ; 80ksi ≡ 550 MPa ; 90ksi ≡ 619 MPa ; 100 ksi ≡ 689 MI

Table 6 Mechanical Properties of Submerged-Arc Weld Joint

Steel	Grade	Pipe size	Transverse weld-tensile properties		Charpy V-notch impact properties		
			T.S. (MPa)	Location of fracture	Test position	Energy at -20°C (J)	50% Shear FATT (°C)
UB-1	X-65	1420 OD x 16 WT	595	Base metal	Weld metal	164	-40
					HAZ	248	-50
UB-2	X-65	1220 OD x 25 WT	617	Base metal	Weld metal	191	≤ -60
					HAZ	272	≤ -40
UB-3	X-70	1420 OD x 20 WT	665	Base metal	Weld metal	148	-40
					HAZ	182	-35
UB-4	X-70	762 OD x 22 WT	633	Base metal	Weld metal	183	-45
					HAZ	62*)	-20
UB-5	X-80	1420 OD x 20 WT	727	Base metal	Weld metal	189	-60
					HAZ	130	-20

*) Low energy due to high-sulfur content

Table 7. Chemical Composition and Mechanical Properties of 0.5% Ni, 0.1% Nb Steel

C	Si	Mn	P	S	Al	Ni	Nb
0.077	0.36	1.56	0.017	0.005	0.02	0.47	0.13

Y.S.	UTS	C_v (+20°C)	50% CVN-FATT	85% BDWTT-FATT
70.1 ksi	84.5 ksi	78J	-85°C	-55°C

56 inch diameter SAW pipe, 17.5 mm wall thickness

Fig. 1. X70 HSLA LINEPIPE STEELS

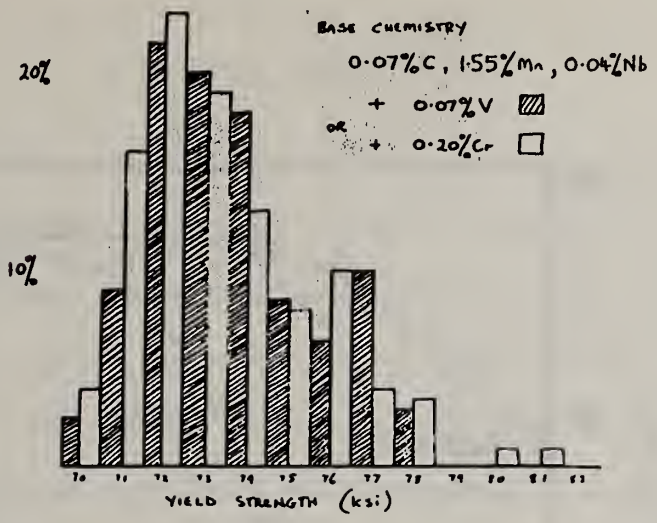

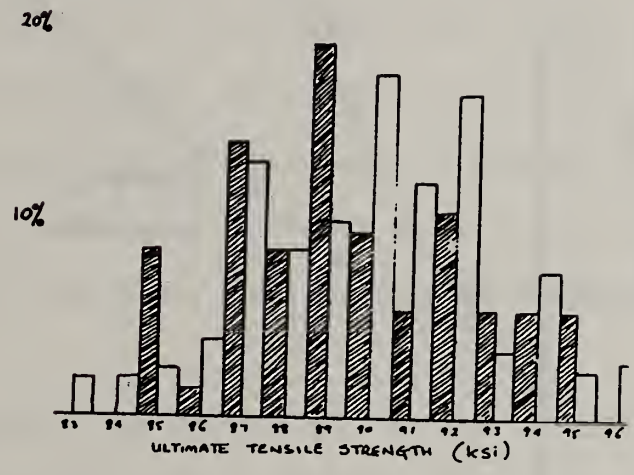

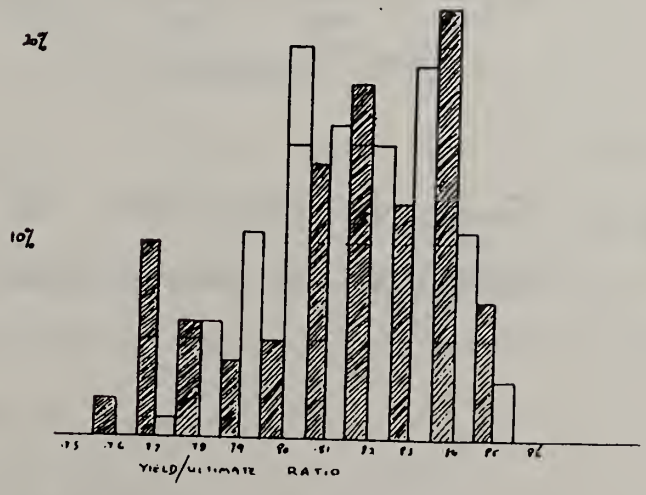

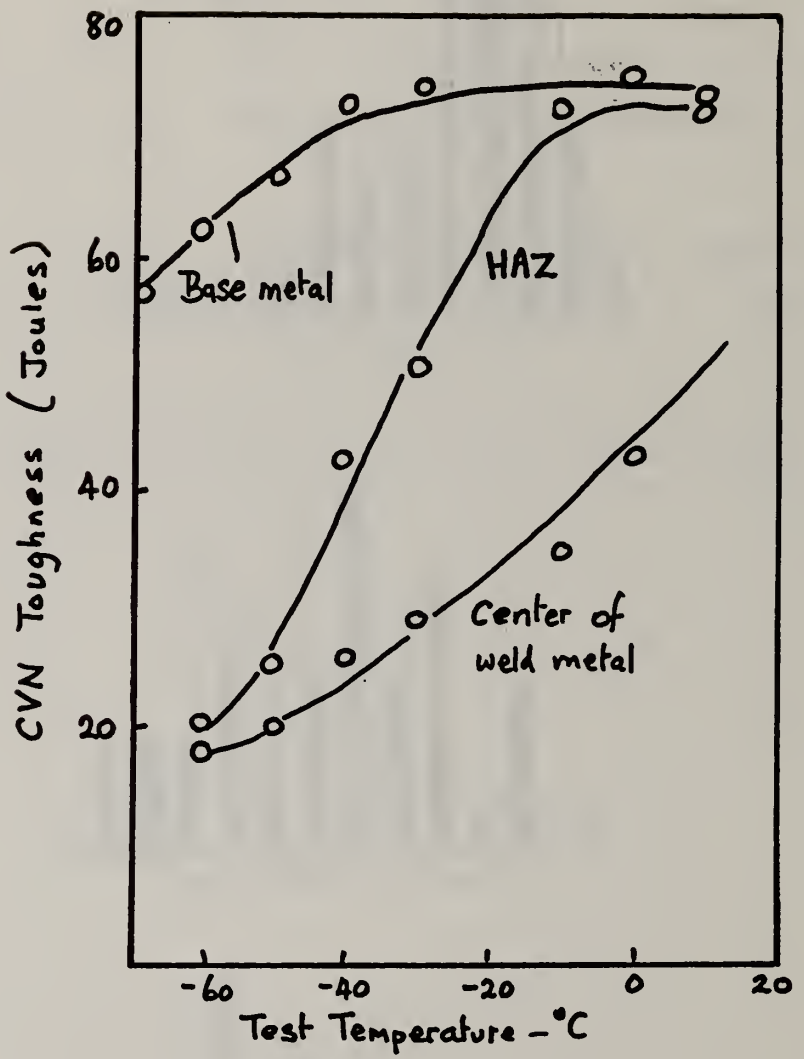

FIG. 2 Toughness properties of Ni-Nb submerged-arc welded pipe (17.5 mm w.t.).

Opportunities for Surface Modification Technology in Conservation of Chromium

by

Peter G. Moore*

Although there are many other uses for chromium, three principal uses are to improve the corrosion-, oxidation- or wear-resistance of structures and materials. Because these properties are surface related, coatings can be used in many cases to reduce the amount of chromium used and to allow the surface properties of structures (as opposed to materials) to be tailored to surface requirements without sacrificing bulk properties. A number of directed energy beam (DEB) processing techniques have been developed in recent years which provide new opportunities for the conservation of chromium through reduced usage and through substitution for chromium by other elements. Today, I will just describe in general terms two classes of processing techniques (ion beam processing and laser beam processing) which produce novel corrosion- and wear-resistant surface layers and then describe several cases in a bit more detail.

With ion beam processing, the surface of the structure is bombarded by ions with energies in the range of 10 to 200 keV. These ions are stopped within 1 μm of the surface of the solid material as a result of a series of collisions. These collisions alter the microstructure of the surface layer and the implanted ions alter the composition of the surface layer. This ion implantation requires the production of an ion beam of the desired species. Ion mixing and ion plating are variations where a thin layer of the desired material is first coated onto the structure and then an argon or xenon ion beam is used to intermix the coating and the substrate atoms.

---

* Peter G. Moore is with the Naval Research Laboratory

With laser processing, the surface of the structure is rapidly heated by a high power laser beam until the surface melts. After the beam is turned off, the liquid rapidly resolidifies and is quenched as the heat is conducted away to the bulk of the structure. Variations on this laser-surface melting process include shock and transformation hardening (where no melting takes place), surface alloying and cladding (where alloying elements are added) and particle injection (where wear resistant particles are incorporated into the melt). There are also many analogous processes using electron beams.

Directed energy beam (DEB) processed coatings in general have several advantages over traditional coatings: (1) a wide range of controlled coating thicknesses is possible, (2) coatings are metallurgically bonded to the substract, (3) there are few thermodynamic constraints for laser processing and fewer still for ion beam processing, and (4) structures and properties can be graded with depth from the surface in order to optimize performance.

There are also several characteristics of DEB processing which restrict its use. Almost all DEB processing is either done in vacuum or in a helium which add to the cost of processing. Because all of the techniques are line-of-sight processing, structures which can be processed by such techniques are restricted to geometries which are relatively open and free of recesses. In addition, processing is limited to relatively small areas and structures, because of the vacuum requirement for ion beam processing and because of warpage due to residual stresses for laser beam processing.

Ion Implantation

As an example of the potential for solving materials problems through the use of ion implantation, consider the study of the effect of implanting various species on the resistance of M50 bearing steel to the pitting corrosion which results in the salt water contaminated aircraft lubricants.

Test specimens of M50 steel were implanted with 150 keV chromium ions to obtain a peak chromium concentration of 24% at a depth of about 400 A below the surface. Electrochemical polarization measurements and simulated field service tests indicated an improved resistance to pitting corrosion and as a result, an improved field performance.

Laser Processing

Three examples illustrate the potential of laser processing for solving materials problems in the areas of corrosion, oxidation and wear. These are the surface melting of 304 stainless steel to improve resistance to localized corrosion, the surface alloying of chromium into steel substrate to produce a stainless steel surface layer, and the production of wear resistant layers by the particle injection method.

Recent work has attempted to improve the resistance of 304 stainless steel to pitting corrosion by laser surface melting. The resolidified material exhibited a very fine dendritic subgrain structure which indicated cooling rates in excess of 10^6K/sec. These materials were electrochemically characterized by potentiodynamic polarization experiments in 0.1 M NaCl which indicated an improved resistance to pitting compared to wrought 304 and comparable to that of 316 stainless steel. A number of possible reasons exist for this improved behavior as a result of the redistribution of both major and minor alloying elements through homogonization during melting and segregation during and after solidification. At this time, it is felt that the improvement is due to the eliminiation of large precipitates which cause the local passive film to be less protective.

Chromium steel surface alloys have been produced on various steel substrates using a variety of processing techniques. The electrochemical behavior

of these alloys has verified that the surface layers passivate in the manner of stainless steels. The broader significance of this and the previous results is that a stainless steel surface layer, suitable to the chemical environment can be rapidly and efficiently produced on the surface of a steel structure.

A third type of laser processing, particle injection, is performed in the fashion of surface melting except that hard, wear-resistant particles are injected into the melt pool. This results in a metal-matrix composite surface layer which is metallurgically bonded to the substrate. Abrasive wear tests of layers produced by the injection of TiC and WC into aluminum-, titanium-, nickel- and iron-base alloys result in performance during abrasive wear tests which are comparable to that of specialty wear coating materials. An especially good example of the potential for this technique is the production of a TiC-aluminum matrix composite on an aluminum substrate; a wear resistant surface combined with a high thermal conductivity high specific-strength base metal which cannot normally be considered for applications where wear is a problem.

Conclusion

Ion implantation and laser processing are both attractive techniques which, when applied to appropriately, can be used to solve wear, corrosion and oxidation problems. The examples presented here have illustrated situations where chromium can be conserved by using these coating techniques, and performance comparable to or better than that of bulk alloys using chromium is obtained. In these applications, chromium was used in a more or less traditional manner and the role of the chromium in enhancing the performance has been the same as its role in conventional alloys. By the nature of these techniques, there are also many possibilities for enhancing performance of structures by pro-

ducing novel materials. It is this two-pronge potential of DEB processing technique which will make them invaluable in the event of critical shortages of key materials.

SALT BATH TREATING AS AN ALTERNATIVE FOR CHROMIUM PLATING

Nitrogen/Oxygen Synergism

The potential for replacing chromium plating by an oxidized nitrided surface (Fig. 1) evolved from a completely unrelated event. Actually the concept of following a liquid nitriding treatment by quenching in an oxidizing fused salt was originally devised to destroy any slight traces of cyanide developed during nitriding and the substantial amount of cyanate present in the salt as the active agent (Fig. 2). The corrosion resistance of the resultant combination diffusion and conversion coating is truly a synergistic effect.

The Aerated Liquid Nitriding Process

A more thorough understanding of the surface produced can be achieved by a brief consideration of the original nitriding process. The aerated liquid nitriding process was introduced into the United States in the late 1950's and early 1960's. The treatment requires immersion in a cyanide/cyanate fused salt at 1060°F (570°C) for a 60 to 180 minute period. The salt is aerated by a sparging ring immersed in the bottom of the fused mixture. Make-up salt which consists of sodium and potassium cyanide is added and reacts with the bubbled air to produce sodium and potassium cyanate according to the following reactions:

$$KCN + 1/2\ O_2 = KCNO \quad (1)$$

$$NaCN + 1/2\ O_2 = NaCNO \quad (2)$$

The formation of the cyanate compounds in situ in conjunction with a 45 to 50% cyanide content and a 45 to 50% cyanate content is the basis for U.S. Patent No. 3,022,204. During the nitriding action on carbon steels a 0.0004 in (.01 mm) to 0.0006 in (.015 mm) compound zone is formed in conjunction with a 0.018 in (0.45 mm) diffusion zone, (Fig. 3). The compound zone is composed of single phase epsilon iron nitride (Fe_3N) (Fig. 4) responsible for its very unique wear resistance and low coefficient of friction properties. The nitrogen dissolved in the diffusion zone (Fig. 5) is responsible for substantial increases in endurance values in both notched and unnotched ferrous structural parts. In addition, the single phase epsilon iron nitride surface exhibits excellent corrosion resistant properties and in many cases the nitriding treatment is performed with this factor as a primary consideration.

Sub-Critical Heat Treatment

Aerated liquid nitriding has the unique characteristic of being a sub-critical single heat treatment capable of increasing corrosion resistance, endurance values and wear resistance. The development of the epsilon iron nitride surface and the nitrogen diffusion at temperatures substantially below the critical temperatures of structural steels permits the elimination of excess material and the subsequent required finishing operations to compensate for growth and distortion during processing. The process is thus ideally suited for treating cylindrical shapes such as cylinder liners and rocker arm shafts, where final finishing costs can be excessive. This capability of retaining dimensional stability is also of vital importance where corrosion protection is dependent upon thin films developed by heat treatment thereby precluding final machining.

Process Changes Required Because of Environment

For many years this specialized heat treatment was documented, tested and specified for crankshafts, gears, rocker arm shafts, connecting rods, valves, valve guides and numerous other engine and chassis parts in all types of industrial applications. Environmental pressures eventually restricted the use of cyanide compounds for metal processing in certain areas and it became necessary to develop a relatively cyanide free liquid nitriding process. At the same time the stated goal was to be able to produce a single phase epsilon iron nitride compound zone (Fig. 6) with a nitrogen diffusion zone that could produce corrosion resistance, endurance values and wear resistance equivalent to those obtained in the existing process. The records accumulated during years of testing of the original process made interchangeability a desired asset.

New Liquid Nitriding Process

The aerated liquid nitriding process introduced in the 1970's met these requirements in all respects. Unfortunately, under certain conditions the fused salt also had the capability of generating small amounts of cyanide during processing, according to:

$$KCNO + 2FeO = KCN + Fe_2O_3 \quad (3)$$

and therefore could not be specified as a complete cyanide free salt. Overcoming this objection involved post treatment in an oxidizing media which began as a standard fused sodium and potassium nitrate/nitrite mixture and then finally evolved into a sodium and potassium hydroxide, carbonate and nitrate composition capable of total destruction of all traces of cyanide and cyanate, (Fig. 7). The hardness patterns (Fig. 8) and (Fig. 9), wear characteristics (Fig. 10) of the quenched nitrided parts exhibited minimal change but the corrosion properties were substantially increased (Fig. 11). Laboratory analyses of the quenched parts revealed that the unexpected corrosion resistant results obtained were not a function of the jet black surface (Fig. 12) but a more complex combination of nitrogen, oxygen and iron.

Auger profiles substantiated the fact that the diffusion of oxygen into the epsilon iron nitrided compound zone was responsible for the corrosion resistance. Studies eventually revealed that optimum dwell times in the fused quenching salt would result in maximum corrosion resistance, although this work is still in progress. The complete mechanism involved in converting a liquid nitrided surface into an effective corrosion barrier in carbon and alloy steels is not completely understood. Test results however continue to indicate that the majority of situations favor the substitution of this treatment for chromium plating and this trend should continue if the projected costs and availability of chromium metal eventually become a reality.

Surface Compatibility with Bearings and Seals

Aerated liquid nitriding in conjunction with oxidizing salt quenching may be a viable substitute for chromium plating but the process as performed lacks compatibility in contact with many non-metallic seals and bushings. With this in mind a third and fourth step was added to the treatment when the finished product is to be subjected to the above conditions. Basically the objection to a standard nitrided and quenched part is the surface residue or roughened finish resulting from nitriding, which can be a lap in contact with softer nonmetallic materials. Fortunately this difficulty can be easily overcome by polishing. Method of polishing is completely optional providing surface removal is uniform and restricted to 0.00005 in (0.0013 mm) per surface. Automated fixtured polishing with 320 grit paper has been used on bearing and contact surfaces of rotating or sliding shafts. Vibratory finishing is completely acceptable where configuration prohibits fixturing. Following the polishing operation the parts are immersed once again in the quench bath for an oxygen diffusion period of twenty minutes.

The effect of this sequence of operations is shown in the bar graph of (Fig. 13). Starting from the outside left bar, the finished carbon steel has very low corrosion resistance and a standard commercial finish. After aerated liquid nitriding, the corrosion resistance has increased dramatically, but directly above, the surface roughness has also increased substantially. The third set of bars illustrates how fine polishing reduces the corrosion resistance slightly but effectively produces a surface finish suitable for bearing contact. Finally, requenching in the oxidizing salt bath develops the ultimate combination of surface finish and corrosion resistance.

The final process with oxygen diffused nitrided surfaces operating against elastomeric and nonferrous seals or bearings is as follows:

1. Aerated liquid nitriding in a cyanide free fused salt -- 60 to 120 minutes at 1070°F (577°C).

2. Quench in controlled rate oxidizing salt at 750°F (400°C).

3. Water rinse.

4. Abrasive polish to desired surface finish with maximum stock removal of 0.00005 in (0.0013 mm).

5. Reimmersion in controlled oxidation bath, dwell time 20 minutes.

6. Water rinse and oil.

Corrosion and Wear Evaluation

Any system that is developed as a substitute for a proven existing product must be subjected to extensive laboratory testing prior to acceptance. Also, the testing has more credence if not restricted to the confines of the developers research facilities.

Automotive spool shafts that are machined from plain carbon steel are subjected to corrosive environmental effects when operating in their under hood locations. A United States manufacturer of these shafts evaluated chromium plating, electroless nickel and the oxidized nitrided coating as suitable protective treatments (Fig. 14). The oxidized nitrided surface after the normal 88 hour test duration reflected less than a 5% corrosion area which is significantly less than the 70% figure shown for both chromium plating and electroless nickel plating. Continuation of the test on the nitrided shafts only (to produce failure) developed a 336 hour corrosion area of 5% to 10% which is significantly less than the results obtained from the chromium and nickel plated shafts during a 72 hour period. The results of these tests which were performed in accordance with ASTM B117 are summarized in (Fig. 15).

One type of corrosion test performed in the research laboratory of a supplier of automotive shock absorbers is shown in (Fig. 16). Two rods with different surface treatments, chromium plating and oxidized liquid nitriding, were subjected to an accelerated life test of 300,000 cycles with a side load applied, followed by 96 hours of ASTM B117 salt spray test. The loading imparts a high pressure contact zone between the O-ring seal and the piston rod in a limited area. The figure illustrates that the chromium plated rod has numerous corrosion sites on the surface while the oxidized nitrided rod shows little effect from the corrosive atmosphere. Smaller rods, chromium plated in the assembly, and liquid nitrided followed by quenching, foreground, are shown in (Fig. 17).

In any discussion involving hard chromium plating, wear resistance properties are usually as important as corrosion characteristics. A program was recently initiated to measure the relative resistance of hard chromium plated with salt quenched aerated liquid nitrided engine valves, (Fig. 18). The test load was applied through a rotating carbide cylinder making contact with a stationary valve stem, oriented at right angles to the cylinder axis. Tests were performed on both the intake valves, AISI 1541 and the exhaust valve 21-2N. After a one minute test period using prescribed loads, the degree of wear was measured as loss of weight in the valve components (Fig. 19).

Summary

In summary, the oxygen diffused nitriding process has the capability of producing a surface comparable or superior to chromium plating with respect to wear resistance and corrosion resistance in numerous industrial applications. Unlike chromium plating, there is no requirement for the utilization of strategic materials. Also, unlike electroplating processes, there is no water or air pollution problems involved when the oxidized liquid nitriding process is practiced. The materials required to produce both of the fused salts involved in the process are readily available common chemicals and none of the compounds present in the effluent rinse waters are presently categorized on a restricted discharge basis. Unit costs of any process are usually suspect after a very short period of time because of our rapidly changing economic conditions but on a comparative basis the total costs involved in chromium plating and the oxygen diffused nitriding process are quite similar and are likely to be that way even with future changes in the Cost of Living Index.

Fig. 1. Ball studs, aerated liquid nitrided and salt bath quenched.

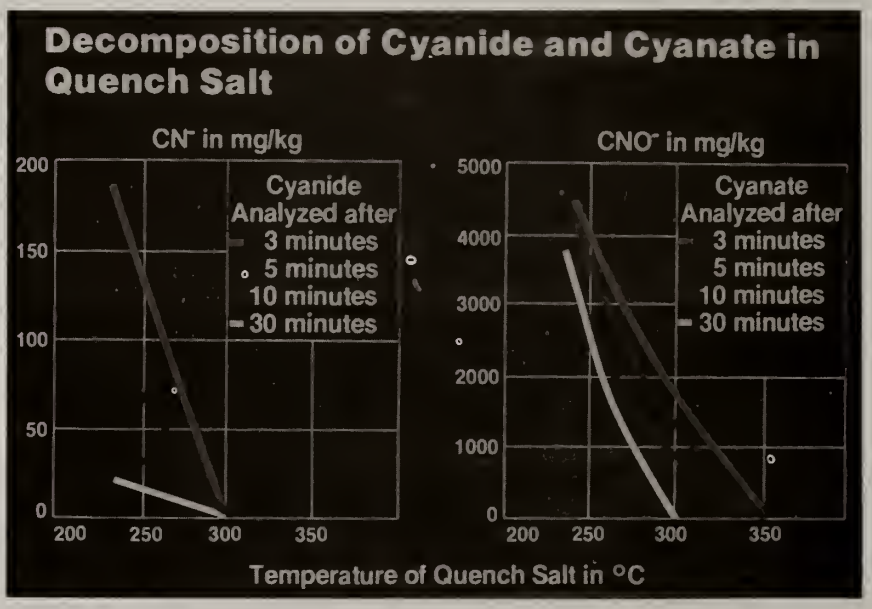

Fig. 2. Chemical destruction of cyanide and cyanate residues, after salt bath quenching, related to time and temperature.

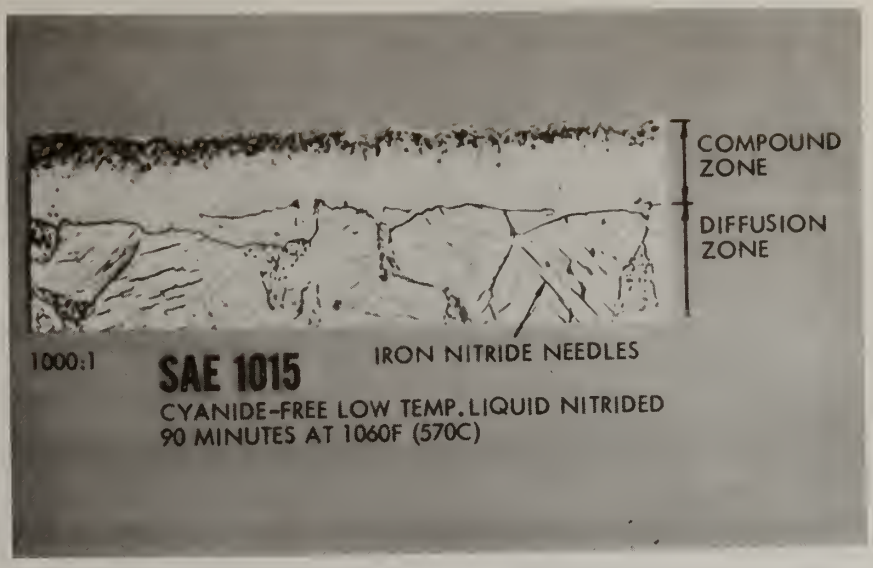

Fig. 3. Compound zone and diffusion zone developed by low temperature liquid nitriding. Note the needle like structure of Fe_4N developed in the diffusion zone by aging.

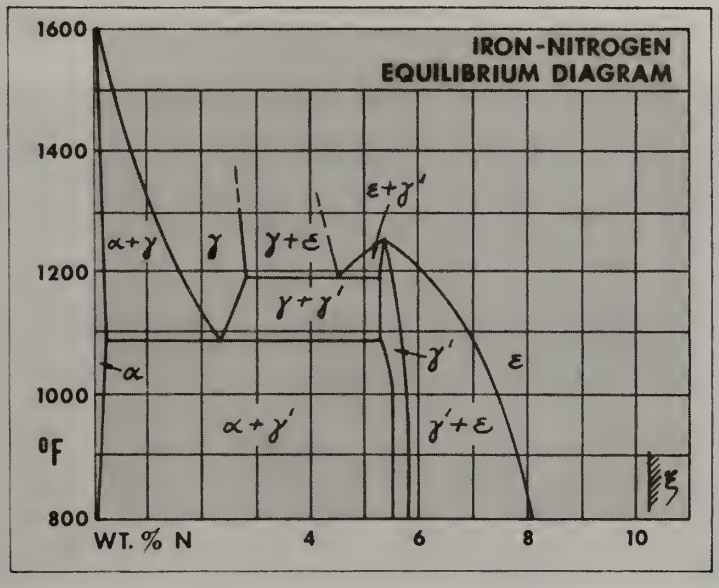

Fig. 4. The epsilon iron nitride phase in aerated liquid nitriding is developed, as shown, slightly to the right of the intersection of the 8% nitrogen line with the 1060°F (570°C) temperature line. The stoichiometric ratio of nitrogen to iron is very close to one to three.

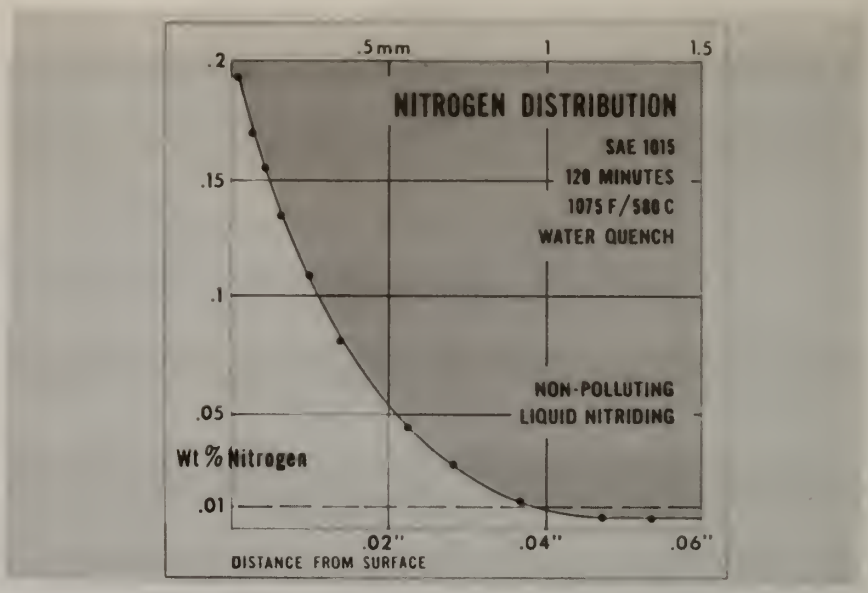

Fig. 5. Nitrogen distribution in the diffusion zone of aerated liquid nitrided carbon steel. It is this nitrogen that is responsible for increases in endurance values from 20% to 100%.

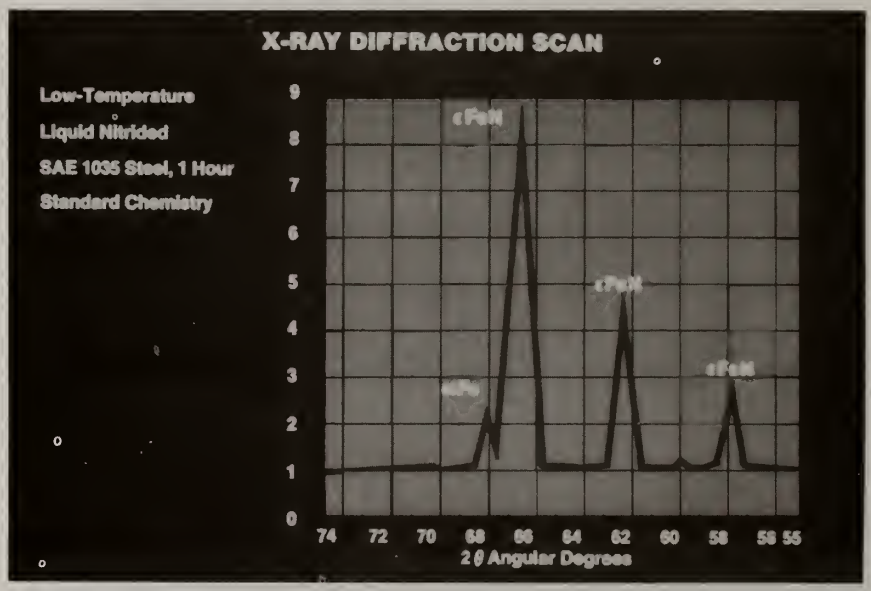

Fig. 6. X-ray diffraction pattern of aerated liquid nitrided carbon steel. The three typical peaks of epsilon iron nitride are present while the absence of other compound peaks indicate that the zone is single phase.

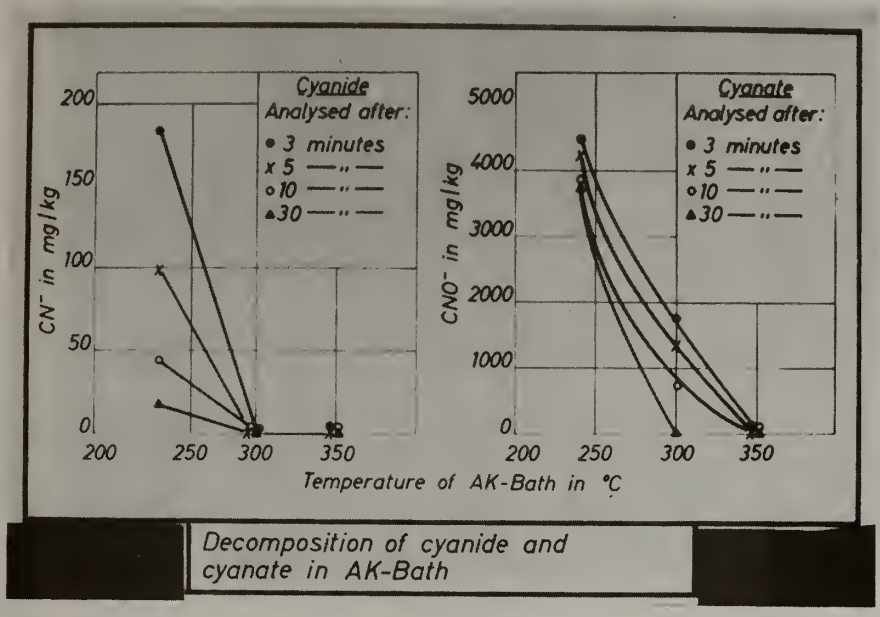

Fig. 7. Chemical destruction of cyanide and cyanate in an oxidizing media.

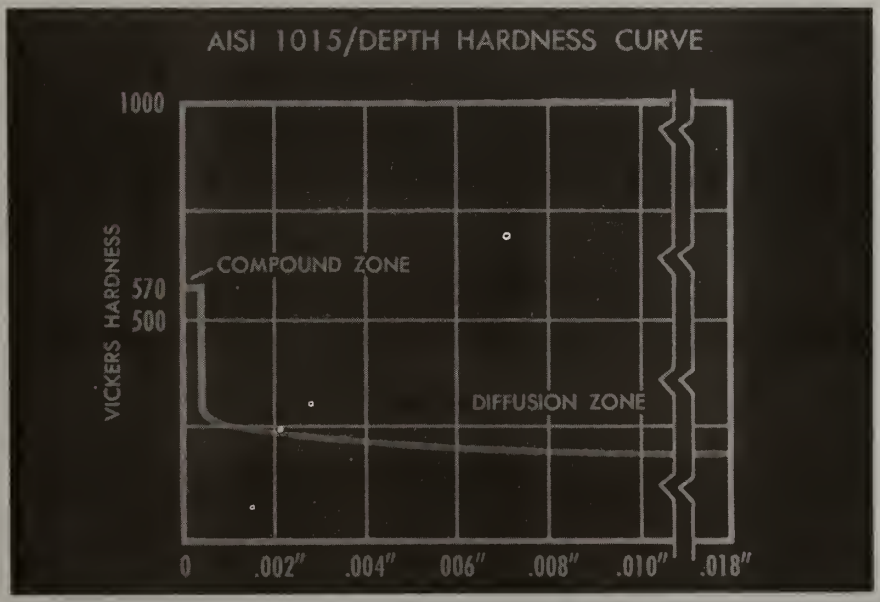

Fig. 8. Hardness pattern resulting from aerated liquid nitriding of plain carbon steel. The sharp drop below the surface measures the depth of the compound zone.

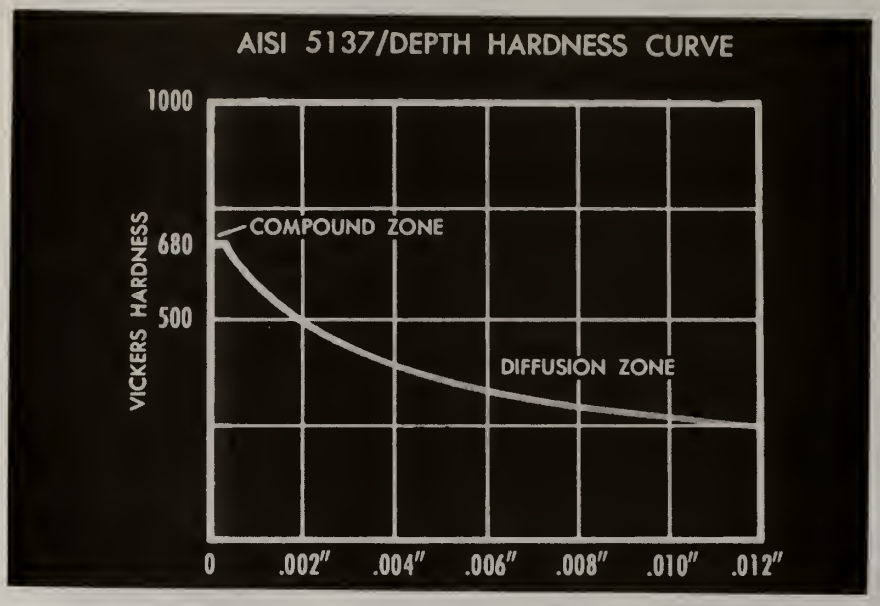

Fig. 9. Hardness pattern developed by aerated liquid nitriding of alloy steel. The higher surface hardness and the measurable retention through the diffusion zone results from alloy influence.

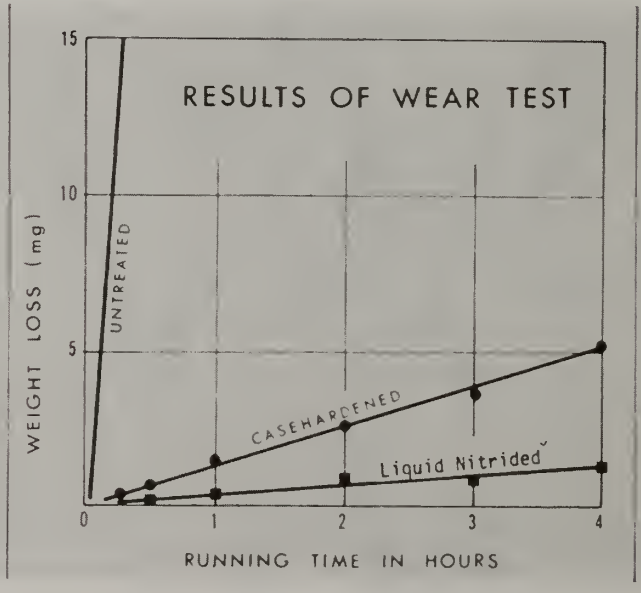

Fig. 10. Wear test comparison of untreated, carburized and aerated liquid nitrided specimens.

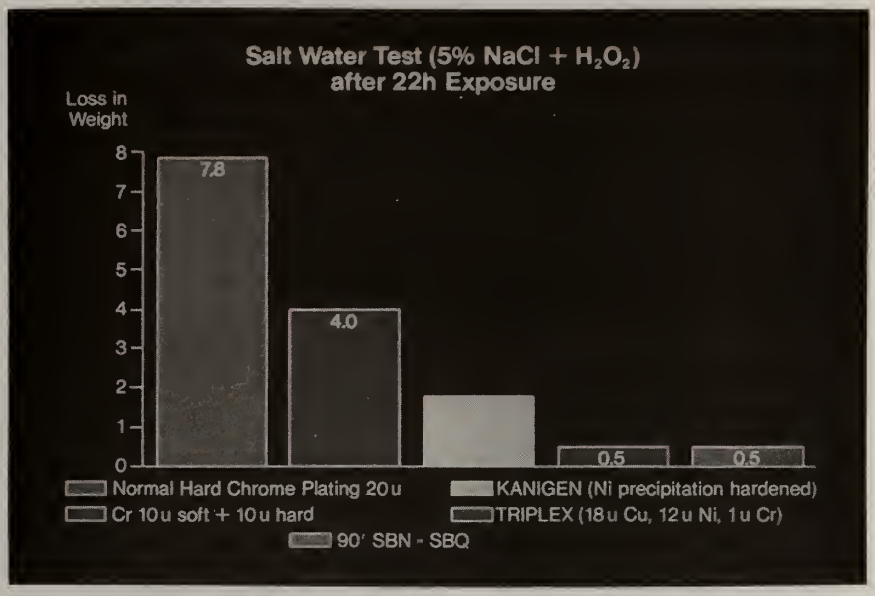

Fig. 11. Salt water corrosion tests on various surface treatments. The SBN-SBQ notation refers to salt bath nitriding followed by salt bath quenching. The other treatments are standard.

Fig. 12. The top gas spring has an aerated liquid nitrided shaft compared to the lower spring with a chromium plated shaft.

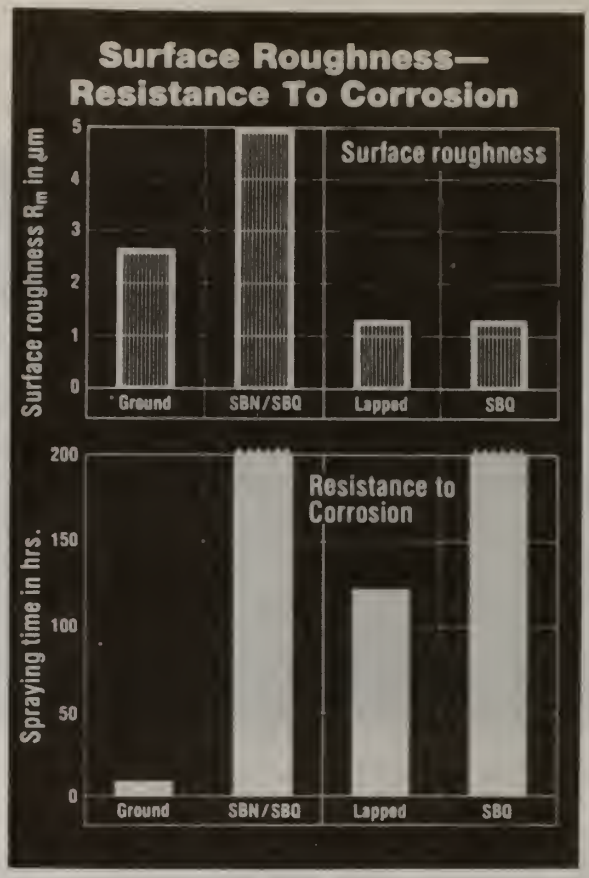

Fig. 13. The effect of sequential surface treatments on surface finish and corrosion resistance. The acronyms for aerated salt bath nitriding, SBN, and oxidizing salt bath quenching, SBQ, are used.

Fig. 14. Automotive spool shafts subjected to salt spray testing according to ASTM B-117. The nitrided/quenched surface is indicated by QPQ.

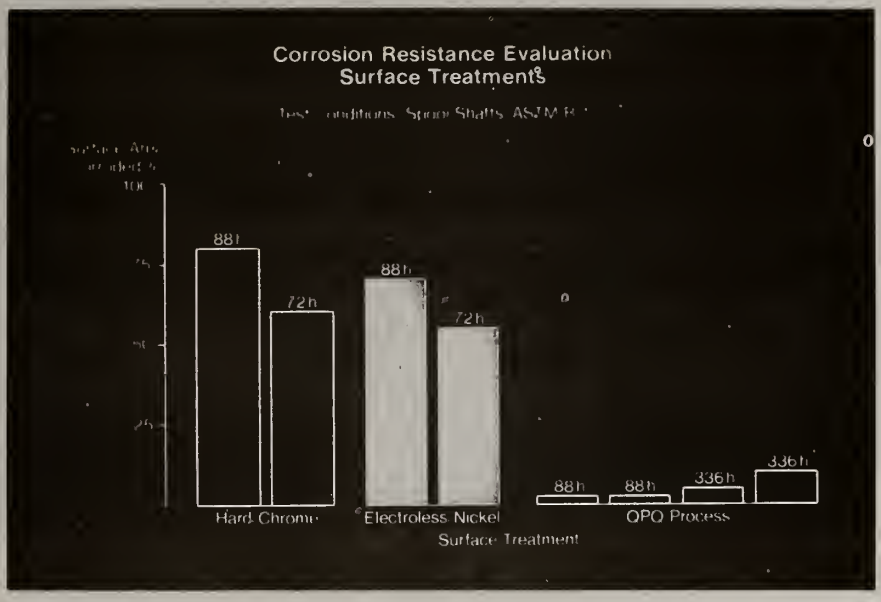

Fig. 15. Resistance of various surface treated spool shafts exposed to corrosion testing according to ASTM B117. QPQ refers to the quenching and polishing of aerated liquid nitrided specimens.

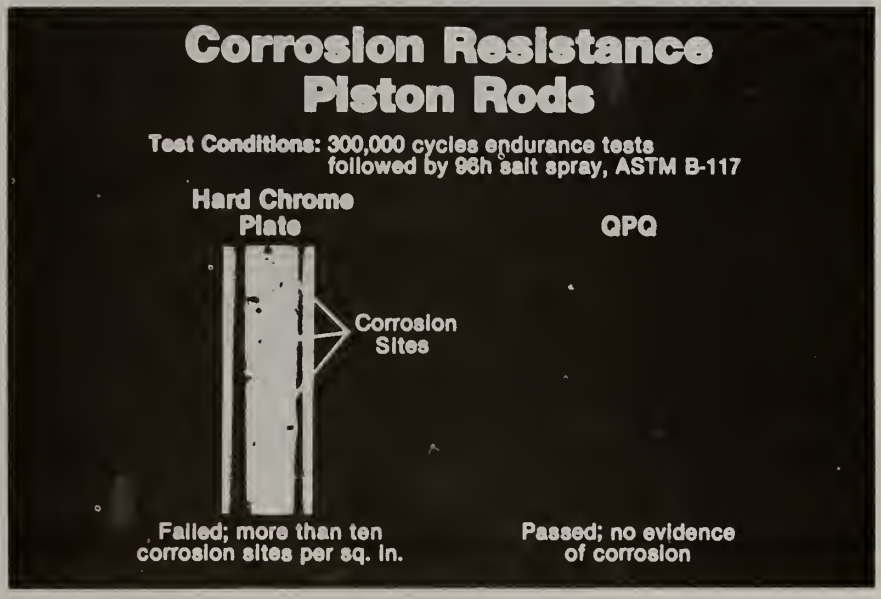

Fig. 16. The aerated liquid nitrided piston rod after salt bath quenching, polishing, and requenching exhibits no evidence of corrosion after endurance testing followed by 96 hours of salt spray.

Fig. 17. Shock absorber assembly and rod. Combinations of endurance properties and corrosion resistance are required.

Fig. 18. Surface treated engine valves.

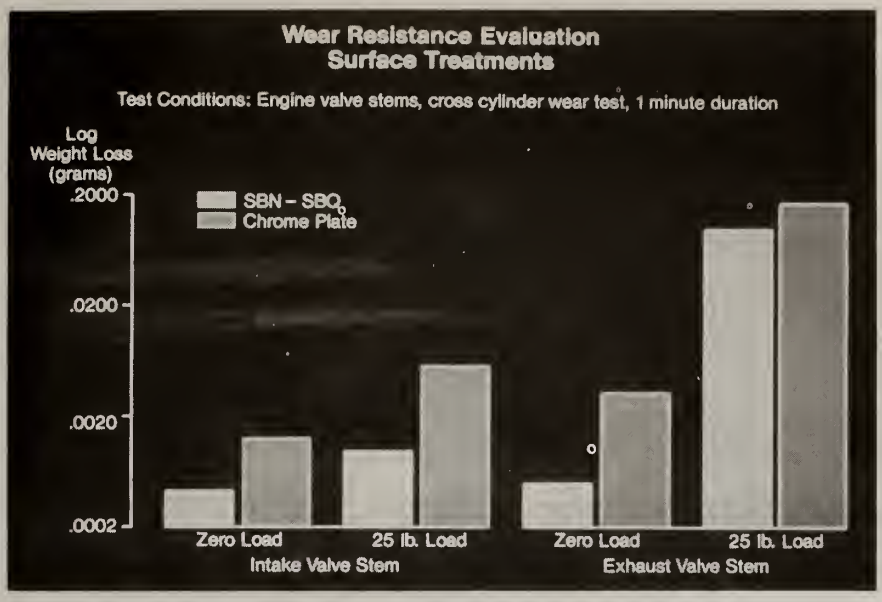

Fig. 19. Comparison of the wear properties of hard chromium plated engine valve stems with stems treated by aerated liquid nitriding followed by salt quenching.

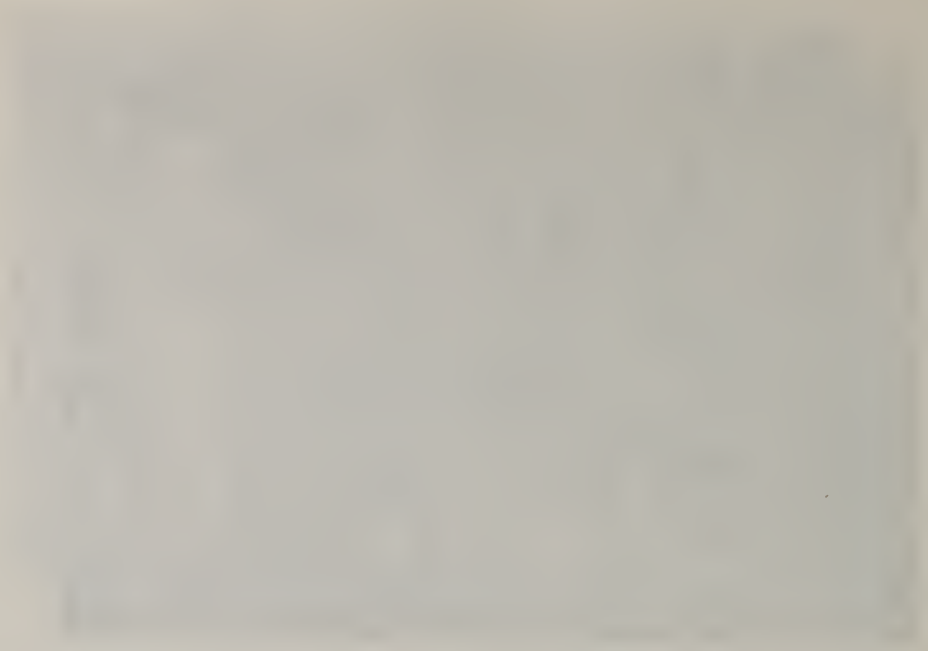

CLAD METALS - MATERIAL CONSERVATION THROUGH DESIGN FOR CORROSION CONTROL AND HIGH PERFORMANCE

James T. Skelly
Metallurgical Materials Division
Texas Instruments Incorporated
Attleboro, MA 02703

Abstract

Growing concern over the continued availability of critical materials at a reasonable cost has spurred the development of new materials, product redesign, and improved conservation and recycling methods. The pursuit of new materials that reduce or even eliminate reliance upon critical materials can offer tremendous payoffs. Numerous research facilities are concentrating on new alloy development, surface coatings, surface modification, ceramics, and composites, all of which hold promise in reducing dependence upon unstable foreign sources for critical materials. Clad metals provide another approach.

By precisely engineering a clad metal system, unique functional benefits can be achieved that are otherwise unavailable or available only with heavy reliance on critical materials. This paper will focus on the design, development, application, and performance of precision clad metals. Specific unique properties and corrosion control benefits will be discussed as will feasible alloy combinations.

Cladding Technology

The modern process for production of clad metal strip is focused upon continuous cold roll bonding of two or more strips. Prior to bonding, the individual strips of metal are rolled to precise gauges and extensively cleaned to provide contaminant-

free surfaces. When passed through the specially-designed high pressure rolling mill, a composite material is formed, deriving its bond integrity from the merging of the atomic lattices of the two metals into a common structure. Subsequent thermal treatment is performed to promote diffusion, improve bond strength, and provide stress relief for further cold work operations. Finishing operations, such as rolling to intermediate and final gauge, annealing, buffing or polishing, and slitting ensure matching clad metal properties to specific and exact product requirements.

These precision clad metals are manufactured by a highly refined process which is based upon the technology of solid state welding. No intermediate brazing alloys or adhesives are used to achieve a permanent bond.

It is important to distinguish clad metals from plated metals. Most importantly, the layers in the clad metal system are wrought metal as opposed to thin and porous plating layers. Also, the thickness of the individual clad metal layers can be precisely controlled over the entire composite metal thickness as opposed to the well-known practical limitations to plating thickness. Figure 1 compares the qualities of cladding versus plating.

Generally, most metals and alloys can be clad. Figure 2 illustrates that many ductile metals and alloys available in wrought form are in production today. Numerous other combinations are technically feasible but require development before commercialization.

The Clad Metal Approach

At first glance, direct substitution of a clad metal system

to conserve critical materials can be envisioned as a surface layer of an alloy containing critical materials clad to a widely available, low cost base metal. In fact, origins of modern clad metal manufacture addressed conservation of precious metals such as gold or silver.

Direct substitution of clad metals for critical materials, however, can only offer a partial solution. The usage of the critical material is only reduced and not eliminated in the end product. The process to clad the critical material will offset much of the apparent economic advantage of the critical material content reduction. We should not be looking for substitutes but should be looking for alternate approaches.

Optimal application of clad metals for conservation of critical materials is derived from obtaining a longer useful life via corrosion control or improved performance of the end product without the heavy reliance upon critical materials.

Metals Design for Corrosion Control

Controlling the effects of corrosion with the use of clad metals necessitates utilization of the galvanic series, which is based upon the electrochemical potential of a metal and a reference cathode. Figure 3 illustrates a typical galvanic series in seawater where a less noble metal would corrode at accelerated rates when coupled electrically to a more noble metal. The application of the galvanic series in design of clad metal systems can result in enhanced corrosion control performance. The corrosion control mechanisms and example applications will be discussed below.

1. By cladding a thin layer of highly corrosion-resistant

metal over a less corrosion-resistant and lower cost metal, it is possible to achieve enhanced and reliable corrosion resistance. The less noble core layer provides the mechanical strength at a low cost. The system differs from plating in the thickness and nonporosity of the noble layer.

An example of this approach, called noble metal cladding, is stainless steel clad aluminum for truck bumpers. The highly corrosion-resistant type 301 stainless steel is 10 times the thickness of chromium plating over a steel or aluminum substrate. As shown in Figure 4, laboratory and field testing has confirmed that defects in the chromium plating layer or damage during installation or service which results in a small anode to cathode ratio, can lead to shorter life for a conventional plated steel or aluminum bumper. The stainless steel clad aluminum bumper has demonstrated beyond a reasonable doubt that it can meet the million-mile-life demands of the heavy duty truck bumper.

2. The combination of a more noble metal clad to a less noble metal, where the purpose of the less noble metal is to protect the more noble metal by corroding preferentially, is an example of a sacrificial corrosion system. This principle has been widely applied in the automotive industry where stainless steel clad aluminum trim has replaced solid stainless steel trim. As illustrated in Figure 5, the attachment of stainless steel directly to the automotive body will promote accelerated corrosion of the body steel. Conversely, as shown in Figure 6 the aluminum

cladding protects the automotive body from corrosion, by corroding preferentially to both the steel and the stainless steel, thereby extending the life of the vehicle.

Solid aluminum trim could provide similar corrosion protection of the body steel, but aluminum itself is far less corrosion resistant than stainless steel, and would rapidly oxidize, detracting from the vehicle's appearance.

3. By cladding a less noble layer over a more noble layer, a corrosion barrier is formed where the more noble inner layer begins to corrode only after the outer layer has been extensively corroded. By designing sufficient mechanical strength for the application into the inner layer, a material system has been created that greatly exceeds the corrosion resistance of the individual components.

A clad system of carbon steel clad to both sides of a core of stainless steel for automotive brake tubing demonstrates this corrosion barrier mechanism. Figure 7 compares the corrosion behavior of carbon steel tubing and carbon steel clad stainless steel tubing. While the conventional terne coated carbon steel tubing deteriorates rapidly due to localized corrosion, the corrosion in the clad tubing is arrested at the stainless steel layer due to the galvanic protection provided by the carbon steel.

4. As an insert between dissimilar metals, a clad transition material eliminates the opportunity for destructive corrosion at the joint. It also simplifies attachment by welding. The joining of aluminum to steel, difficult by welding and doomed to crevice corrosion failure, can be

accomplished by placing an insert of aluminum clad steel. The aluminum component is welded to the aluminum layer and the steel is welded to the steel layer. The presence of the metallurgical bond eliminates the opportunity for crevice corrosion.

5. For a material system to withstand differing corrosive environments on each side of a strip requires a monometal or alloy to resist the corrosive effects of both environments. An alternate approach is to develop a clad metal system with each layer designed to resist the corrosive effects of the individual environment.

An example of a complex multilayer clad system has been developed for anode caps for battery button cells. The inner copper layer is compatible with the internal chemistry of the battery cell while the outer nickel layer resists the corrosive effects of the external environment. The middle stainless steel layer provides the formability and mechanical strength.

As illustrated in Figure 8, another example is a three-layer system of titanium clad copper clad nickel for a bipolar electrode in fuel cells. The nickel is required for its resistance to hydrogren permeability on the cathode side. The highly corrosive environment necessitates titanium on the anode side. The copper core is required for its thermal and electrical conductivity to carry electrical current and dissipate heat.

Through appropriate design, the five clad metal approaches to corrosion control described above can greatly extend the useful

life of end products. This extended life itself can have dramatic reduction in the demands for critical materials.

Clad Metal Design for High Performance

In a similar fashion to corrosion control with clad metals, the combination of materials into a clad metal system can often result in a unique combination of physical properties or properties that might otherwise be achieved only through the use of expensive or critical materials. Properties, such as strength, ductility, electrical and thermal conductivity, thermal expansion, magnetism, and surface appearance can be tailored to a specific requirements in a clad metal system with exacting precision.

A key tool in the development of clad metal sytems is the rule of mixtures, which is a series of calculations used to determine the new composite's properties, based upon the known properties of the individual metals. The rule of mixtures equation can provide a good approximation of the composite's properties in order to narrow the field of potential clad metal systems during the design phase, without actually fabricating the composite.

The general equation which can be applied to calculate properties such as density, lateral thermal conductivity, electrical conductivity, and thermal expansion through the thickness of the composite is shown below:

$$D = \frac{A_1 \times D_1 + A_2 \times D_2 + \ldots . An \times Dn}{100}$$

Where A_1, A_2, etc., are the thicknesses, in percent, of the

components of the clad metal.

D_1, D_2, etc., are properties of the same components.

Properties such as thermal conductivity normal to the surface, thermal expansion along the length, and modulus of elasticity can be calculated with different equations. For fatigue and mechanical strength properties, testing of actual sample specimens or prototypes is recommended.

1. An example of functional benefits offered by a precision clad metal is high thermal and electrical conductivity copper clad to both sides of a low thermal expansion rate 64% iron-36% nickel alloy known as Invar. As illustrated in Figure 9, it is being successfully applied as a printed wiring board core material for direct surface mounting of ceramic chip carriers.

In order to achieve more dense electronic packaging, ceramic chip carriers were developed to replace the existing dual inline packages (DIP), thereby reducing component area by factors of 2-5:1. Because the solder joint is both the mechanical and electrical attachment medium for these components, an exact match is required in thermal coefficient of expansion (TCE) between the ceramic chip carrier and the printed wiring board. This is especially critical when wide operating temperatures are encountered such as in military, automotive, and telecommunication applications. Also, the greater packaging density achievable with chip carriers can generate more heat per unit area, which needs to be dissipated to prevent high temperature failure of the integrated circuit. Additionally, strength,

stiffness, and flatness are key criteria in selection of a printed wiring board material system.

Unlike other material systems, copper clad Invar offers a combination of properties that allow the electronics packaging engineer to achieve all the required performance levels. Copper clad Invar is now being designed into applications which had previously utilized cobalt-containing Kovar due to its low thermal expansion rate. With copper clad Invar, it is possible to achieve a thermal expansion rate comparable to Kovar as well as superior thermal and electrical conductivity properties. Figure 10 compares the thermal properties for copper clad Invar to other printed wiring board materials.

2. Another example of the synergistic attributes of clad metals is the application of stainless steel clad aluminum for aircraft firewalls. Titanium had been considered due to its excellent strength-to-weight characteristics and its high temperature performance. However, titanium's cost and availability make it an undesirable choice.

Stainless steel clad aluminum provides strength-to-weight properties similar to that of titanium and has passed the stringent FAA flame test (15 minutes at 2000°F). Best of all, this material is readily available at a fraction of the cost of titanium.

3. Another high performance clad metal system is copper clad to both sides of a ferritic stainless steel core for integrated circuit lead frames. Copper clad stainless steel lead frame material has the ductility and strength

equivalent to or better than the traditional lead frame material, Alloy 42 (nickel-iron alloy), yet provides six times the thermal conductivity of Alloy 42.

With integrated circuit devices becoming increasingly complex, they need improved thermal dissipation to avoid high temperature failures. The copper layer provides the excellent lateral thermal conductivity while the stainless steel layer provides the strength and ductility. Copper alloys, which are also being used in high power IC devices, have marginal mechanical properties for many lead frame applications.

4. Heat exchangers for industrial and transportation applications have traditionally been made by inserting copper shims between the structural layers and furnace brazing the entire assembly. The approach can be highly labor intensive in compactly designed units and can also lead to defective braze joints due to improper location of the copper shims. As illustrated in Figure 11, the clad metal approach utilizes a composite of copper clad to both sides of a core of carbon steel or stainless steel. The copper acts as the brazing alloy and thus eliminates the cost of manufacturing and handling the copper shims. The clad metal system also ensures a sufficient presence of copper for requisite braze joint strength.

Application of Clad Metals for Critical Material Conservation

New alloy development, which holds promise in reducing dependence upon materials such as chromium, cobalt, manganese, and titanium, requires up to ten years and often increases

material cost or reduces performance.

Innovative design and application of clad metal systems can sharply reduce the demand for critical material without sacrificing performance and cost. Additionally, clad metal development can take as little as one year. In most cases, readily available materials can be combined into clad metal systems that yield unique functional properties and corrosion control capabilties.

When the U. S. Mint was searching for alternate material systems to silver bearing coinage, cupronickel clad copper clad cupronickel was developed in approximately one year. Furthermore, the clad coins met strict Mint requirements for corrosion resistance, formability, appearance, abrasion resistance, Rho density, reclaimable scrap, and availabilty.

Innovative design and production of clad metals have resulted in widespread use in numerous industrial and consumer applications. The capability to engineer a clad metal to operate in hostile, corrosive environments and meet exacting performance requirements can be readily applied to the conservation of critical materials. Our engineering community, designing tomorrow's products, must include potential clad metal systems early in the design and evaluation phase of these new products. When designed in from the beginning, the full payback in terms of material conservation, optimal performance, and inherent corrosion control can be achieved through clad metal technology.

Many engineers, unaware of the large volume availability and advanced technology of clad metals, do not consider clad metal systems but specify alloys that consume large amounts of critical

materials. Often design engineers make trade-offs among engineering properties by accepting some properties that are marginal to retain other more critical properties, or by overdesigning the entire system often using critical materials. This overuse or misuse of materials can led to marginal performance of the end product, shortened life in the operating environment as well as increased cost.

An example of this is the use of Kovar (17% Co/29% Ni/ balance Fe) in numerous electronic components utilizing glass-to-metal seals due to its low TCE and glass-matching capability up to 450°C. Kovar, however, is extremely costly, consumes precious cobalt, and is a poor thermal conductor. Copper clad Invar offers a similarly low TCE through 225°C, improved thermal conductivity, a solderable surface, and eliminates the consumption of cobalt. Process modifications to allow copper clad Invar usage might necessitate a shift to a solder seal approach to accommodate the transition of Invar to a higher expansion rate at 225°C. However, it is these kinds of process changes that can reduce demand for critical materials with the added benefit of reducing cost.

Summary

Material conservation begins with the product design and evaluation stage. The design engineer must comprehend not only the initial product design but also its life cycle-performance requirements. The design engineer must seek innovative designs and processes that reduce dependence upon critical materials. The competitive marketplace demands such innovation; the motivation is lower cost as well as improved performance.

COMPARATIVE QUALITIES OF CLAD VERSUS ELECTROPLATED COATINGS

Clad Laminate

Advantages

Clad layers have low porosity.

- Composition is precisely controlled.
- Alloys and active metals (Al, Ti, etc.) can be clad.
- Thickness of cladding is continuously variable and precisely controlled.
- Properties do not vary with cladding thickness.
- Complex, multilayer systems can be produced.

Limitations

- Fabricated parts cannot be clad.
- Cut edges may require special treatment.
- Brittle metals cannot be clad.
- Width of stock is limited.

Electroplate

Advantages

- Fabricated parts can be plated.
- Brittle materials can be plated.
- Finish brightness can be controlled.
- Selective areas can be plated.

Limitations

- Deposited metal may be porous.
- Codeposition (with S, H_2, etc.) is common.
- Active metals (Al, Ti, etc.) cannot be deposited.
- Substrates with stable oxides cannot be plated.
- Thickness is limited by plating time.
- Properties can vary with plating thickness.
- Thickness and uniformity can vary.

Figure 1

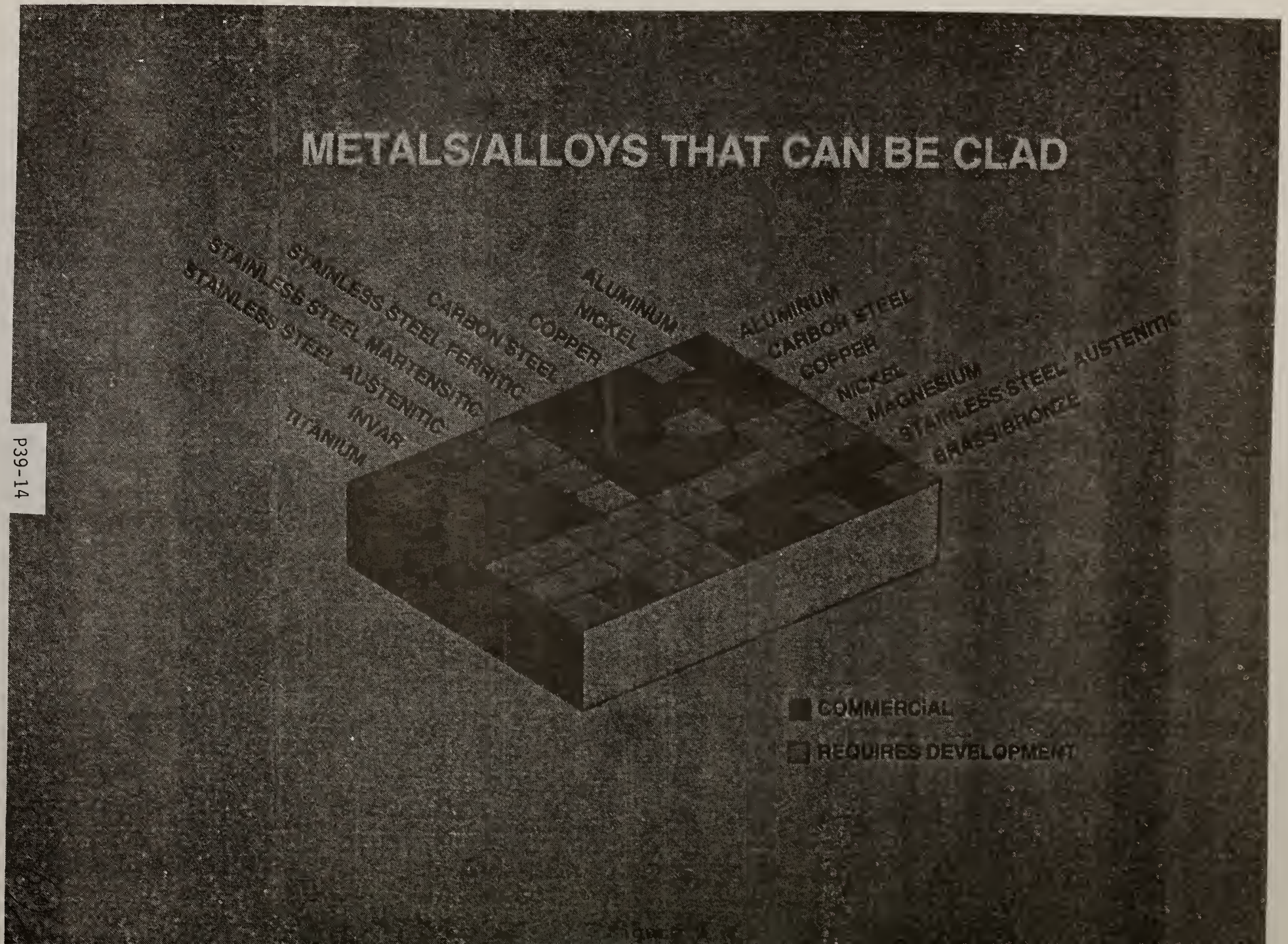
METALS/ALLOYS THAT CAN BE CLAD
STAINLESS STEEL MARTENSITIC
STAINLESS STEEL FERRITIC
STAINLESS STEEL AUSTENITIC
CARBON STEEL
INVAR
COPPER
TITANIUM
ALUMINUM
NICKEL
ALUMINUM
CARBON STEEL
COPPER
NICKEL
MAGNESIUM
STAINLESS STEEL AUSTENITIC
BRASS/BRONZE
COMMERCIAL
REQUIRES DEVELOPMENT

GALVANIC SERIES IN SEAWATER

NOBLE END

Platinum
Gold
Silver
Titanium
316 Stainless Steel (passive)
304 Stainless Steel (passive)
410 Stainless Steel (passive)
Nickel (passive)
Cupronickel
Bronzes
Nickel (active)
Tin
Lead
316 Stainless Steel (active)
304 Stainless Steel (active)
Lead-Tin Solder
410 Stainless Steel (active)
Cast Iron
Steel
Cadmium
Aluminum
Zinc
Magnesium

ACTIVE END

Figure 3

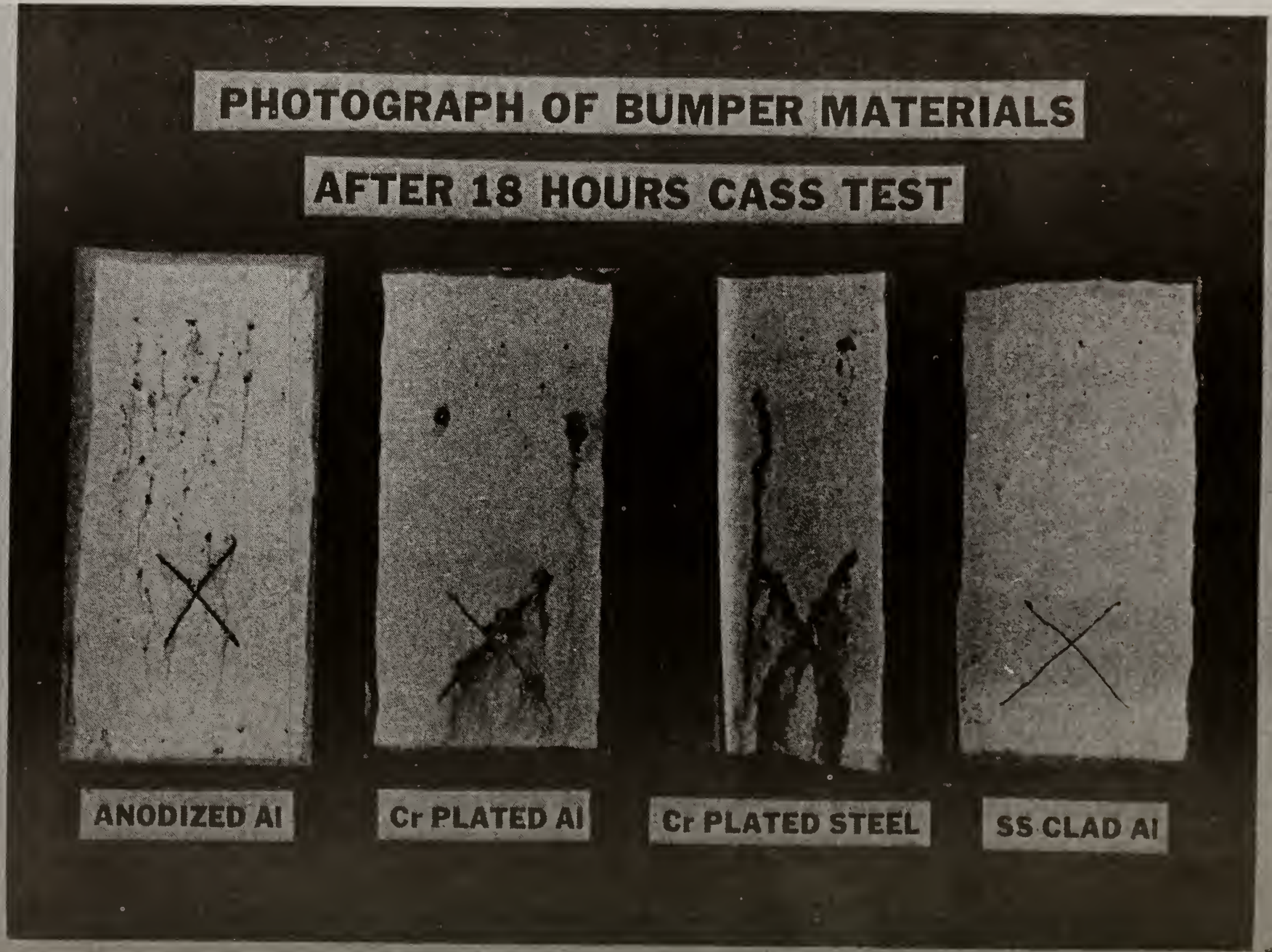

P39-16

Figure 4

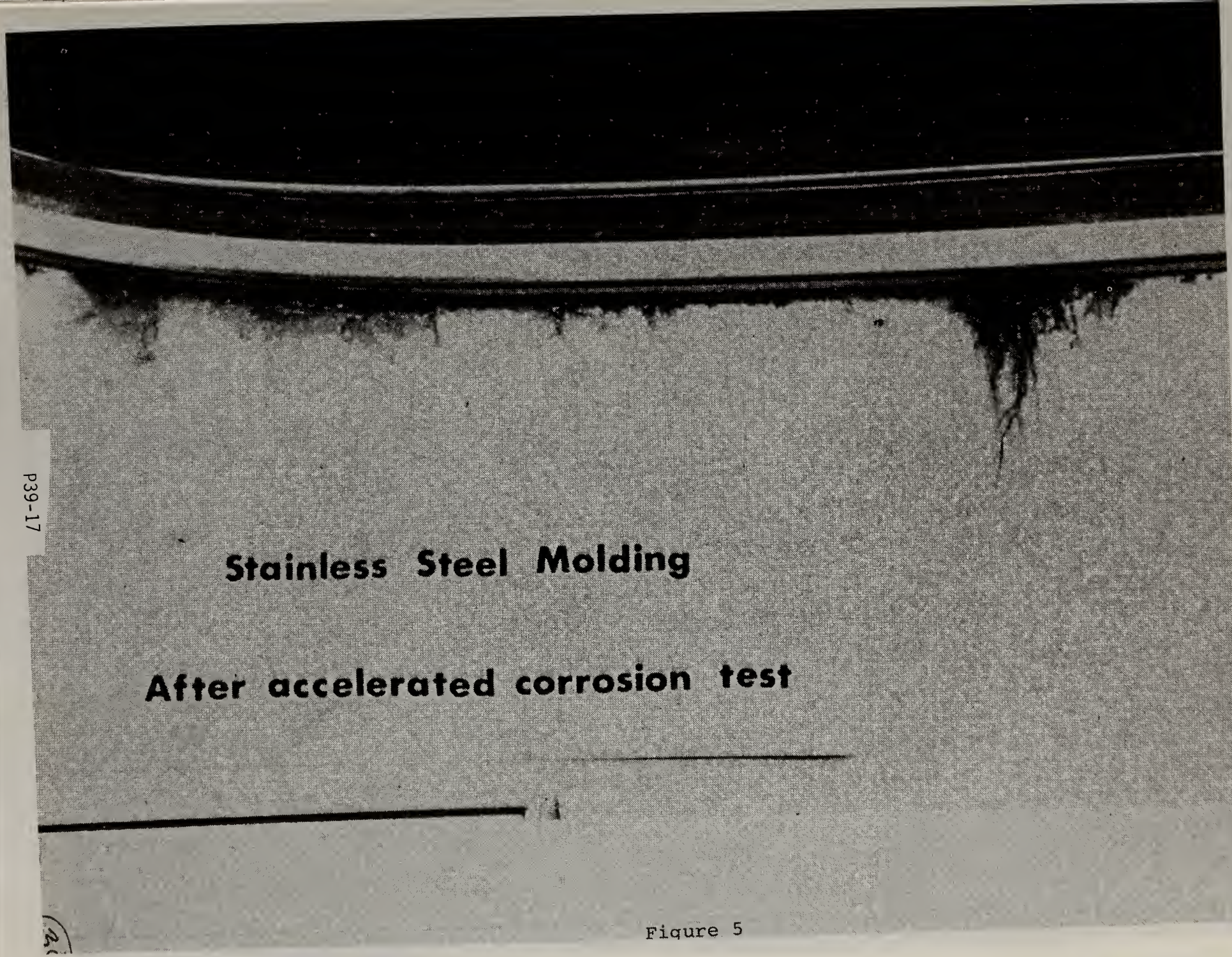

P39-17

Figure 5

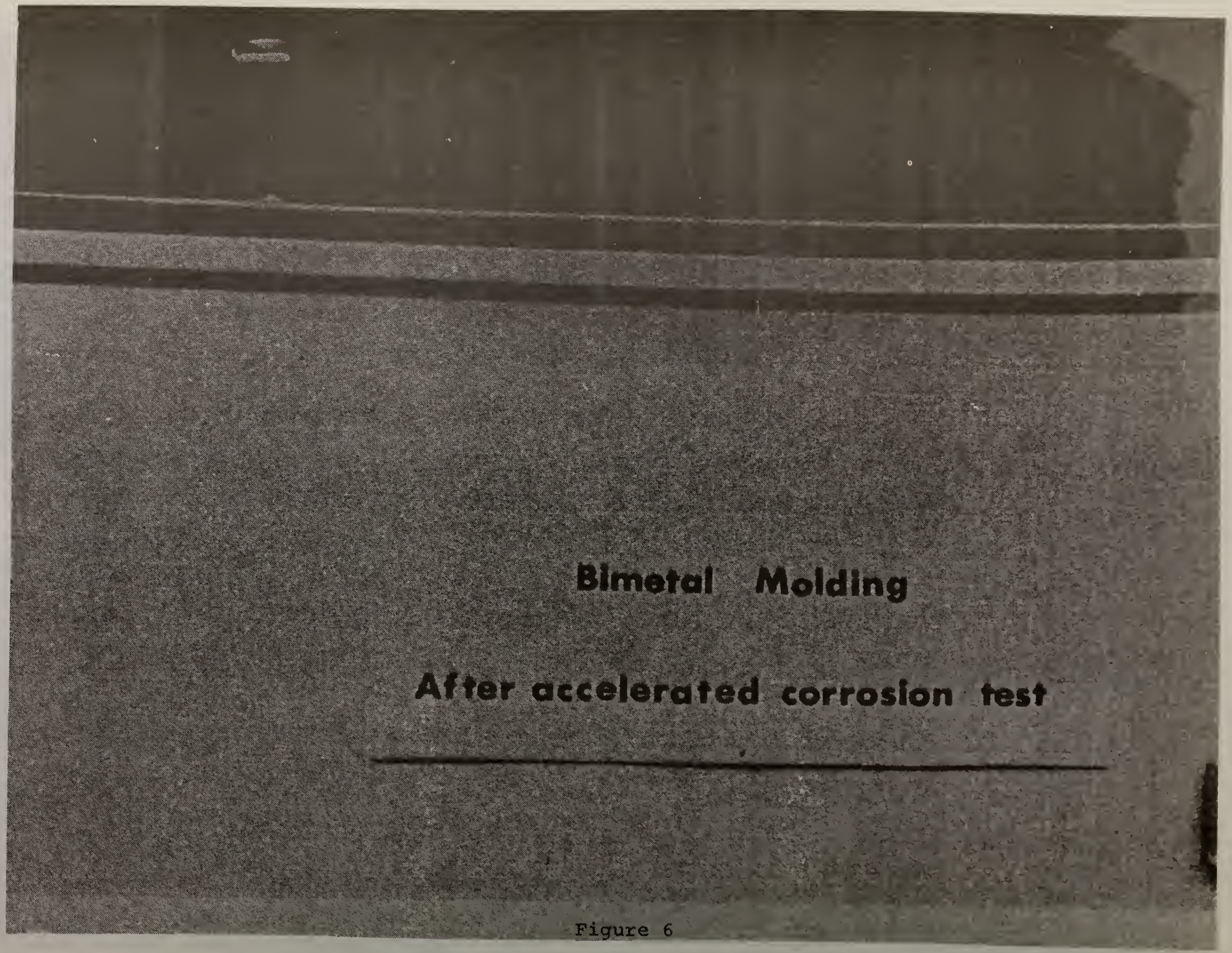

Figure 6

CYCLIC IMMERSION (DIP AND DRY) CORROSION TEST OF BRAZED AND TERNECOATED BRAKE LINE TUBING IN SIMULATED ROAD SALT ENVIRONMENT

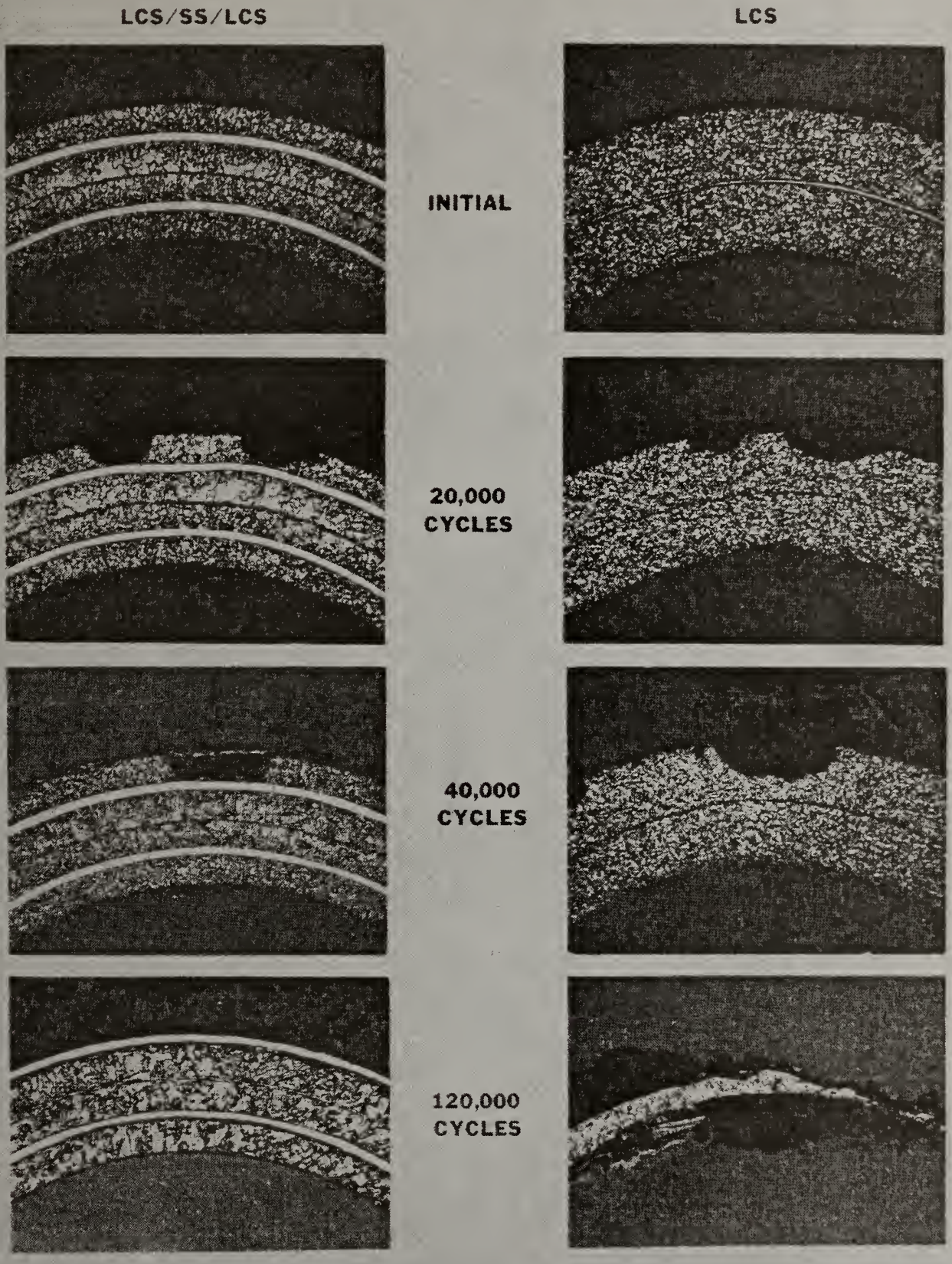

Figure 7

PHOTOMICROGRAPH OF CROSS SECTION (75 X) OF TITANIUM/COPPER/NICKEL BIPOLAR ELECTRODE MATERIAL

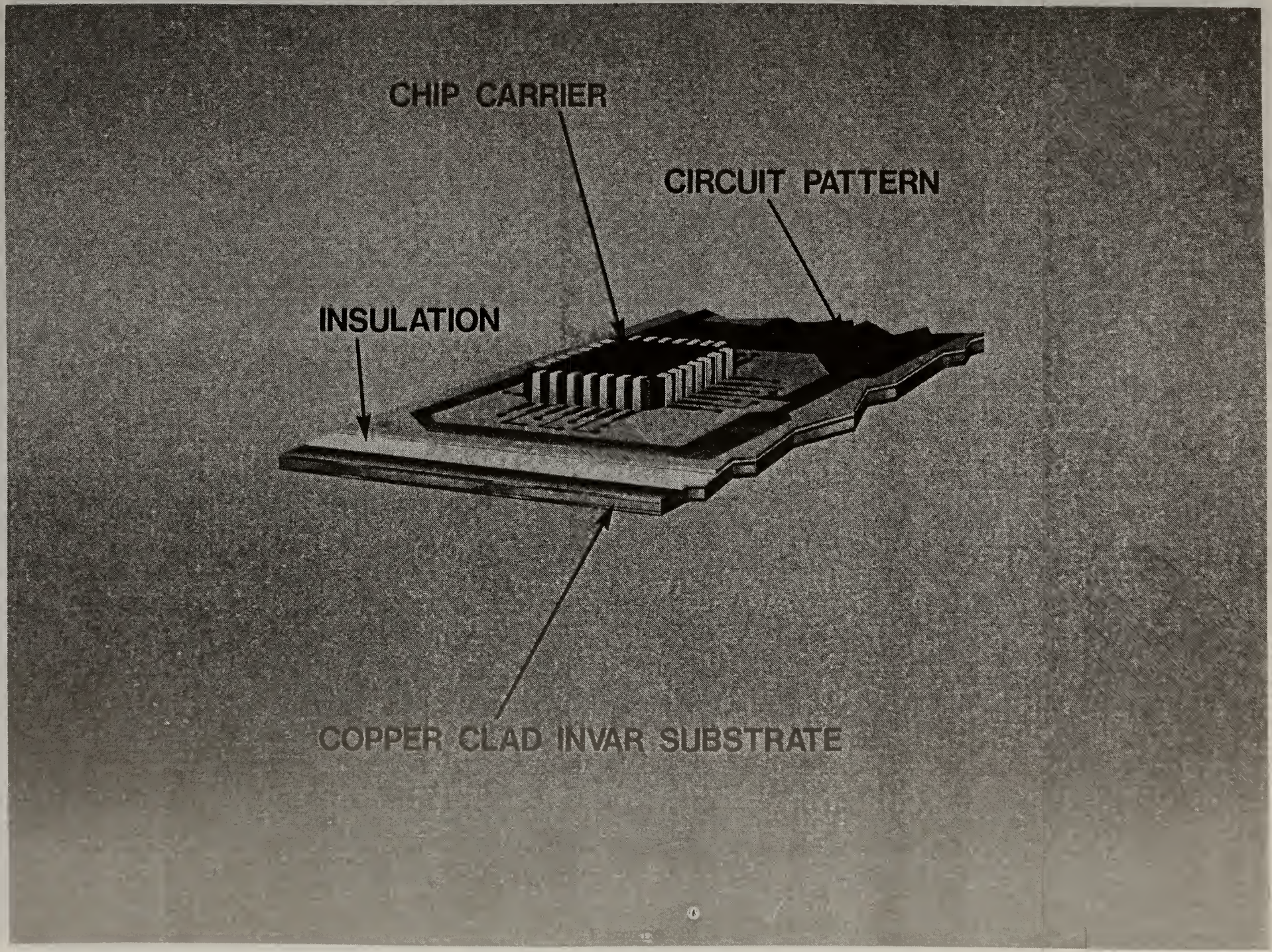
CHIP CARRIER
CIRCUIT PATTERN
INSULATION
COPPER CLAD INVAR SUBSTRATE

THERMAL PROPERTIES OF COPPER CLAD INVAR

SUBSTRATE MATERIAL	THERMAL CONDUCTIVITY (BTU/H/FT²/(°F)/FT)	TCE (IN./IN./°C X10⁻⁶)
CDA 101 COPPER	226	17.3
99.5% BeO	120	6.4
6061 ALUMINUM	110	23.6
COPPER CLAD INVAR	76*	6.4
LOW CARBON STEEL	27	12.0
94% ALUMINA	10.4	6.4
ALLOY 42	8.8	5.3
KOVAR	8.2	5.9
EPOXY-GLASS	0.2	15.8

*LATERAL CONDUCTIVITY

Figure 10

HEAT EXCHANGER MATERIAL

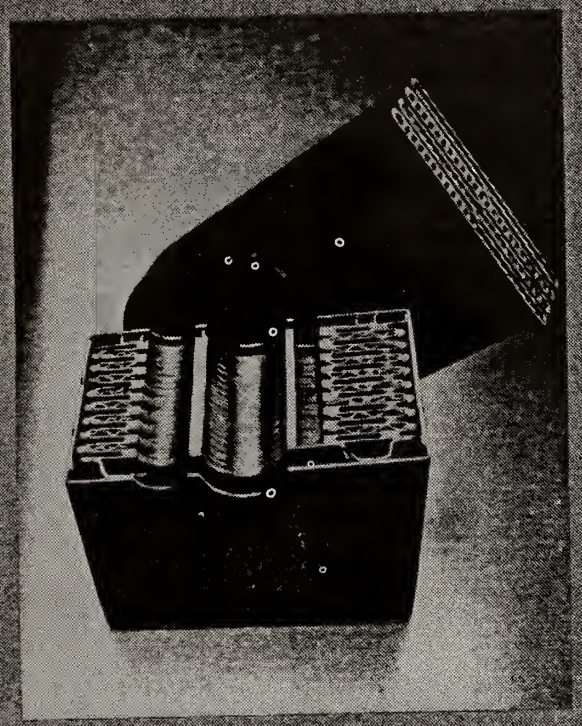

- JOINABILITY
- STRENGTH
- MANUFACTURING COST REDUCTION

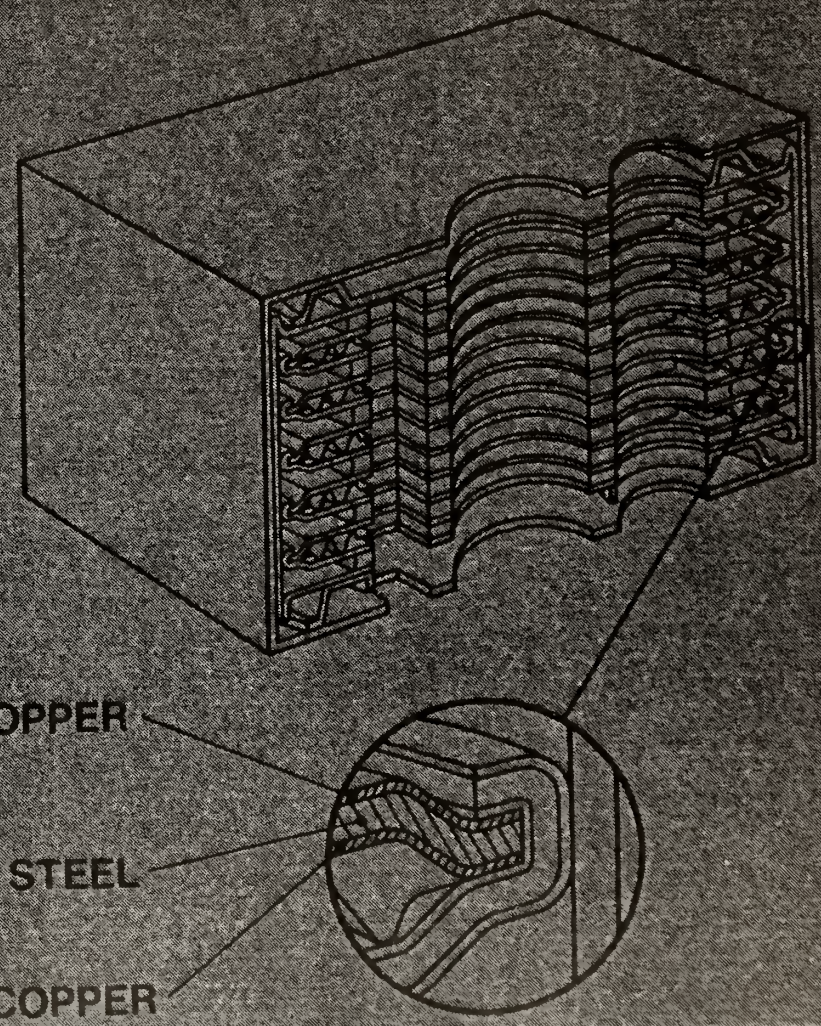

Figure 11

References

1) Hodesblatt, S., Alternatives to Strategic Materials, Design Engineering, January, 1982, pp 44-49

2) Dance, F.J., Clad Metal Circuit Board Substrates for Direct Mounting of Ceramic Chip Carriers, Electronic Packaging and Production, January, 1982

3) Dance, F.J., Mounting Leadless Ceramic Chip Carriers Directly to Printed Wiring Boards - A Technology Review and Update, Nepcon West, February 24, 1982

4) Bowers, E. W., the U.S. Engaged in Another Kind of War - Strategic Minerals, Iron Age, April 14, 1982, pp 38-41

5) Hurlich, A., Strategic Materials - Technology Trends, Mechanical Engineering, July, 1982, pp 44-53

6) Baboian, R., Designing Clad Metals for Corrosion Control, SAE Trans., 81, pp 1763, 1973

7) Baboian, R., Clad Metals in Automotive Trim Applications, Paper 710276 SAE Automotive Engineering Congress, January, 1971

8) Baboian, R., Corrosion Resistant, High Strength Clad Metal System for Hydraulic Brake Line Tubing, SAE Trans., 81, pg 1117, 1973

9) Baboian, R., and Haynes, G., Joining Dissimilar Metals with Transition Materials, paper 760714, SAE Automotive Engineering Congress, January, 1976

10) Baboian, R. and Haynes, G., Corrosion Barrier Materials for Communication Industry, Materials Performance, 16, pg 30, 1977

11) Baboian, R., Controlling Galvanic Corrosion, Machine Design, October 11, 1979

12) Delagi, R., Designing with Clad Metals, Machine Design, November 20, 1980

13) Regan, R., Metals Industries Waiting for Reagan's Minerals Policy, Iron Age, December 16, 1981, pp 31-33

14) Cassidy, R., Strategics: The New Gold?, Sky, August, 1981, pp 10-16

15) Baboian, R., Clad Metals Respond to a Changing Automotive Environment, Body Engineering, pp 69-74, Spring, 1981

16) Verink, E.D., Our Next National Crisis: Materials, Mechanical Engineering, pg 42, August, 1980

17) Baboian, R., Conservation of Critical Materials with Clad Metal Systems, Electrochemical Society Transactions

18) Gomez, P. J., A Systems Approach to the Economic Use of Natural Resources, Wire Association Convention, October, 1966

19) Quimby, W. G., Production Methods, Properties and Applications for Clad Metals, American Society for Metals Meeting, March 21, 1979

Autobiography

James T. Skelly is a graduate of the University of Rhode Island where he received his B.S. in Industrial Engineering. He also has an MBA from Northeastern University. He has been employed by Texas Instruments in finance, production control in the Control Products Division, and automotive program manager for the Metallurgical Materials Division. Jim is currently product manager in the Metallurgical Materials Division.

ABSTRACT

It has long been known that carbon steel exposed to geothermal brine is aggressively attacked and large corrosion allowances must be made in the design of vessels and piping used in such environments. The economics of geothermal power presents a real need for the use of functional low-cost materials as liners for exposed carbon steel surfaces.

Polymer concrete (PC) has been identified as a promising liner material. PC is defined as a concrete in which the aggregate is bound in a dense matrix with a polymer binder. Several high-temperature PC systems have been formulated and tested in the laboratory in brine, flashing brine, and steam at temperatures up to 260°C. Results are also available on field exposures lasting up to 36 months from at least one of six geothermal test sites. Good durability is indicated in all tests.

A study has indicated that the use of PC liners as a replacement for the corrosion allowance in carbon steel components for a 50-MWe geothermal plant will reduce the cost of electrical generated power by ~6.2 mills per kilowatt hour.

INTRODUCTION

The demand for the development of geothermal energy increased as the transitory era of cheap imported fuel came to an end. The constant increase in global energy consumption has made even greater demands for the production of a cheaper energy source.

One such source being investigated is the extraction of heat energy from the earth, i.e., geothermal energy. Worldwide commercial utilization of geothermal energy was reported to be over 7000 megawatts in 1979.[1] A 1980 survey performed by EPRI indicated that current geothermal electricity generation in North America was 663 megawatts and projected a growth to about 10,000 megawatts by the year 2000. In addition, potential direct utilization of geothermal energy by a wide range of industries was also indicated.[2]

The development of geothermal energy has encountered some serious technical problems in the handling of hot brine and steam. Hot brine and other aerated geothermal fluids are highly corrosive and they chemically attack most conventional construction materials. Corrosion and scale encrustations have been encountered in all geothermal plants, and to various degrees they adversely affect plant lifetimes and power output. To date, carbon steel has been the primary material of construction but the use of expensive materials such as chrome-moly steel and titanium base alloys may be required for long term operation. Corrosion studies of several different steels exposed to high-temperature geothermal brines were made by the Lawrence Livermore Laboratory at the Salton Sea Geothermal Field.[2] Six-month exposure studies indicated corrosion rates of 1.65 mm/year for mild steel (AISI-1009) while chrome-moly steel (ASTM-A387-9) had a corrosion rate of 0.13 mm/year. Chrome-moly steels, however, cost about four to six times as much as the carbon steels, thereby substantially increasing plant construction costs.

The availability of low-cost materials with suitable properties will enhance the development of a stable geothermal industry. Brookhaven National Laboratory (BNL) under contract tc the Department of Energy (DOE) has been developing non metallic construction materials suitable for use with geothermal fluids. Calculations indicate that if successfully implemented, the use of materials such as polymer concrete (PC) in geothermal electrical generating processes could result in a 10 to 20% cost reduction. On the basis of projections of USA direct utilization applications by the year 2000, energy cost savings equivalent to an annual saving of $\$50 \times 10^6$ to $\$300 \times 10^6$ have also been estimated.

Development of non metallic construction materials for use in geothermal systems was initiated in the early 70s. Since that time, several high-temperature PC systems have been formulated. Laboratory and field tests have been performed in brine, flashing brine, and steam at temperatures up to 250°C. Laboratory data for exposure times of up to 2 years are available. Field test data from six geothermal sites with exposures of up to 3 years are also available. Durability of the PC has been good in almost all cases. The results to date have indicated the potential for the successful use of a specially formulated PC as a lining material for process piping and vessels in geothermal power systems. PC glass filament wound pipe, with low thermal conductivity, can be made for process heat and district heating applications.[3]

Economic studies performed concurrently with the research program have identified several cost-effective uses for PC in geothermal processes. One study has indicated that the use of PC liners as a replacement for the corrosion allowance in carbon steel components for a 50-MWe geothermal plant will reduce the cost of power by ~6.2 mills per kilowatt hour. Greater savings are indicated if PC is substituted for stainless steel, titanium, or Hasteloy in acid-handling systems, condensate-piping systems, reinjection lines, and steel separators. Uses in cooling towers, district heating systems, and the protection of concrete surfaces also appear to be cost effective.

PRODUCTION METHODS

Polymer concrete is defined as a concrete in which the aggregate is bound in a dense matrix with a polymer binder. The techniques used for mixing and placement are similar to those used for portland cement concrete, and after curing a high-strength durable material is produced. The most important process variables are monomer and aggregate composition and the aggregate particle-size distribution. Specimens can be produced with compressive strengths up to 207 MPa. Full strength is attained immediately after the polymerization reaction is completed. Polymerization can be accomplished with initiators and promoters at ambient temperatures or with initiators in conjunction with heat. Combinations of both methods are also used to ensure complete polymerization of the monomers used.

A. Monomer Formulations

Several monomer systems that can be used in high-temperature PC formulations have been developed. Some of these will be briefly reviewed. Long-term test data are available for the following systems:

1. 60 wt% styrene, 40 wt% trimethylolpropane-trimethacrylate (TMPTMA)
2. 50 wt % styrene, 33 wt% acrylonitrile, 17 wt % TMPTMA
3. 55 wt % styrene, 36 wt % acrylonitrile, 9 wt % TMPTMA

These systems can be polymerized using chemical initiators (benzoyl peroxide, di-tert-butyl peroxide) and heat or by chemical initiators (benzoyl peroxide) and promoters (dimethyl aniline). The styrene-TMPTMA mixture is suitable for the manufacture of PC which is stable to 150°C, while the last two systems can be used at temperatures up to 250°C.

B. Aggregate Selection

The durability of PC to geothermal fluids is highly dependent upon the composition of the aggregate. Materials such as quartz, silica, flyash, and portland cement have been investigated. All of the aggregates have

been used successfully in materials at temperatures <210°C. Above this temperature, only PC materials containing a mixture of silica sand and portland cement have been durable when subjected to brine and steam.

Experimental work at BNL indicated that composites formed with a monomer system containing styrene(S), acrylonitrile (ACN), and TMPTMA, in conjunction with an aggregate system containing silica sand and portland cement (10 to 40% by weight of aggregate mixture), were stable in 25% brine solutions and steam at temperatures up to 250°C. Bonding of the monomers to the silica sand was enhanced by the use of a silane coupling agent. It was also observed that Type III portland cement gave better results than Type I or IV. This led to the belief that a bond was formed with the vinyl monomers and the tricalcium silicate (highest in Type III cement) which resulted in increased thermal and chemical stability.[4,5] Later experimental work at BNL verified that a bond does exist between vinyl-type monomers and the cement phase;[6] thus cement-containing PC would be expected to have higher thermal stability and long-term durability.

The compressive strengths of PC specimens tested at the Geysers, California (Figure 1), and duplicated in laboratory autoclave tests show that they decay for the first 30 to 60 days and then remain constant. Test data have been collected for periods up to 2 years, and some of the data are given in Table 1. Additional data collected from specimens exposed to 25% brine solutions at 177°C in laboratory autoclaves are given in Table 2. The data indicate that the strengths of the samples are essentially constant after the first 60 days of exposure, with samples containing acrylonitrile having higher compressive strengths.

C. Manufacturing

PC-lined pipes were manufactured at BNL and installed at the U.S. Bureau of Mines Corrosion Facility at Niland, California, in the Salton Sea geothermal field. This is considered to be the most aggressive corrosive fluid known to date. It contains 280,000 ppm dissolved solids in the brine at wellhead temperatures of 240° to 260°C. The lined pipe was installed in

the inlet line of the corrosion facility and was in continuous service for 3 months (Figure 2). The pipe was 1.2 m long and had an inside diameter of 7.6 cm.

The liner was made of PC containing 55 wt% S, 36 wt% ACN, 9 wt% TMPTMA. The aggregate system was 70 wt% graded silica sand, 30 wt% Type III portland cement. The inside of the steel pipe was sandblasted to remove any scale and/or rust. The inner core was made of rubber (7.6 cm diam) and installed in the center of the steel pipe to leave an annulus of 1.25 cm. Benzoyl peroxide 98 (1%) and di-tert-butyl peroxide (0.5%) initiators were dissolved in the monomer mixture. The aggregate system (~90%) was loaded in a Day rotating blade mixer and the monomer mixture (~10%) added. When the composite was thoroughly mixed the PC mortar was placed in the annulus while the pipe was mounted on a table vibrator. Longer or larger-diameter pipes would have additional vibrators on the pipe wall. When the annulus was filled, the PC was allowed to cure in situ. After the initial cure, the inner rubber hose was removed and the lined pipe placed in an oven at 150°to 190°C for a final cure.

Numerous steel pipes have been lined with PC and tested at various geothermal sites. Pipe diameters have ranged from 7.6 to 30.5 cm and lengths from 1.5 to 2.5 m. At East Mesa, California, PC-lined pipes (Figure 3) were in service for up to 3 years with no apparent decay.

Polymer Concrete Research, Inc. under contract to BNL has developed a centrifugal casting process that can be used for the commercial manufacture of PC-lined steel pipe.[7] A steel shell is placed in the centrifugal casting machine and using a lance the inside of the shell is cleaned by sandblasting (Figure 4). Preweighed PC batches are mixed and placed inside the pipe. End caps are attached and then the pipe is spun, first at 115 rpm to distribute the material and then at 1700 rpm for 2 minutes to compact the PC (Figure 5). One end cap is removed and any excess slurry is removed. A prelilminary cure at ambient temperature is accomplished with the end caps in place. The pipe is then placed in a hot air circulating oven (Figure 6) at 190°C and a final cure is attained in ~8 hours. The PC liner can be seen in Figure 7.

D. Materials Properties Testing

Since the steel shell of the pipe can be expected to carry all or most of the mechanical stresses, high physical strength in the PC are not of primary concern. There are several properties that PC must have to provide protection for the carbon steel shell. These include low permeability, good bond strength to the steel inner surface, good corrosion and acid resistance, and low erosion rates.

1. Permeability. Since the purpose of the liner is to provide a barrier between the geothermal fluid carried in the pipe and the mild steel shell, the permeability coefficient of the lining material is important. Studies were made on cylindrical samples 10 mm thick in the apparatus shown in Figure 8. An average permeability coefficient was calculated, using Darcy's Law, to be 22×10^{-12} cm/sec. This is about 23 times less permeable than portand cement concrete.[7]

Sections of 15.2-cm-i.d. pipe with a nominal 2.54-cm wall thickness have been cast in PC with formulations previously mentioned. Specimens have maintained fluid pressures as high as 2.75 MPa before bursting or showing any signs of leakage.[8] Attempts at measuring the permeability coefficient of centrifugally cast PC pipes have been unsuccessful because of leakage at the gaskets between the pipe ends and the fixture (Figure 9).

2. Bond Strengths. Bond strength between PC liner and the steel pipe has also been tested. Bond strengths are measured on sections of PC-lined steel pipe in a fixture as shown in Figure 10. Laboratory-cast sections have shown bond strength to average ~5.5 MPa.

Sections of a PC-lined pipe that had been exposed to the 280,000-ppm flowing brine at 235° to 250°C for 90 days at the Bureau of Mines Materials Testing Facility at Niland, California, were tested at 25°, 100°, and 200°C. The bond strengths were 10.3, 10.4, and 8.9 MPa respectively. A section of the pipe after the bond test is shown in Figure 11. The ability of the PC liner to withstand the high force required to disbond it from the

steel and the absence of salts or corrosion products on the steel are indications of the high strength and impermeability of the liner.

3. Corrosion and Acid Resistance. Testing of PC samples in the laboratory and in the field in various geothermal environments has shown the material able to withstand the most adverse conditions. Loss of strength is generally noted for 30 to 60 days, then the materials stabilize and exposures of up to 3 years in several geothermal environments indicate good durability.

The feasibility of using PC materials in high temperature - low pH environments has also been investigated. PC samples have been exposed to a pH 1 HCl solution at 90°C for more than 440 days. No evidence of deterioration of the PC as determined by weight loss or volume change has been detected. Additional tests have been conducted in an environment of pH 1 HCl at 200°C. PC samples manufactured with several monomer systems with a silica sand - portland cement aggregate system have been exposed for 180 days with no apparent deterioration (Figure 12).

4. Erosion Resistance. No definitive studies have been conducted to determine the erosion capabilities of PC. However, several PC-lined steel pipes have been exposed to flowing brine for periods of up to three years at the East Mesa geothermal site near El Centro, California. The brine flow rate was 226-302 lit/min at a temperature of 160°C. No deterioration, erosion, or scale accumulation was detected upon completion of the test.

E. Economic Assessment

The Bechtel Corporation has performed conceptual designs for two 50-MWe power plants operating on geothermal brines.[9] One plant utilized a moderate-temperature low-salinity brine as produced near Heber, California, in the Imperial Valley, and the other utilized a high-temperature, high-salinity brine as produced in Niland, California, near the Salton Sea. In both plants extensive use was made of carbon steel for vessels and

piping, with Type 316 L stainless steel or titanium used only when carbon steel was considered to be unsuitable.

Burns and Roe Industrial Services Corporation (BRISC) reviewed the two designs with the view of substituting, where possible, PC materials for the metals used by Bechtel.[10] Each plant was considered separately and estimates of cost savings which could be made in the capital cost of the two plants were calculated. The capital cost estimates covered the battery limits plants and the brine supply and reinjection costs as delineated in the report for the Heber plant. No estimate of the piping was included for the Niland plant because of the limited amount of detail provided in the original report.

In the case of the Heber plant, it was shown that a savings of ~$880,000 can be achieved, based on the equipment and lines within the battery limits, and ~$2,800,000 for brine supply and reinjection lines outside the battery limits (Table 3). In the Niland case a savings of ~$550,000 for equipment and lines within the battery limits was shown.

These savings in capital costs have a direct impact on the cost of electric power and could result in a cost reduction of 2.72 mills per kilowatt hour for the Heber plant. A similar savings is expected for the Niland plant. It was also estimated that the use of PC-lined vessels and piping would allow for an on-stream time of ~74% versus 70% using unlined carbon steel components. This higher on-stream availability could result in additional savings of ~3.46 mills per kilowatt hour. Thus a net savings of ~6.2 mills per kilowatt hour could be realized by using PC materials wherever possible.

CONCLUSIONS

1. The durability of PC in geothermal fluid environments has been demonstrated by extensive long-term tests conducted at BNL and at six geothermal sites.

2. PC may be used in the design of geothermal or saline water facilities to counter corrosion at temperatures up to 250°C.

3. The cost of PC liners in most cases is less than other alternative methods of providing corrosion protection.

4. PC, made with properly selected monomers and aggregates, can protect carbon steel surfaces at temperatures above the expected geothermal operating range and preserve structural integrity without the use of corrosion allowances.

5. The need for exotic materials such as titanium, molybdenum, or austenitic stainless steels (Type 316 L) is reduced or eliminated by using PC-lined carbon steel.

6. Material costs for vessels and piping within the Heber plant battery limits results in a 44% savings through the use of PC linings.

7. Brine supply and reinjection piping material costs can be reduced by 40% using PC linings.

8. The use of PC materials at the Heber Plant can result in a reduction in the cost of electric power production by 2.72 mills per kilowatt hour.

9. A 4% increase in on-stream availability for the Heber plant, due to the use of PC liners, will result in a net cost reduction of ~3.46 mills per kilowatt hour.

10. The reduction in capital cost and anticipated improvements in on-stream availability through the use of PC in the Heber plant will result in an overall saving of ~6.2 mills per kilowatt hour.

References

1, Anderson, David N., and Lund, John W., Editors, Direct Utilization of Geothermal Energy: A Technical Handbook, Geothermal Resources Council Special Report No. 7, ISSN 0149-8991, ISBN 0-934412-07-03, 1979.

2. McCright, R.D., Frey, W. F., and Tardiff, G. E., Localized Corrosion of Steels in Geothermal Steam/Brine Mixtures, Geothermal: Energy for the Eighties, Transactions, Volume 4, Geothermal Resources Council, ISSN 10193-5933, ASBN 0-934412-54-5, Davis, California, 1990.

3. Schroeder, J.E., Design and Fabrication of Polymer Concrete Pipe for Testing in Geothermal Energy Processes, Final Report, July 1981.

4. Kukacka, L. E., Fontana, J., Auskern, A., Concrete Polymer Materials for Geothermal Applilcations, Report No. 6, BNL 20571, July 1975.

5. Kukacka, L. E., et al., Alternate Materials of Construction for Geothermal Applications, Progress Report No. 14, BNL 50751, September 1977.

6. Sugama, T. and Kukacka, L.E., Cement and Concrete Research, Vol. 9, pp. 69-76, 1979.

7. Kaeding, A., Design and Fabrication of Polymer Concrete-Lined Pipe for Testing in Geothermal Energy Processes, Final Report, December 1981.

8. Kukacka, L.E., et al., Concrete-Polymer Materials for Geothermal Applications, Progress Report No. 9, BNL 21665, June 1976.

9. Conceptual Design of Commercial 50 MWe (net) Geothermal Power Plants at Heber and Niland, California. October 1976, Energy Research and Development Administration, Division of Geothermal Energy, SAN-1124-1.

10. Economic Assessment of Polymer Concrete Usage in Geothermal Power Plants, November 1977, Prepared by Burns and Roe Industrial Services Corporation, BNL 50777.

Table 1

Polymer Concrete Specimens Exposed to Flowing Dry Steam at 238°C at the Geysers, Calif.[A]

Exposure time, days	Monomer system, weight percent	Compressive strength, MPa
0	50 S[B]-33 ACN[C]-17 TMPTMA[D]	75
0	55 S-36 ACN-9 TMPTMA	75
60	50 S-33 ACN-17 TMPTMA	31
90	50 S-33 ACN-17 TMPTMA	30
90	55 S-36 ACN-9 TMPTMA	34
360	50 S-33 ACN-17 TMPTMA	30
360	55 S-36 ACN-9 TMPTMA	30

A) All PC specimens contained an aggregate system composed of 90 wt% silica sand-10 wt% Type III portland cement.

B) S = styrene monomer.

C) ACN = acrylonitrile monomer.

D) TMPTMA = trimethylolpropane - trimethacrylate cross-linking agent.

Table 2

Compressive Strength of PC After Exposure to 25 percent Brine at 177°C

Exposure time, days	PC No. 1 Compressive strength, MPa	PC No. 2 Compressive strength, MPa
0	66	75
63	31	48
142	27	42
280	30	52
466	30	52
960	34	50

PC No. 1 60 wt% styrene - 40 wt% TMPTMA.
PC No. 2 50 wt% styrene - 33 wt% acrylonitrile - 17 wt% TMPTMA.
Aggregate, 90 wt% silica sand - 10 wt% Type III portland cement.
Specimen size, 19 mm diam x 38 mm long.
Strengths measured at 20°C.

TABLE 3

SAVINGS WITH POLYMER CONCRETE

	ORIGINAL METAL	POLYMER CONCRETE	SAVINGS	% REDUCTION OR SAVINGS
BATTERY LIMITS				
EQUIPMENT				
FLASH TANKS	561,610	90,548	471,062	83.9
EJECTORS AND CONDENSERS	18,634	20,206	-1,572	-8.4
VENT SCRUBBER	11,019	5,784	5,235	47.5
SUB TOTAL	$ 591,263	$ 116,538	$474,725	$80.3
LINES	1,408,112	1,001,763	406,349	28.9
TOTAL B.L.	$1,999,375	$1,118,301	$881,074	$44.1
OUTSIDE BATTERY LIMITS				
BRINE SUPPLY LINES	$1,090,080	$ 713,028	$ 377,052	$34.6
BRINE REINJECTION LINES	6,134,860	3,654,187	$2,480,673	40.4
TOTAL O.B.L.	$7,224,940	$4,367,215	$2,857,725	$39.6
GRAND TOTAL	$9,224,315	$5,485,516	$3,738,799	$40.4

List of Figures

FIGURE 1

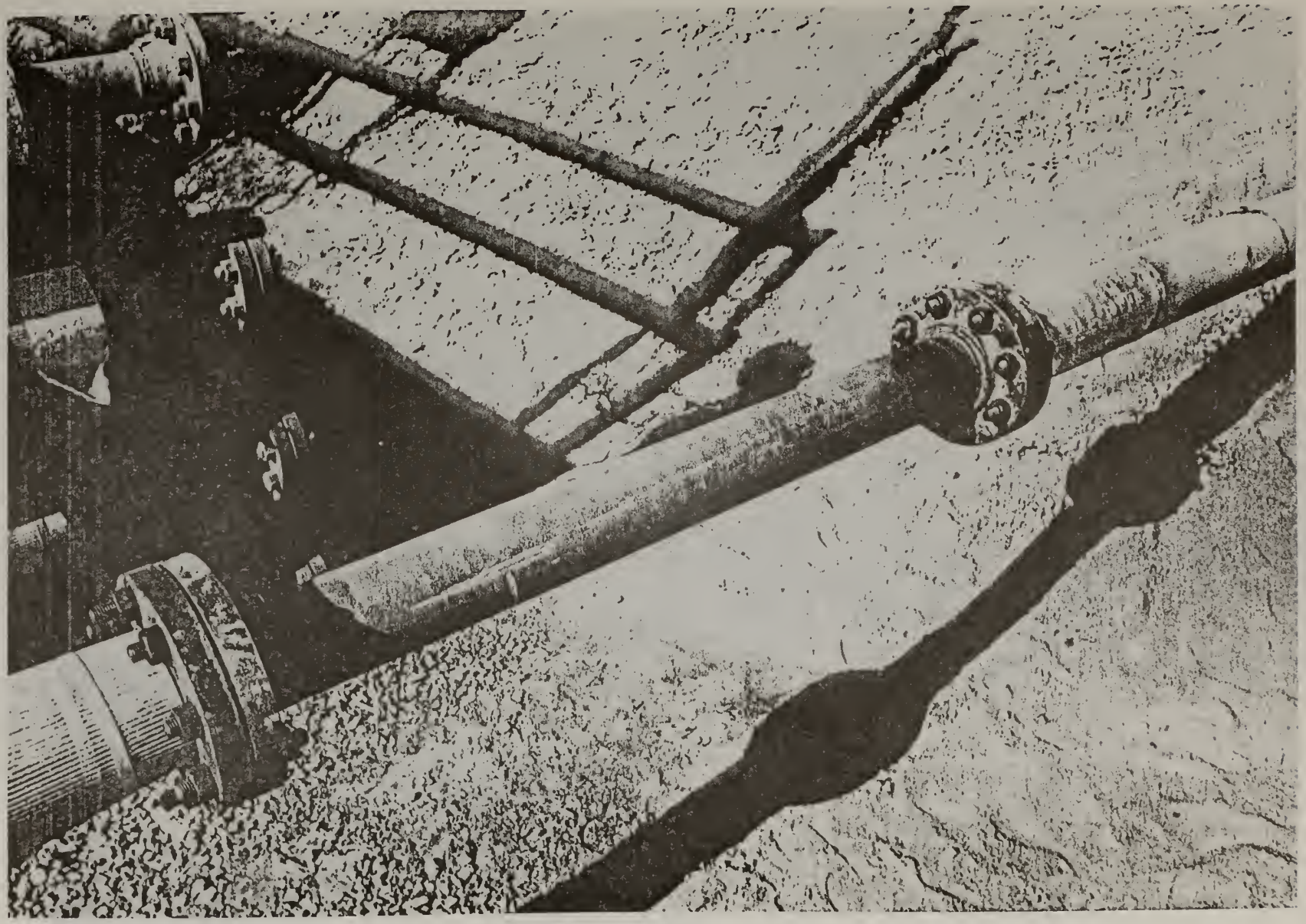

FIGURE 2

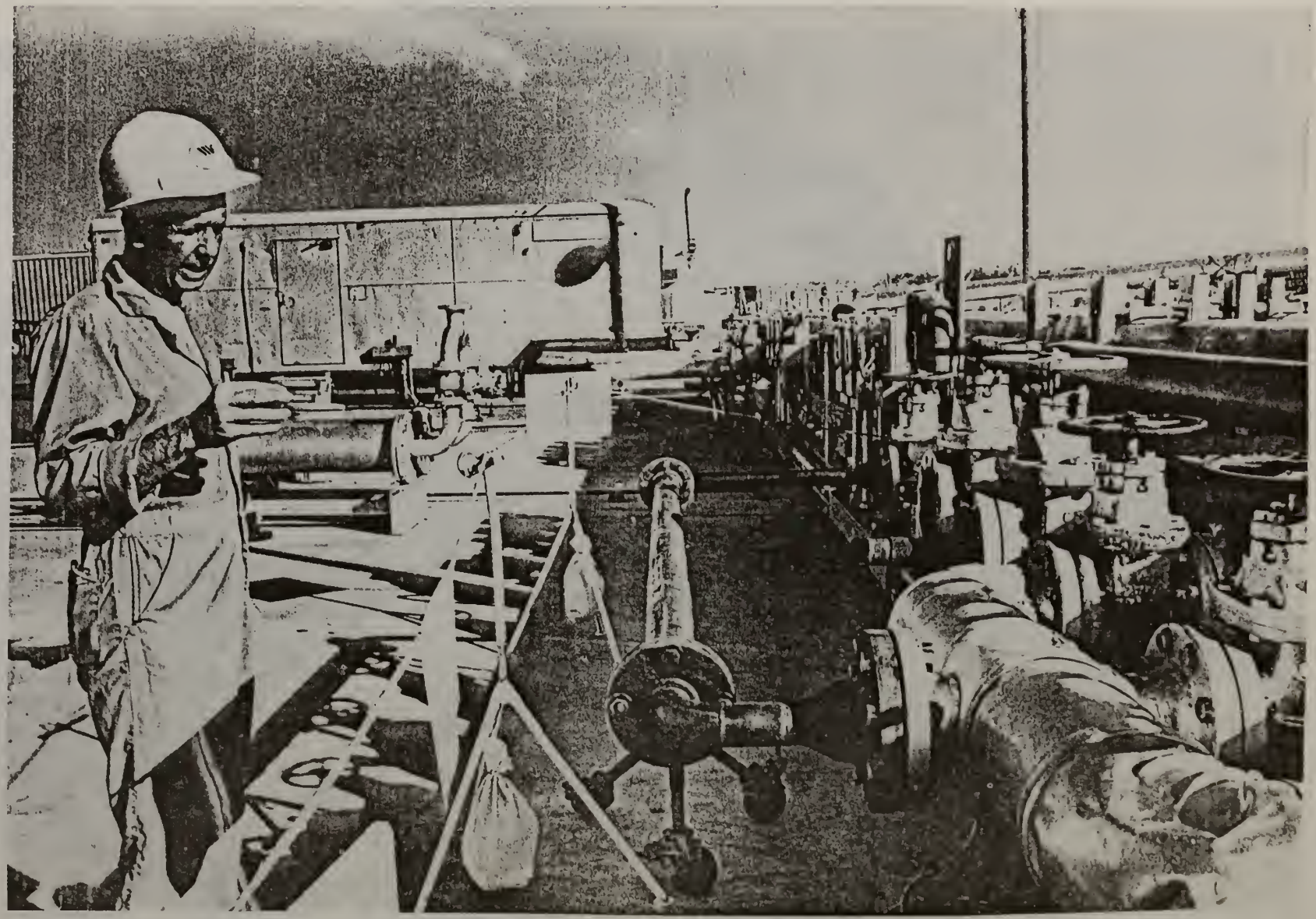

FIGURE 3

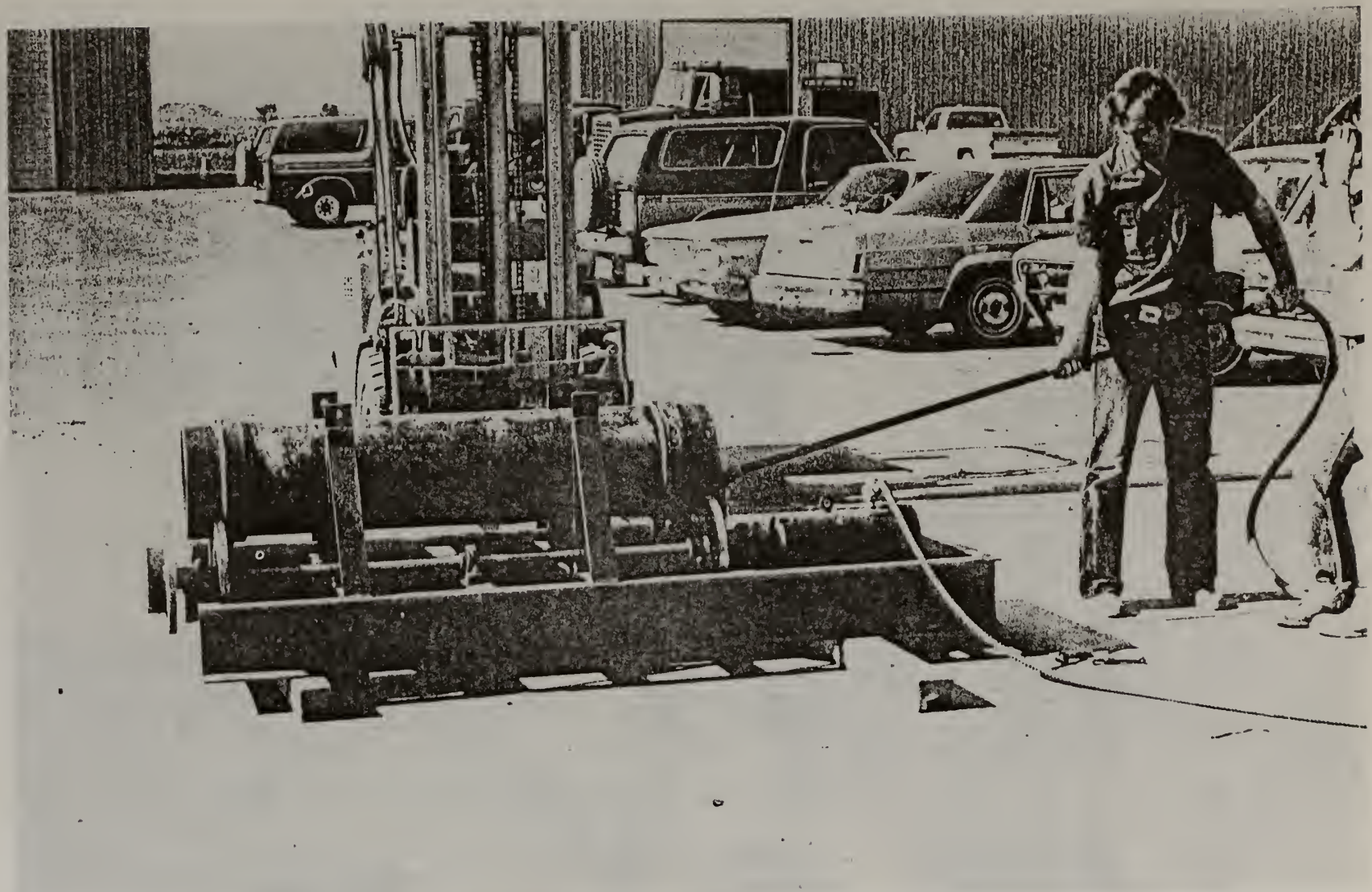

FIGURE 4

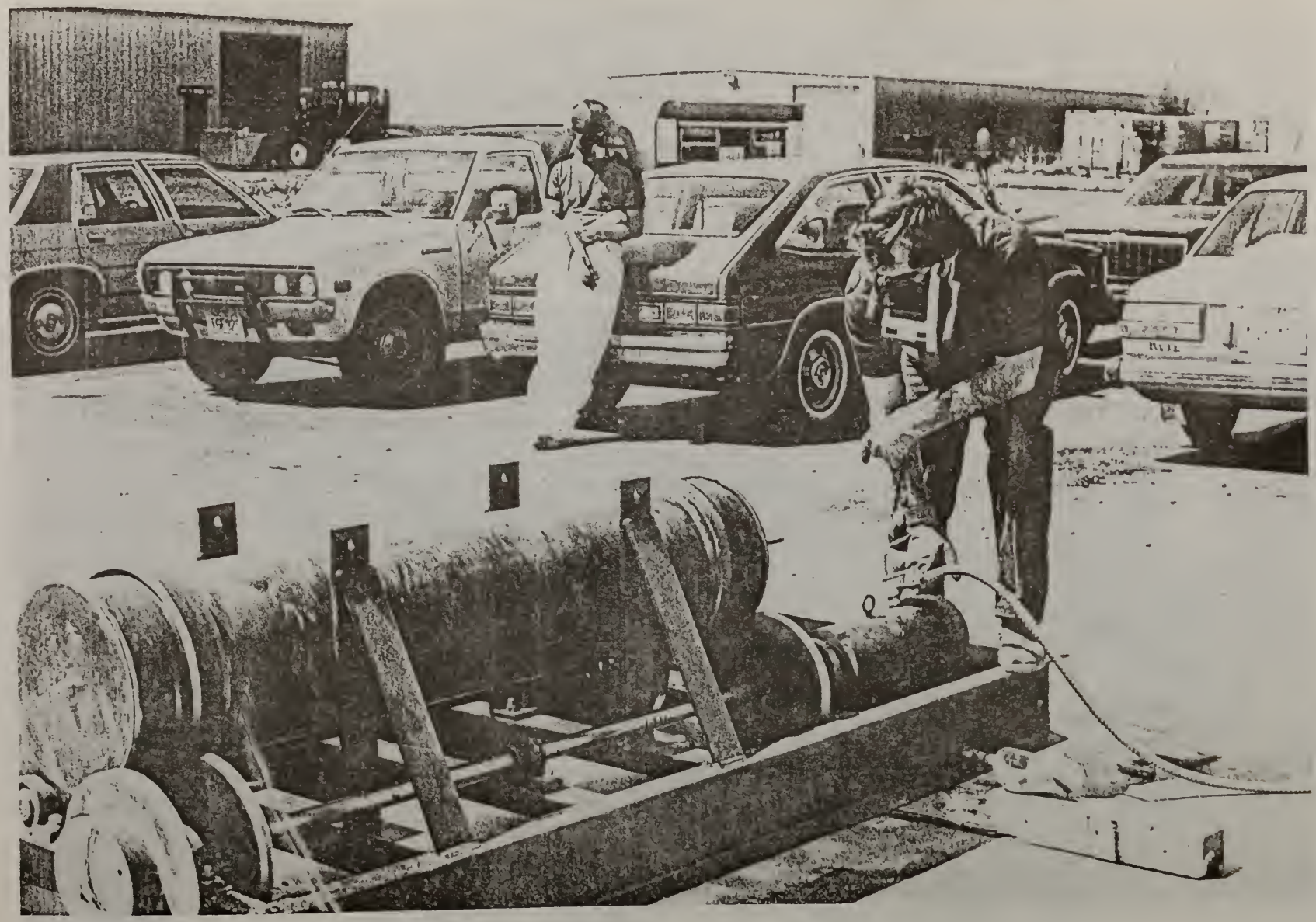

FIGURE 5

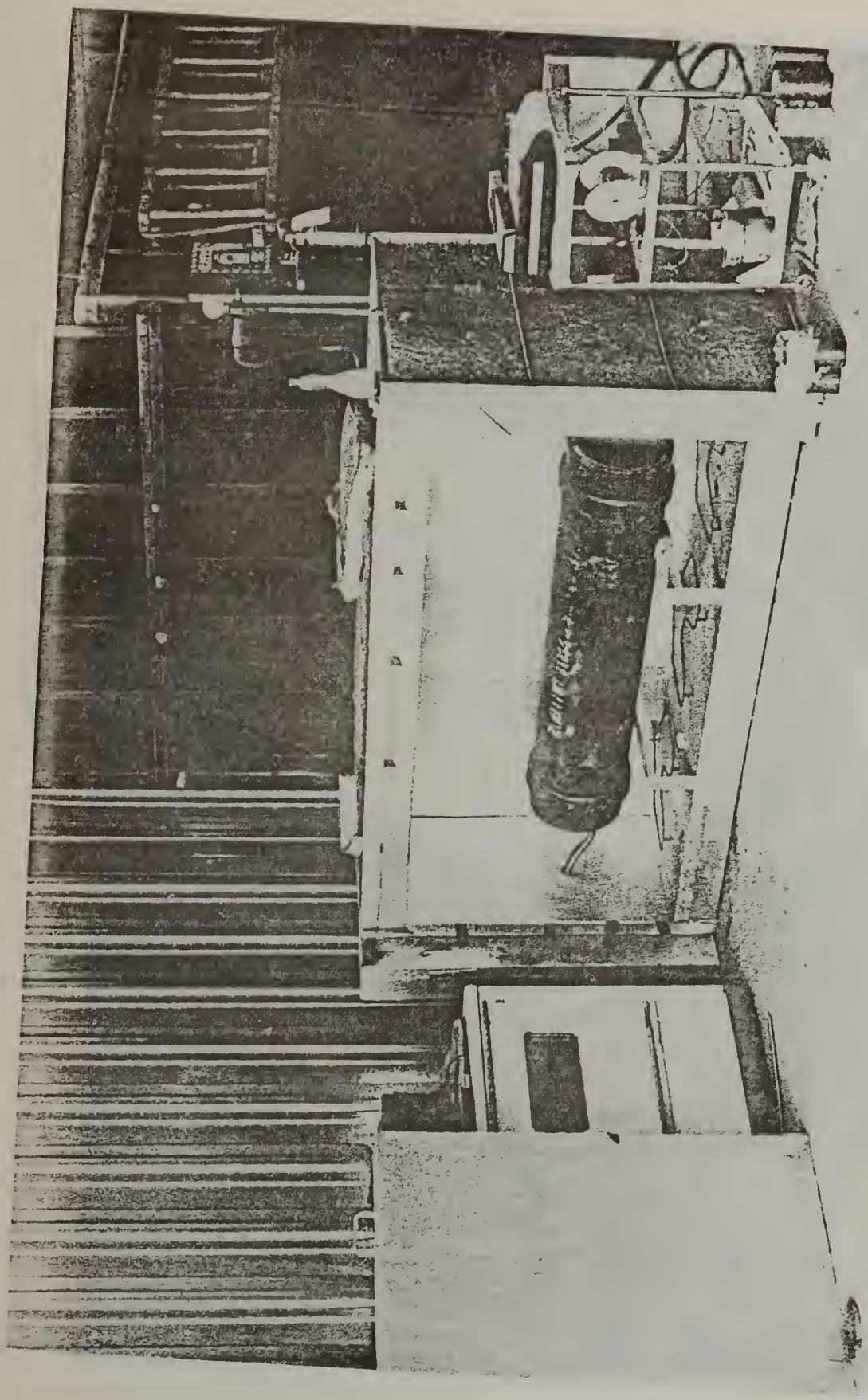

FIGURE 6

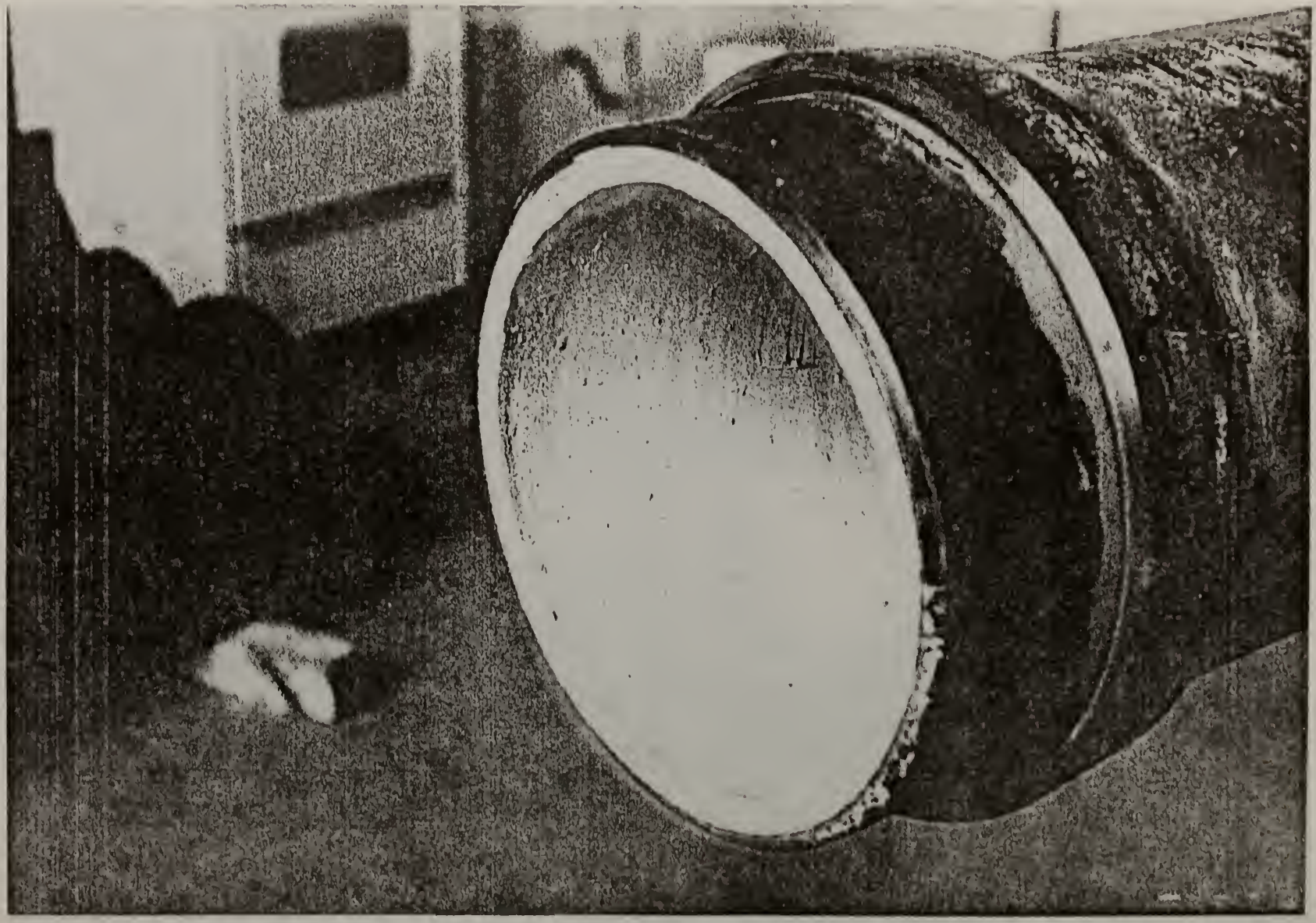

FIGURE 7

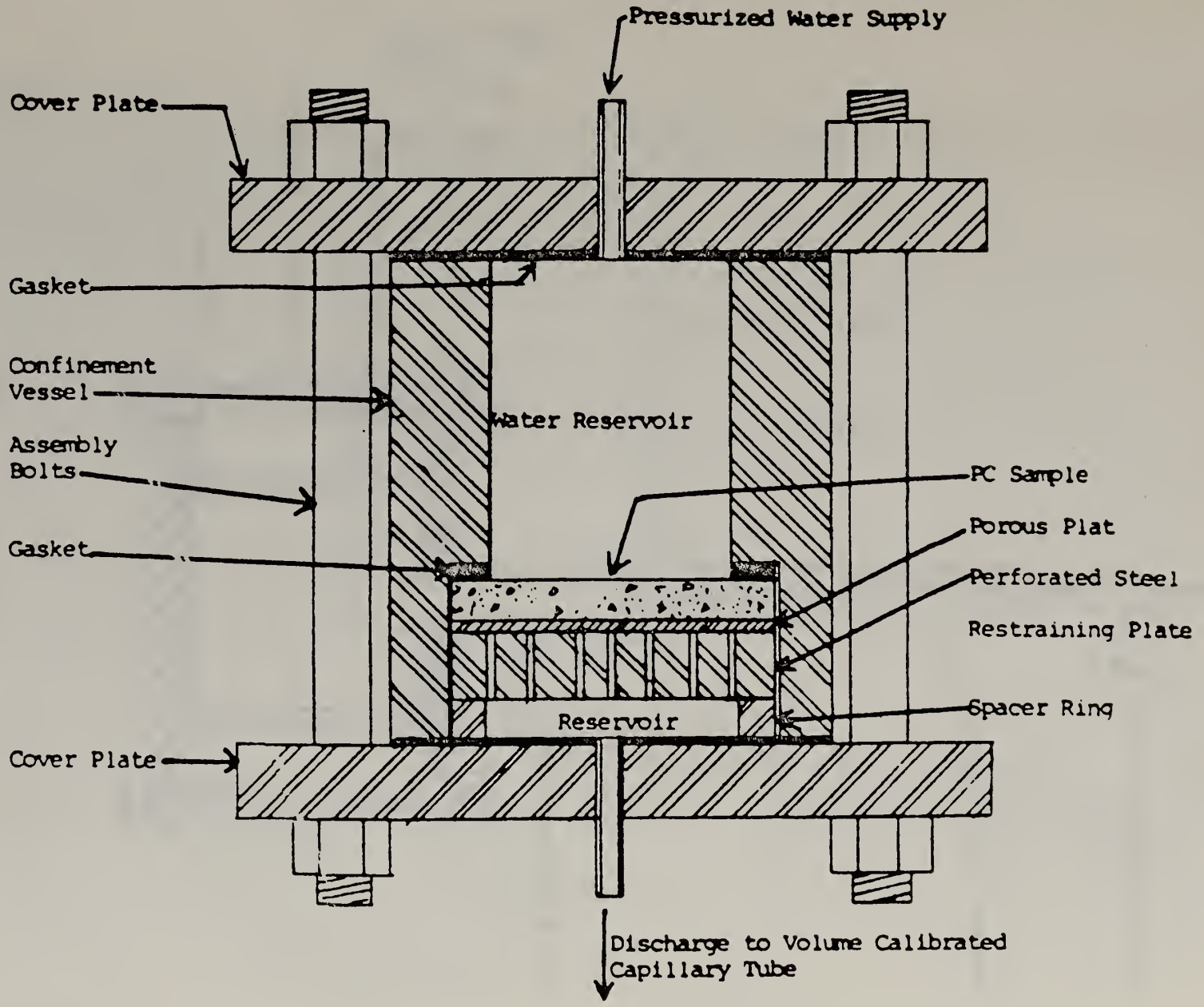
Pressurized Water Supply
Cover Plate
Gasket
Confinement Vessel
Water Reservoir
Assembly Bolts
PC Sample
Porous Plat
Gasket
Perforated Steel
Restraining Plate
Spacer Ring
Reservoir
Cover Plate
Discharge to Volume Calibrated Capillary Tube

FIGURE 8

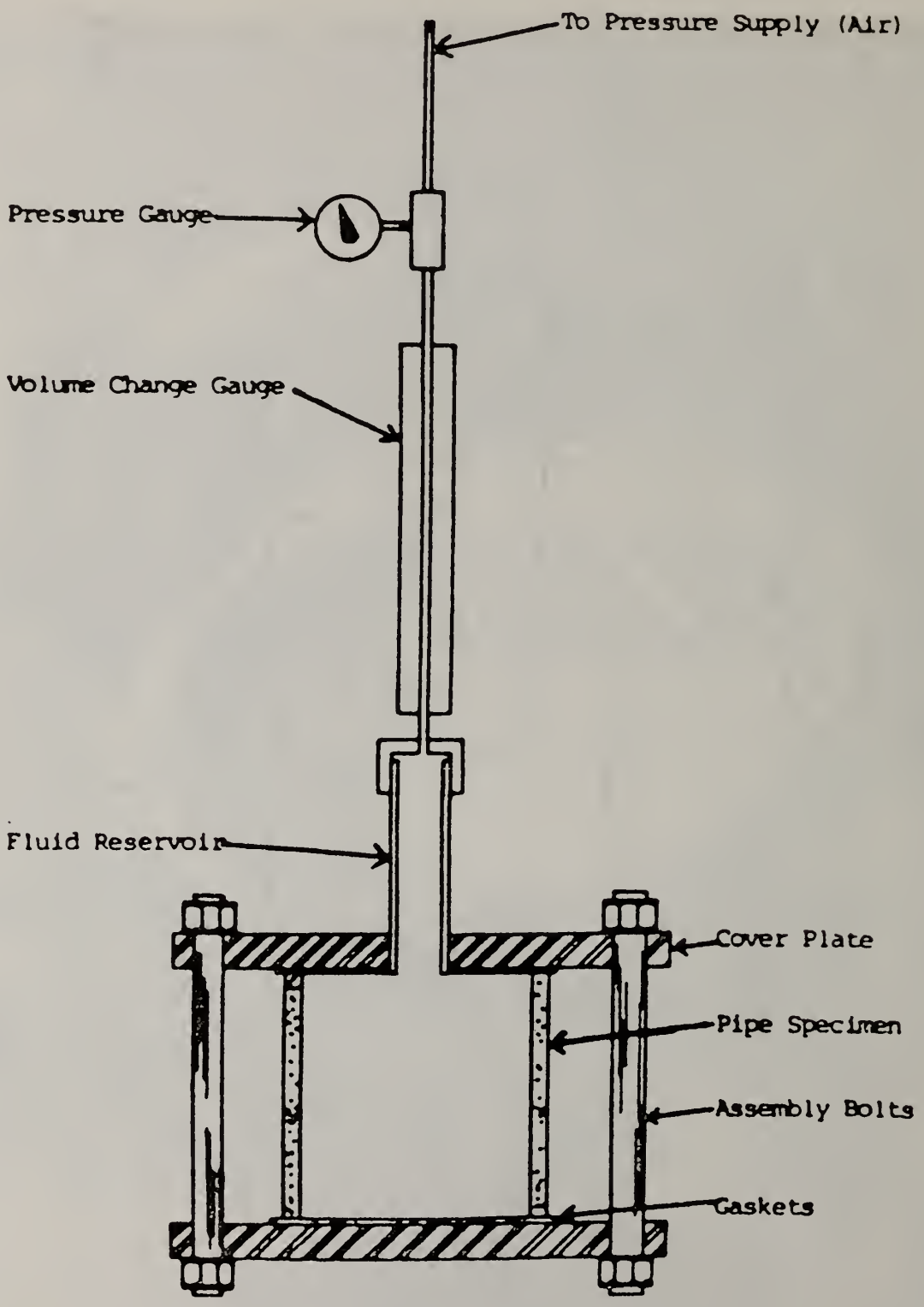
To Pressure Supply (Air)
Pressure Gauge
Volume Change Gauge
Fluid Reservoir
Cover Plate
Pipe Specimen
Assembly Bolts
Gaskets

FIGURE 9

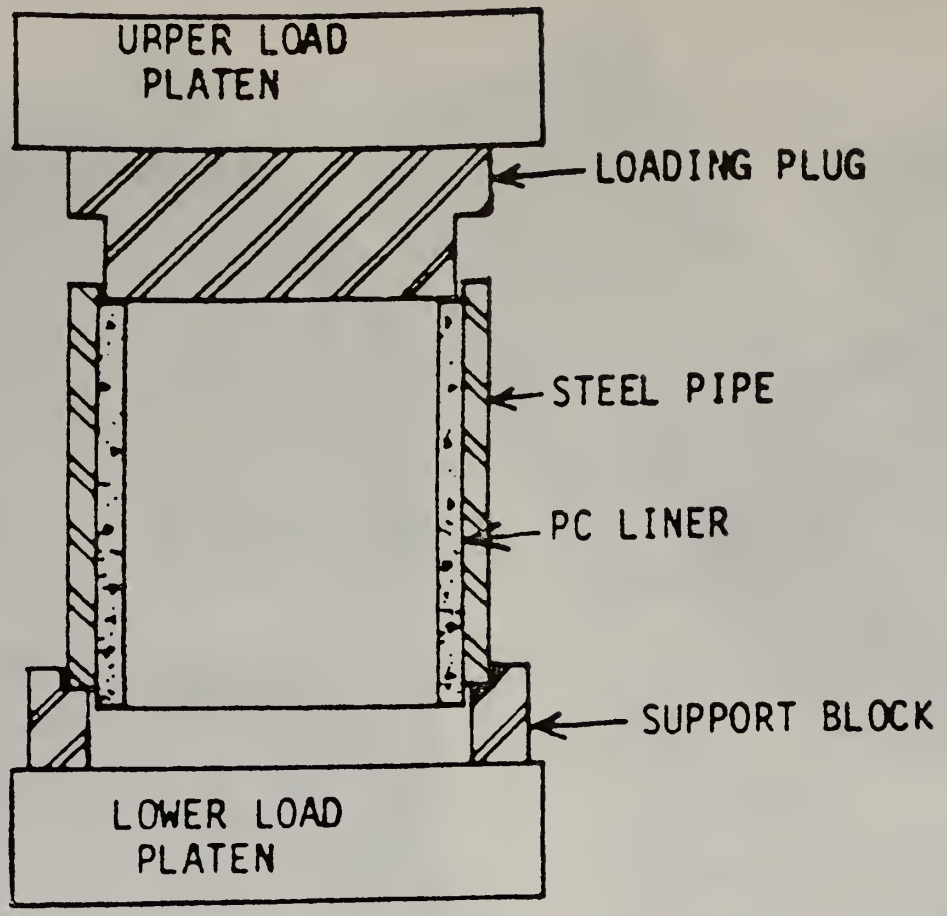

$$F_b = \frac{P}{3.14dL}$$

Where: F_b = Bond Strength
P = Initial Breakout Force
d = ID of Steel Pipe
L = Length of PC Liner

FIGURE 10

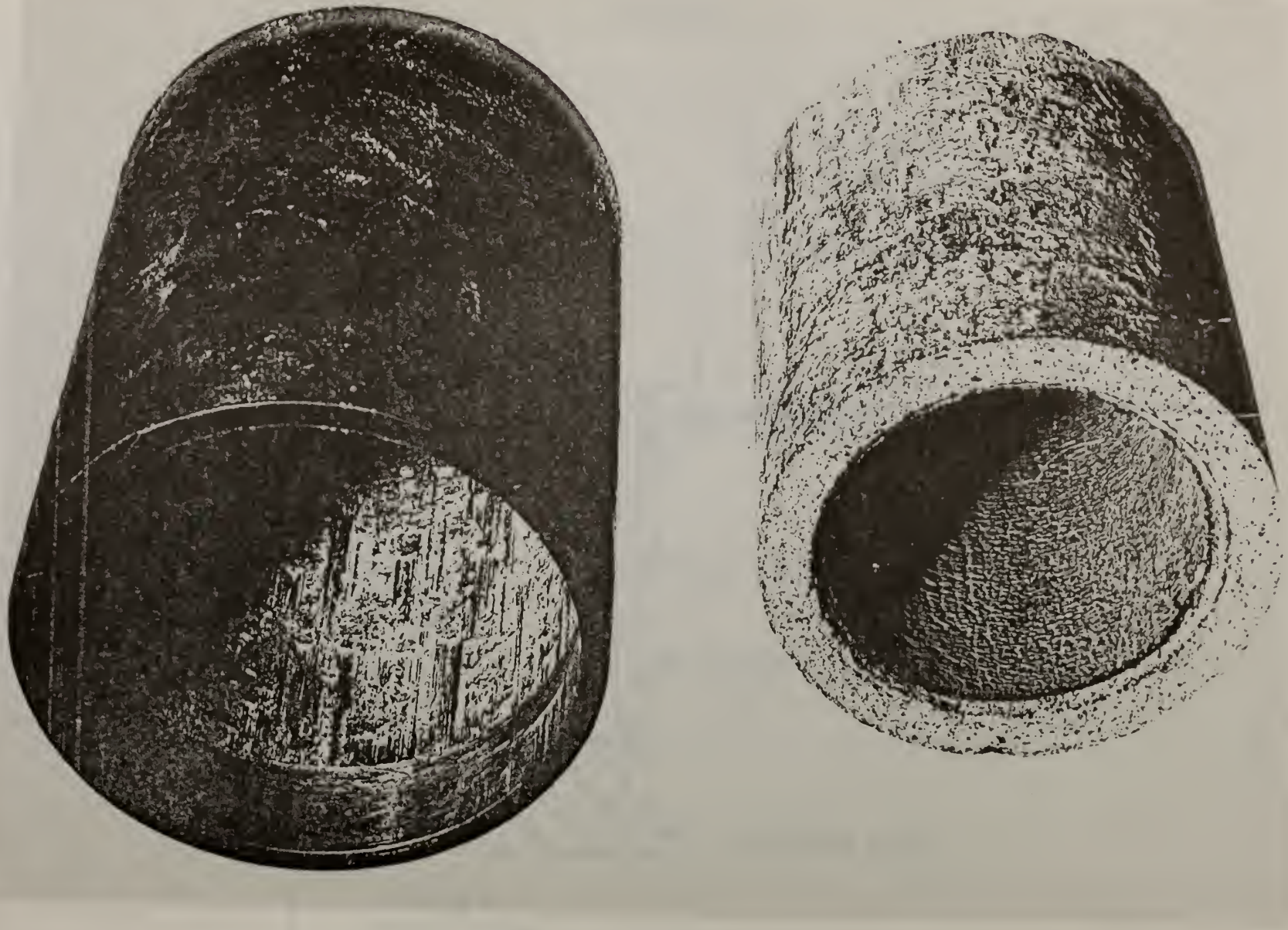

FIGURE 11

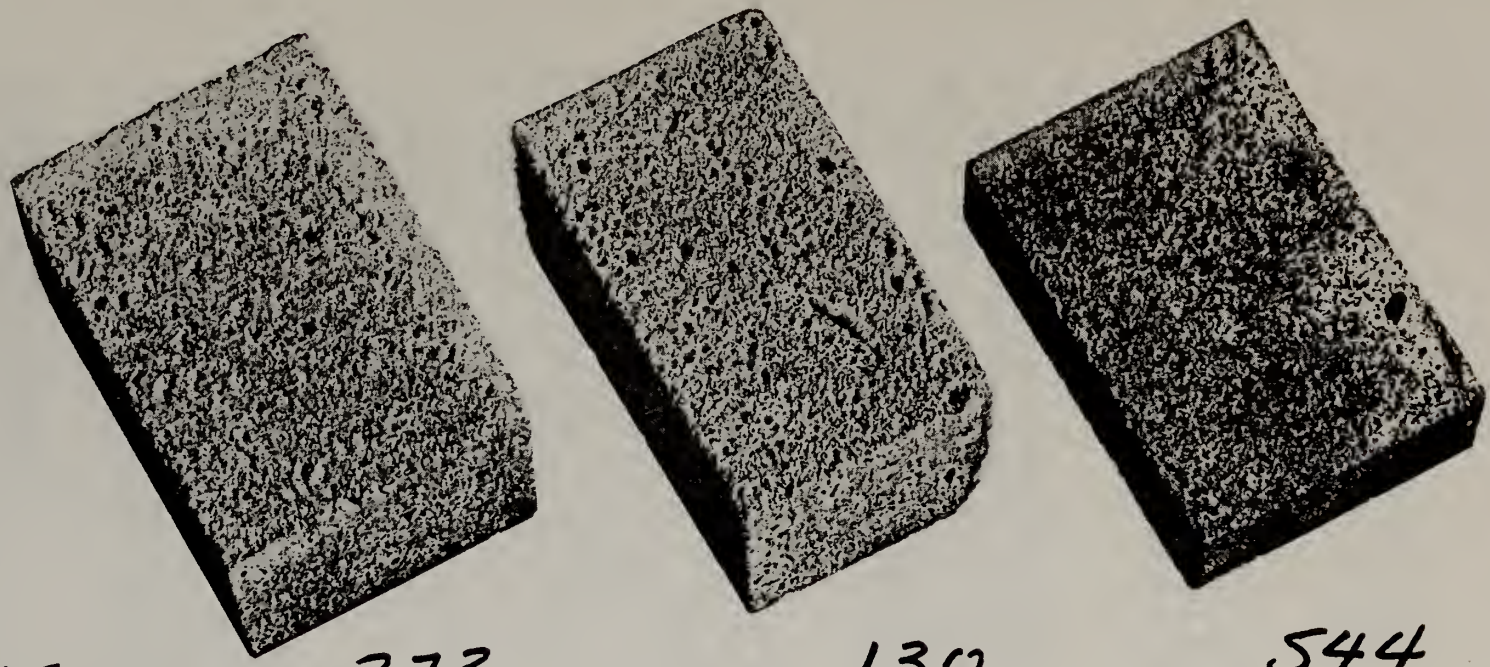

SAMPLE	273	130	544
EXPOSURE, hrs	1668	1668	2258

TEMPERATURE 200°C @ PH 1

FIGURE 12

ELECTROLESS NICKEL AS A SUBSTITUTE FOR CHROMIUM PLATING IN INDUSTRIAL APPLICATIONS

Ronald N. Duncan
ELNIC, Inc.
Nashville, Tennessee

In the last decade American industry has become almost totally dependent upon foreign supplies for strategic metals and minerals. While presently we import only 42 percent of the petroleum we use, more than 80 percent of the chromium, cobalt, manganese, niobium, tantalum and platinum required for industry is supplied by foreign producers.

Of these strategic metals, chromium is probably the most critical. Chromium is indispensable for the manufacture of stainless and alloy steels and is essential to the metal finishing industry. The United States presently consumes 25 percent of the world's production of chromium and has no domestic reserves. Worse yet, 98 percent of the world's chromium supply is located in southern Africa. Because of this area's political instability, a stoppage or reduction of its production is very possible(1,2).

In the National Materials Advisory Board's study on "Contingency Plans for Chromium Utilization"(3), electroless nickel was cited as the only true substitute for chromium. All other suggestions were techniques to merely reduce, not eliminate, chromium usage. Electroless nickel was also described in this report as a probable improvement over chromium in many applications. This paper describes this coating and its properties and discusses how it can be used as a substitute for industrial chromium coatings and for other more expensive or less readily available materials.

AN AMORPHOUS MATERIAL

Electroless nickel is an alloy of nickel and phosphorus. Those coatings used for functional (rather than decorative) applications typically contain 10 to 11 percent phosphorus dissolved in nickel and less than 0.05 percent other impurities. Unlike chromium or other electrolytic coatings, electroless nickel is completely amorphous.

It has no crystal structure and contains no segregation or separate phases. Its lack of long range order has been confirmed by electron diffraction studies at magnifications of 150,000[4]. An example of this coating is the 75 μm (3 mil) thick deposit shown in Figure 1. It is the lack of structure of this alloy which produces its unusual properties and makes it well suited for protection against corrosion, erosion and wear. Some of the properties of electroless nickel are compared to those of commercial hard chromium coatings in Table 1.

Because of their purity and homogeneity, the internal stress of high phosphorus electroless nickel coatings is very low on most substrates. As shown by Figure 2[5], on steel the coating is typically compressively stressed at 4 MPa (0.5 ksi). This helps to ensure the deposits integrity and the coatings performance.

The internal stress of commercial hard chromium coatings is always very highly tensile, and usually exceeds 200 MPa (30 ksi). This, combined with chromium's brittleness, causes the coatings to be cracked and often produces fissures through its thickness to the substrate. An example of the cracks in hard chromium deposits is shown in Figure 3.

A similar problem occurs with electroless nickel coatings containing less than 10 percent phosphorus. As illustrated by Figure 2, the internal stress level of low phosphorus deposits is also high. This also causes these deposits to be cracked and porous. The discontinuities present in both chromium and low phosphorus, electroless nickel coatings reduce their strength, ductility, and wear and corrosion resistance.

UNIFORMITY PROVIDES MANY BENEFITS

Unlike electroplated coatings, electroless nickel is applied without an electric current. Instead, the coating is produced by autocatalytic chemical reduction. Electroless nickel is plated onto a substrate by reducing nickel ions to metallic nickel with sodium hypophosphite. This chemical process avoids the non-uniformity associated with most other metallic coatings.

The thickness of electroplated coatings like chromium will vary significantly depending upon the part's configuration and proximity to the anodes. The coating tends to buildup on corners, edges and the like, and to be reduced on internal surfaces. Not only do these variations effect

the ultimate performance of the coating, but they can also cause additional finishing or machining to be needed after plating. With electroless nickel, the coating thickness is the same on any area of the part that is exposed to fresh plating solution. Grooves, slots, blind holes, and even the inside of tubing will have the same amount of coating as the outside surface of the part.

The benefits of electroless nickel's uniformity are illustrated by its substitution for chromium on many of the cylinders and rolls used in the printing and textile industries. This change has reduced chromium usage, and has also significantly reduced the finishing costs of these components. Previously the cylinders had to be ground, plated to a thickness of about 250 μm (12 mils), and ground a second time, before they could be balanced and installed. With electroless nickel they are now ground only once, balanced, plated to the desired diameter -- usually with 25 to 37 μm (1 to 1½ mil) -- and installed. Not only has this reduced the cost of plating by 40 percent, but 55 percent of the grinding time is also saved, freeing the machines for the production of new parts and increasing productivity (6).

The thickness of electroless nickel coatings can be controlled to suit the application. Coatings as thin as 2½ μm (0.1 mil) are commonly applied to electronic components, while those as thick as 75 μm (3 mils) are typical for chemical or petroleum equipment. Coatings thicker than 250 μm (10 mils) are also easily applied, but because of cost are normally used only for salvage or repair of worn or mis-machined parts.

GLASS-LIKE PROPERTIES

The mechanical and physical properties of electroless nickel deposits resemble those of other glasses. They have high strength, limited ductility and relatively low conductivity. The ultimate tensile strength of high phosphorus deposits exceeds 700 MPa (100 ksi). This is equal to many alloy steels and 5 to 10 times higher than chromium. This allows the coating to withstand considerable abuse without damage. Accordingly, it is commonly used to protect compressor blades, turbines, valves, pumps, extruders, blowers, and the like, and has often replaced stainless steel and exotic alloys.

The ductility of electroless nickel is only about 1 to 1½ percent. While this is less than that of most alloys, it is adequate for most coating applications and much superior to chromium. Thin films of the deposit can be bent

completely upon themselves without fracture, and the coating has been used successfully for springs and bellows. Electroless nickel, however, should not be applied to articles which subsequently will be bent or drawn. Severe deformation will crack the deposit, reducing corrosion and abrasion resistance.

The electrical and thermal conductivity of electroless nickel is low. Its conductivity can be increased by heat treatment, but is still much less than that of conventional conductors like copper or silver. Because of the relatively thin layers used, however, for most applications its resistance is not significant. Electroless nickel coatings are being successfully used for such applications as exchanger tubing and electrical switches and contacts.

Electroless nickel can be easily soldered, braised, and bonded and is often used to ease joining of non-metals and aluminum and stainless steel. This, combined with its uniformity and corrosion resistance, have made electroless nickel an ideal coating for electronic components. Accordingly, it is being increasingly used to reduce or eliminate gold and precious metal requirements in the electronic industry(7).

PROVIDES EXCELLENT RESISTANCE TO WEAR

One of the most important properties of electroless nickel for many industrial applications is its hardness and wear resistance. As deposited, high phosphorus coatings have a microhardness of 480 to 500 VHN_{100}, approximately equal to 48 HRC. This is similar to many hardened steels. Heat treatments, similar to age hardening procedures for aluminum alloys, can produce significant increases in coating hardness. As shown by Figure 4, hardness values as high as 1100 VHN_{100} (approximately 69 HRC) can be produced. This is equal to the hardness of commercial hard chromium and comparable to that of some hard facing alloys and ceramics.

Hardening of electroless nickel is due primarily to the formation of nickel phosphide particles within the alloy. At temperatures above 260°C (500°F) coherent and then distinct particles of Ni_3P begin to form, and at temperatures above 320°C (600°F) the glass begins to crystallize. This causes its hardness and wear resistance to increase rapidly. Maximum hardening is obtained through treatments at 400°C (750°F).

Both heat treated and non-heat treated electroless nickel coatings are commonly used to minimize the effects of erosion, abrasion and wear. Laboratory tests have shown fully hardened coatings to have wear resistance equal to hard chromium. This is illustrated by Table 2, which shows the results of Taber Abraser Wear tests of electroless nickel coatings, and compares them to electroplated nickel and chromium[8]. The excellent resistance of electroless nickel often allows it to replace high alloy materials, hard chromium, and even hard facings.

An example of the ability of electroless nickel to make common materials behave like superior ones is the polyethylene pelletizer bowl shown in Figure 5. This bowl, with a 125 μm (5 mil) thick high phosphorus coating, was in service for two months with no measurable loss or attack. Previous uncoated aluminum bowls failed in less than three weeks after 40 percent of their weight was eroded away. Other typical wear applications include feed screws and extruders, computer drive mechanisms, textile and fiber equipment, hydraulic cylinders, molds and dies, and packaging equipment.

Another property related to wear is lubricity. Under sliding or abrasive conditions, low friction surfaces minimize heat buildup and experience less scoring and galling than higher friction surfaces. Because of the phosphorus they contain, electroless nickel deposits have a low coefficient of friction, typically 0.13 (lubricated) to 0.4 (unlubricated). This is approximately 20 percent lower than chromium, one-half of that of steel, and significantly better than aluminum or stainless steel.

One disadvantage of electroless nickel is that, unlike chromium, it is not hydrophilic. Electroless nickel lacks the crack pattern present in chromium which can hold an oil or water film. Thus for applications like ink rollers, which depend upon surface wetting, electroless nickel may not always be suitable.

ADHESION STRENGTH IS OUTSTANDING

The performance of a coating is often dependent upon its adhesion to its substrate. Without adequate adhesion even the most resistant coating can become dislodged or broken, allowing attack of the underlying metal. The adhesion of electroless nickel coatings to steel, aluminum, copper and their alloys normally exceeds the sheer strength of the substrate.

The high bond strength of these coatings is due to the ability of the plating solution to completely remove microscopic contaminants from the substrate prior to the deposition of the first nickel-phosphorus layer. This allows the coating to develop both mechanical and metallic bonds with the substrate metal. The adhesion of electroless nickel coatings to steel and aluminum is typically 300 to 400 MPa (40 to 60 ksi). This is similar to and often superior to that of chromium coatings.

PROVIDES SUPERIOR CORROSION RESISTANCE

One of the most important differences between electroless nickel and chromium coatings is their corrosion resistance. Both are barrier coatings. Both protect the underlying metal by sealing it off from the environment rather than by sacrificial action. Thus, to be completely protective the coatings must be defect free.

Because of the cracks present through even thick deposits, hard chromium coatings offer only limited protection against corrosion. These cracks offer pathways through the coating for a corrosive environment to reach and attack the substrate. Accordingly, chromium coatings will oftentimes develop a network of rust spots or rust lines across its surface. In addition, unlike electroless nickel, chromium coatings are subject to interface or underdeposit attack. With chromium, corrosion not only will extend into the substrate at the bottom of cracks or pores, but will also travel out from these areas along the coating-to-substrate interface, loosening and lifting the coating(9).

Because of its homogeneity and freedom from defects, electroless nickel coatings provide a true barrier to corrosion. They do not offer any pathways to the substrate. The metallic bonds these coatings form with their substrate also prevent underdeposit attack. Even if a pore were to be produced by improper processing or mechanical damage, in most environments it rapidly fills with corrosion product, stifling further attack. Corrosion will not spread out from the defect and thus it is contained.

High phosphorus electroless nickel coatings are almost totally resistant to alkalis, like caustics and potash; to salt solutions and brines, like sea water or those present in food or chemical environments; to acid gas environments, like those in the petroleum industry; and to all types of organic media and solvents. The coating also has good resistance to ammonia solutions; to organic

acids, like lactic or acetic; and to reducing acids, like hydrochloric or sulfuric. It is only significantly attacked by strongly oxidizing solutions like concentrated sulfuric or nitric acid(10).

In most environments, the corrosion resistance of hard chromium is much less than that of electroless nickel. Chromium is rapidly attacked by reducing environments and is subject to pitting and localized attack in halogens, especially oxidizing halogens like ferric chloride. This is illustrated by Table 3, which compares the corrosion of electroplated and cast chromium to that of electroless nickel in different environments(9,10,11).

The petroleum and chemical process industries are the largest users of electroless nickel for corrosion protection. Because of its superior resistance to attack in these environments, the coating ensures easy and reliable operation and extends the equipment life. Accordingly, it is often used in place of more critical or expensive materials, especially stainless steel. For instance, oil field valves coated with 75 μm (3 mils) of electroless nickel cost approximately one-third that of equivalent stainless steel valves and in most environments provide equal protection(12).

Many petroleum components now coated with electroless nickel were originally plated with hard chromium. The poor performance of chromium in oil field environments, however, lead to a reduction in its use and to the increased specification of electroless nickel(13). Specific applications in these industries include ball, gate, plug and check valves, blow out preventers, chokes, heat exchange equipment, pumps, compressors, tubing, vessels, packers, and all types of down hole equipment(12).

CONCLUSION

Electroless nickel has many unique properties which make it a superior engineering material. The coating offers high strength, excellent abrasion and wear resistance, lubricity, solderability, and superior corrosion resistance, together with ease of application and uniform thickness. Accordingly, electroless nickel has proved to be useful in improving reliability, in reducing cost, and in avoiding the use of critical or strategic materials.

RND:ss
October 4, 1982

REFERENCES

1. Gray, A.G., Metal Progress, Vol. 117, No. 3, p. 33 (1980).

2. Swinburn, J., Materials Performance, Vol. 21, No. 1, p. 54 (1982).

3. National Materials Advisory Board, "Contingency Plans for Chromium Utilization", National Academy of Sciences, Washington, D.C., 1978.

4. Weil, R., Stevens Institute of Technology, private communication, January 24, 1980.

5. Parker, K. and Shah, H., Plating, Vol. 58, No. 3, p. 230 (1971).

6. Paliotta, J.V., "Functional and Economic Impact of Electroless Nickel on the Printing Press Industry", Electroless Nickel Conference II, Cincinnati, March, 1981.

7. Bandrand, D.W., Plating and Surface Finishing, Vol. 68, No. 12, p. 57 (1981).

8. Industrial Nickel Plating and Coating, International Nickel Company, New York, 1976.

9. Uhlig, H.H., Editor, Corrosion Handbook, John Wiley and Sons, New York, 1948, p. 825-828.

10. Duncan, R.N., "Corrosion Control With Electroless Nickel Coatings", AES Electroless Plating Symposium, American Electroplating Society, St. Louis, March, 1982.

11. LaQue, F.L., and Copson, H.R., Corrosion Resistance of Metals and Alloys, Reinhold Publishing, New York, 1963, p. 448-449.

12. Duncan, R.N., "Performance of Electroless Nickel Coatings in Oil Field Environments", Corrosion/82 Conference, National Association of Corrosion Engineers, Houston, March, 1982.

13. King, J.A., and Badelek, P.S.C., Oil and Gas Journal, Vol. 80, No. 28, p. 115 (1982).

TABLE 1

COMPARISON OF ELECTROLESS NICKEL AND COMMERCIAL HARD CHROMIUM COATINGS

PROPERTY	ELECTROLESS NICKEL	COMMERCIAL HARD CHROME
MATERIAL	Alloy of 10 to 11 percent dissolved in nickel.	Chromium plus trace amounts of oxides and hydrogen.
STRUCTURE	Amorphous; no phase structure, lamination or segregation.	Crystalline; fine grained with numerous cracks.
INTERNAL STRESS ON STEEL, MPa	<7	200-300
DENSITY, g/cm^3	7.75	6.90-7.18
MELTING POINT, °C	890	1610
ELECTRICAL RESISTIVITY, μΩ-cm	90	14-66
THERMAL CONDUCTIVITY, W/cm-°K	0.08	0.67
MAGNETIC COERCITY	Non-magnetic	Non-magnetic
TENSILE STRENGTH, MPa	>700	<200
DUCTILITY, % ELONGATION	1 to 1½	<<0.1
MODULAS OF ELASTICITY, GPa	200	100-200
COEFFICIENT OF THERMAL EXPANSION, μm/m/°C	12	6
ADHESION STRENGTH, MPa	300-400	Good
HARDNESS, VHN_{100}	480 to 500, as deposited; heat treatable to 1100	800 to 1000
COEFFICIENT OF FRICTION VS STEEL (LUBRICATED)	0.13	0.16
TABER WEAR RESISTANCE, mg/1000 cycles	15 to 20, as deposited; 2 to 9 after heat treatment	2 to 3
CORROSION RESISTANCE	Excellent resistance to attack by all but the most severely oxidizing environments.	Poor due to cracks; resists oxidizing environments; attacked by halogens and reducing solutions.

RND:ss
October 4, 1982

TABLE 2

COMPARISON OF THE TABER ABRASER RESISTANCE OF DIFFERENT ENGINEERING COATINGS.

COATING	HEAT TREATMENT	TWI, mg/1000 CYCLES(1)
Watts Nickel	None	25
Electroless Nickel	None	17
Electroless Nickel	300°C/1 hr	10
Electroless Nickel	500°C/1 hr	6
Electroless Nickel	650°C/1 hr	4
Hard Chromium	None	2

(1) Taber Wear Index, CS-10 abraser wheels, 1000 gram load, determined as average weight loss per 1000 cycles for total test of 6000 cycles.

RND:ss
October 4, 1982

TABLE 3

COMPARISON OF THE CORROSION BEHAVIOR OF CHROMIUM AND ELECTROLESS NICKEL IN DIFFERENT ENVIRONMENTS

ENVIRONMENT	CORROSION RATE, μm/y		
	CHROMIUM		ELECTROLESS NICKEL
TEMPERATURE	12°C(1)	16°C(2)	20°C(3)
10% Acetic acid	nil	660	25
10% Citric acid	nil	--	19
Conc. Hydrochloric acid	--	100,000	46
10% Hydrofluoric acid	25,000	--	30
10% Lactic acid	nil	--	19
10% Malic acid	51	--	17
10% Nitric acid	nil	--	44
Conc. Nitric acid	nil	--	>25,000
10% Phosphoric acid	25	5	16
10% Sulfuric acid	280	--	12
Conc. Sulfuric acid	760	--	25
10% Sodium hydroxide	nil	--	nil
10% Ammonium chloride	nil	--	nil
10% Cupric chloride	380	--	25
10% Cupric nitrate	51	--	12
10% Ferric chloride	nil	--	780
10% Sodium chloride	nil	--	0.5

(1) Commercial hard chromium deposit; corrosion rates less than 25 μm/y reported as nil.

(2) Cast chromium metal.

(3) Electroless nickel containing 10½% phosphorus and less than 0.05% other elements.

RND:ss
October 4, 1982

FIGURE 1

Typical high phosphorus electroless nickel deposit on a mild steel substrate. The coating thickness is 75 µm (3 mils). Lighter layer at top is a copper overplate applied for edge resolution. 400X magnification. Nital etchant.

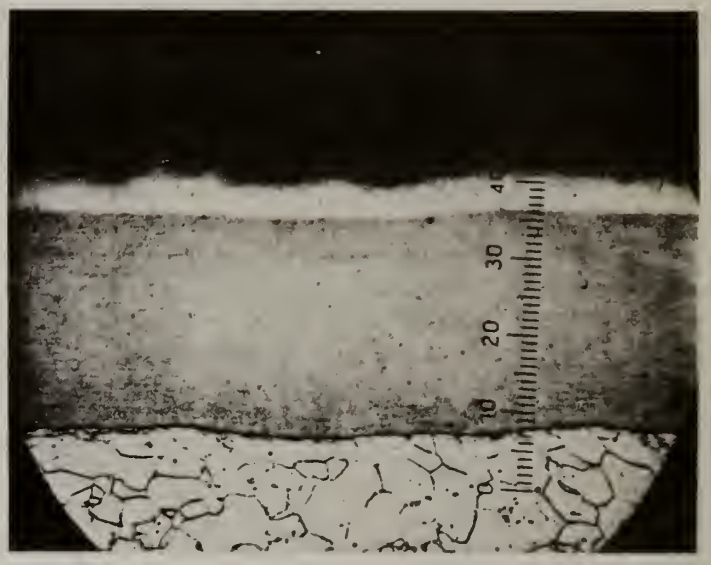

FIGURE 2

Effect of phosphorus content on the internal stress of electroless nickel deposits on steel. (1 ksi = 6.89 MPa)

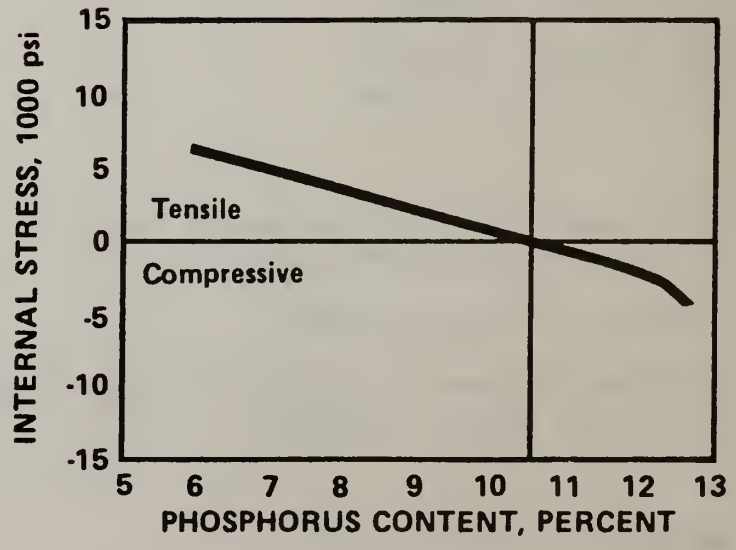

FIGURE 3

Typical cracks in a commercial hard chromium deposit. 1000X magnification. Not etched.

FIGURE 4

Effect of different one hour heat treatments on the hardness of electroless nickel containing 10½% phosphorus.

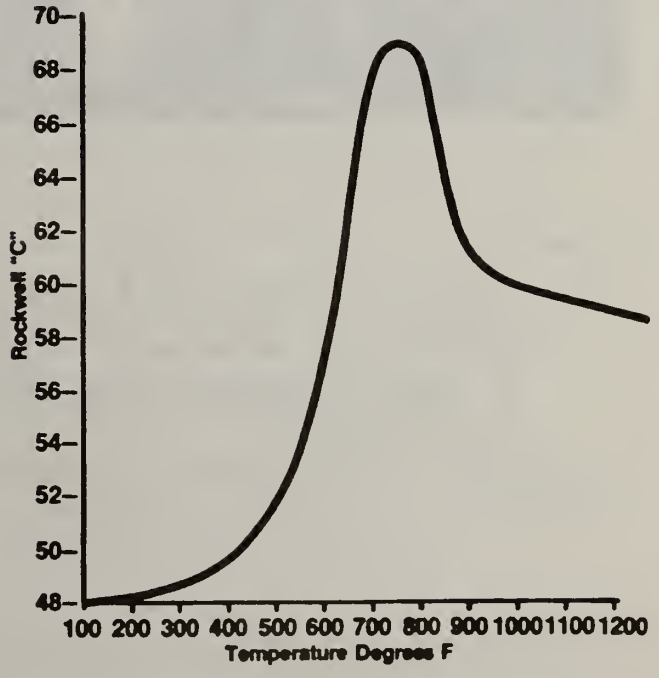

FIGURE 5

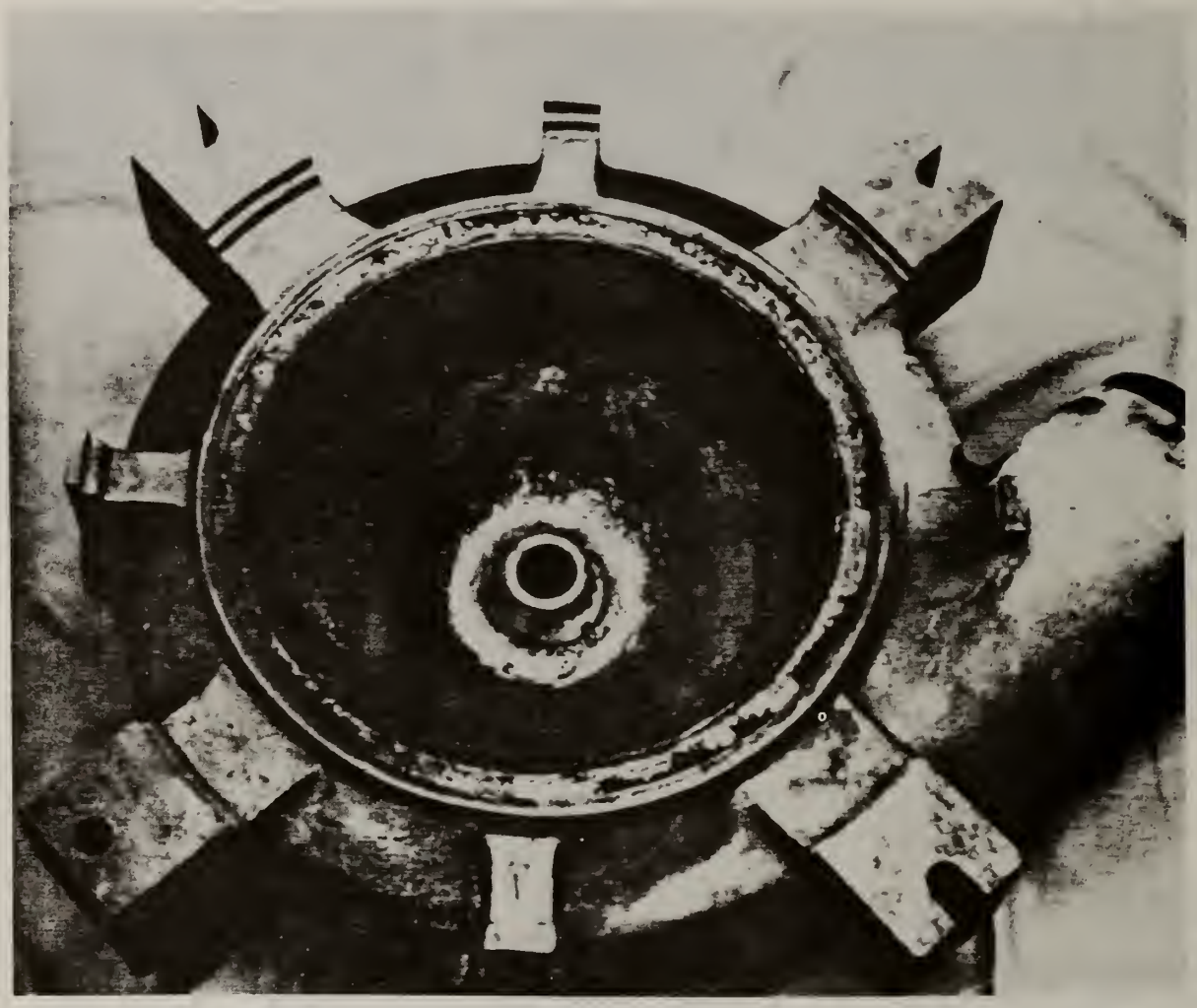

Plated aluminum pelletizer bowl, after two months of exposure to high velocity, polyethylene pellets and Mississippi River water. Bowl is coated with 125 μm of high phosphorus electroless nickel. Previously, uncoated bowls failed in 3 weeks with weight losses of 40 percent.

DEVELOPMENT OF DUCTILE POLYCRYSTALLINE Ni_3Al FOR HIGH-TEMPERATURE APPLICATIONS*

C. T. Liu and C. C. Koch
Metals and Ceramics Division
Oak Ridge National Laboratory
Oak Ridge, Tennessee 37830

ABSTRACT

The nickel aluminide, Ni_3Al, is strong and stable at elevated temperatures; however, low ductility and brittle fracture restrict its use for structural applications. Microalloying has been employed to overcome the embrittlement associated with grain-boundary separation. Among the dopants added, boron has been found to be most effective in improving fabricability and ductility of polycrystalline Ni_3Al. Tensile elongations of >50% have been achieved by control of boron concentration and thermomechanical treatment. The B-doped Ni_3Al shows excellent strength and oxidation resistance at high temperatures. Unlike conventional alloys, the yield strength of the aluminide increases rather than decreases with increasing test temperature. The potential for developing the aluminide as a substitute for Cr-containing heat-resistant alloys is assessed.

INTRODUCTION

Austenitic stainless steels and superalloys are the common heat-resistant materials for structural use at elevated temperatures. The alloys typically contain substantial quantities (15~30 wt %) of chromium for oxidation and corrosion resistance. Because of the strategic nature of the chromium supply, there has been an increasing interest in development of aluminides as a substitute for Cr containing alloys.

---

*Research sponsored by the Exploratory Studies Program, Oak Ridge National Laboratory and Division of Materials Sciences, U. S. Department of Energy under contract W-7405-eng-26 with the Union Carbide Corporation.

Nickel and iron aluminides are in a class of materials usually referred to as intermetallic compounds. The aluminides are typically strong, stable, and resistant to oxidation and corrosion[1] at elevated temperatures. Unlike conventional alloys, the static strength of many aluminides shows an increase rather than a decrease with increasing test temperature.[2,3] A major problem with using aluminides as structural materials is their reported brittle fracture and low ductility, particularly at lower temperatures.[2,4] Because of the poor fabricability and low fracture toughness, the aluminides have not been considered as serious candidates for structural engineering applications.

The nickel aluminide based on Ni_3Al (γ') is an important strengthening constituent of commercial nickel-base superalloys. It has been known for years that single crystals of Ni_3Al are quite ductile,[5] but its polycrystalline forms are extremely brittle.[6,7] The brittleness of such poly-crystals is associated with weak grain boundaries that cause brittle intergranular fracture without much plastic deformation within the grains. During the past 20 years, efforts have been spent on improving the ductility of aluminides,[8,10] but significant progress has been achieved only recently through microalloying processes.[11] Microalloying involves adding a small amount of dopants (usually <1%) for controlling chemistry and cohesion of the grain boundaries. In this study, a microalloying approach was employed to alleviate the grain boundary embrittlement problem of Ni_3Al. Emphasis will be placed on the effect of boron additions on ductilization of Ni_3Al alloys.

EXPERIMENTAL PROCEDURES

The Ni_3Al alloys containing 26 and 24 at. % Al (13.9 and 12.7 wt % Al) were doped with a small amount of Ce (0.1 wt %), Mn (2.1 wt %), and B (0 to 0.1 wt %). The alloys were prepared by arc melting and drop casting, using pure metal elements and Ni—4 wt % B and Ni—4 wt % Ce master alloys. There was no significant change in weight during the alloy preparation. The alloy ingots (2.5 × 5.3 × 0.6 cm) were first

homogenized at 1000-1200°C, and then fabricated to sheets by either hot rolling at 1200°C or cold rolling at room temperature with intermediate annealing at 1000°C.

The microstructure of Ni_3Al alloys annealed for various times at 1000°C was examined metallographically. The specimens polished by standard techniques were etched in a solution of 20 parts of H_2O, 20 parts of HNO_3, 10 parts of HF, 20 parts of H_3PO_4, 10 parts of acetic acid, and 10 parts of HCl. The crystal structures of Ni_3Al alloys were determined by x-ray diffraction using Cu K_α radiation.

Sheet specimens with a gage section of 12.7 × 3.2 × 0.7 mm were used for tensile and creep tests. Tensile tests were conducted on an Instron testing machine at a crosshead speed of 150 mm/s. To perform the tensile tests at elevated temperature, a water-cooled quartz-tube vacuum system was attached to the Instron machine, and specimens were heated inductively inside a tantalum susceptor. Creep tests were done in vacuum under dead-load arrangement. During the tests, the temperature was monitored by a Pt/Pt–10% Rh thermocouple centrally located on the specimen. Fracture surfaces of selected tensile specimens were examined by a JSM-U3 scanning electron microscope (SEM) operated at 25 kV.

RESULTS

Undoped Ni3Al alloys containing 26 and 24 at. % Al cracked badly during hot and cold fabrication. Figure 1(a) shows part of the ingot hot rolled at 1200°C. The ingot was almost pulverized due to extensive cracking along the grain boundaries, indicating the grain-boundary brittleness in Ni_3Al. The alloys doped separately with 0.1 wt % Ce, 0.1% B, and 2.1% Mn all cracked during fabrication except the B-doped Ni–24 at. % Al alloy (12.7 wt. % Al), designated as IC-6. It was possible to fabricate the IC-6 ingot into sheet by repeated cold rolling at room temperature and heat treatment at 1000°C. The amount of cold work was initially ~15% reduction in thickness, and was gradually increased to 50% between each intermediate annealing. Figure 1(b) shows the 0.76-mm-thick sheet of IC-6 fabricated by cold rolling.

(a)

(b)

Fig. 1. Comparison of fabricability of Ni_3Al alloys containing 24 at. % Al; (a) A part of Ni_3Al ingot hot rolled at 1200°C, showing extensive grain-boundary cracking; (b) A sheet of Ni_3Al doped with 1000 ppm B, fabricated by cold rolling at room temperature.

To study the effect of B additions on fabricability, a series of alloys was prepared based on Ni-24 at. % Al, in which various levels of B were added. Table 1 summarizes the results. The alloys containing 100 ppm B or less cannot be fabricated by cold rolling. IC-18 containing 250 ppm B was fabricated into sheets, but it exhibited numerous shallow surface cracks. The alloys containing 400 ppm and above were fabricated into good quality sheets.

Table 1. Effect of boron additions on fabricability[a] of Ni-24 at. % (Ni-12.7 wt %) Al

Alloy	B Addition (ppm)	Fabricability
IC-2	0	Cracked badly
IC-20	50	Cracked badly
IC-19	100	Cracked
IC-18	250	Sheet fabricated but exhibited shallow surface cracks
IC-21	400	Sheet fabricated
IC-15	500	Sheet fabricated
IC-28	700	Sheet fabricated
IC-6	1000	Sheet fabricated

[a]Ingots were fabricated by repeated cold rolling (15 ~ 50% reduction in thickness) and softening heat treatment at 1000°C.

The crystal structure in undoped and B-doped Ni_3Al alloys was determined by x-ray diffraction. The superlattice lines, which were clearly visible, characterize the $L1_2$-type ordered crystal structure. Thus, the small amount of B does not affect the long-range ordered crystal structure in Ni_3Al. The microstructure of B-doped Ni_3Al alloys (24 at. % Al) was examined as a function of aging time at 1000°C. The alloys show a "regular" equiaxed grain structure with few annealing twins and second-phase particles (Fig. 2). Grain growth occurs at

(a)

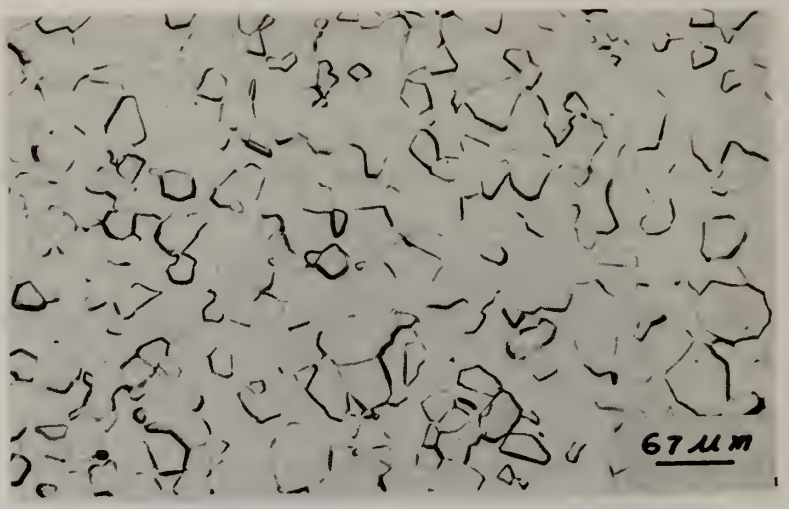

(b)

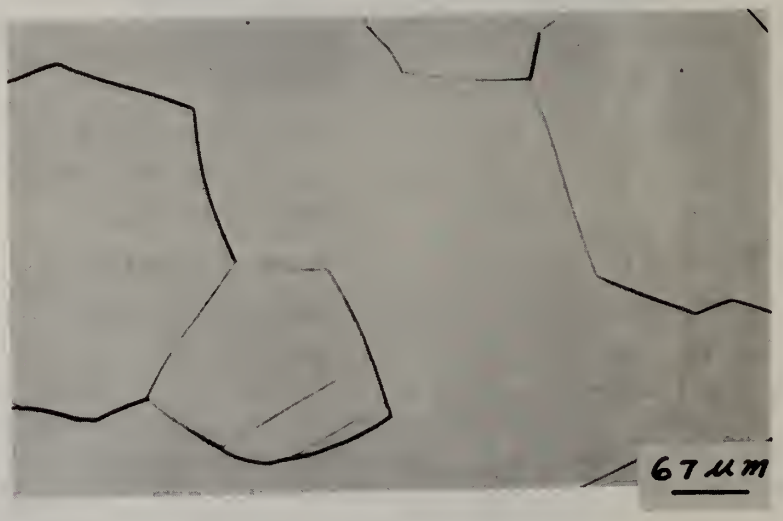

Fig. 2. Microstructures of Ni_3Al doped with 1000 ppm B. (a) 10 min anneal at 1000°C; (b) 16 d anneal at 1000°C.

1000°C; however, there is no apparent difference in grain size for specimens containing 500 and 1000 ppm B after the same annealing treatment.

Tensile properties of B-doped Ni_3Al alloys were characterized as functions of B concentration, heat treatment, and test temperatures. Table 2 shows the room-temperature properties of the alloys doped with different levels of B. For the specimens annealed 30 min at 1000°C, the yield strength showed a linear increase with the B concentration [Fig. 3(a)] but the tensile strength was essentially insensitive to the B concentration. All the B-doped alloys exhibited transgranular ductile fracture [like Fig. 4(a)] with the ductility exceeding 40%. The tensile elongation increased with the B content [Fig. 3(b)] and reached 53.8% for the IC-6 specimen containing 1000 ppm B. After being annealed for 16 d at 1000°C, the IC-6 specimen showed a higher yield strength but distinctly lower ductility. In accompanying the decrease in ductility, the fracture mode changed from the transgranular to a mixed one [Fig. 4(b)]. On the other hand, the IC-15 specimen containing 500 ppm B displayed a lower yield strength with ductility remaining unchanged after the long term anneal.

Figure 5 is a plot of yield strength as a function of test temperature for the B-doped Ni_3Al (IC-15) and commercial fabricable alloys such as Hastelloy-X and type 316 stainless steel. Unlike the conventional alloys, the strength of IC-15 increases with increasing temperature and reaches a maximum around 600°C. As a result of this increase, the aluminide is much stronger than the commercial alloys at elevated temperatures. For example, the aluminide displays a yield strength of 550 MPa (80,000 psi) and a ductility of 45% at 600°C. In comparison, the yield strengths of Hastelloy-X and type 316 stainless steel are 210 and 120 MPa (31,000 and 17,000 psi), respectively. Thus, the aluminide has the superior high-temperature strength.

Table 3 shows the results of preliminary measurements of creep properties of the B-doped alloys tested at 760°C (1400°F) and 138 MPa (20,000 psi). The minimum creep rate of the aluminides is insensitive to the B concentration between 250 and 1000 ppm. IC-6 specimens exhibited a sharp drop in creep rate with an increase in grain size from

Table. 2. Tensile properties of B-doped Ni_3Al alloys tested at room temperature at a crosshead speed of 150 mm/s

Alloy Number	B Concentration (ppm)	Yield Strength MPa (ksi)	Tensile Strength MPa (ksi)	Total Elongation (%)
		Annealed 30 min at 1000°C		
IC-18	250	269.4 (39.1)	1304.3 (189.3)	43.8
IC-21	400	281.1 (40.8)	1297.4 (188.3)	46.5
IC-15	500	290.8 (42.2)	1314.6 (190.8)	49.4
IC-28	700	301.8 (43.8)	1296.7 (188.2)	50.6
IC-6	1000	321.8 (46.7)	1253.3 (181.9)	53.8
		Annealed 16 d at 1000°C		
IC-15	500	163.3 (23.7)	1027.3 (149.1)	53.0
IC-6	1000	447.2 (64.9)	549.8 (79.8)	8.0

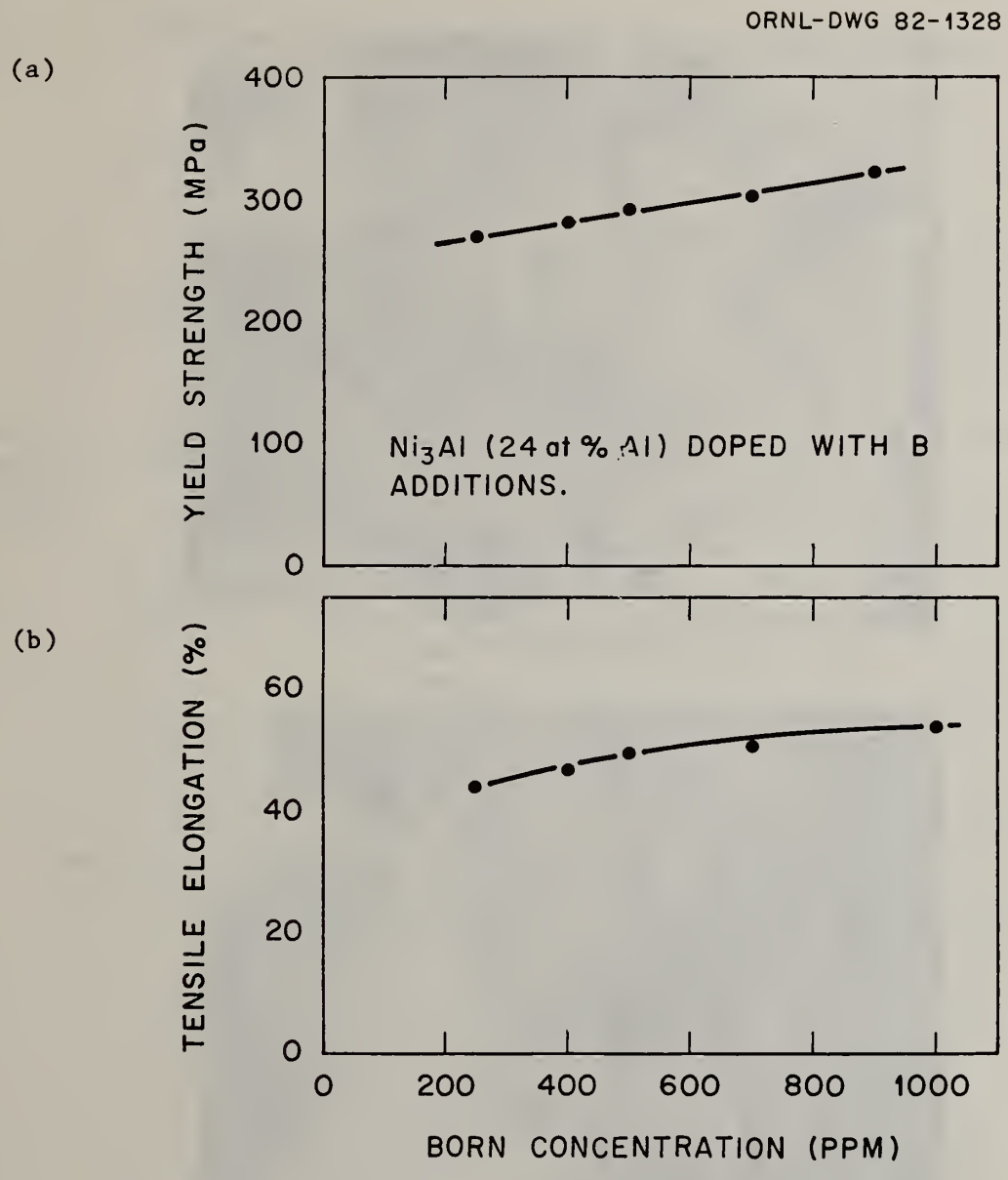

Fig. 3. Yield strength and tensile elongation of B-doped Ni_3Al alloys (24 at. % Al) as a function of boron content.

(a)

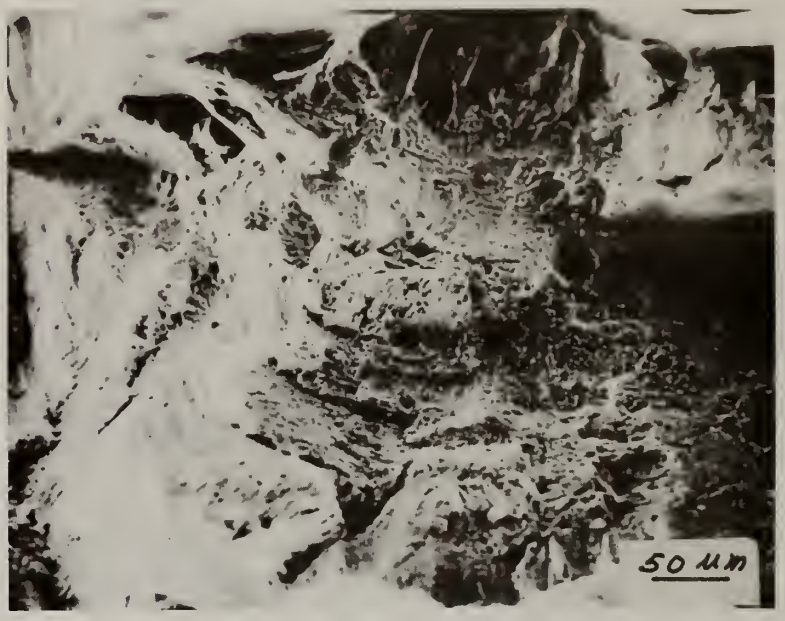

(b)

Fig. 4. SEM fractographs of B-doped Ni_3Al (1000 ppm B) tested in tension at room temperature. (a) Specimen annealed for 3 d and 15 h at 1000°C. (b) Specimen annealed for 16 d at 1000°C.

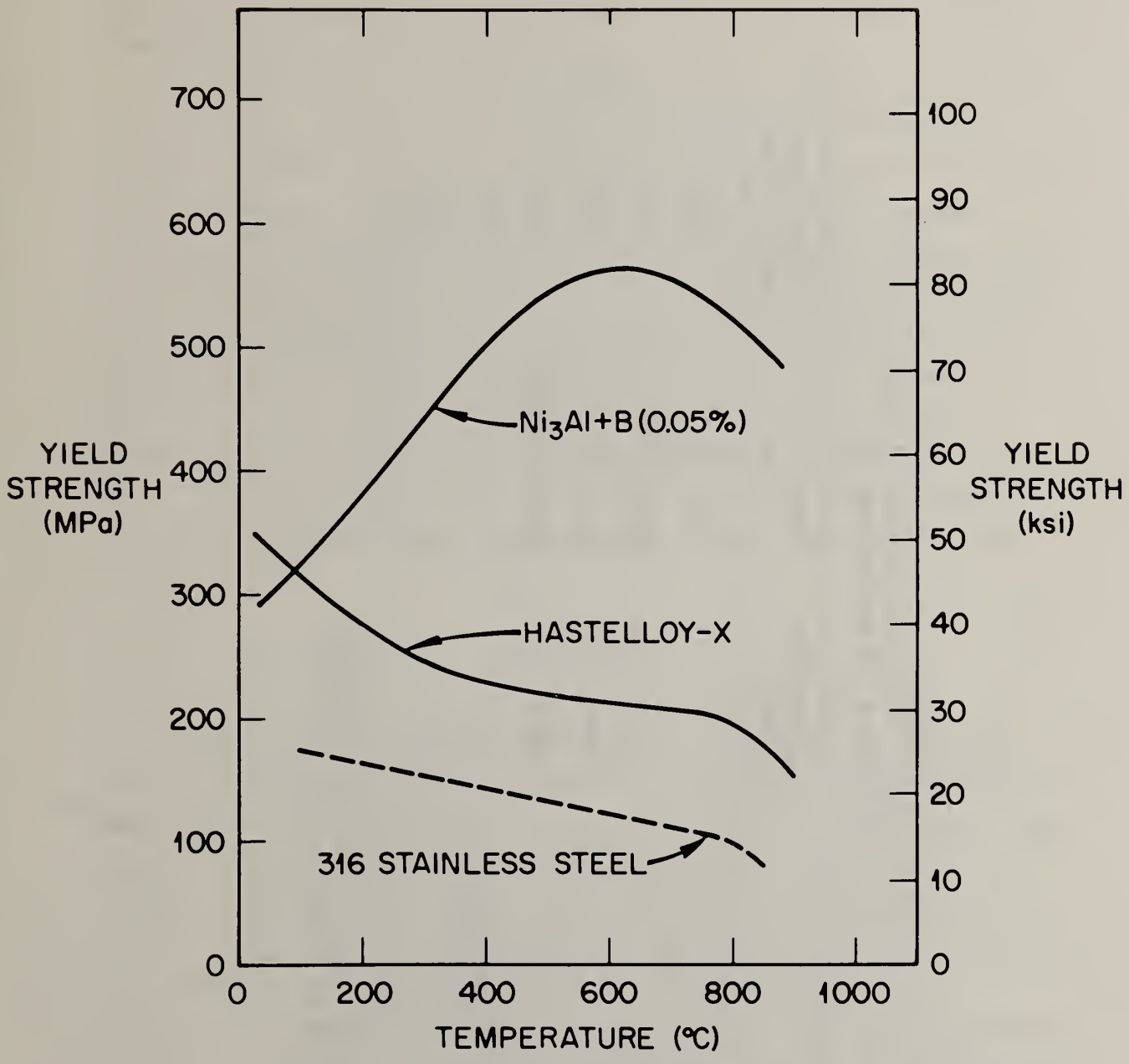

Fig. 5. Yield strength as a function of test temperature for Ni_3Al (24 at. % Al) doped with 500 ppm B and commercial fabricable alloys Hastelloy X and type 316 stainless steel.

Table. 3. Comparison of creep properties of B-doped Ni_3Al alloys with type 316 stainless steel and Hastelloy X tested at 760°C (1400°F) and 138 MPa (20,000 psi)

Alloy	B concentration (ppm)	Grain size (μm)	Minimum creep Rate (10^{-5}/h)
Ni_3Al (IC-18)	250	Fine (25)[a]	41.8
Ni_3Al (IC-15)	500	Fine (25)[a]	40.4
Ni_3Al (IC-6)	1000	Fine (15)[a]	39.3
Ni_3Al (IC-6)	1000	Coarse (120)[b]	1.8
Type 316 stainless steel			854.0
Hastelloy X			132.0

[a]Produced by annealing 30 min at 1000°C.
[b]Produced by annealing 16 d at 1000°C.

25 to 120 μm produced by annealing at 1000°C. The creep rate of B-doped Ni_3Al is substantially lower than that of type 316 stainless steel[12] and Hastelloy X,[13] as indicated in Table 3.

An alloy coupon of IC-6 was exposed to air at 900°C for a study of air oxidation. The sample was removed from the furnace after each 100-150 h exposure. The exposed sample displayed no apparent spalling with a weight gain of 0.61 mg/cm^2 after a total of 524-h exposure. Metallographic examination indicates the formation of a thin oxide scale [Fig. 6(a)] (~2.6 μm thick) which is enriched with aluminum as revealed by electron microprobe analysis [Fig. 6(b)]. Line scanning revealed a depletion of Al in the base metal beneath the Al-rich oxide scale. A strip cut from the oxidized coupon was bent to ~360 degrees without failure (Fig. 7), indicating the B-doped aluminide remained ductile after the exposure. All the results demonstrate the good oxidation resistance of B-doped Ni_3Al containing no Cr, the critical strategic element.

DISCUSSION

Since Ni_3Al classically exhibits brittle intergranular fracture, microalloying has been used to alleviate the grain-boundary embrittlement problem of the aluminide. In this study, two types of dopants were added to Ni_3Al. Type I dopants are Ce and Mn that, based on thermodynamic considerations,[14] have a strong affinity for impurities such as sulfur. Sulfur has been known to have a strong tendency to segregate to grain boundaries in Ni-base alloys[15] as well as in Ni_3Al[16] and $Ni_3(Al,Ti)$.[16] The purpose of adding the dopants was to scavenge sulfur and other harmful impurities from grain boundaries through a precipitation reaction. A Type II dopant is B, which tends to segregate at grain boundaries and possibly increase the cohesive strength of the boundaries. Among the dopants we added, boron is found to be the most effective in improving fabricability and ductility of the nickel aluminide. This finding is in agreement with the results of Aoki and Izumi[11] who first discovered the beneficial effect of B in Ni_3Al. They reported a tensile ductility of ~35% elongation at room temperature. By

(a)

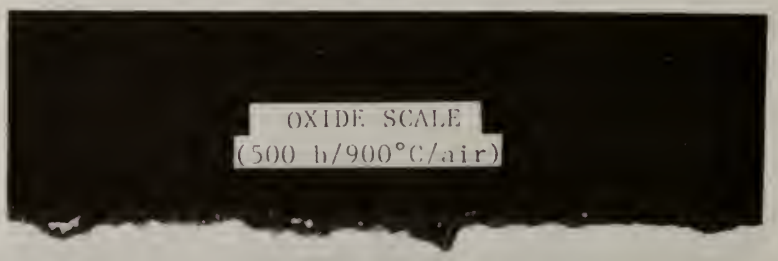

(b)

Fig. 6. Formation of Al-rich oxide scale on the surface of the B-doped Ni_3Al (1000 ppm B) specimen exposed for 524 h in air at 900°C. (a) oxide scale with an average thickness of 2.6 μm. (b) Al mapping obtained by electron microprobe analysis.

Fig. 7. A bent strip of B-doped Ni_3Al (1000 ppm B) oxidized for 500 h at 900°C in air.

control of B concentration and thermomechanical treatment, we have observed a tensile ductility of 53.8% elongation at room temperature — the highest tensile ductility ever achieved by polycrystalline aluminides. Using Auger electron spectroscopy, White[17] has detected a strong segregation of B to grain boundaries in B-doped Ni_3Al. We believe the presence of B at grain boundaries improves the cohesion of the boundary and thus reduces the tendency toward the integranular fracture in Ni_3Al. It should be pointed out that B additions only effectively ductilize the Ni_3Al alloys containing 24 at. % Al, but not the alloy containing 26 at. % Al. The reason for this behavior is not well understood, but it is possibly related to the alloy stoichiometry, which is known to affect the chemistry of grain boundaries and consequently their segregation behavior.[18,19]

The ductility and fabrication behavior of B-doped Ni_3Al (24 at. % Al) are dependent on the B concentration. The Ni_3Al alloys doped with <250 ppm B cannot be satisfactorily fabricated into sheets

because of grain-boundary cracking. On the other hand, sheet fabrication becomes somewhat difficult for the aluminide doped with 1000 ppm. Also, Ni_3Al containing 1000 ppm B loses most of its ductility after long-term annealing at 1000°C. Thus, the optimium level of B in Ni_3Al should be around 500 ± 200 ppm, based on the consideration of ductility and fabricability.

The yield strength of the B-doped Ni_3Al (IC-15), just like undoped Ni_3Al,[20] shows an increase with temperature, and reaches a maximum around 600°C. The positive temperature dependence of the yield strength, which has been observed in other $L1_2$ ordered alloys, is generally believed to be associated with a thermally activated hardening process[21] in connection with the {111} slip system. The strength starts to decrease with temperature above 600°C, corresponding to a gradual change in slip systems from {111} to {100} planes.(22,23) The B-doped Ni_3Al alloys are much stronger than the existing commercial fabricable heat-resistant alloys as shown in Fig. 5. Currently we are working to increase the strength of Ni_3Al further by both solid solution hardening and particle strengthening.

The B-doped Ni_3Al alloys are quite resistant to creep deformation and air oxidation. The minimum creep rate of the fine-grained Ni_3Al specimens is significantly lower than that of type 316 stainless steels[12] and Hastelloy X.[13] Furthermore, the creep rate of Ni_3Al specimens can be substantially reduced (by a factor of 20) by an increase in grain size from 25 to 120 μm. The higher creep rate in the fine-grained specimens may be related to grain-boundary sliding which can be minimized by coarsening the grain structure. Metallographic examination reveals numerous cracks formed along grain boundaries in these creep-ruptured specimens. The oxidation rate of B-doped Ni_3Al (IC-6) is comparable or lower than that of current heat resistant alloys[24] (depending on the Cr content in these alloys). The good oxidation resistance results from the formation of aluminum oxide scales which protect the alloy from excessive oxidation. Recent work[25] in coating materials has demonstrated that alumina-forming materials provide an excellent resistance to hot corrosion in coal energy conversion systems. This indicates the potential use of the aluminides as structural materials in sulfiding environments.

In summary, the aluminide Ni_3Al can be made ductile by microalloying with a few hundred ppm boron. The B-doped Ni_3Al alloys, possessing a unique combination of high-temperature strength, oxidation resistance, and adequate ductility and fabricability, have the potential to be developed as new structural materials containing no critical strategic elements such as Cr and Co.

ACKNOWLEDGMENTS

The authors wish to express their sincere thanks to J. O. Stiegler and C. L. White for valuable technical discussions. Thanks are also due to R. L. Heestand and L. Queener for alloy preparation and fabrication, R. E. Clausing for electron microprobe analysis, O. B. Cavin for x-ray diffraction, W. H. Farmer for metallography, and E. L. Lee and J. F. Newsome for technical assistance. The authors are also grateful to Connie Dowker for preparation of the manuscript.

REFERENCES

1. E. A. Aitken, *Intermetallic Compounds,* J. H. Westbrook, ed., pp. 491–515, John Wiley & Sons, Inc., New York, 1967.

2 N. S. Stoloff and R. G. Davis, *Prog. Mater. Sci.* **13**(1), 1–34 (1966).

3. B. H. Kear, C. T. Sims, N. S. Stoloff, and J. H. Westbrook, eds. "Ordered Alloys - Structural Applications and Physical Metallurgy," *Proc. 3rd Bolton Landing Conf.*, September 1969, Baton Rouge, Claitor's Publishing Division, 1970.

4. H. A. Lipsitt, D. Shechtman, and R. E. Schafrik, *Met. Trans. A* **11A**, 1369 (1980).

5. S. M. Copley and B. H. Kear, *Trans. AIME* **239**, 977 (1967).

6. R. Moskovic, *J. Mater. Sci.* **13**, 1901 (1978).

7. K. Aoki and O. Izumi, *Trans. Jpn. Inst. Met.* **19**, 203 (1978).

8. E. M. Grala, *Mechanical Properties of Intermetallic Compounds*, J. H. Westbook, ed., p. 358, John Wiley & Sons, Inc., New York, 1960.

9. A. V. Seybolt and J. H. Westbrook, *Acta Metall.* **12**, 449 (1964).

10. M. J. Blackburn, et al., AFML-TR-78-18 and 78, Air Force Materials Lab., Wright-Patterson Air Force Base, Ohio, 1977–78.

11. K. Aoki and O. Izumi, *Nippon Kinzoku Gakkaishi*, **43**, 1190 (1979).

12. V. K. Sikka, et al., ORNL-5285, Oak Ridge National Laboratory, October 1977.

13. C. R. Brinkman, et al., ORNL/TM-5405, Oak Ridge National Laboratory, October 1976.

14. O. Kubaschewski and C. B. Alcock, *Metallurgical Thermochemistry 5th ed.*, Pergamon, New York, 1979.

15. W. C. Johnson, J. E. Doherty, B. H. Kear, and A. F. Giamei, *Scr. Metall.* 8, 971 (1974).

16. C. L. White and D. F. Stein, *Metall. Trans. A.* **9A**, 13 (1978).

17. C. L. White, unpublished results, Oak Ridge National Laboratory, 1982.

18. A. V. Seybolt and J. H. Westbrook, *Acta Metall*, **12**, 449 (1964).

19. J. H. Westbrook and D. L. Wood, *J. Inst. Met.* **91**, 174 (1963).

20. O. Noguthi, Y, Oya, and T. Suzuki, *Metall. Trans. A* **12A**, 1647 (1981).

21. S. Takenchi and E. Kuramoto, *Acta Metall.* **21**, 415 (1973).

22. R. G. Davies and N. S. Stoloff, *Trans. Metall. Soc. AIME* **233**, 714 (1965).

23. C. Lall, S. Chin, and D. P. Pope, *Metall. Trans. A* **10A**, 1323 (1979).

24. J. Stringer and I. G. Wright, *Oxid. Met.* 5, 59 (1972).

25. P. R. Clark, C. M. Packer and R. A. Perkins, FE-2592-29, Lockheed Palo Alto Research Laboratory, March 15, 1981.

INTRODUCTION

During the past 12 years, the interest in ceramics as high-temperature structural material has grown in the major industrial countries. Through various governmental agencies, each country has channelled substantial funds for producing and evaluating critical ceramic components for such applications. Around 1970, the Advanced Research Projects Agency (ARPA) of the U.S. Department of Defense, initiated a program to demonstrate successful use of ceramics in demanding high-temperature structural applications.

Components for the hot flow path of a vehicular gas turbine engine and some diesel engine parts are being extensively investigated. Of the ceramic materials, dense silicon nitride and dense silicon carbide are considered the favorite candidates. Lately, toughened zirconia has been considered favorably for some specific applications.

Shapes for most of these component parts are extremely complex. Furthermore, the components must meet strict dimension tolerances and maintain very high reliability in use. Even so, it is a prerequisite to produce these components in large numbers at a competitive cost. Several fabrication techniques can be used to produce such complex components. Many of these techniques are being explored. The complexity of the components and the need for large quantities dictated the consideration of injection molding as a technologically and economically feasible fabrication approach.

As a result of worldwide interest in this technology, Battelle offered an industrial group research program to determine the important factors in the ceramic injection molding process and in molding advanced ceramics. Due to proprietary nature of our study, we have kept this paper fairly broad and used information available in the open literature. Still, the paper contains sufficient detail to underscore the various technical aspects of ceramic injection molding.

COMPONENTS OF CURRENT INTEREST

Current efforts are focused on fabricating the following four components:

- Turbine Rotors: To operate at an equivalent turbine inlet temperature of 1200 to 1400 C over the complete speed range (Figure 1a).

- Turbine Stators: To operate at 1400 C turbine inlet temperature and withstand prevailing thermal and mechanical stresses during startup, steady-state, and shutdown conditions (Figure 1b).
- Supercharger Rotors: To replace expensive nickel alloys by lower cost, nonstrategic materials. To investigate the possibility of developing a 3-shaft regenerative turbine operating at 1300 C. It is believed that a 3-shaft turbine may have a better partial load economy, two stages of compression would allow intercooling between compressor stages and improve the specific fuel consumption at high load factors and also the specific power output; also, with two stages of compression, relatively small turbines driving the compressors can be designed to operate at modest rotational speed and with reduced centrifugal stresses (Figure 1c).
- Combustion Prechamber Inserts: To replace high-nickel alloy in diesel engine combustor components. Also to reduce ignition delay on cold start up and to reduce idling/light-load noise (Figure 1d).

INJECTION MOLDING PROCESS

For some years, ceramic manufacturers have been aware of the potential for injection molding; nevertheless, acceptance of this process as a routine production approach has been extremely slow. This skepticism can be better understood if one presents the process technology in some perspective.

Ceramic injection molding consists, essentially, of the following steps:

- Tailoring the ceramic powder
- Developing some organic binder formulations
- Producing a homogeneous ceramic and organic binder mix
- Forming parts by injection molding
- Processing the parts to remove the organic binder and densifying the parts.

Injection molding is obviously not a direct analog of the plastic molding process. Successful ceramic injection molding depends on several process steps. In this paper, we briefly discuss all these process steps and include some experimental data. A silicon nitride powder has been chosen as an example.

Tailoring the Powder

Trend in ceramic industries is to use powders with high surface reactivity to reduce the sintering temperature and time, and to achieve improved end properties. GTE Sylvania's SN502 (characterized in Table 1) is one of the few appropriate commercially available silicon nitride powders. It is typically composed of a mixture of amorphous, alpha and beta phases with the alpha phase predominant. Its major contaminants are oxygen and free silicon. The SEM micrograph in Figure 2 indicates that this powder is composed of a variety of shapes and sizes with a large fraction of submicron-size particles and some agglomerates. Because the powder is a mixture of both needle shaped (α-Si_3N_4) and equiaxed particles, a reliable size distribution can not be achieved. The needles vary from 0.1 to 7 or 8 microns in diameter and from submicron to 20 to 30 microns in length, although the majority are much shorter. The surface area indicates a large fraction of particles less than 1 micron. The mixture of shapes in this powder drastically affects its packing and flow characteristics. One can easily understand this in considering how a pile of needles or pins pack. Needle shapes persist throughout the compaction process and lead to a relatively low compact density. Low compact density causes excessive shrinkage during sintering. High and nonuniform shrinkage becomes very critical for complex parts with tight tolerances. Furthermore, such powders create problems when mixed with relatively small amounts of organic binder, thus affecting the rheology of the molding composition.

Moreover, covalent silicon nitride is not sinterable without an added sintering aid. In recent years, extensive research has been undertaken to find chemical additives that would help the densification process. Currently, Y_2O_3 or a mixture of Y_2O_3 and Al_2O_3 are widely used as a suitable

aid for pressureless sintering of silicon nitride. Homogeneous mixing of the additive(s) with silicon nitride powder is extremely critical. Thus, a powder processing step is essential with SN502 silicon nitride to improve its flow and packing and to render homogeneous dispersion of the additive(s). The powder processing in this context refers to one of several methods of milling, such as ball milling, fluid energy milling, or attrition milling. For silicon nitride, dry ball milling has received the most attention and has been used as a standard practice. The milling conditions and results are given in Table 2. Irrespective of the type of milling aid, compaction density increased significantly after 16 hours. However, the breakdown of agglomerates and needles became significant only after 24 hours of milling, as shown in the micrograph in Figure 3 for the powder milled with stearic acid. This improvement represents deagglomeration and reduction in needle size. It is not necessarily a result of real particle size reduction during milling process. This powder was used in a subsequent injection molding process.

Developing a Binder Formulation

Of primary importance is the selection of a binder formulation that will give correct flow properties to a ceramic and binder combination such that a void-free, stress-free, and uniformly dense molded shape can be achieved. The flow behavior of such materials (shown in Figure 4 from Metzner, 1959) can be described as:

- St. Venant where the viscosity is inversely proportional to shear rate
- Bingham plastic which does not show any flow unless the shear stress reaches a critical unit. The nonlinearity has been attributed to changes in the network structure and alignment within the network structure of the flowing material as the stresses change. The network structure can support a stress before any material flow can be initiated. This finite stress is known as the yield stress.

- Pseudoplastic where the viscosity decreases continually with shear rate.
- Dilatant where the viscosity increases with shear rate.

Ideally, in injection molding, the mix leaving the gate of the mold cavity should spread like a liquid sweeping the air before it, the air escaping through mold clearances or vents. However, the absence of a yield point would mean that the molded part may deform at the dewaxing stage. On the other hand, if the mix has a high yield point, it will extrude into the mold cavity as a thread or ribbon which coils upon itself, tending to trap air and induce mechanical stresses as shown in Figure 5. To obtain best results, it is necessary to select a binder formulation that will have a yield point consistent with the shape, size, and dimensional stability of the molded part. In other words, the ceramic/polymer or wax formulations should have either Bingham or pseudoplastic flow characteristic. Furthermore, the binder should be easily degradable or extractable in a subsequent dewaxing process.

A binder formulation that will meet the criteria mentioned above has been sought since 1932. An impressive list of patents that can be produced covers almost all the natural and synthetic organics available in commercial quantities. In general, low-molecular-weight polyethylene, polystyrene, polypropylene, and, more recently, paraffin and microcrystalline waxes with small additions of other organic modifiers have been used successfully as binders for ceramic injection molding. In the light of flow behavior and safe dewaxing, we have chosen a molecular weight ($\sim$5000) polyethylene with a melt index of 250.

Rheological Behavior. Experience has shown that good flow during molding requires a viscosity of less than 10^4 poise. As the shear rate often ranges between 100 sec^{-1} and 1000 sec^{-1}, it is assumed that any binder formulation with a viscosity less than 10^4 poise within the shear rate range indicated will be suitable for molding. An Instron Capillary Rheometer which has a shear rate range from 1 to 10^4 sec^{-1} has been used to describe the flow behavior. Figure 6a shows the viscosity shear rate curves for unfilled polyethylene and polyethylene containing silicon nitride at different levels of loading. Obviously, the addition of silicon nitride has significantly

increased the viscosity at each shear rate but not changed the general shape of the curve. At low shear rates, the viscosity of this formulation rises sharply indicating a yield stress below which the material does not flow. It also shows that the viscosity is outside the molding range at silicon nitride loading of only 48 volume percent. Therefore, the viscosity of this formulation should be reduced so as to increase the silicon nitride loading, thereby, increasing the density of the part and reducing the shrinkage.

The viscosity of such a formulation can be reduced by introducing some organic additives in small concentrations. These are broadly known as modifying agents. Modifying agents should be compatible with the polyethylene and should easily wet the silicon nitride powder surface. Paraffin, microcrystalline waxes, stearates, oleates, and many saturated and unsaturated fatty acids can be used as modifying agents. Figure 6b illustrates the effect of modifying agents on the silicon nitride loading and viscosity. By adding 18 volume percent of modifying agent the viscosity of the binder formulation has been significantly reduced, even with an increased silicon nitride loading of 60 volume percent. Obviously, the role of these modifying agents is rather complex and some studies are in progress to develop some basic understanding.

Producing a Homogeneous Mix

A workable binder formulation thus developed can be used to produce a sizable quantity of materials for molding. Production of such mix requires an effective mixing technique. The following factors should be taken into account when selecting a mixing technique:

- Knowing and defining where a homogeneous mix is attained
- Selecting a mixing system that moves the ingredients to be mixed into a pattern that fulfills the requirements of the desired mix.

In mixing viscous materials, the major mechanism is shear. Shear performs mixing by drawing out the components over thinner layers, which reduces the size of the region occupied exclusively by one component. Various types of commercial shear mixers are available. The Brabender Plastograph with a sigma mixing head is an efficient mixing system.

Forming the Parts

Basically, injection molding is a simple cyclic process in which the granular mix is heated until softened, then forced into a mold where it cools and resolidifies to produce a part in the desired shape.

Molding Machines. Many types and sizes of machines are available, however, schematics of two basic types are shown in Figure 7. The screw-type injection molding machine differs from a plunger type in material conveying and plasticizing. A plunger machine heats the material by conduction and convection only. In a screw machine, a major portion of heat comes from the frictional forces between screw, material, and cylinder. In a plunger machine, the pressure loss in the cylinder could be significant, and the pressure at the end of the plunger is much higher than the pressure at the nozzle. In a screw machine, the ram pressure and nozzle pressure are almost the same.

Selection of a specific machine type is influenced by the requirements of the molded product and by the degree of versatility desired. Regardless of the type, the following features in an injection molding machine are of absolute necessity.

- Injection cylinder should have three individually controlled heater zones. (Nozzle temperature should be separately controlled.)
- Injection and follow-up pressures should be variable up to at least 14 MPa, and be controlled by individual timers.
- Variable speed ram should be controlled either by a flow control valve or by a timed hydraulic pump.
- Feed adjustment should be precise.
- Cycle timers should control plunger-forward time, mold-close time, etc.
- Preposition and multiple prepack controls should be on the plunger-type machine.

Molding Cycle. A molding cycle is based on time, temperature, and pressure. Being a dynamic process, its steps usually overlap; however, they need to be characterized as identifable increments if analysis and control are to be attempted. The cycle time is best represented by the diagram shown in Figure 8 (from Gilmore and Spencer, 1950). The sequence is as follows:

- Period A (dead period) is the time (after the mold closes and the screw/plunger starts forward) before material starts to flow into the sprue bushing.
- Period B (mold filling period) is the time during which material flows into the mold and fills the cavity.
- Period C (pressure build-up period) is the time (after the cavity is filled and the material begins to cool) during which pressure in the cavity builds up to injection pressure.
- Period D (packing period) is the time (including Period C) during which material flows into the cavity at a relatively low rate. The injection cycle ends with this period and the screw/plunger retracts.
- Period E (discharge period) is the time during which material in the gate is still fluid and, with zero pressure on the runner side and slightly less than hold pressure in the cavity, the material flow reverses. (Flow rate is determined by the seal or follow-up pressure).
- Period F (cooling period) is the time during which material in the cavity cools with no flow through the gate in either direction.
- At the end of the mold closed time, the mold opens with some pressure remaining in the cavity. This pressure has been termed the residual mold pressure.

Along with time sequence, it is essential to have the correct temperature and pressure sequence. The pressure-temperature functions in molding have been presented as "ideal gas" equation

$$(P + \pi)\ (V - W) = RT,$$

where P is the hydrostatic pressure, V is the specific volume, T is the material temperature, and π, W, and R are constants for specific molding

material. It can be argued, if the melt temperature is constant in the cavity immediately upon injection, the effective specific volume (V-W) is inversely proportional to the effective applied pressure (P+π). Once the gate is frozen, the effective specific volume (V-W) is constant, and the effective applied pressure (P+π) drops in proportion to the temperature. It is possible to construct a model from this equation and obtain some temperatures and pressures for a specific material being molded into a fairly simple shape.

In the final analysis, molding success depends on the balance between these parameters, the mold design, and the rheology of the molding compound.

Mold Design. The success of injection molding may be measured by the efficiency of the mold design and the quality of the mold construction. Initial consideration should be given to parts design before designing a mold. Feasibility of molding a part by injection molding should be based on such facts as size and weight of the part, section thickness, shrinkage, tolerances, draft, threads, radii, and holes. After careful review of all information on a part, the actual mold design should be considered in the light of the following factors:

- Runner length should be short; but diameter can be varied.
- Preferred runner shape is circular.
- Runner should be placed in the ejector half.
- Preferred gate shape is either round or rectangular.
- Gate size rather than shape appears to have more influence on the manner in which the cavity is filled.
- Larger gate sizes appear beneficial because:
  - -- As the gate size is increased, the probability of jetting is reduced by the lower velocity of the material entering the mold
  - -- The evidence of knit lines is reduced
  - -- Cavity filling is more rapid and there is less opportunity for the material to freeze prior to complete filling of cavity.

- Changes in gate location can reduce or eliminate jetting of the material.
- Vent location in mold is most effective when jetting is reduced and the cavity is filled from the gate area through the remainder of the cavity. (Jetting may cause covering of the vent during the initial stages of cavity filling.)
- Filling is more controlled when the material comes into contact with a surface of the cavity immediately upon entry.
- Mix being injected into the cavity takes the path of least resistance; thus, using gates of different sizes simultaneously may not be advisable.
- Depending upon the freezing rate of the material, it may not be undesirable to use cavities of different sizes simultaneously.
- Rheological characteristics of the material influence the retention of weld marks and knit lines in the molded parts.
- Wear on the machine parts and mold is still an unknown factor.

Removing the Binder

The binder must be removed (dewaxed) from the parts prior to sintering. Binder removal is a key operation in the success of injection molding. In the experimental design, the following factors should be taken into account:

- The binder systems may be composed of more than one organic ingredient with markedly different melt viscosity and decomposition ranges. Hence, in such systems, attempts should be made to remove the ingredients slowly and gradually to create passages within the part with increasing temperature and time, and to allow the major binder ingredient to escape at high temperatures without causing any failure.
- Thermal degradation of nonoxide injection molded ceramics in air could cause a serious oxidation problem. Under these conditions, silicon carbide is more likely to suffer from oxidation than silicon nitride. With silicon nitride, it is generally believed

that silica on the powder surface forms a protective layer and provides more stability during dewaxing in an oxidizing atmosphere; while silicon carbide (in the presence of the excess carbon necessary for densification) cannot tolerate an oxidizing environment. Therefore, various methods of dewaxing should be considered:

- Evaporation and oxidation at elevated temperature
- Pyrolysis in an atmosphere other than air
- Vacuum extraction at elevated temperature
- Solvent extraction.

The dewaxing rate is very dependent on the heating rate, temperature range, partial pressure of gaseous species, part size, and total quantity in an oven load. It is also imperative to devise a technique to reduce the total dewaxing time. Finally, successful dewaxing of thick sections is a limiting factor in ceramic injection molding.

Sintering and Product Evaluation

The ability to form complex shapes with silicon nitride in mass-production quantities at acceptable costs depends on finding an alternative to the current hot pressing approach--one such approach is pressureless sintering. However, silicon nitride, like many other nonoxide ceramics, is difficult to sinter by itself because of its covalent bonding. In the early seventies, Jack (1972) suggested that sialon-type materials (silicon aluminum oxynitride--it is often loosely applied to any composition containing the elements Si-M-O-N, M being the metal atom) are sinterable without applying pressure. Prochasza et al (1978) have successfully densified SiC using only small quantities of sintering aids. Deeley et al (1961) have shown MgO as one of the most effective additives for hot pressing silicon nitride. Terwilliger and Lange (1975) have shown that silicon nitride can be sintered in nitrogen at atmospheric pressure to a density of 90 percent theoretical using 5 percent MgO as sintering aid. However, they noted a considerable weight loss which resulted fom the dissociation of silicon nitride. Mitomo (1976) and Priest et al (1977) have been able to densify silicon nitride in the presence of a

sintering aid to 95 percent and reduce the dissociation using 1.0 to 2.0 MPa of nitrogen overpressure. Giachello et al (1979) have densified silicon nitride with MgO as sintering aid at atmospheric pressure and control both the silicon nitride dissociation and MgO volatilization by embedding the parts in a loose powder mixture. Meanwhile, the sintering mechanism involving MgO has been studied extensively; its shortcomings are pointed out and alternative sintering aids are proposed (Brook et al, 1977). Silicon nitride can be sintered to densities greater than 90 percent theoretical using oxide or nonoxide additions and a nitrogen pressure from 0.1 to 8.0 MPa. Using an amorphous powder (SN 402) and 4 weight percent Y_2O_3 as sintering aid, Rowcliffe and Jorgensen (1977) achieved 90-99 percent theoretical density in (2 atm) N_2. Priest et al (1977) achieved 90-95 percent theoretical density using SN 502 powder and 20 weight percent CeO in 2.0 MPa N_2. Masaki and Kamigaito (1976) could densify a silicon nitride plus 10 weight percent $MgAl_2O_4$ mixture to about 96 percent theoretical in 0.1 MPa N_2. Stewart, Wills, and Wimmer (1977) densified a mixture of Si_3N_4-Al_2O_3-AlN to 98 percent theoretical in 0.1 MPa N_2. Greskovitch et al (1979) densified Si_3N_4 with Be_3N_2 plus Mg_2Si additives or Be_2SiN_2 plus Mg_3N_2 additives. For present advanced gas-turbine programs, silicon nitride with the Y_2O_3 or Y_2O_3-Al_2O_3 additive system is actively being developed (Gazza and Katz, 1980).

While a wide variety of furnaces are used for sintering studies, a graphite induction-heated furnace is most common. The sintering temperature ranges from 1300 to 2000 C. Parts are usually placed in BN crucibles to protect against carbon in the furnace atmosphere.

The extent of densification is usually determined from the density and shrinkage data. The weight loss records any dissociation of Si_3N_4 at the sintering temperature. Typical results are presented in Table 3.

We have used density and room temperature flexure strength as the typical end properties to demonstrate the influence of process variables on the properties of sintered silicon nitride. Table 4 compares the density and strength data of three injection molded silicon nitride parts with similar composition and sintering temperature (1750 C/2 hr). In all three cases, the density and strength are within a comparable range; also, this strength is equivalent to the value reported by Galasso and Veltri (1981) for cold

isostatically pressed material. Yet, better control on injection molding process parameters would be necessary to achieve higher strength as obtained with hot pressed, and machined silicon nitride of similar composition.

A fracture surface (Figure 9) indicates a large pore on the edge of the specimen is the fracture origin. Such pores are associated in injection molding with nonuniform dispersion of binder ingredients that are subsequently removed in the dewaxing process.

SUMMARY

In this paper we have attempted to demonstrate that injection molding of ceramic parts is a viable production process. The work described indicates that while the process is viable, the basic knowledge on this technology still leaves much to be desired. The five major steps in injection molding ceramic parts are covered, using silicon nitride powder as the material of interest. While ultimate parts characteristics and economics are not achieved, at least many of the ramifications in each of the steps are discussed, and suggestions are promulgated toward achieving at least acceptable results in each step. Also touched upon are some testing methods, and basic theory indicating the interrelationships of the steps and their processes. Molding machines and mold designs and their effect on ceramic parts are touched on. Binder removal methods are indicated and sintering is touched on as the final step toward useable ceramic injection molded parts.

Currently achievable density and strength data on silicon nitride shapes that are presented indicate that the ceramic molding process is technologically and economically feasible.

REFERENCES

Brook, R. S., Carruthers, T. G., Bowen, L. J., and Weston, R. J., 1977. "Mass Transport in the Hot Pressing of Alpha Si_3N_4", Nitrogen Ceramics, edited by F. L. Riley, p 383.

Deeley, G. G., Herbert, J. M., and Moore, N. C., 1961. Powder Met., 8, 145.

Galasso, S. F., and Veltri, D. R., 1981. "Sintering of Si_3N_4 Under Nitrogen Pressure", AMMRC TR81-28, September 1979 - September 1980.

Gazza, G. E., and Katz, R. N., 1980. "Development of Sinterable Si_3N_4", DOE/AMMRC 1AG EC-77-A-01-1017.

Giachello, A., Martinengo, P. C., and Tommasini, G., 1979. "Sintering of Si_3N_4 in a Powder Bed", J. Mater. Sci. 14, 2825-2850.

Gilmore, A. D., and Spencer, R. S., 1950. Plastics, 143-228.

Greskovitch, C., Prochaza, S., and Resolowski, J. M., 1979, "Basic Research on Technology Development for Sintered Ceramics", Technical Report, AFML-TR-76179, Contract F-33615-76-6-5033, General Electric.

Jack, K. M., and Wilson, W. I., 1972. "Ceramics Based on the Si-Al-O-N and Related Systems", Nature (Phys. Sci.) 238 (80) 28-29.

Mann, L. D., 1978. "Injection Molding of Sinterable Silicon Base, Non-oxide Ceramics", Technical Report AFML-TR-78-200, September 1977 - October 1978.

Masaki, H., and Kamigaito, O., 1967. "Pressureless Sintering of Si_3N_4 with Additions of MgO, Al_2O_3, and/or Spinel, YOGYO-Kyokai-Shi, 84 (10), 508-12.

Metzner, B. A., 1959, "Flow Behavior of Thermoplastics", edited by Bernhardt, C. E., p 19.

Mitomo, M., 1976, J. Mater. Sci., 11, 1103.

Priest, H. F., Priest, G. L., and Gazza, G. E., 1977, "Sintering of Si_3N_4 Under High Nitrogen Pressure", J. Am. Cer. Soc., 60 (1-2), 81.

Prochaza, S., 1978. "The Role of Boron and Carbon in the Sintering of Silicon Carbide", Special Ceramics, 6, edited by P. Popper, p 171.

Quackenbush, L. C., French, K., and Neil, T. J., 1982. "Fabrication of Sinterable Silicon Nitride by Injection Molding", Ceramic Engineering and Science Proceedings, 20-28, Am. Ceram. Soc.

Rowcliff, D. J., and Jorgensen, P. J., 1977. "Proceedings of the Workshop on Ceramics for Advanced Heat Engines", Contract 770110UC95a-ERDA-Rep.

Stewart, R. W., Wills, R. R., and Wimmer, J. M., 1977. "Fabrication of Reaction Sintered Silicon", J. Am. Cer. Soc. 60 (1-2) 65-67.

Terwilliger, G. R., and Lange, F. F., 1975. J. Mater. Sci., 11, 1169.

Table 1. Characterization of SN 502 Si_3N_4 Powder

Composition, percent		
Amorphous	Si_3N_4	40.
Alpha	Si_3N_4	57.6
Beta	Si_3N_4	2.4
	O_2	2.70
	Cl_2	0.20
	Si	Trace
Mean Particle Size		Submicron
Surface Area, m^2/g		4.389
Apparent Density, percent of theoretical		9.4
Tap Density, percent of theoretical		15.0
Compaction Ratio, percent		4.7

Table 2. Milling Conditions and Results for SN 502

Milling Parameters	
Porcelain Mill	1890 cc
Si_3N_4, Y_2O_3, Al_2O_3 Powder	250 g
Al_2O_3 Cylinders, Coors High Purity 1.27 x 1.27 cm	2100 g
Loading Ratio, by weight	5.4:1
Milling Aid, weight percent	1
Mill Speed	100 rpm

Compact Density

Milling Time, hr	Pressing Pressure MN/m^2	Milling Aids, Percent Theoretical Density			
		Stearic	Oleic	Naphthenic	Triethanalamine
8	172	45.1	43.0	46.3	40.4
16	"	50.8	54.8	51.5	51.0
24	"	51.1	55.4	47.4	52.7
48	"	56.7	54.4	48.2	56.8

Table 3. Sintering Results on SN 502 Si_3N_4 Vanes, Cups, and Test Bars

Sample	Density After Burnout, Percent of Theoretical	Density After Sintering, Percent of Theoretical	Shrinkage After Burnout, percent	Shrinkage After Sintering, percent	Weight Loss During Sintering, percent
Vanes:					
1	—	97.8	ND*	18.8	1.20
2	—	98.1	ND*	19.1	1.07
3	—	98.8	ND*	18.8	1.32
4	—	98.3	ND*	19.3	0.96
5	—	97.6	ND*	18.6	1.01
Cups:					
1	—	97.5	ND*	18.5	0.91
2	—	98.4	ND*	18.4	1.11
3	—	98.2	ND*	18.2	1.18
4	—	98.6	ND*	18.6	1.14
5	—	98.5	ND*	18.5	—
Test Bars:					
1	55.2	98.4	0.71	19.5	0.77
2	55.6	97.5	0.74	18.6	0.75
3	54.8	98.8	0.60	18.8	0.84
4	55.5	97.8	0.56	19.2	0.95
5	55.8	98.0	0.64	19.0	0.88

*ND = Not determined.

Table 4. Density and Room Temperature Flexure Strength of Sintered Silicon Nitride

Source	Composition	Fabrication Method	Density, g/cc	RT Flexure Strength,* MPa
Galasso and Veltri (1981)	Si_3N_4-15Y_2O_3-3Al_2O_3	Cold Isopressed	3.141	432 (3-Point)
Mann (1978)	Si_3N_4-8Y_2O_3-4Al_2O_3	Injection Molded	3.09	402 (4-Point)
BCL (unpublished)	Si_3N_4-8Y_2O_3-4Al_2O_3	Injection Molded	3.04	380 (4-Point)
Quackenbush et al (1982)	Si_3N_4-6Y_2O_3-2Al_2O_3	Injection Molded	3.13	385.8 (4-Point)

*Unmachined.

Figure 1. Typical Injection Molded Silicon Nitride Components

a. Rotor Ring b. Stator c. Supercharger Rotor

d. Combustion Prechamber Insert

Figure 2. SEM of As-Received GTE SN 502 Silicon Nitride Powder

Figure 3. SEM of SN 502 Silicon Nitride Dry Ball Milled With 1 Weight Percent Stearic Acid for 24 Hours

Figure 4. Types of Flow Behavior

Figure 5. Stages in Mold Filling with a Silicon Nitride Mix

Figure 6. Viscosity Versus Shear Rate for Various Mixes

6a. Polyethylene with Different Si_3N_4 Loadings

6b. Effects of Modifying Agents on Si_3N_4 Loading and Viscosity

Figure 7. Injection Molding Machines

7a. Screw Type Machine

7b. Plunger Type Machine

Figure 8. Molding Cycle
A, Dead Time; B, Mold-Filling Period;
C, Pressure Build-Up Phase;
D, Packing Period;
E, Discharge;
F, Cooling With Gate Frozen

Figure 9. SEM on Fracture Surface of Injection Molded Silicon Nitride

COMPONENTS OF CURRENT INTEREST

INJECTION MOLDED SILICON NITRIDE ROTOR RING

1 a.

SILICON NITRIDE STATOR

1 b.

COMPONENTS OF CURRENT INTEREST

INJECTION MOLDED SILICON NITRIDE SUPERCHARGER ROTOR

1 c.

COMBUSTION PRECHAMBER INSERT

1 d.

CERAMIC POWDER CHARACTERISTICS

AS RECEIVED GTE SN502 Si_3N_4 POWDER

Figure 2.

Figure 3.

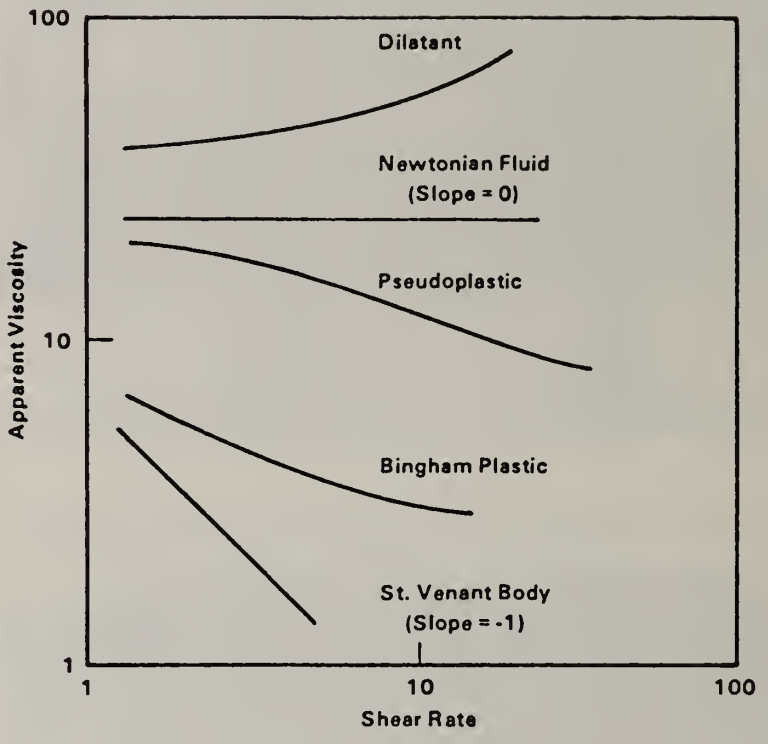

APPARENT VISCOSITY AS A FUNCTION OF SHEAR RATE FOR VISCOUS FLUIDS

Figure 4.

EFFECT OF VISCOSITY ON THE MOLD FILLING CHARACTERISTICS

Figure 5.

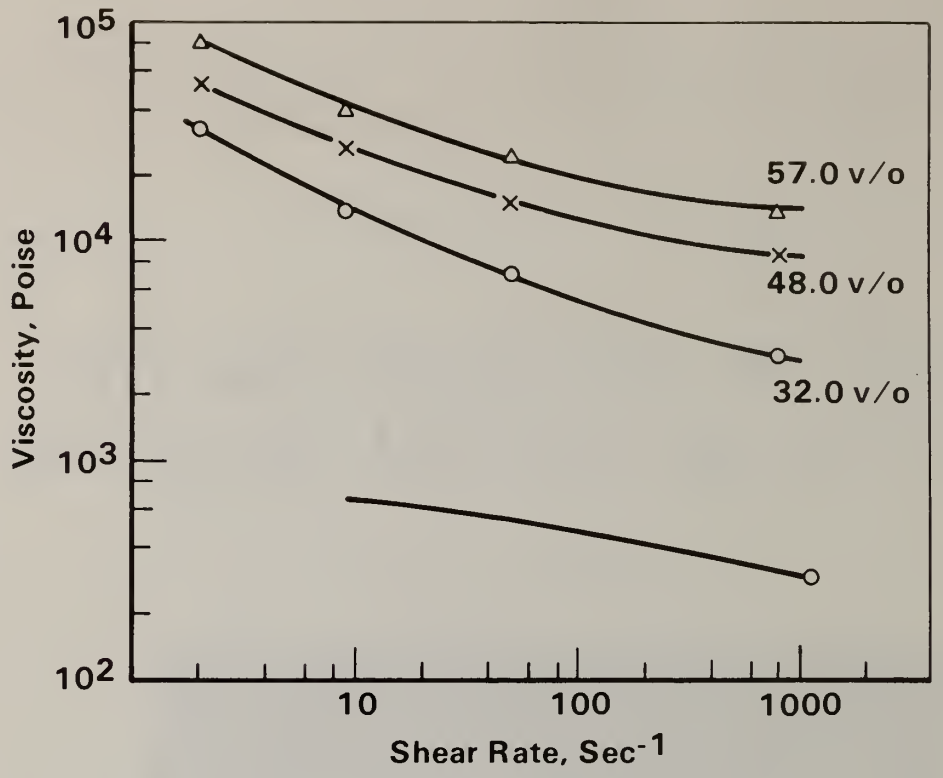

6a. Viscosity of Polyethylene at Different Levels of Silicon Nitride Loading

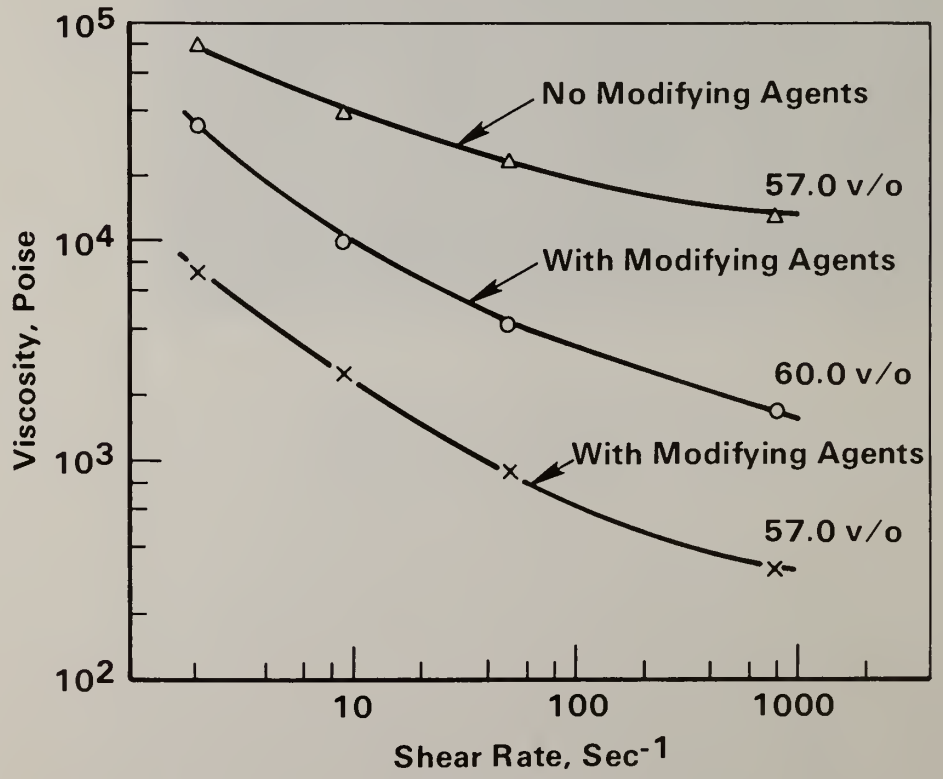

6b. Effects of Modifying Agents on Silicon Nitride Loading and Viscosity

Figure 6. Viscosity Versus Shear Rate for Various Mixes

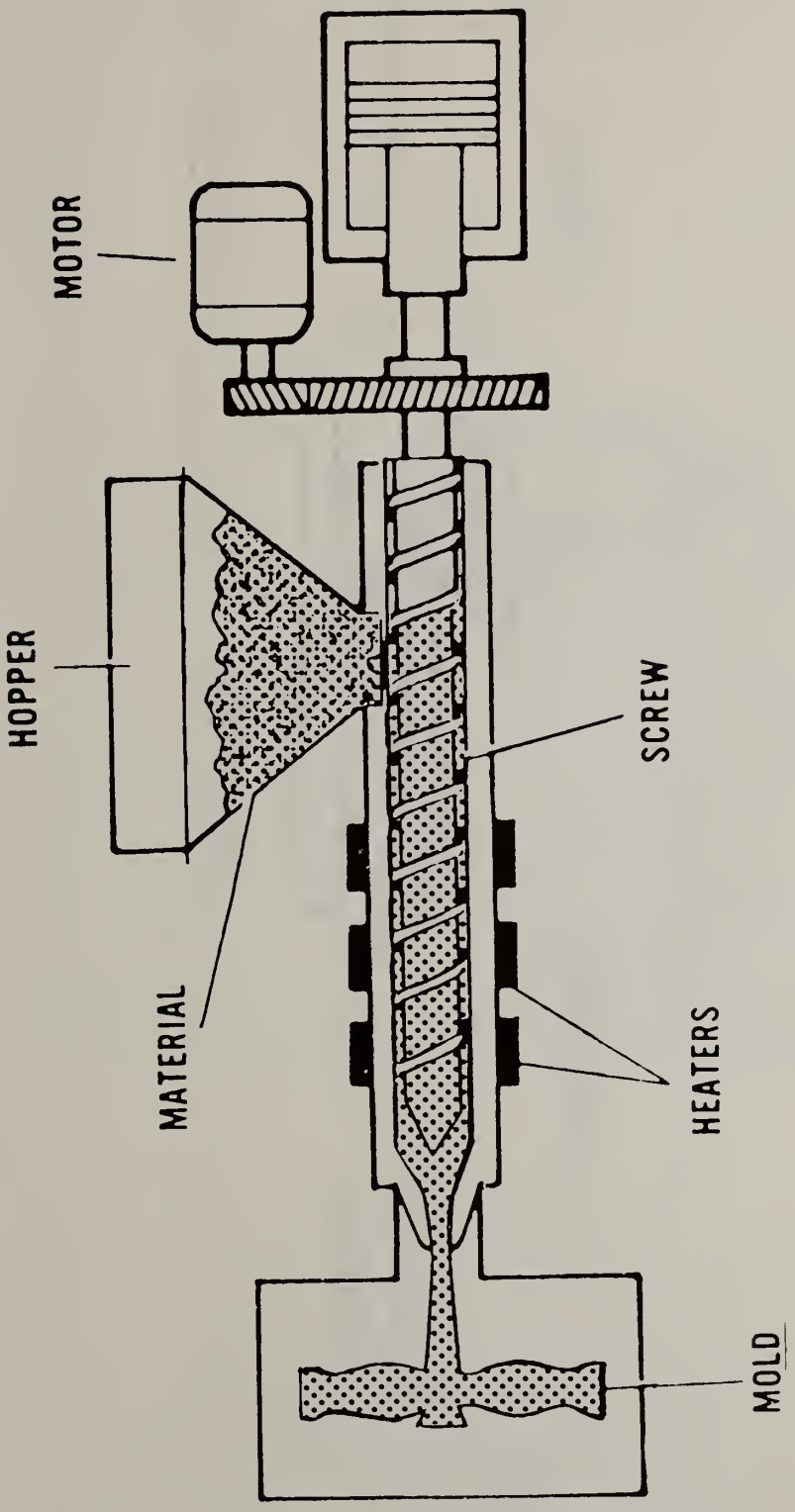

Figure 7a.

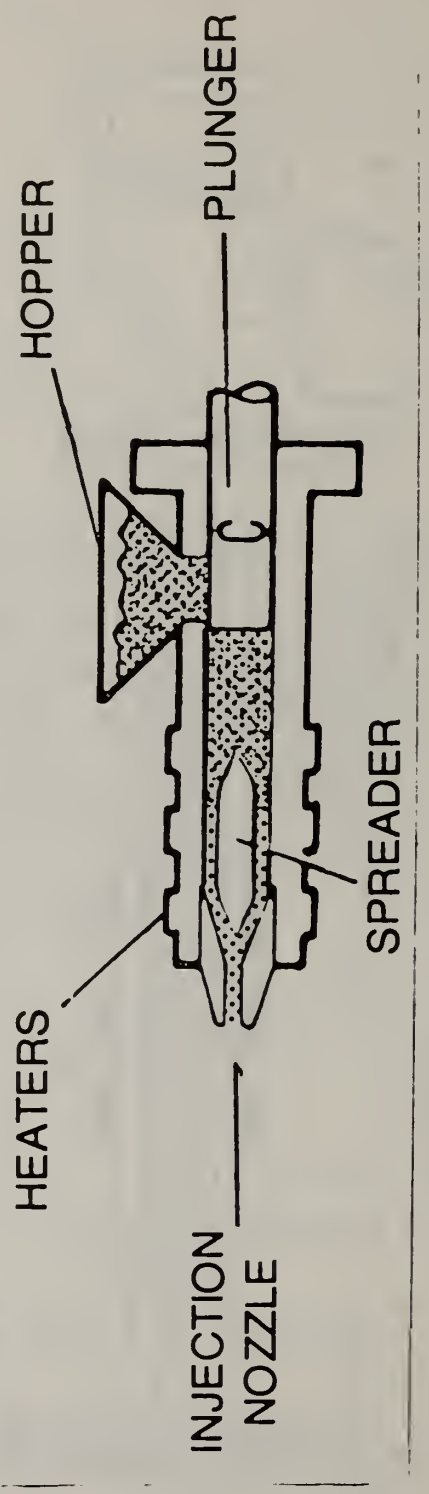

Figure 7b.

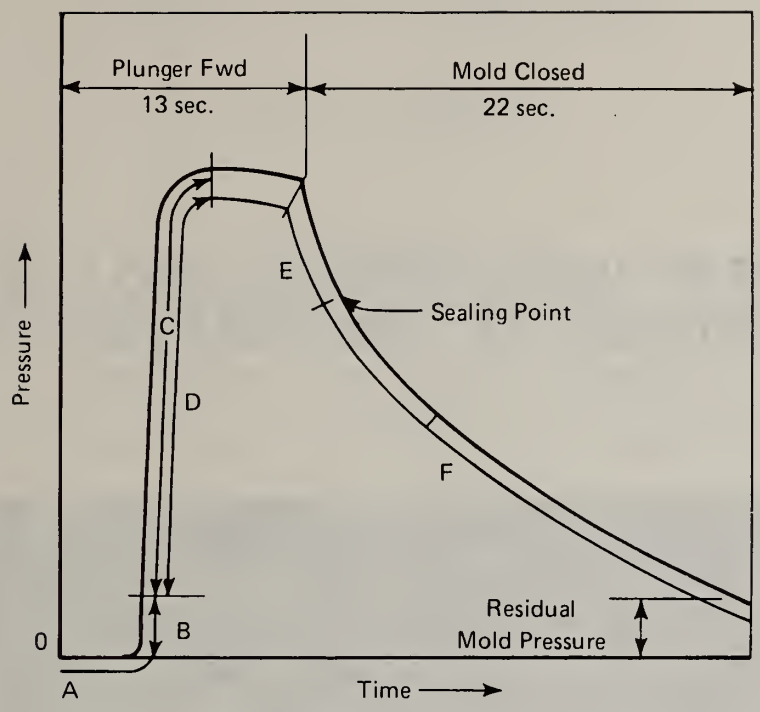
Plunger Fwd
13 sec.
Mold Closed
22 sec.
Pressure
E
Sealing Point
C
D
F
Residual
Mold Pressure
0
B
A
Time

Figure 8

SEM PICTURE OF INJECTION MOLDED AND SINTERED SILICON NITRIDE ON THE FRACTURE SURFACE

Figure 9

DEVELOPING AN INFORMATION STOCKPILE TO AID IN SUBSTITUTION PREPAREDNESS

Robert T. Nash
Vanderbilt University

Introduction

During the workshop the attendees had the opportunity to provide their written views on the acquisition, organization and dissemination of information describing alternative technologies which could be used if shortages of critical materials occurred. Thoughtful comments were obtained which in combination provide a coherent picture of the issue of stockpiling information.

The following five elements of the information stockpile issue were identified in the responses from the workshop participants which are:

- Types of Information Explaining Alternative Technologies
- Uses and Sources of Information Explaining Alternative Technologies
- Channels for Disseminating Information
- Influential Organizations
- Qualification of a Material

Each of these five elements will be discussed separately.

Types of Information Explaining Alternative Technologies

There was a consensus that the following types of information should be included in a substitution preparedness stockpile.

Case Histories by Application
Substitution Plans by Companies
Structure - Property Relations
Substitution Tables

Invariably, changes in processes are associated with any change in the use of materials. Consequently, an alternative technology consists of both a change

in material and the associated processes which are employed in the production and subsequent fabrication of the material into a finished part.

In addition to technical and economic information the participants felt that administrative information would be necessary. In particular, government agencies should keep industrial organizations informed about plans which would be employed during an emergency if a shortage of materials occurred.

It was recognized that much useful information is proprietary and hence not likely to appear in any publication. Further, information concerning processes is usually not amenable to publication in any but the most rudimentary form. Hence, the workshop participants thought that it would be useful to develop lists of people that are expert on alternative technologies who could be contacted during an emergency.

Uses and Sources of Information Explaining Technological Alternatives

An important distinction exists between changes in materials for which qualification is required and those for which it is not. At one extreme a change can be made in a tool steel through a manufacturer's decision. At the other, materials used in nuclear power systems and aircraft can only be changed after lengthy qualification procedures.

Only those technological alternatives which have undergone at least limited application in an industrial organization would be used by industry during an emergency. Therefore, a consensus supported the position that only a technology which has actually been employed in serial production, or at a minimum in prototype testing, should be included in the information stockpile. Any changes in the use of critical materials during an emergency must be simple, or they will not be implemented due to lack of time.

Technological alternatives which are used by industry often originate in government laboratories and universities. However, this work is only technological information in process until applied to the manufacture of actual materials and finished parts by industry. Laboratory results, no matter how promising, would be of little or no value in an emergency.

Channels for Disseminating Information

Existing channels of information transfer should be employed to the greatest extent possible in disseminating information on substitution preparedness. The regular sources include:

- Journals
- Conference Proceedings
- Handbooks
- Government Publications

It was also the view of the workshop participants that these regular sources of information should be supplemented. The principal means would be to publish abstracts of papers already appearing in the open literature. These abstracts could be made available through existing electronic information retrieval systems as soon as they are prepared. In addition, hard copy summaries of the abstracts could be published annually. When a suitable body of information had been accumulated on a particular topic, publication of a monograph or handbook would become appropriate.

Influential Organizations

A number of public and quasi public organizations were mentioned which would play a role in the organization of a materials substitution stockpile. These include:

NMAB	Department of Commerce
ASTM	Department of Interior
MPC	(Bureau of Mines)
AISI	Department of Defense

To guide the development of an information stockpile, an advisory group could be organized which would include representatives from industry and each of the influential organizations listed above. This group could provide advice on the most effective means of organizing a stockpile of information pertinent to substitution preparedness.

Qualification of a Material

A crucial element in determining what information should be included in an information stockpile is the role of qualification procedures. These procedures help determine the length of time required to make any type of change in the use of a material. Therefore, the role of qualification in substitution preparedness should be evaluated carefully. The workshop participants felt that an alternative technology should only be included in the information stockpile after qualification of the material.

Findings Concerning an Information Stockpile

The following findings were obtained during the workshop concerning the organization of an information stockpile.

1) Since qualification procedures greatly influence the period of time required to change the use of a material, only that information concerning materials which have been qualified should be included in the stockpile where qualification is necessary.
2) Only that information concerning technologies which have been carried through prototype testing should be included in the stockpile where qualification is not necessary.
3) Existing channels for disseminating primary information should be employed to the greatest extent possible. The existing channels should

be augmented with Substitution Preparedness Abstracts which could be used to locate primary information.

4) Those organizations which can influence the adoption of new types of materials should be instrumental in the development of the information stockpile.

5) Much information is never published. Hence, the names of people should be made available who would provide advice on alternative materials and processes for use during an emergency.

6) Information should only be included in the stockpile if the substitute technology can be implemented within a reasonable period of time. If too much time is required, the substitute technology will not be used in an emergency.

NBS-114A (REV. 2-8C)

U.S. DEPT. OF COMM. BIBLIOGRAPHIC DATA SHEET (See instructions)	1. PUBLICATION OR REPORT NO. NBSIR 83-2679-2	2. Performing Organ. Report No.	3. Publication Date July 1983

4. TITLE AND SUBTITLE

Technical Aspects of Critical Materials Use by the Steel Industry Volume II B: Proceedings of a Public Workshop; "Trends in Critical Materials Requirements for Steels of the Future; Conservation and Substitution Technology for Chromium".

5. AUTHOR(S)

Edited by R. Mehrabian

6. PERFORMING ORGANIZATION (If joint or other than NBS, see instructions)

NATIONAL BUREAU OF STANDARDS
DEPARTMENT OF COMMERCE
WASHINGTON, D.C. 20234

7. Contract/Grant No.

8. Type of Report & Period Covered

9. SPONSORING ORGANIZATION NAME AND COMPLETE ADDRESS (Street, City, State, ZIP)

U.S. Department of Commerce, National Bureau of Standards
U.S. Department of the Interior, Bureau of Mines
U.S. Department of Defense, Army Research Office

10. SUPPLEMENTARY NOTES

☐ Document describes a computer program; SF-185, FIPS Software Summary, is attached.

11. ABSTRACT (A 200-word or less factual summary of most significant information. If document includes a significant bibliography or literature survey, mention it here)

This volume presents papers given at a public workshop sponsored jointly by the National Bureau of Standards, Bureau of Mines, Army Research Office, and Vanderbilt University. The workship "Critical Materials Requirements for Steels of the Future; Conservation and Substitution for Chromium," was held at Vanderbilt University, October 4-7, 1982; it featured 50 presentations by technical authorities from steel producing and using industries.

Volume I of this publication draws extensively on these proceedings and reviews technical opportunities for research in process improvement and in alternative materiald development that would reduce U.S. dependency in critical materials. The advanced technologies reviewed in Volume I in addition to their implications for critical materials conservation represent trends leading to better quality, lower cost steel products, and therefore they may contribute positively to the industry's more immediate concern for improved markets.

12. KEY WORDS (Six to twelve entries; alphabetical order; capitalize only proper names; and separate key words by semicolons)

Advance coatings; alternative materials; chromium; processing; steel; strategic materials

13. AVAILABILITY

☐ Unlimited

☒ For Official Distribution. Do Not Release to NTIS

☐ Order From Superintendent of Documents, U.S. Government Printing Office, Washington, D.C. 20402.

☐ Order From National Technical Information Service (NTIS), Springfield, VA. 22161

14. NO. OF PRINTED PAGES

415

15. Price